STARS

2016

Modeling Mass Transfer and Assessing Cost and Performance of a Hollow Fiber Nanofiltration Membrane Process

David Yonge
University of Central Florida

MODELING MASS TRANSFER AND ASSESSING COST AND PERFORMANCE OF A
HOLLOW FIBER NANOFILTRATION MEMBRANE PROCESS

by

DAVID T. YONGE, E.I.

B.S.C.E., University of Central Florida, 2011
B.S.Env.E., University of Central Florida, 2011
M.S.Env.E., University of Central Florida, 2012

A dissertation submitted in partial fulfillment of the requirements
for the degree of Doctor of Philosophy
in the Department of Civil, Environmental, and Construction Engineering
in the College of Engineering and Computer Science
at the University of Central Florida
Orlando, Florida

Spring Term
2016

Major Professor: Steven J. Duranceau

ABSTRACT

Bench-scale water treatment testing of three next generation hollow-fiber (HF) nanofiltration (NF) membranes was conducted to characterize divalent ion rejection capabilities and investigate removal mechanisms. Existing mathematical models were investigated to describe solute transport using synthetic magnesium sulfate solutions including the size exclusion model, homogenous solution diffusion (HSD) model, dimensional analysis, and the HSD model incorporating film theory. Solute transport for two of the membranes were described by HSD theory and were predictive of their 90% divalent ion removal. A third membrane was more accurately modeled using size exclusion and was found to be predictive of its 40% divalent ion rejection. Feed ionic strength variation was shown to significantly impact rejection. In this work, semi-empirical models were developed to describe solute transport under varying feed ionic strength conditions. Bench-scale testing of aerated groundwater confirmed the HFNF membrane divalent ion rejection capabilities. Pilot testing of a commercially available HFNF membrane was shown to remove divalent ions and dissolved organic carbon (DOC) by 10% and 25%, respectively. Financial evaluations indicated that HFNF offered cost savings over traditional spiral-wound (SW) NF, $0.60/kgal versus $0.85/kgal operating costs, respectively. Traditional SWNF membranes produced superior water quality achieving 90% divalent ion removal and 96% DOC removal but required media and membrane filtration pretreatment. When considering the costs of constructing a new 2 million gallon per day (permeate) HFNF process, conceptual cost comparisons revealed that HFNF technologies could reduce capital costs by approximately $1 million, and operating costs by $0.27/kgal for an 85% recovery plant.

This dissertation is dedicated to God, my lovely wife, Stephanie, and my supportive family.

ACKNOWLEDGMENTS

TABLE OF CONTENTS

LIST OF FIGURES

LIST OF TABLES

LIST OF EQUATIONS

LIST OF ABBREVIATIONS

A	amperes
AASHTO	American Association of State Highway and Transportation Officials
ACS	American Chemical Society
ASTM	American Standard for Testing Materials
C	Celsius
CEB	chemically enhanced backwash
CECE	Civil, Environmental, and Construction Engineering
CF	cartridge filter
cfs	cubic feet per second
cfu	colony-forming unit
CIP	clean in place
DA	dimensional analysis
DBP	disinfection byproducts
EC	electrical conductance
EEM	excitation-emission matrix
ESEI	environmental systems engineering institute
FT	film theory
ft	feet
gpm	gallons per minute
gfd	gallons per square foot day
gpd	gallons per day
hr	hour
Hz	hertz
HF	hollow fiber
HFC	hollow fiber concentrate
HFF	hollow fiber feed
HFP	hollow fiber permeate
HSD/HSDM	homogenous solution diffusion / model
HSDM-FT	homogenous solution diffusion film theory model
HSD-IS	homogenous solution diffusion ionic strength model
I&C	instrumentation and controls
IC	ion Chromatography
ICP	inductively coupled plasma
in	inch
IX	ion exchange
KHP	potassium acid phthalate
kW	kilowatt

L	liter or length
LCL/LWL	lower control limit / lower warning limit
m	meter
M	mass
MCE	mixed cellulose ester
MCL	maximum contaminant level
MCLG	maximum contaminant level goal
MFI	modified fouling index
min	minute
MPFI	mini plugging factor index
MTC	mass transfer coefficient
MF	microfiltration
MG/MGD	million gallons / million gallons per day
mM	millimolar
MWCO	molecular weight cut-off
NF	nanofiltration
NOM	natural organic matter
NPDOC/DOC	(non-purgeable) / dissolved organic carbon
NSDWR	national secondary drinking water regulations
NTU	Nephleometric tubidity units
O&M	operation and maintenance
OES	optical emission spectrophotometry
ORP	oxidation reduction potential
PDT	pressure decay test
PES	polyethersulfone
PPSU	polyphenylsulfone
PSF	polysulfone
PV	pressure vessel
PVC	polyvinyl chloride
PVP	polyvinylpyrrolidone
psi	pounds per square inch
psig	pounds per square inch gauge
RBSMT	rapid bench scale membrane tests
R^2	coefficient of determination
Re	Reynolds number
RegSS	sum of squares due to the regression
RMSE	root mean squared error
RO	reverse osmosis
RPD	relative percent difference

RSS	residual sum of squares
RV	raw Verna
Sc	Schimdt number
SDI	silt density index
SE	size exclusion
SEBST	single element bench scale tests
SF	sand filtration
SFF	sand filter filtrate
Sh	Sherwood number
SM	standard method
SMCL	secondary maximum contaminant level
SPEEK	sulfonated poly ether ether keytone
SST	total sum of squares
SW	spiral wound
SWDA	safe water drinking act
t	time
TCF	temperature correction factor
TDS	total dissolved solids
TMP	transmembrane pressure
TOC	total organic carbon
TSS	total suspended solids
UCF	University of Central Florida
UCL / UWL	upper control limit / upper warning limit
UF	ultrafiltration
USEPA	United States of America Environmental Protection Agency
USGS	United States of America Geological Survey
V	volts
WTF	water treatment facility

1.   INTRODUCTION

The drinking water community of today requires more effective, efficient, and cost-effective water processing methods to overcome the challenges of more stringent regulatory mandates amidst increasing demands due to population growth and diminished access to higher quality water supplies. Significant advancements in membrane technology has led to a growth in the number of water purveyors adopting synthetic membrane processes to address these challenges (Jacangelo & Laine, 1994; Shannon, Bohn et al., 2008; Van der Bruggen & Vandecasteele, 2003). Low-pressure hollow-fiber ultrafiltration (HFUF) membranes are commonly used to remove turbidity and particles while providing a barrier for pathogens such as *cryptosporidium* (AWWA, 2005). Likewise water treatment facilities can achieve removal of hardness through the use of spiral-wound nanofiltration (SWNF) membrane technology (Conlon, Hornburg et al., 1990) which was originally developed in the 1980s (Cadotte, Forester et al., 1988). However compared to a hollow-fiber configuration, SW membranes are more energy intensive, prone to fouling and often require advanced pretreatment (Wintgens, Salehi et al., 2008). Therefore, research has continued regarding hollow-fiber nanofiltration (HFNF) technology.

A number of studies have been conducted on the development and construction of HFNF membranes finding HFNF technologies exhibit greater packing density, higher surface area to volume ratios, self-support capability, and cost effective operation (Darvishmanesh, Tasselli et al., 2011; Fang, Shi et al., 2014; Futselaar, Schonewille et al., 2002; Kiso, Mizuno et al., 2002). Additional bench-scale studies have included the applicability of HFNF membranes for NOM removal (DiGiano, Braghetta et al., 1995) and comparisons between HFNF and flat sheet membrane pretreatment requirements (Van der Bruggen, Hawrijk et al., 2003). While the transition

from bench-scale to full-scale plant implementation has occurred for HFUF and SWNF technologies, advancements in HFNF have primarily been limited to bench-scale applications with few studies advancing to the pilot-scale. Sethi and Wiesner (2000) performed pilot studies investigating a HFNF with a membrane length of one meter and a molecular weight cutoff (MWCO) of 250 Daltons (Da). HFNF membranes were shown to handle higher concentrations of particulate and colloidal fouling compared to SWNF membranes which required HFUF as pretreatment. The cost of HFNF compared to the integrated HFUF-SWNF process was found to offer significant cost savings (approximately 30%) for small scale treatment plants. Additional pilot-scale HFNF research includes treatment of wastewater effluent (Duin, Wessels et al., 2000; Futselaar et al., 2002) and the use of air sparging for cleaning HFNF membranes (Bonné, Hiemstra et al., 2003; Verberk & Van Dijk, 2006).

More recent pilot studies conducted by Knops and colleagues (2012) showed HFNF technology was successful at removing dissolved constituents of a surface water supply in the Netherlands. Although several HFNF membrane facilities have been constructed and are operating in northern Europe, the facilities tend to be small-scale (< 1 million gallons per day) and focused on color and natural organic matter (NOM) rather than divalent ions (Knops, 2016). However, additional work is necessary to determine removals capabilities, describe rejection mechanisms, and assess hydraulic membrane performance before full-scale implementation. The research presented in this dissertation included the application of HFNF membranes for treatment of a biologically active aerated groundwater supply containing sulfate, hardness, and dissolved NOM through bench-scale and pilot-scale applications.

2. SITE DESCRIPTION AND BACKGROUND

The City of Sarasota's (City) water treatment facility (WTF) is located at 1750 12th Street, Sarasota FL. The City is permitted by state regulatory authorities to withdraw water from two main groundwater sources, one brackish and one freshwater. The combination of well fields allows the City to produce 12 MGD of finished water at their downtown water treatment facility location. The two well fields have significantly different water quality and are treated by two different processes as portrayed from Figure 2-1. The downtown brackish well field is treated by reverse osmosis (RO) and the aerated Verna groundwater is treated by ion exchange (IX). This chapter provides a description of the City's treatment processes and presents the limitations and concerns with the current technology treating the Verna groundwater supply.

Downtown Brackish Well Field

Six million gallons per day (MGD) of raw water are pumped from the downtown well field and processed via the RO system. The RO system operates at approximately 75% recovery, producing 4.5 MGD of permeate which accounts for approximately 65% of the City's current drinking water production. Permeate refers to the portion of the RO feed stream that passes through the membrane. Subsequently, concentrate refers to the membrane output stream that contains water that has not passed through the membrane and includes the concentrated constituents rejected by the membrane. The RO permeate is piped to the next unit operation where it is aerated through packed towers for degasification of hydrogen sulfide and carbon dioxide. Caustic soda is added to the permeate for pH adjustment and enters a wet well where it is blended with IX softened water and aerated Verna bypass water for stabilization and mineralization.

Water Plant Schematic
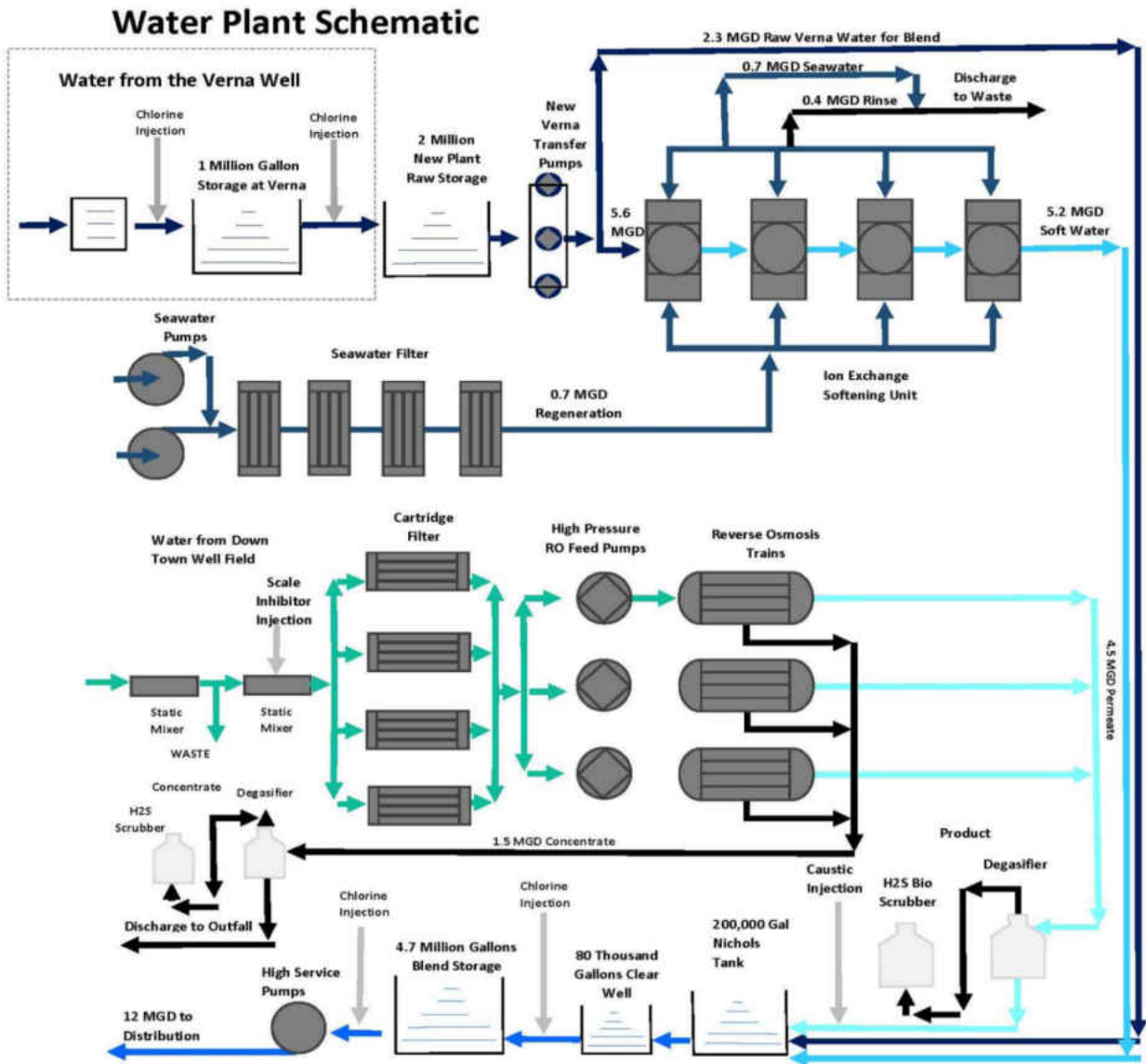
Figure 2-1: City of Sarasota WTF Schematic (Courtesy of City of Sarasota, FL)

The blended water is disinfected with chlorine and stored in an onsite ground storage reservoir until it is pumped to the distribution system. The RO concentrate is combined with the IX backwash water and discharged to a nearby deep well.

<div align="center">Verna Aerated Well Field</div>

The second water source the City utilizes is referred to as the Verna well field. The Verna groundwater contains elevated levels of hydrogen sulfide, hardness, and sulfate as seen from historical data found in Table 2-1 (Boyle Engineering Corporation, 1998; Tharamapalan, 2012b). Hydrogen sulfide is often identified as a rotten-egg odor or musty scent and is the most common odor problem in groundwater (White, 1999). Dockins and coworkers (1980) found the main source of hydrogen sulfide in groundwater is from the biological conversion of sulfate to sulfide. Hydrogen sulfide is often removed from ground water sources through aeration (Powell & von Lossberg, 1948) or oxidation using chlorine, hydrogen peroxide, potassium permanganate or ozone (Cadena & Peters, 1988). The City utilizes natural draft tray aeration for hydrogen sulfide removal although packed tower, spray tower, and cascade aerators are also common in Florida (Duranceau, Trupiano et al., 2010; Lovins & J., 2003). The tray aeration system located at the Verna well field simultaneously performs two main functions. The anoxic groundwater is oxygenated by gas adsorption while carbon dioxide and hydrogen sulfide are stripped from the groundwater (Powell et al., 1948). After aeration the Verna water is chlorinated for biological control and piped approximately 20 miles to the City's water treatment facility.

The aerated water is either treated using IX or bypassed and blended with the IX product water (Tharamapalan, Duranceau et al., 2011). Approximately 5.2 MGD of Verna groundwater is produced through the cation exchange process used for hardness control. The Verna water source

contains approximately 450 mg/L as CaCO$_3$ of hardness originating from the dissolution of underground rock formations such as calcite (CaCO$_3$), and dolomite (CaMg(CO$_3$)$_2$) (Macpherson, 2009). Water hardness is not a health concern, rather, it is an aesthetic concern. Hardness-causing ions are capable of reacting with soap to form precipitates, adversely affecting the soap-lathering process, and causing scaling in pipes and appurtenances (de França Doria, 2010).

Table 2-1: Historical Verna Water Quality

Parameter	Units	Historical Average
Alkalinity	mg/L as CaCO3	159
Bromide	mg/L	0.06
Calcium	mg/L	91
Chloride	mg/L	18
Conductivity	μS/cm	935
Color (True)	CPU	3.0
Magnesium	mg/L	135
Sulfate	mg/L	405
Sulfide	mg/L	6.2
TDS	mg/L	846
TOC	mg/L	2.00
UV-254	cm^{-1}	0.03

The IX system employed at the City's WTF utilizes a synthetic polystyrene cation resin to exchange sodium for calcium and magnesium ions. However the IX resin must be periodically regenerated and the selective nature of ion exchange resin hinders the simultaneous removal of cations, anions, and organics (Bergman, 1995). The RO permeate is blended with the IX effluent to dilute the sulfate and total dissolved solids (TDS) concentrations in the treated Verna water. However, by relying on blending for dilution, the ratio of Verna groundwater to RO permeate production is of significant concern relative to compliance with the National Secondary Drinking Water Regulations (NSDWR) for sulfate. Sulfate has a secondary maximum contaminant level (SMCL) of 250 mg/L under the Safe Water Drinking Act (SDWA), established for aesthetic effects

relating to taste and order. Therefore the flow and mass balance of the system must be monitored

to maximize production while meeting regulations regarding sulfate and TDS. Figure 2-2

summarizes the water quality of specific contaminants in the three blended streams.
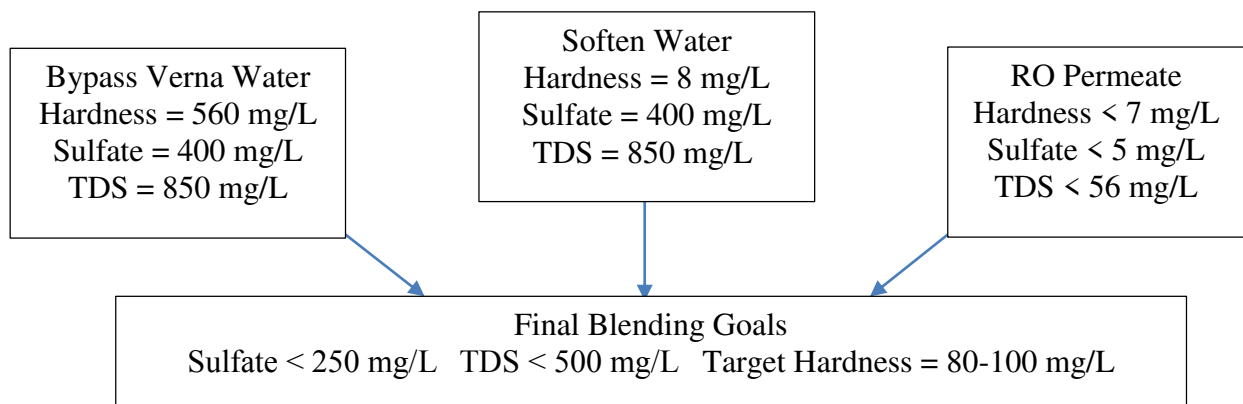
Figure 2-2: Blending Stream Concentrations for the City of Sarasota Utilities

<u>Current System Limitations and Concerns</u>

Currently the City uses approximately 37% of the allowance of the Verna ground water source due

to process limitations. An increase in the use of Verna groundwater would require more advanced

treatment in order for the plant to continue to reduce hardness and meet the NSDWRs for sulfate

and TDS (250 mg/L and 500 mg/L, respectively). Furthermore, the City has expressed concerns

regarding the ion-exchange water treatment process reliability. The City currently relies on filtered

seawater withdrawn from Sarasota Bay that is treated and used to regenerate the City's ion

exchange process. The dependency on the seawater intake system potentially places the City at

risk to a number of anthropogenic and natural environmental events that may render Sarasota Bay

unusable. Possible natural events affecting the reliability of the current ion exchange regeneration system include hurricanes and storm surge that could cause significant structural damage to the intake system in Sarasota Bay. Additionally, harmful algae blooms and red tide events are common in the Gulf of Mexico, and these events could cause a significant change in seawater quality. Anthropogenic disasters such as the Deep Water Horizon oil spill are of particular concern due to possible impact to Sarasota Bay and subsequent risks to the ion exchange regeneration process.

In order to utilize the allotted amount of Verna water and subsequently reduce reliance on Sarasota Bay, the City has considered NF membrane softening as a replacement for the existing cation exchange system. However, the aeration process at the Verna well field presents a challenge for successful implementation of traditional NF processes that rely on a spiral-wound configuration. The tray aerators located at the Verna well field provide optimal conditions for the growth of sulfur-oxidizing bacteria which thrive in transition zones where anoxic condition and aerobic conditions meet (Brigmon, Bitton et al., 1995). Incomplete oxidation of sulfate leads to the formation of colloidal sulfur which is problematic for filters and appurtenances downstream of the aeration process (Lyn & Taylor, 1992). The colloidal sulfur contributes to turbidity that contributes to the fouling of SWNF membranes without extensive pretreatment. Modifications to the City's tray aeration system was completed in 2012 which improved the sulfide removal by approximately 20%, but the formation of colloidal sulfur persists (Tharamapalan, 2012b). Previous pilot studies in Sarasota conducted by Tharamapalan and coworkers (2012b) demonstrated that to effectively process aerated Verna groundwater successfully to control sulfate requires a combination of sand filtration (SF), HFUF, and traditional SWNF. While Florida leads the industry in terms of installed SWNF capacity for groundwater treatment, the technology has not been successfully applied to the treatment of aerated water streams. This research was conducted in part, to assess the cost and

performance of an alternative HFNF membrane process for treatment of the City's Verna water supply. The HFNF membranes are anticipated to have the robustness of ultrafiltration and the mass transfer characteristics of nanofiltration which may prove to be more effective in treating the aerated groundwater supply than more traditional SWNF membrane technologies. An assessment of HFNF mass transfer to study solute rejection mechanisms based on solute-membrane interactions was also performed in this work.

3.   APPLICABLE LITERATURE

In this chapter, the literature related to pressure-driven membrane processes for drinking water treatment is reviewed. The literature review includes an overview of membrane characteristics, configuration, operation, fouling potential, hydraulic performance, and removal capabilities for low and high pressure membranes. Several mathematical modeling approaches are discussed for predicting membrane performance including size and diffusion based removal mechanisms. In addition, bench and pilot-scale membrane testing techniques as well as the application challenges associated with these methods are also included. The literature pertaining to the development and testing of HFNF membranes in laboratory and pilot settings is examined in this review.

Pressure-Driven Membrane Processes

The four main pressure-driven synthetic membrane processes for drinking water treatment include microfiltration (MF), ultrafiltration (UF), nanofiltration (NF), and reverse osmosis (RO). Membranes are classified by their removal capabilities and the mechanisms that drive the removal, however, the membrane design and configuration also plays a role when identifying membranes. Zhao and Taylor (2005) have reported that the generally accepted removal mechanism for MF and UF is size exclusion, whereas diffusion is the prevalent solute removal mechanism for NF and RO. Table 3-1 provides a summary of the conditions and characteristics of pressure-driven membrane processes, including typical operating pressures and targeted constituents.

Table 3-1: Characteristics of Pressure-Driven Membrane Processes (AWWA, 2007)

Membrane Technology	Operating Pressures	Minimum Approximate Particle Size Removed	Molecular Weight Cut-Off	Targeted Contaminants for Removal
MF	4-70 psi	0.1 μm	N/A	Particles, turbidity, bacteria & protozoa, coagulated organic matter, inorganic precipitates
UF	4-70 psi	0.01 μm	10,000 - 500,000 Da	Includes the above plus, viruses, organic macromolecules, colloids
NF	70-140 psi	0.001 μm	200 - 1,000 Da	Includes the above plus, hardness, color, DBP precursors, larger monovalent ions, pesticides.
RO	140-700 psi	0.0001μm	< 100 Da	Includes the above plus, monovalent ions.

Microfiltration & Ultrafiltration

MF and UF are low pressure driven membrane filtration techniques primarily used to remove particles and microorganisms by straining or size exclusion. The most common membrane configuration for MF and UF is hollow-fiber (Howe, Marwah et al., 2007). There are two different flow paths for HF membranes: flow can be from the inside-out, or from outside-in of the HF. In the case of outside-in flow direction, there is more flexibility in the amount of feed to flow across the hollow fibers, whereas the inside-out flow direction has to consider the pressure drop through the inner volume of the hollow fibers. Inside-out flow, however, offers much more uniform flow distribution through the lumen of HF compared to the outside-in flow as found by Xu and coworkers (2008); it is noted that the inside-out flow patterns are more susceptible to plugging (USEPA, 2005). The remaining discussion on low-pressure membranes is mainly focused on HFUF membranes as MF membranes were not evaluated in this research.

UF membranes can be operated in either cross-flow or dead-end filtration modes. In the case of cross-flow filtration, there are three streams, one inlet and two outlet streams referred to as the feed, filtrate, and retentate. In this process, the components in the water are separated by a semi-permeable membrane through application of pressure and flow parallel to the membrane surface. The cross-flow mode of filtration has a lower recovery rate compared to dead-end filtration (USEPA, 2005). In dead-end filtration, feed water is forced through the hollow fibers which capture and retain particles. Dead-end filtration involves one inlet and outlet stream resulting in 100% of the feed water passing through the fibers without a recycle stream. For dead-end filtration, periodic backwashes with filtrate water and/or cleaning chemicals are required to recover membrane productivity and prevent irreversible fouling.

Fouling of UF membranes can be caused by: (1) operation of membranes beyond a critical flux value (AWWA, 2005); (2) foulant compaction that reduces the effectiveness of backwashing (Smith, Vigneswaran et al., 2006); and (3) membrane material compatibility with feed water (Liu, Caothien et al., 2001). A UF system can be considered to be fouling if the operating parameters such as feed pressure, temperature and flow rates are held constant, but the flux rate or mass transfer coefficient (MTC) of water through the membrane is decreased (Cheryan, 1998). The flux rate and mass transfer coefficient can be calculated using Equations 3-2 through 3-3. Once a membrane experiences fouling, it is common to clean the membrane by performing a chemically enhanced backwash (CEB) or a clean in place (CIP) to restore hydraulic performance.

Hydraulic performance is determined by monitoring trends in the specific flux and transmembrane pressure (TMP). TMP is defined as the change in pressure from the feed to filtrate side of the membrane. For cross-flow applications, the TMP is calculated from the average of the feed and

retentate pressures minus the permeate pressure as shown in Equation 3-1 (Ahmad, Ismail et al., 2005). The water flux can be calculated by dividing the filtrate flow by the active membrane area as seen in Equation 3-2. In pressure-driven processes feed pumps are required to drive the water through the membrane process. The temperature of the water affects the permeate flow. The flux values can be normalized and corrected for temperature changes using a temperature correction factor (TCF) shown in Equation 3-3. Alternatively Equation 3-4 can be used to account for changes in TMP that are related to temperature changes that affect the viscosity of water rather than from fouling.

$$TMP = \Delta P = \left(\frac{P_F + P_C}{2} - P_P \right) \tag{3-1}$$

$$J_W = \frac{Q_P}{A} \tag{3-2}$$

$$K_W = \frac{J_W}{TMP \times TCF} \tag{3-3}$$

$$TMP_{(TC)} = TMP \times TCF \tag{3-4}$$

Where:
P_F = feed pressure (M/L^2)
P_C = retentate pressure (M/L^2)
P_P = filtrate pressure (M/L^2)
J_W = flux ($L^3/L^2 \cdot t$)
Q_P = filtrate flow rate (L^3/t)
A = membrane area (L^2)
K_w = specific water flux normalized at standard temperature 20 ˚C (t^{-1})
TMP = transmembrane pressure ($M//L^2$)
TCF = temperature correction (TC) factor (˚C)

The reporting standard for normalized temperature of water is 25 ℃ (ASTM, 2010), but the reference testing temperature in this study was set at 20 ℃ to be consistent with manufacturer specifications. There are two common methods for accounting for temperature variations and their effect on flux in pressure driven membranes including a theoretical method, and a membrane specific empirical method. A theoretical temperature correction factor (TCF) was derived from the Hagan-Poiseuille given in Equation 3-5, and the ratio given in Equation 3-6 (Cheryan, 1986).

$$J_W = \frac{\Delta P}{R_W} = \frac{\varepsilon r^2 \Delta P}{8 \delta \mu} \qquad (3\text{-}5)$$

$$TCF = \frac{J_{T°C}}{J_{25°C}} = \theta^{(T-25)} \qquad (3\text{-}6)$$

Assuming membrane surface porosity (ε), pore radius (r), viscosity (μ), and thickness (δ) are constant, Equation 3-5 can be substituted into Equation 3-6 and linearized. The resulting equation can then be solved by regression to yield Equation 3-7. This method has been simplified in some texts to be a value of 1.03 (ASTM, 2010; AWWA, 2011).

$$TCF = \frac{J_{T°C}}{J_{25°C}} = 1.026^{(T-25)} \qquad (3\text{-}7)$$

However, the theoretical method only accounts for the change in viscosity with temperature and assumes no change to the physical membrane. The second method for normalizing flux involves developing a statistical relationship using operational temperature and mass transfer coefficient data. Since the MTC is proportional to flux, it can be substituted into Equation 3-6 and linearized to yield Equation 3-8. This method is typically performed by the manufacturer using deionized-distilled water and assumes the membrane is effectively clean when collecting operational data. TCF determined in this way accounts for the temperature effects of both the membrane and the water.

$$log\left(\frac{J_{T°C}}{J_{25°C}}\right) = log\left(\frac{MTC_{25°C}}{MTC_{T°C}}\right) = (T-25)log\theta \qquad (3\text{-}8)$$

Safar and coworkers (1998) compared the temperature correction factors using the ASTM method membrane manufacturer's equation and found deviations between the two numbers as high as 22% in temperatures lower than 20 ºC. Their work emphasized the importance of using the manufacturer's recommended TCF. The manufacturer has specified the temperature correction factors for the membranes evaluated in this research to be calculated using Equations 3-9 and 3-10.

$$TCF_{(20°C)} = \frac{0.99712}{1.855 - 0.05596T + 0.0006533T^2} \qquad (3\text{-}9)$$

$$TCF_{(20°C)} = 0.002024 \times (42.5 + T)^{1.5} \qquad (3\text{-}10)$$

Much research has demonstrating the removal capabilities of MF and UF membranes. Hirata and Hashimoto (1998) demonstrated a > 7 log removal for C*ryptosporidium* oocyst using HFUF membranes. Jacangelo and coworkers (1995) found removals greater than 6.8 log for MS2 bacteriophage agreeing with earlier research conducted by Olivieri and coworkers (1991). Suspended solids, colloidal, and dissolved organic compounds can also be removed depending on their molecular mass and on the molecular mass cut-off of the membrane. UF membranes have pore size of approximately 0.01-0.05 µm in size and have a molecular weight cut-off of about 10,000-500,000 Daltons (AWWA, 2007; Simmons, Sobsey et al., 2001). These characteristics enable UF membranes to remove particulate matter, bacteria, viruses, and parasites including *Cryptosporidium* and *Giardia* (Jacangelo, Rhodes et al., 1997). In well-designed and operated systems, UF membranes can consistently produce filtered water with turbidity values below 0.05 Nephelometric turbidity units (NTU) (Duranceau & Taylor, 2011) and can result in SDI<1 (Solutions, 2010). MF and UF often operate at transmembrane pressures between 3-15 psi

(AWWA, 2005). However, UF membranes have historically not been designed to remove dissolved solids such as hardness but rather are implemented as a pretreatment step to NF or RO or as a replacement to media filtration in conventional treatment (Jacangelo et al., 1994).

Nanofiltration & Reverse Osmosis

The first RO desalination research in the United States was performed by Reid and Brenton at the University of Florida using cellulose acetate membranes (Reid & Breton, 1959). RO membranes became commercially viable due to the development of the asymmetric membrane in the early 1960s and have since been competing with electrodialysis for the removal of salts (Lonsdale, 1982; Stevens & Loeb, 1967). Softening membranes were first introduced in 1976 and marketed as RO softening membranes. The technology became more popular in the 1980s when FilmTec Corporation introduced spiral-wound thin film composite NF membrane elements as reported by Cadotte and coworkers (1988).

NF membranes are now used for a variety of applications including the removal of disinfection byproduct precursors and pesticides in drinking water. NF membranes often have a molecular weight cut-off between 200 and 1000 Daltons which enables NF membranes to target rejection of divalent ions (AWWA, 2011). Additionally, NF membranes are generally able to remove 95% of naturally occurring color and DBP precursors (Taylor, Mulford et al., 1989; Watson & Hornburg, 1989). Dissolved organic carbon with a molecular weight greater than 400, hardness ions, and limited monovalent ions can be removed by tight nanofiltration membranes (Hilal, Al-Zoubi et al., 2004). Spiral-wound RO and NF processes operate in cross-flow filtration where the feed water flows tangential to the membrane surface and produces two output streams.

Spiral-wound RO and NF membranes are designed to operate at a constant flux by increasing the feed pressure of the system. The operating pressure, TMP and salt rejection are monitored over time to assess membrane performance (Kucera, 2010). Eventually the membranes are cleaned or replaced by flowing chemicals through the membranes until membrane performance is restored. The calculations for RO and NF membranes regarding flux, specific flux, and TCF are similar to Equations 3-2 through 3-3 with the exception of Equation 3-1. The transmembrane pressure in RO and NF applications incorporates the osmotic pressure of the system using Equation 3-11 (Zhao & Taylor, 2005). The osmotic pressure for an incompressible solvent can be thermodynamically calculated using Equation 3-12 which considers the ideal gas constant (R_g), temperature (T), volume of solvent (V_A), and the vapor pressures in the dilute (P_A^0) and concentrated solutions (P_A).

$$\text{TMP} = \Delta\text{P-}\Delta\Pi \tag{3-11}$$

$$\Pi = \frac{R_g T}{V_A} \ln \frac{P_A^0}{P_A} \tag{3-12}$$

The osmotic pressure for dilute solutions can be related to the molar concentration of the dissolved substances (c) in the concentrated solution using van't Hoff relationship shown in Equation 3-13 (Sawyer, McCarty et al., 2003). Some membrane manufactures have developed empirical models which use feed water concentrations to estimate the osmotic pressure in RO systems but in general osmotic pressure of a brackish water can be estimated using Equation 3-14 (Weber, 1972).

$$\Pi = c R_g \text{T} \tag{3-13}$$

$$\Delta\Pi = \frac{1 psi}{100 mg/L} \left(\frac{C_f + C_c}{2} - C_p \right) \tag{3-14}$$

Where:
C_c = solute concentration in the concentrate stream (M/L^3)
C_f = solute concentration in the feed stream (M/L^3)
C_p = solute concentration in the permeate stream (M/L^3)

<u>Predicting Membrane Performance</u>

As membrane technologies grew in application over the last few decades, extensive research has been conducted to predict NF and RO membrane performance. As a result many theories and models were developed to describe the mass transfer of solvent and solutes through membranes.

Mass Transfer Coefficients

In membrane separation, mass transfer refers to the net movement of a constituent in a mixture from one region to another region of a different concentration across the membrane interface. The drinking water industry typically uses the symbol (K_w) to refer to the mass transfer coefficient (MTC) of solvent with the (w) term representing water. The solutes are often referred to using K_s since solute rejection can be applied to any number of contaminants. There are numerous factors affecting solute mass transfer including molecular weight, molecular size, acid disassociation constant, hydrophobicity, and hydrophilicity (Bellona, Drewes et al., 2004). The characteristics of the solvent also affect solute mass transfer as well as the properties of the membrane, such as molecular weight cut-off, pore size, surface charge, surface morphology and module geometry (Zhao, 2004). There are four common ways to obtain the mass transfer coefficients. MTCs can sometimes be obtained from literature sources or from the membrane manufacturer. Membrane manufacturers typically determine MTCs for a particular membrane by fitting experimental data to diffusion model equations. Lastly MTCs can be determined by empirical correlations expressed in terms of Schmidt, Reynolds, and Sherwood numbers. The Schmidt number is a dimensionless number of the ratio of momentum transfer to mass transfer given by Equation 3-15 (Cheryan, 1986).

$$Sc = \frac{\mu}{\rho D_0} \hspace{11cm} (3\text{-}15)$$

Where:
D_0 = diffusion coefficient (L²/t)
ρ = density of water (M/L³)
μ = kinematic viscosity of water (M/L•t)

Diffusion coefficients in liquids are difficult to measure accurately and much of the literature is limited to a temperature range between 0 ºC and 40 ºC. Furthermore ionic strength and pH of the solution can also effect diffusion coefficient values which cause difficulties when developing theories to estimate diffusivity. However, semi-theoretical and empirical correlations have been proposed for nonelectrolyte solutions including one developed by Wilke and Chang (1955) shown in Equation 3-16.

$$D = 7.4 \times 10^{-8} \left(\frac{(xMW)^{0.5}T}{\mu V^{0.6}} \right) \qquad (3\text{-}16)$$

Where:
x = association parameter (2.6 for water)
MW = molecular weight of solvent (M/mol) (18.8 g/gmol for water)
T = temperature (K)
μ = viscosity of solution (M/L•t)
V = molal volume of solute at normal boiling point (L³)

The diffusion coefficient of an electrolyte can be predicted at infinite dilution using the Equation 3-17 as given by the Nernst equation (Kuznetsova, 2007). The ionic conductance of common ions in infinite dilute aqueous solutions at 25 ºC can be found in the literature (Perry, Chilton et al., 1963).

$$D_i^o = \psi_i^0 \left(\frac{R_g T}{z_i F^2} \right) \qquad (3\text{-}17)$$

Where:
R_g = universal gas constant (8.314 J/ mol•K)
T = temperature (K)
F = Faraday number (96,000 coulombs)
ψ_i^0 = equivalent conductance of ion i (L/mol•ohm)
z_i = charge on ion i

The Reynolds number (Re) is a dimensionless quantity that represents the ratio of momentum forces to viscous forces. Reynolds numbers are characterized as laminar where viscous forces are dominant and turbulent where inertial forces dominate. Reynolds numbers less than 1800 reflect laminar flow conditions while Reynolds numbers greater than 4000 are considered turbulent flow conditions. The Reynolds number is calculated using Equation 3-18.

$$Re = \frac{d_h V \rho}{\mu} \tag{3-18}$$

Where:
d_h = hydraulic diameter (L)
V = fluid velocity (L/t)

The Sherwood number (Sh) is a dimensionless quantity of the ratio of convective mass transfer to molecular mass transfer which considers the boundary layer thickness (D_o) and the hydraulic diameter (d_h) of the channel using Equation 3-19 (Sourirajan & Kimura, 1967).

$$Sh = \frac{k d_h}{D_0} \tag{3-19}$$

It can be correlated to the Reynolds and Schmidt numbers by Equation 3-20 assuming the velocity profile if fully developed under laminar flow conditions and the concentration boundary layer is developing along the entire length of the channel (Sieder & Tate, 1936).

$$Sh = 0.664(Re)^{0.33}(Sc)^{0.33}\left(\frac{d_h}{L}\right)^{0.33} \tag{3-20}$$

Where:
L = length of the membrane (L)

The previously described method using empirical correlations and dimensional analysis can be used to estimate the mass transfer of the solute but typically under predicts the actual MTC. Dimensional analysis does not consider membrane properties or the effect of multi-solute solutions

on individual solute diffusivities. Therefore MTCs are often estimated using experimental data and mathematical models. The most common predictive models include the size exclusion model, the homogenous solution diffusion model, and the film theory model.

Size Exclusion Model

The size exclusion model is often used to describe the behavior of MF and UF membranes where solute rejection is independent of flux and recovery. The permeate concentration can be predicted by the size exclusion constant and Equation 3-22.

$$Rej = \frac{C_f - C_p}{C_f} \tag{3-21}$$

$$C_p = (1 - Rej)C_f = aC_f \tag{3-22}$$

Where:
Rej = rejection
C_p = solute concentration in the permeate stream (M/L^3)
C_f = solute concentration in the feed stream (M/L^3)

Homogenous Solution Diffusion Model

Mass transport through NF and RO processes have historically been described using the homogenous solution diffusion model (HSDM). The HSDM was the first model developed for high recovery RO and NF systems (Lonsdale, Merten et al., 1965). The model is developed using fundamental mass balance equations considering a single membrane element while assuming the mass transfer of water and solutes occur due to pressure and concentration gradients, respectively. A diagram of a single membrane element has been provided in Figure 3-1. The diagram illustrates the flows, solute concentrations, and pressures of the raw, feed, recycle, concentrate and permeate streams of a single membrane element.
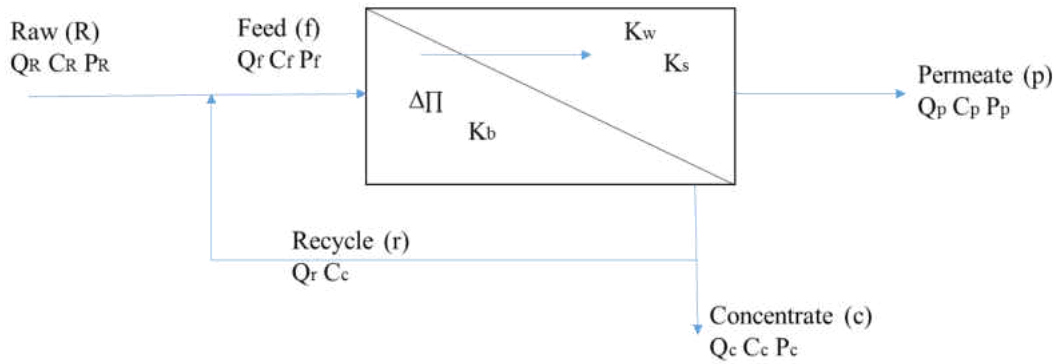
Figure 3-1: Mass Balance Single Element Membrane Diagram

Assuming recycle is not implemented, Equation 3-23 and Equation 3-24 can be derived from a mass balance around the membrane illustrated in Figure 3-1. Recovery is defined as the ratio of the permeate flow to the feed flow and is calculated using Equation 3-25. Typical RO processes treating seawater or hard colored ground water can achieve recoveries of 50% to 90%, respectively. Recoveries for MF or UF systems are often greater than 90% (Nakatsuka, Nakate et al., 1996).

$$Q_f = Q_c + Q_p \qquad \text{(3-23)}$$

$$Q_f C_f = Q_c C_c + Q_p C_p \qquad \text{(3-24)}$$

$$R = \frac{Q_p}{Q_f} \qquad \text{(3-25)}$$

The water flux is related to the pressure differential across the membrane by the mass transfer coefficient of water. Equation 3-26 describes the water flux through a membrane accounting for the change in osmotic pressure.

$$J_w = K_w(\Delta P - \Delta \Pi) = \frac{Q_p}{A} \qquad \text{(3-26)}$$

Where,
J_w = flux of water through the membrane ($L^3/L^2 \cdot t$)
K_w = mass transfer coefficient of water (L/t)
ΔP = transmembrane pressure (M/L^2)
$\Delta \Pi$ = transmembrane osmotic pressure (M/L^2)
A = membrane area (L^2)
Q = flow (L^3/t)
Subscripts f, c, p = feed, concentrate, permeate

Solute transport in the HDSM is driven by the difference in concentration gradient between the feed and permeate sides of the membrane and is calculated using Equation 3-27 (Ozaki, Sharma et al., 2002). The solute mass transfer coefficient is typically assumed to be constant in linear models despite the non-linear behavior of the variable which is due to varying influent water quality, operating conditions, and membrane properties (Zhao, Taylor et al., 2005).

$$J_s = K_s(\Delta C) = \frac{Q_p C_p}{A} \qquad (3\text{-}27)$$

Where,
J_s = mass flux of solute ($M/L^2 \cdot t$)
K_s = solute mass transfer coefficient (L/t)
$\Delta C = 0.5(C_f + C_c) - C_p$ (M/L^3)
C = concentration (M/L^3)

The HSDM is developed by algebraic manipulation of Equations 3-24 through 3-27 and often rearranged to express solute flux in terms of recovery as seen in Equation 3-28 (Duranceau, 1990). The HSDM illustrates the effect of feed concentration, membrane characteristics, recovery, and operational parameters to predict permeate quality. However, the model does not account for certain physical and chemical constraints and makes some simplifying assumptions common in linear and film theory models (AWWA, 2007; Zhao, Taylor, et al., 2005).

$$C_p = \frac{C_f K_s}{K_w(\Delta P - \Delta \Pi)\left(\frac{2-2R}{2-R}\right) + K_s} \qquad (3\text{-}28)$$

If a recycle stream is utilized within the system as used in many laboratory apparatuses the recycle stream can be accounted for using the recycle ratio (r). The recycle ratio is defined as the flow of the recycle stream divided by the flow of the feed stream and it has been incorporated into the HSDM in Equation 3-29.

$$C_p = \frac{C_f K_s}{K_W(\Delta P - \Delta \Pi)\left(\frac{(1+r)(2-2R)}{2+2r-R}\right)\left(\frac{2-2R}{2-R}\right) + K_s} \tag{3-29}$$

Film Theory Model and HSDM-FT

Another common method for modeling solute mass transfer considers the increased concentration of solutes at the membrane-liquid interface referred to as concentration polarization. Solutes and solvent are brought to the membrane surface by convective transport as described by Equation 3-30. As the solvent passes through the membrane, the concentration of the solutes increases near the membrane surface resulting in a concentration gradient. The concentration gradient causes diffusional mass transport to occur in the reverse direction toward the bulk solution. The rate of solute transport from the surface to the bulk solution can be described using Equation 3-31 if axial concentrations are neglected.

$$J_s = J_W C_b \tag{3-30}$$

$$J_s = -D_s \frac{dC}{dx} \tag{3-31}$$

The film theory model has been depicted in Figure 3-2 and can be described by the mass balance shown in Equation 3-32 which assumes the solute flux is constant through the film and membrane under steady state conditions. Integration of Equation 3-32 over the film boundary conditions yields Equation 3-33.
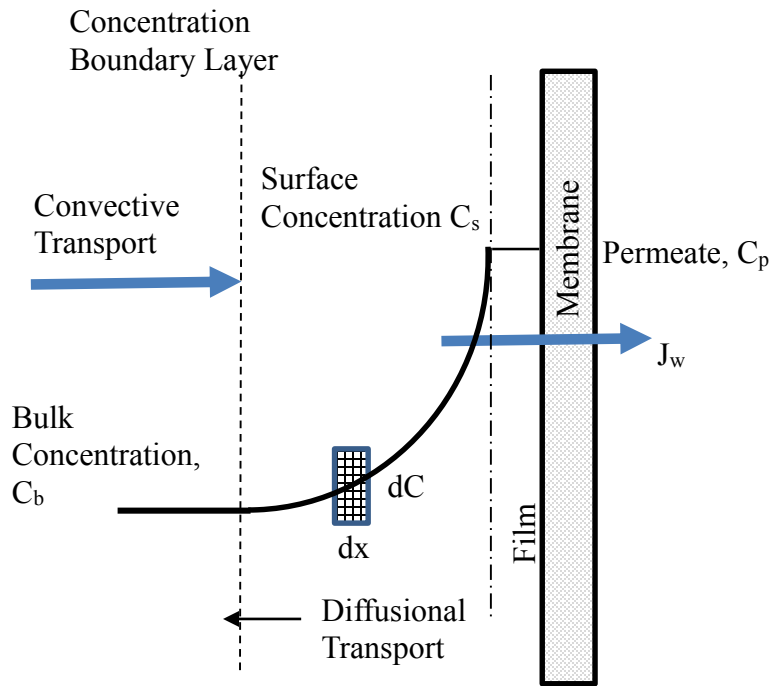
Figure 3-2: Mass Balance Film Theory Diagram

$$J_i = -D_s \frac{dC}{dx} + J_W C_i \qquad\qquad (3\text{-}32)$$

$$\frac{C_s - C_p}{C_b - C_p} = e^{J_w/k_b} \qquad\qquad (3\text{-}33)$$

Where:
J_i = flux of solute I
D_s = diffusivity
x = film thickness (L)
C_i = solute concentration from the bulk to the membrane surface (M/L^3)
C_b = solute concentration in the bulk solution (M/L^3)
$k_b = D_s/x$ diffusion coefficient from the surface to the bulk solution (L/t)
C_s = solute concentration at the surface of the membrane (M/L^3)
C_p = solute concentration in the permeate stream (M/L^3)

The film theory model does not account for pressure and therefore its validity is limited to systems operating a flux in a pressure independent system (Cheryan, 1986). Sung (1993) modified the HSDM to account for concentration polarization by incorporating the film theory model (HSDM-FT) shown in Equation 3-34. This model has been used by a number of researchers including (Zhao, Taylor, et al., 2005) and Cussler (2009). The HSDM-FT can also account for a recycle stream by using Equation 3-35.

$$C_p = \frac{C_f K_s e^{J_w/k_b}}{K_w(\Delta P - \Delta \Pi)\left(\frac{2-2R}{2-R}\right) + K_s e^{J_w/k_b}} \tag{3-34}$$

$$C_p = \frac{C_f K_s e^{J_w/k_b}}{K_w(\Delta P - \Delta \Pi)\left(\frac{(1+r)(2-2R)}{2+2r-R}\right)\left(\frac{2-2R}{2-R}\right) + K_s e^{J_w/k_b}} \tag{3-35}$$

The previously discussed models attempt to describe the rejection mechanisms of membrane systems but the factors affecting rejection remain complex and not fully understood. Therefore, it is typically recommended that significant testing of membranes is conducted through bench and pilot-scale application before implementing a full-scale design.

<u>Membrane Testing & Application Challenges</u>

Batch bench-scale simulations are typically used to test multiple membrane types, determine membrane rejection characteristics, and select a membrane for pilot testing (Cissé, Vaillant et al., 2011; Comerton, Andrews et al., 2008; Ladner, Subramani et al., 2010). Rapid bench scale membrane tests (RBSMT) can be used to simulate a differential element of a full scale SW membrane module (Westrick & Allgeier, 1996). Tests are conducted using a flat sheet of membrane placed within a flow cell equipped with a mesh feed spacer. The water flows tangential to the membrane producing a permeate and concentrate stream. RBSMTs can be conducted off-

site through batch experiments using small volumes of water (< 200 liters). The tests can be used to evaluate the impact of recovery, pressure, and crossflow velocity for several membranes quickly and at a low cost. Single element bench scale tests (SEBST) are typically performed over longer periods of time (up to 1 year) and offer more information than RBSMTs with regards to hydraulic performance (Xu, Drewes et al., 2008). SEBSTs utilize a standard 4" by 40" single membrane element operated in continuous flow mode to test membrane performance. SEBSTs can be used to test HF and SW membrane configurations but due to continuous flow requirements the tests must be conducted on-site. While SEBSTs provide more information than RBSMTs the procedure does not serve as a replacement to pilot testing as this technique does not provide sufficient data for full scale plant design. Pilot-scale systems are typically comprised of multiple staged full-scale membrane elements operated continuously over a period of one year. Although the pilot scale systems can be costly they provide the most accurate operational data with regards to TMP, flux and permeability. Pilot systems can also be operated over longer periods of time to assess pretreatment requirements, seasonal effects and the fouling potential for the full-scale membrane process.

Fouling on spiral-wound RO and NF generally occurs via a number of mechanisms including (1) scale deposits due to the precipitation of soluble salts (Hasson, Drak et al., 2001) (2) the presence of excessive biological growth (Ridgway, Justice et al., 1984) (3) membrane interaction with organics and (4) deposition of particulate and colloidal matter. Semiat and colleagues (2003) found scaling can be controlled with the addition of acid or scale inhibitors. Biological, organic and particulate fouling is often addressed by instituting advanced pretreatment such as conventional media filtration, HFMF or HFUF as discussed by Vrouwenvelder and van der Kooij (2001).

The operating pressures of NF and RO membranes range from 70 -140 psi and 140-700 psi, respectively (Younos & Tulou, 2005). The SW configuration of NF and RO membranes are less resilient to particulate matter and require advanced pretreatment to prevent fouling. Previous research found treatment of aerated groundwater with high sulfate levels using SWNF was only feasible with SF-UF pretreatment (Tharamapalan, 2012b). While HF configurations are common for both RO and UF applications, HFNF membranes have not been extensively researched nor produced on a pilot scale. Newer technology has led to advancements in membrane development causing a cross between HFUF and hollow fine fiber RO processes.

<div align="center">Hollow-Fiber Nanofiltration Membrane Technology</div>

The most prevalent RO membrane configurations are spiral-wound (SW) elements (AWWA, 2007) but hollow fine fiber elements have been used for treating seawater and have shown higher salt rejection at the cost of higher operating pressures (Teuler, Glucina et al., 1999). The application of NF membranes has typically been limited to high-pressure SW configurations. This configuration typically has a lower capital cost relative to HF membranes. However, compared to HF membranes, SWNF membranes are more prone to fouling, more difficult to clean, and often require advanced pretreatment when treating water containing colloidal and particular matter (Sethi et al., 2000).

A technological "gap" currently exists in membrane technology in that the removal of dissolved multi-valent ions is currently limited to high-pressure SWNF membranes. A low-pressure HF membrane that is capable of softening could prove useful to the drinking water industry. For example, this type of configuration may allow the City to treat Verna groundwater without the need for extensive pretreatment that is currently required for a SW application.

Sethi and Wiesner (2000) conducted modeling to investigate the different conditions under which the HFNF configuration or HFUF and SWNF configuration would be the optimal selection for cost-effectiveness. Their study was conducted by modeling the operation of both a HFNF and a HFUF-SWNF application. The model parameters were estimated using operational data collected from a HFNF pilot conducted in previous research by Jacangelo and colleagues (1994). At the time of the study the cost difference between a HFNF application and a HFUF-SWNF application made the HFUF-SWNF more economical for large scale implementation. However, additional research and development of HFNF has continued over the past decade and the parameters used in this modeling effort may no longer be valid.

Kiso and researchers (2002) tested a HFNF for rejection of pesticides. The HFNF used in their study (referred to as HFNF-1) was a composite membrane with polyamide skin layer and polysulfone (PSF) support layer. The HFNF-1 demonstrated a salt rejection of 35% and a $MgSO_4$ rejection of 93% at 0.5 MPa. Their work investigated the rejection properties of HFNF using hydrophilic compounds that do not adsorb to the membrane material and are often used to evaluate if a membrane rejects solutes through size exclusion. The results of their study indicated that rejection was highly correlated to molecular weight and molecular width. Adsorption of pesticides on the membrane surface was controlled by the hydrophobicity (log P) of the solute. In their work the effects of concentration polarization were not considered.

Darvishmanesh and coworkers (2011) prepared and characterized a polyphenylsulfone (PPSU) HFNF for organic solvent removal. PPSU has better solvent resistance than polyethersulfone (PES) or PSF. He and researchers (2008) developed a new type of HFNF membrane by dip coating a PES support membrane with a sulfonated poly ether keytone (SPEEK) layer. Rejection was

characterized with dextran mixtures and various salt solutions. Salt transport was modeled using the Donnan Steric Pore Model. These examples of HFNF research describe efforts to characterize HFNF membranes through a variety of fashions. However, few researchers have attempted to model HFNF rejection and transport of dissolved salts under purely diffusion-control principles historically applied to SWNF.

The three HFNF membranes under investigation in this study have been designed to be oxidant tolerant HF membranes that can achieve varying removals of color, hardness, and organics retention. However, the rejection capabilities, transport mechanism, and system configuration are untested. Literature does not describe a model that is applicable to water treatment using HF membranes for diffusion-controlled rejection of dissolved constituents. Such a model would be necessary for industry consideration of HFNF membrane technology. This research was conducted to characterize and model HFNF membranes and investigate how the technology could be applied to treatment of aerated sulfide-containing ground water supplies.

4. METHODS AND MATERIALS

This chapter provides a description of the equipment, materials, and experimental procedures used throughout this research. Accomplishing the objectives of this research required the planning, design, construction, and operation of four treatment systems.

1. The first system included the development of a bench-scale HFNF membrane testing apparatus, constructed to characterize and model three next generation HFNF membranes. The experiments using this system were conducted within University of Central Florida's (UCF) laboratories under controlled conditions using synthetic solutions.

2. The second treatment system incorporated a bench-scale parallel sand filtration (SF) unit, installed at the City's WTF. The SF unit served to pretreat aerated groundwater before conducting bench-scale HFNF membrane tests in the UCF laboratories. These studies were conducted to assess the performance of the HFNF membranes on aerated groundwater with regards to water quality.

3. The third treatment system was a HFNF pilot system that utilized a full-scale membrane module for treating the City's aerated Verna water supply at the City's drinking WTF. This system was used to assess water quality, hydraulic operating conditions, and pretreatment requirements of the HFNF membrane.

4. The fourth treatment system included an integrated SF-HFNF-SWNF membrane pilot used for treating the City's aerated groundwater supply. This system was tested to provide a benchmark for comparing the performance of traditional SWNF with next generation HFNF membranes.

A discussion of laboratory and field analyses is presented for reference purposes. Additionally a summary of the quality control procedures including accuracy and precision are reviewed in this chapter.

<u>Bench-Scale Equipment, Materials & Procedures</u>

Bench-Scale Membrane Testing Equipment

Three next generation HFNF membranes, referred to as membranes A, B, and C, were investigated at the bench-scale in a laboratory setting. The fibers for membranes A, B, and C are chemically resistant to chlorine and can be operated over a wide pH range, from pH 2 to pH 11. Membranes A and B are not yet commercially available but are expected to meet the performance of membrane C while also providing additional TOC and divalent ion rejection as specified in Table 4-1. Membrane C is commercially available and was designed to remove particulate matter, colloids, bacteria, viruses, color, and dissolved organics. Membrane C has a molecular weight cut off (MWCO) of 1000 Daltons with an expected TOC removal of approximately 90%. It is capable of producing a consistent permeate turbidity of less than 0.1 NTU. The manufacturer specified a 4-log virus retention and 6-log bacteria retention, viable for treating sources of drinking water.

Table 4-1: Membrane Characteristics

Membrane	MWCO (Daltons)	TOC Rejection %	Divalent Ion Rejection %	Commercially Available
A	500	95 - 99	50 - 85	No
B	700	93 - 97	30 - 60	No
C	1000	80 - 95	< 30	Yes

The membranes were designed to operate inside-out with cross-flow filtration allowing for backwash capability and lower power consumption as compared to traditional SWNF membranes (USEPA, 2005). The membrane manufacturer recommends operating with cross-flow velocities between 0.7 and 6.5 ft/s (0.2 and 2.0 m/s) with 1.6 ft/s (0.5 m/s) for optimal performance. While the membranes were capable of operating at flux values between 6 and 15 gfd (10 and 25 lmh) the manufacturer suggested operating the flux between 9 and 12 gfd (15 and 20 lmh). In comparison, typical spiral-wound nanofiltration membranes operate at 18 gfd (30 lmh) (USEPA, 2005). The membrane lumens exhibit inner diameters of 0.03 in (0.8 mm), significantly larger than that of hollow fine reverse osmosis fibers which have inner diameters of 0.003 in (0.08 mm) (Wilf, Awerbuch et al., 2007). The miniature modules are comprised of 120 fibers and have an active length of 0.82 ft (0.25 m). Each membrane module area is 0.812 ft^2 (0.0754 m^2). The resin thickness is 0.082 ft (0.025 m). Each module was tested in the laboratory using the bench-scale system shown in Figure 4-1.
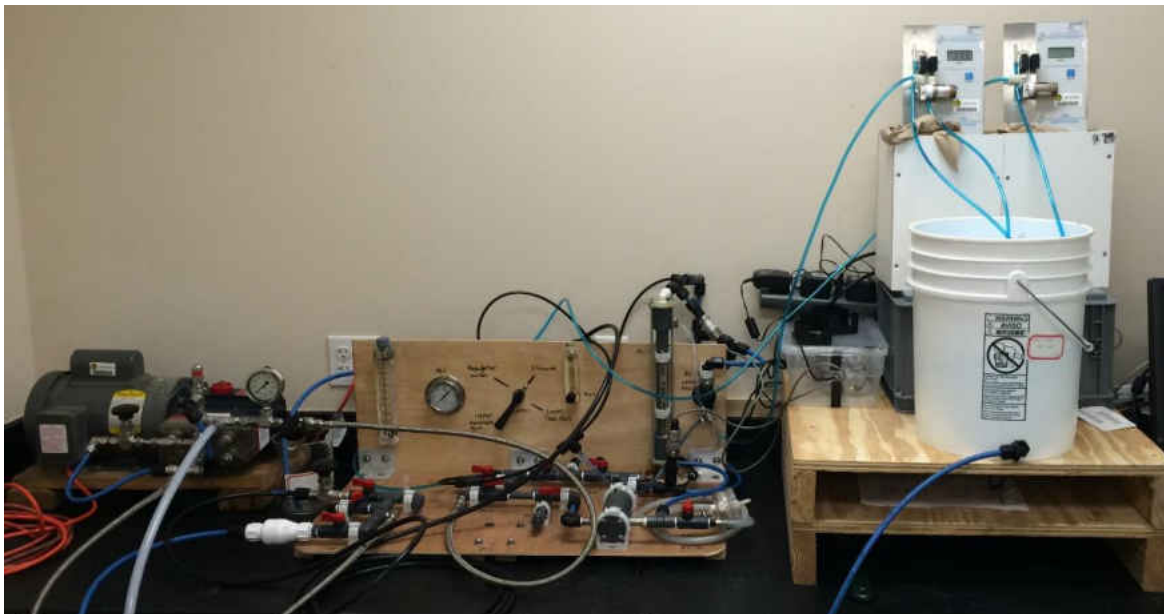
Figure 4-1: Photograph of Bench-scale Membrane Testing Equipment

This bench-scale system utilized a 5 gallon feed tank, a 0-160 psi feed McDaniel pressure gauge (Boutte, LA), a 0-30 psi permeate McDaniel pressure gauge (Boutte, LA), a 0-2 gpm King flow meter (Garden Grove, CA), two Omega pressure transducers (Stamford, CT), one Omega thermocouple (Stamford, CT), one electronic McMillan flow meters (Georgetown, TX), two Optiflow 1000 Agilent Technologies bubble flowmeters (Palo Alto, CA), and a Hydracell constant flow diaphragm feed pump (Minneapolis, MN) with motor as shown in Figure 4-2. The feed pump required power requirements included 110 V and 60 Hz. The maximum flow capacity was 1.8 gpm. Ball valves with 150 psi pressure rating and ¾" schedule 80 polyvinyl chloride (PVC) piping were used under pressurized appurtenances. Plastic tubing was also used for piping where pressures were below 5 psi (such as in the permeate stream). Swagelok (Solon, OH) needle valves were used to adjust and fine-tune flows. A data acquisition system was used to record feed pressure, concentrate pressure, feed temperature, and permeate flow 4 times per minute during experimental test runs. Recycle and concentrate flows were recorded manually.
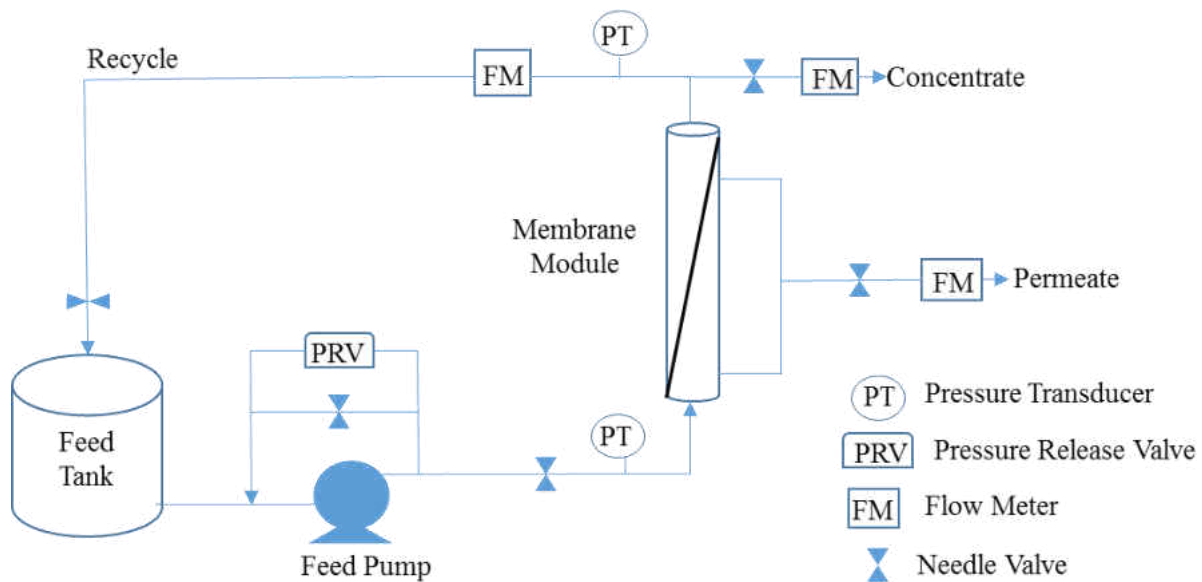
Figure 4-2: Process Flow Diagram of Membrane Testing Equipment

Five synthetic water solutions and an aerated groundwater of known water quality were prepared or collected for bench-scale membrane testing. The first solution was composed of magnesium sulfate ($MgSO_4$) dissolved into deionized water to create a 5 mM synthetic blend as suggested by the membrane manufacturer. This solution was used to assess the divalent ion removal capabilities of each membrane. The second and third solutions were composed of 8 mM and 2 mM $MgSO_4$, respectively, and were used to determine if varying the concentration of the compound effected removal. These concentrations were chosen to represent waters as very hard and soft water, respectively, as described by Briggs and Ficke (1977) and provided in Table 4-2.

Table 4-2: General Hardness Classification of Waters

Degree of Hardness	mg/L as $CaCO_3$
Soft	0-60
Moderately Hard	61-120
Hard	121-180
Very Hard	> 180

The fourth and fifth synthetic solutions were used to assess the effect that varying ionic strength had on membrane performance. Maung and Song (2009) found the removal efficiency of diffusion controlled membranes are not only affected by pH, temperature, system hydraulics, and water quality, but also ionic strength. The ionic strength of the solution has significant impact on mass transfer and membrane stability. In coastal states, such as Florida and California, drinking water demand is often met by using brackish ground waters supplies (Dykes & Conlon, 1989). Membrane performance, with regards to ionic strength, becomes relevant for regions where ground water has an elevated level of TDS. To assess the impact of salinity on HFNF performance, solutions four and five were prepared. These solutions comprised of a mixture of 5 mM $MgSO4$ and varying concentrations of sodium chloride (NaCl) as described in Table 4-3.

35

Table 4-3: Testing Solutions Summary

Solution	MgSO$_4$•7H$_2$O Concentration mg/L (mM)	NaCl Concentration mg/L (mM)	TDS (mg/L)	Ionic Strength (IS)	Hardness Class
Deionized Water	<1 (<1)	<1 (<1)	<1	N/A	N/A
Solution 1	600 (5)	<1 (<1)	700	0.023	Hard
Solution 2	960 (8)	<1 (<1)	960	0.032	Very Hard
Solution 3	240 (2)	<1 (<1)	260	0.009	Soft
Solution 4	600 (5)	730 (12.5)	1,200	0.030	Hard
Solution 5	600 (5)	2,340 (40)	2,600	0.054	Hard
Filtered Verna	n/a	n/a	≈800	≈0.020	Hard

Bench-Scale Parallel Sand Filtration Equipment

The sixth solution used during bench-scale membrane testing was filtered aerated groundwater sampled from the City's Verna well field. The sample was pre-filtered through the bench-scale parallel SF apparatus shown in Figure 4-3. The SF unit utilized two 35" tall high density polyethylene pressure vessels (PV) each having a diameter of 6 inches. Piping and appurtenances were composed of 3/4" schedule 80 PVC. The pressure vessels were rated for a maximum pressure of 150 psi within a temperature range of 1 to 49 °C. Each vessel was filled with 4inches of 1/8"-1/4" gravel as a support layer and topped with 18" of silica sand. PV1 housed fine sand (0.45 to 0.55 mm) and PV2 housed course sand (0.65 to 0.75 mm). Each vessel was equipped with a 0 to 30 psi pressure gauge on the feed side of the filter for monitoring head loss and calculating energy requirements. Prior to the startup of the SF pilot, each media was prepared by rinsing the sand with chlorine to inactivate bacteria and disinfect the media. Standard American Association of State Highway and Transportation Officials (ASASHTO) sieves (No. 18 and No. 25) were used to achieve the proper particle size for pressure filter (PV) 1 and 2, respectively. After the media was prepared, it was transferred into the pressure vessels.

Figure 4-3: Bench-Scale Parallel Sand Filtration Unit

Each pressure vessel was rinsed and backwashed for a minimum of three cycles before initial startup of the sand filter commenced. Flows were tested between 0.4 and 0.75 gpm, to attain filtration rates of approximately 2 and 4 gpm/sf. Feed pressures were monitored for estimating energy requirements and determining backwash requirements. A two-step backwash was necessary to clean the filters and restore filter productivity. Low flow backwashes (5 gpm) were conducted using City-treated finished water to control biological growth and high flow backwashes (10 gpm) using aerated Verna water were conducted to reach an approximate bed expansion of 40%. Typical backwash durations were between 5 and 30 min until turbidity values of the effluent water reflected the influent water. Following backwashes the system was operated in forward filtration for a minimum of 30 min before conducting filtration tests to determine fouling indices. Sample locations for the aerated raw Verna water and the filtrate water are illustrated in Figure 4-4. Turbidity analysis was conducted daily to estimate fouling potential of the filtrated water. The least fouling filtrate stream was used for bench-scale membrane testing.
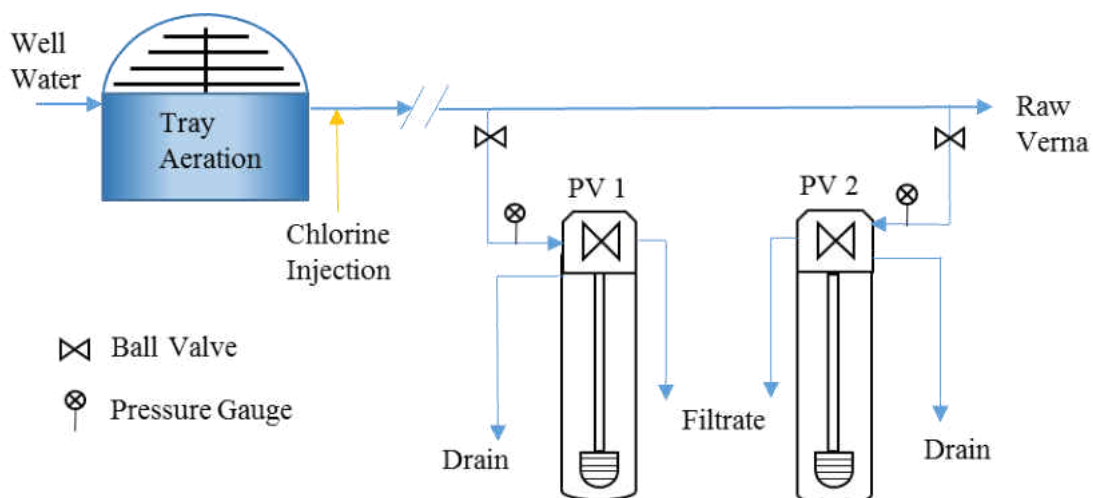
Figure 4-4: Process Flow Diagram of Parallel Sand Filter Pilot

Model development and membrane characterization for predicting solute mass transfer required varying the operational conditions and solute concentrations for multiple bench-scale membrane tests. This required conducting controlled experiments at three water flux settings, three recovery settings, and using multiple testing solutions for each membrane. The nomenclature used to describe a particular target flux with a particular membrane recovery using a specific testing solution is herein referred to as a retention test.

The membranes were stored at room temperature per manufacturer's specifications until bench-scale experiments were conducted. The feed solutions were created at least one day prior to membrane testing to allow the solid chemicals (i.e. $MgSO_4$ and NaCl) to dissolve completely. Each membrane module was installed onto the unit and flushed with deionized water until the system was free of air bubbles. Initial permeability tests were conducted prior to testing synthetic blends. Permeability tests were conducted at 50% recovery with a flux setting of 12 gfd (20 lmh) using deionized water. After a 15 minute (min) stabilization period, the data logger was used to record the pressures and flows of the system which were then used to calculate the membrane

permeability. Permeability tests were performed for each membrane before and after testing solutions 1 to 5 to monitor fouling or fiber breakage. Each retention test was conducted using a five-step procedure:

1. The feed tank was filled with the desired testing solution. Initial flushing of the system was conducted for a minimum of 15 minutes (solution was wasted before recycling to feed bucket).

2. Targeted flux and recovery were set by adjusting ball and needle valves to the desired settings.

3. The bench-scale system was operated for an additional 15 minute stabilization period.

4. Computer software () was turned on to initiate data recording for the feed and concentrate pressures and flows, as well as the feed temperature.

5. A total of five samples for the concentrate and permeate were continuously collected during each retention test. In addition initial and final feed samples were collected for each retention test.

The procedure was repeated for each retention test. Temperature and conductivity were measured upon collection. Sample preparation for sulfate and magnesium analysis was conducted within four days of collection and analyzed within the proper holding time as specified in the standard methods. Additional analysis for alkalinity, chloride, potassium, silica, sodium, total dissolved solid, total suspended solids and turbidity were conducted for applicable retentions tests such as when testing filtered Verna groundwater. At the conclusion of the research, additional testing was conducted by the membrane manufacturer to confirm estimated permeability and magnesium sulfate rejection.

Pilot-Scale Equipment and Procedures

HFNF Membrane Pilot System

The HFNF pilot was installed at the City's WTF located in Sarasota FL for treatment of the Verna groundwater supply discussed in Chapter 2 of this document. The HFNF membrane pilot equipment was provided by Pentair X-Flow (Pentair) (Enschde, Netherlands) and incorporated one pre-assembled filtration unit, consisting of a feed pump, a strainer, one membrane module, and an electrical cabinet. PVC piping and additional appurtenances such as pressure gauges, flow valves, and flow meters were included in the system. The power requirements of the system required 230 V, 50 Hz, and 25 A and consumed an average of 2.95 kW. The process requirements for the system were designed to operate under the conditions listed herein: operating pressures between 0-95 psi (0-6.5 bar); operating ambient temperature between 0 and 40 ℃, acidity of the medium between 3 and 11 pH units, and a flow rate of 2.64 gpm (0.6 m^3/hr) (Pentair, 2011). The membrane module was equipped with Pentair's HFW1000 membrane, referring to a hollow fiber membrane with a molecular weight cut off of 1000 Daltons. The membrane is hydrophilic and composed of PES/modified PES. HFW1000 lumens have hydraulic diameters of 0.8 mm contributing to a total membrane area of 430 ft^2 (40 m^2). The membranes are chlorine tolerant and designed for organics retention, turbidity removal, and 4-log reduction of viruses.

A portion of testing the HFNF membrane pilot required the use of a media filter for pretreatment. The media filtration system utilized in the HFNF and SWNF membrane pilot studies used a filament-wound fiberglass filter with a 56" sidewall length and 30" diameter. The media filter housed 12" of 1/8"-1/4" gravel and 33" of 0.45 to 0.55 mm fine silica sand. The sand filter was operated in declining rate down-flow filtration using the pressure head (approximately 20 psi)

available in the Verna pipeline due to the elevation difference of the Verna wellfield and the City's downtown WTF. The SF pilot and HFNF membrane pilot are shown in Figure 4-5. Originally the HFNF pilot system was designed to operate at a constant flux of 9 gfd (15 lmh) and a 50% recovery by providing backpressure on the permeate stream to maintain the recovery. However, in order to conduct an analysis on the hydraulic performance of the pilot, a system with variable parameters was required. This was accomplished by retrofitting the pilot provided by Pentair with flow and pressure appurtenances. The pilot retrofit performed by Harn-R/O Systems (Harn) (Venice, FL) allowed for the recovery to be altered and the backpressure decreased to better represent the implementation of a full-scale system. The HFNF pilot modifications increased the functionality of the unit by: installing flow meters to visually measure the filtrate, concentrate, and recycle flows; installing sample ports for filtrate, concentrate, and recycle streams; allowing for adjustments in the filtrate, concentrate, and feed flows; lowering system pressure while maintaining flows by decreasing filtrate backpressure and feed pressure (Pentair, 2011).

Figure 4-5: SF Pilot (featured left) and HFNF Pilot (featured right)

The pilot unit included multiple data transmitters which were used to monitor the permeate flow, temperature, and permeate, feed, and concentrate pressures. The data from the transmitters were logged using a data acquisition system, set to record information on five-minute intervals accessible remotely on the manufacturer's server. This data was analyzed to determine the flux, specific flux, and transmembrane pressure for the assessment of membrane productivity, rejection, and solute accumulation (inorganic, organic and biological) over time. The formulas and equations used to determine hydraulic parameters were previously discussed in Chapter 3. Additionally, example calculations are provided in Appendix B of this document.

The HFNF membrane pilot was tested at multiple settings to determine feed pressure requirements, operating flux values, and pretreatment requirements. Each setting was tested for a duration lasting a minimum of two weeks. Tharamapalan (2012b) observed rapid membrane fouling without the integration of SF-HFUF and cartridge filter (CF) pretreatment. Therefore SF was implemented as a pretreatment process for the initial operation of the HFNF pilot system. The sand filter was bypassed for the last 600 hours of operation to determine membrane performance without SF pretreatment. Performance was determined at each setting by monitoring the stability of hydraulic conditions such as specific flux and TMP as well as monitoring water quality.

According to Boyd (2013), at minimum, a typical pilot-scale water quality monitoring plan should include the collection of pH, temperature, conductivity, TSS, TDS, turbidity, alkalinity and TOC data. Consequently, additional water quality parameters were monitored and recorded at the time of sampling for each sample location including pH, temperature, conductivity, turbidity, and alkalinity. Hydraulic parameters that included temperature, flows, and pressures were manually recorded three times a day to provide a quality control check of the electronic pilot data logger.

Bucket tests were required for the initial startup, until the flow meters were installed on the pilot unit. Pressures were recorded directly from the pressure gauges on the pilot unit. Table 4-4 lists the location and frequency of each analysis performed throughout the study. An example of a daily field sampling sheet has been provided in Appendix C. Water quality assessments were conducted at each setting by monitoring the mass transfer of hardness ions, sulfate, and TOC. Due to the frequency of sample collection, the assistance of the City's operation personnel in the collection of data and sets of samples was necessary. A sample set included five to six samples taken daily in one-liter amber bottles. Samples representative of the aerated raw Verna (RV) water, SF filtrate, HF feed, HF concentrate, and HF permeate were taken at the corresponding sampling points shown in Figure 4-6. The raw Verna water was chlorinated after aeration to control biological growth.

Table 4-4: Pilot Testing Matrix

Analysis / Test	Analysis Location	Testing Frequency
Alkalinity	City's Laboratory	Twice per week
Conductivity	City's Laboratory	Five times per week
pH	City's Laboratory	Five times per week
Temperature	City's Laboratory	Five times per week
Turbidity	City's Laboratory	Five times per week
Concentrate Flow	Pilot Unit	Daily
Concentrate Pressure	Pilot Unit	Daily
Feed Flow	Pilot Unit	Daily
Feed Pressure	Pilot Unit	Daily
Permeate Flow	Pilot Unit	Daily
Permeate Pressure	Pilot Unit	Daily
Total Dissolved Solids	UCF Laboratory	Twice per week
Total Suspended Solids	UCF Laboratory	Twice per week
Anions	UCF Laboratory	Five times per week
Cations	UCF Laboratory	Five times per week
Total Organic Carbon	UCF Laboratory	Five times per week
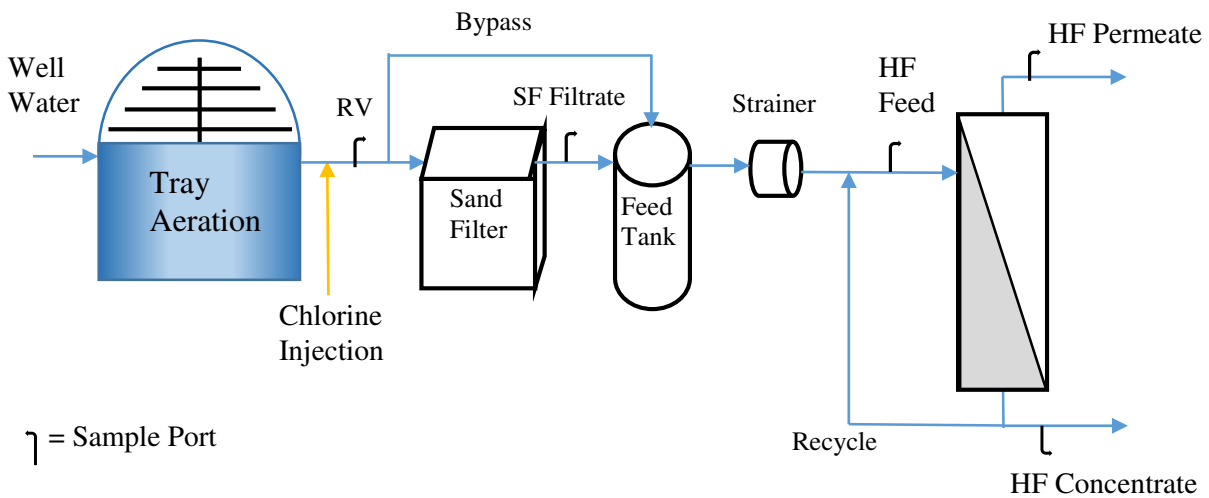
Figure 4-6: Process Flow Diagram of HFNF Membrane Pilot

SWNF Membrane Pilot System

One component of this research included a pilot-scale assessment of the feasibility of treating Verna water through a combination of SF, HFUF, and traditional SWNF membranes. The HFUF and SWNF pilot systems used in this component of the research are displayed in Figure 4-7. The treatment system utilized the sand filter pilot discussed and shown previously. The HFUF pilot system utilized two Pentair X-Flow (Enschede, The Netherlands) Xiga 40 HFUF membranes housed within a PVC module. The asymmetric HFUF hydrophilic membranes were composed of polyethersulfone (PES) modified by polyvinylpyrrolidone (PVP). Membrane elements were composed of lumens with 0.8 mm diameters and lengths of 5 ft (1.5 m). The total membrane area for each element was 430 ft^2 (40 m^2). The system was operated in dead end filtration mode with an inside-out configuration. The HFUF system was continuously injected with chlorine to control the growth of algae and prevent biofouling for a portion of the testing period. Chemical enhanced backwashed (CEBs) were performed using either citric acid, caustic, or sodium hypochlorite.

Figure 4-7: Ultrafiltration Pilot (featured left) and SW Nanofiltration Pilot (featured right)

The SWNF pilot skid utilized 18 Hydranautics (Oceanside, CA) ESNA1-LF-4040 polyamide SWNF membranes. The SWNF pilot skid was constructed in a two-stage 2:1 array, with the first and second stages housing 12 and 6 membrane elements, respectively. Each membrane element provided an active surface filtration area of 85 ft^2 (7.9 m^2). One micron polypropylene cartridge filters were installed directly before the NF process to prevent suspended particles from entering the feed stream. The SWNF pilot feed stream was dosed with sodium metabisulfide for hypochlorite sequestration and Avista Technologies (San Marcos, CA) Vitec® 1000 as a scale inhibitor.

The SWNF pilot system implemented in this research is depicted in the process flow diagram in Figure 4-8. The system includes a number of pretreatment operations and processes to provide adequate protection of the SWNF membranes including SF and HFUF. The sand filter was backwashed approximately once a week to provide sufficient flows and minimize head loss. The HFUF pilot automatically recorded process data in 2 minute intervals including the temperature and turbidity of the feed stream, the pH, conductivity, turbidity and flow of the filtrate stream, and the pressure of the feed and filtrate streams. CEBs were performed as necessary to maintain filtrate

production. Pressure decay tests were performed periodically to monitor membrane integrity. The SWNF process data was recorded automatically at 10 min intervals and included time, feed temperature, pH, conductivity, oxidation reduction potential (ORP), and the pressure and flows of the concentrate and permeate for each stage. Process data was collected weekly and used in data analysis and pilot performance evaluations. It should be noted the implementation of this technology on a full scale system is substantially costly. Previous studies conducted by Tharamapalan and coworkers (2012b) have documented the successful implementation of this technology while meeting sufficient removals of hardness, sulfate, and TDS. This pilot system was used to verify the findings of previous work and establish a benchmark and performance criteria to use in the comparison of traditional SWNF membrane technologies and next generation HFNF membrane technologies. Intermittent samples for water quality analysis of metals, anions, and solids were sampled for each of the pilots. However sampling was conducted less frequent than the HFNF testing period, due to the large amount of historical data collected in previous research.
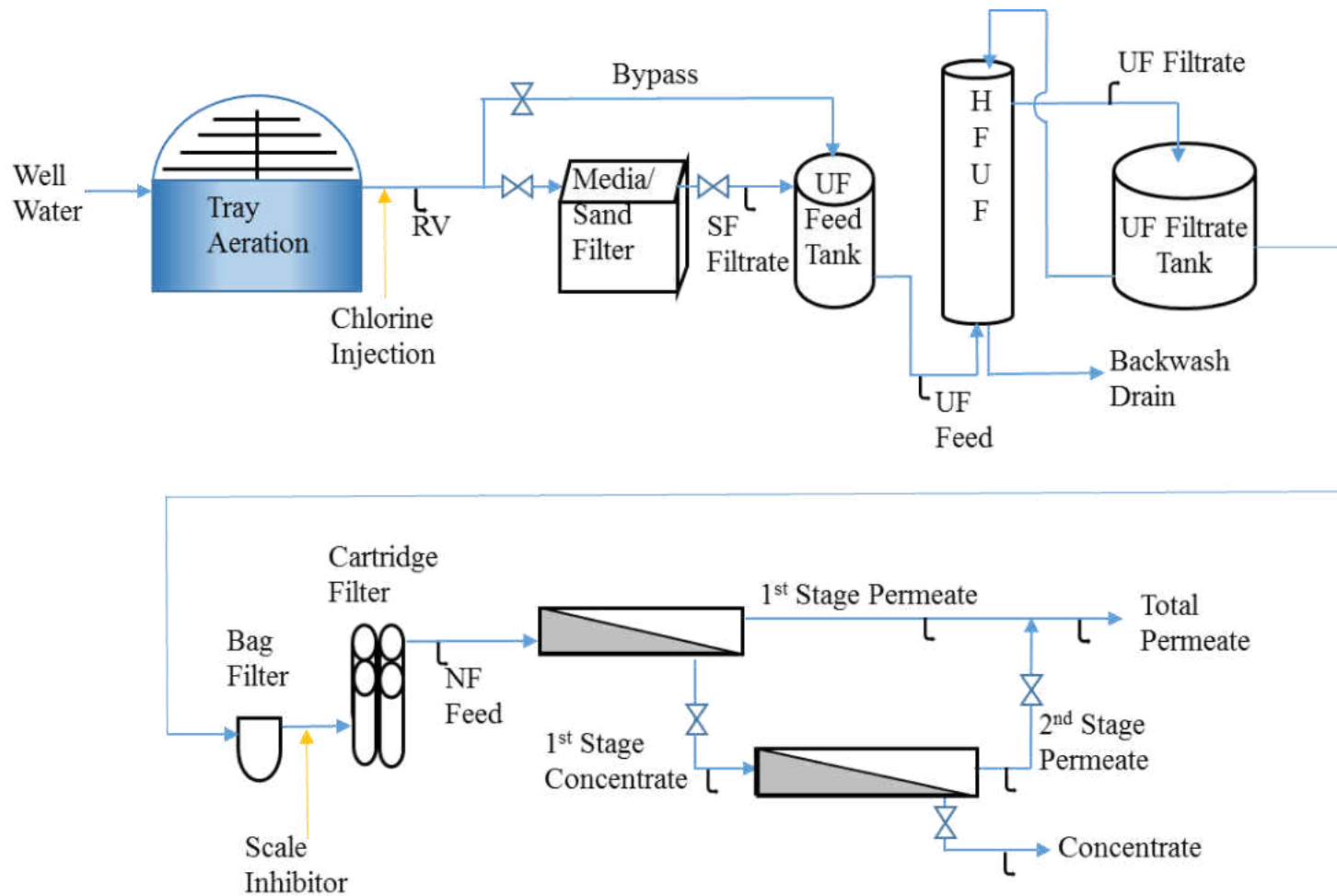
Figure 4-8: Process Flow Diagram of SWNF Membrane Pilot

Water Quality Methods and Analysis Description

Table 4-5 provides a list of water quality parameters that were conducted in the UCF and City of Sarasota laboratories during the study. These parameters include the major constituents of concern such as hardness, sulfate, TDS and TOC as well as additional constituents commonly found in water supplies to assess the performance of each membrane. This data served as a quality control in the methodical procedures conducted throughout this research. The data from tests not directly related to membrane testing were used to further characterize the overall treatability of the Verna water source. Constituents were measured in accordance with the *Standard Methods for the Examination of Water and Wastewater (AWWA, WEF et al., 2005)* or when appropriate as described by the U.S. Environmental Protection Agency.

It was necessary to conduct select water quality analysis in the field at the sample location. Table 4-6 summarizes the parameters measured on-site during field testing. Calibration procedures and measuring ranges have been specified as well. Dissolved oxygen and sulfide were conducted in the field due to the short holding time for measuring the constituents. Previous studies have documented biological fouling on membranes treating the Verna water source (Duranceau, Tharamapalan et al., 2014). For membrane pilot studies conducted in this research, total plate counts and biological activity reaction tests (BARTs) were used to verify and classify biological activity present in the water sources.

Table 4-5: Summary of Analytical Methods for Laboratory Water Quality Analyses

Analyte	Method Reference Number (Standard Method); Instrument	Method Reporting Level (MRL)	Method Detection Level goal (MDL)	Hold Time	Minimum Sample Volume	Container Type	Preservative
Alkalinity	SM: 2320 B. Titration Method Bromocresol green/ methyl red	5 mg/L as $CaCO_3$	5 mg/L as $CaCO_3$	Preferably 24 hours 14 days max.	100 mL	Glass or Plastic (filled completely and capped)	Cool, 4 °C
Barium	EPA 200.7 / SM: 3120 B. Inductively Coupled Plasma (ICP) Method/Inductively Coupled Plasma Spectrometer	0.01 mg/L	0.002 mg/L	180 days	250 mL	Plastic or Glass	Cool, 4 °C; Acidify with 2% concentrated HNO_3 to pH < 2
Calcium	EPA 200.7 / SM: 3120 B. Inductively Coupled Plasma (ICP) Method/Inductively Coupled Plasma Spectrometer	0.01 mg/L	0.01 mg/L	180 days	250 mL	Plastic or Glass	Cool, 4 °C; Acidify with 2% concentrated HNO_3 to pH < 2
Calcium Hardness	SM: 2340 C.EDTA Titrimetric Method	5.0 mg/L as $CaCO_3$	0.300 mg/L as $CaCO_3$	180 days	250 mL	Plastic or Glass	1-mL HNO_3, pH < 2
Chloride	EPA 300.0 / SM: 4110 B. Ion Chromatography (IC) with Chemical Suppression of Eluent Conductivity	0.10 mg/L	0.004 mg/L	28 days	500 mL	Plastic or Glass	None
Chlorine	SM: 4500-Cl G. DPD Colorimetric Method/HACH Spectrophotometer DR5000	0.02 mg/L	0.02 mg/L	0.25 hours	10 mL	Plastic or Glass	Analyze immediately
Color (True)	SM: 2120 C. Single Wavelength Method (254 nm)	1 PCU	1 PCU	24 hours	100 mL	Plastic or Glass	None
Conductivity	2510B. Laboratory Method; Fisher Scientific Traceable Conductivity, Resistivity and TDS Meter	N/A	N/A	28 days	125 mL	Glass	Cool, 4 °C
Iron	EPA 200.7 / SM: 3120 B. Inductively Coupled Plasma (ICP) Method/Inductively Coupled Plasma Spectrometer	0.005 mg/L	0.007 mg/L	180 days	250 mL	Plastic or Glass	Cool, 4 °C; Acidify with 2% concentrated HNO_3 to pH < 2

Table 4-5: Summary of Analytical Methods for Laboratory Water Quality Analyses

Analyte	Method Reference Number (Standard Method); Instrument	Method Reporting Level (MRL)	Method Detection Level goal (MDL)	Hold Time	Minimum Sample Volume	Container Type	Preservative
Magnesium	EPA 200.7 / SM: 3120 B. Inductively Coupled Plasma (ICP) Method/Inductively Coupled Plasma Spectrometer	0.1 mg/L	0.03 mg/L	180 days	250 mL	Plastic or Glass	Cool, 4 °C; Acidify with 2% concentrated HNO_3 to pH < 2
Manganese	EPA 200.7 / SM: 3120 B. Inductively Coupled Plasma	0.001 mg/L	0.002 mg/L	180 days	250 mL	Plastic or Glass	Cool, 4 °C; Acidify with 2% concentrated HNO3 to pH < 2
pH	SM: 4500-H+ B. Electrometric Method/ HQ40d Portable pH, Conductivity and Temperature Meter	0.01 units	0.01 units	0.25 hours	125 mL	Plastic or Glass	Analyze immediately
Potassium	EPA 200.7 / SM: 3120 B. Inductively Coupled Plasma (ICP) Method/Inductively Coupled Plasma Spectrometer	0.1 mg/L	0.1 mg/L	180 days	250 mL	Plastic or Glass	Cool, 4 °C; Acidify with 2% concentrated HNO_3 to pH < 2
Silica	EPA 200.7 / SM: 3120 B. Inductively Coupled Plasma (ICP) Method/Inductively Coupled Plasma Spectrometer	0.02 mg/L	0.02 mg/L	180 days	250 mL	Plastic (Borosilicate glassware should be avoided)	Cool, 4 °C; Acidify with 2% concentrated HNO_3 to pH < 2
Sodium	EPA 200.7 / SM: 3120 B. Inductively Coupled Plasma (ICP) Method/Inductively Coupled Plasma Spectrometer	0.03 mg/L	0.03 mg/L	180 days	250 mL	Plastic or Glass	Cool, 4 °C; Acidify with 2% concentrated HNO_3 to pH < 2
Sulfate	SM: 4110 B. Ion Chromatography (IC) with Chemical Suppression of Eluent Conductivity / SM: 4500	0.018 mg/L / 1.0 mg/L	0.018 mg/L / 1.0 mg/L	28 days	500 mL	Plastic or Glass	Cool, 4°C
Temperature	SM: 2550 B. Laboratory Method/ HQ40d Portable pH, Conductivity and Temperature Probe	0.1 °C	0.01 °C	0.25 hours	125 mL	Glass / Plastic	Analyze immediately

Table 4-5: Summary of Analytical Methods for Laboratory Water Quality Analyses

Analyte	Method Reference Number (Standard Method); Instrument	Method Reporting Level (MRL)	Method Detection Level goal (MDL)	Hold Time	Minimum Sample Volume	Container Type	Preservative
Total Dissolved Solids (TDS)	SM: 2520 B. Electrical Conductivity Method; Fisher Scientific Traceable Conductivity, Resistivity and TDS Meter / SM: 2540C	10 mg/L / 1 mg/L	7.661 mg/L / 4 mg/L	7 days	125 mL	Plastic	Cool, 4 °C
Total Organic Carbon	SM: 5310 C. Persulfate-Ultraviolet Oxidation Method/Tekmarr-Dohrmann Phoenix 8000: The UV-Persulfate TOC Analyzer	0.1 mg/L	0.01 mg/L	Preferred 24-hrs; limit 7-days	100 mL	Plastic	Analyze immediately; Or add HCl, H_3PO_4 or H_2SO_4 to pH<2, Cool, 4°C
Total Suspended Solids (TSS)	SM: 2540 D. Total Suspended Solids Dried at 103-105°C	1 mg/L	4 mg/L	Preferred 24-hrs; limit 7-days	100 mL	Plastic	Cool, 4 °C
Total Hardness	SM: 2340 B. Hardness by Calculation	3.0 mg/L as $CaCO_3$	0.346 mg/L as $CaCO_3$	180 days	250 mL	Plastic or Glass	Cool, 4 °C; 1-mL HNO_3, pH < 2
Turbidity	SM: 2130 B. Nephelometric Method	0.020 NTU	0.012 NTU	48 hours	100 mL	Plastic/ Glass	For best results, analyze immediately without altering sample; If storage is required, cool to 4 °C.
UV- Absorbing Organic Constituents UV-254	SM: 5910 B. Ultraviolet Absorption Method	0.01 cm^{-1}	0.001 cm^{-1}	48 hours	125 mL	Amber glass bottle; teflon lined cap	For best results, analyze samples as soon as possible. If storage is required, cool to 4 °C.

Table 4-6: Summary of Field Analytical Methods

Test/Analyte	Standard Method (SM) Reference Number; Instrument	Range / Resolution	Calibration Procedures
BART-APB	Acid Producing Bacteria - BART	MDL-100 cfu/ml	Fill VOA glass with 40 mL of sample store at room temperature
BART-IRB	Iron Released Bacteria - BART	MDL-100 cfu/ml	Fill VOA glass with 40 mL of sample store at room temperature
BART-SFB	Slime Forming Bacteria - BART	MDL-100 cfu/ml	Fill VOA glass with 40 mL of sample store at room temperature
BART-SRB	Sulfate Reducing Bacteria - BART	MDL-100 cfu/ml	Fill VOA glass with 40 mL of sample store at room temperature
Conductivity	LaMotte Con 5 Field Probe (with temperature compensation)	0 – 20 mS Range 1 µS resolution	Calibrated against manufacturer's internal method and frequent membrane inspection
Color (True)	SM: 2120C Single Wavelength Method (254 nm)	1 – 50 PCU	Calibrated against prepared standards from stock PCU solution
Dissolved Oxygen	YSI 550A Sensor	0 – 50 mg/L O_2 Range	Calibrated against manufacturer's internal method and frequent membrane inspection
Hydrogen Sulfide	LaMotte 4630 Drop Count Method or SM 4500F Iodometric Method	0.01 mg/L S resolution	Check with samples collected for laboratory analysis using zinc acetate preservation method.
pH	LaMotte pH 5 Series Field probe (with temperature compensation)	0 – 14 Range, 0.01 resolution	Commercial pH calibration buffers, pH 4, 7, 10. Calibrated prior to analyzing any batch of samples using 2 point calibration with standard buffers
Temperature	Mercury-filled Celsius Thermometer	0 – 100 ºC range; 0.1 ºC resolution	Calibrated against NIST-certified thermometer
Turbidity	SM: 2130 B. Nephelometric Method; HACH 2100q Portable Turbidimeter	0.02 – 200 NTU	Calibrated against 0.1, 10, 20, 100, 200, and 800 NTU standards

Sample containers were cleaned in accordance with the methods and procedures outlined in (AWWA et al., 2005). Cleaning procedure steps varied by sample container type. Each sample container was labeled and identified by sampling location, sampling date, sample number and personnel. Sample blanks, spikes, duplicates, as well as the presence of preservation and dechlorination agents were specified on the label when appropriate. If preservation techniques were necessary, such as with metals samples, samples were prepared and preserved within 48 hours of collection. The holding times, container requirements and preservations techniques have been included in Table 4-5.

Table 4-7: Cleaning Procedures for Various Sample Containers

Container Type	Purpose	Required Cleaning Steps
1 L Glass Amber bottles	Field sampling	Steps 2-7, 9 and 10
Analytical Glassware	Laboratory analyses	Steps 2-6 and let dry
15 gallon drums	Field collection	Step 1
55 gallon drums	Laboratory storage	Step 1
High-density polyethylene bottles	Laboratory sampling	Step 1
Glass vials	Laboratory analyses	Steps 2-6, 8 and 9

1. Rinse sufficiently with sample water.

2. Remove outside labels with tap water and scrub brush.

3. Wash inside with tap water and laboratory detergent.

4. Rinse three times with tap water.

5. Rinse with ACS grade 1:1 HCl.

6. Rinse three times with distilled water.

7. Cover lid with aluminum foil and puncture foil to allow moisture to escape.

8. Air dry and wrap with aluminum foil.

9. Bake for at least two hours at 400°C, and cool to room temperature.

10. Cover lid with aluminum foil.

The quality of data produced in this research was dependent upon the integrity of the samples and materials used to perform analyses. Method specific sample containers, analytical grade reagents and preservatives were administered as described in Table 4-5. Field sampling for metals and anion analysis was completed with the use of 1L amber bottles. Sample containers were completely filed to minimize headspace and sealed with Teflon-lined septas and caps. Turbidity, pH, conductivity, temperature, and alkalinity were measured in the field at the time of sampling. Samples were stored at 4°C in darkness before being transported in coolers to UCF facilities for additional analyses. Samples were analyzed for parameters within the appropriate holding times specified in Table 4-5. Fifteen-gallon drums were used for the collection of larger (>2 L) sample quantities. The drums were rinsed three times with sample water, capped, and immediately transported to UCF laboratories.

Laboratory Analysis Description

<u>Organic Analysis</u>

Non-purgeable dissolved organic carbon concentrations were analyzed according to SM 5310 persulfate-ultraviolet oxidation method using a Dohrmann Phoenix 8000 (Mason, OH) UV-Persulfate TOC analyzer equipped with a Tekmarr autosampler. This method converts organic carbon to carbon dioxide through persulfate oxidation. The inorganic carbon species are converted to carbon dioxide and purged from the system into the atmosphere. The carbon dioxide remaining in the liquid is measured by a non-dispersive infrared analyzer. Results are provided in terms of absorbance and concentrations are calibrated using NPDOC standards. The NPDOC standards were diluted from a stock concentration of 200 mg/L organic carbon prepared by dissolving 425

mg of potassium acid phthalate (KHP) in one liter of distilled water. The KHP was dried at 105 ºC overnight, then stored in a desiccator before preparing the stock solution. A two system check was performed on TOC analysis by verifying samples against the laboratory-prepared standard and a manufactured standard. NPDOC standards included concentrations of 0.5, 1, 2, 5, 10, 20 mg/L C for water samples. Additional lower level standards of 0.25, 0.75, 1.5 and 3 mg/L C were added when analyzing permeate samples. Blank samples of distilled water were analyzed before and after the standards to monitor carry over and assess the analytical detection limit.

Fluorescence excitation-emission spectroscopy was conducted to further characterize the dissolved organic matter. A fluorescence excitation-emission matrix (EEM) can be used to differentiate between humic acid-like, fulvic acid-like, and protein-like substances. Prior to fluorescence analysis, samples were filtered with a 0.45 µm membrane filter to remove particulates. Without further pretreatment, fluorescent EEM spectra were collected using a Shimadzu RF-6000 spectrofluorophotometer (Kyoto, Japan). The emission intensity readings were captured in 1-nm wavelength intervals between 280 nm and 600 nm for excitation wavelengths ranging from 200 nm to 400 nm in 5-nm intervals. The excitation and emission slits were set to a 10-nm band-pass. The Raleigh scattering effect was minimized by subtracting the fluorescence spectra collected from a blank sample of deionized water.

Inorganic Analysis

Inorganic analyses for sulfate and chloride were conducted using a Thermo Scientific Dionex™ ICS-1100 (Sunnyvale, CA) Ion Chromatography System (IC) with an AS40 autosampler. The system is equipped with a high pressure pump, sample injector, IonPac® MFC-1 RFIC TM 3x27mm metal free trap column, IonPac® AG23 RFIC TM 4x55mm guard column and IonPac®

AS23 analytical separator column, chemical suppressor, heated conductivity cell, and an electrochemical detector. The IC machine performs ion analyses using suppressed chemical detection. Each IC sample is pumped through the trap column and guard before entering the separator column where each anion is isocratically separated. The data collection system produces chromatograms for each of ions in solution. The ion chromatography system utilizes a liquid eluent prepared by diluting a manufactured stock solution (AS23 eluent concentrate) by a factor of 100 to yield 4.5 mM sodium carbonate and 0.8 mM sodium bicarbonate solution. The IC system is calibrated using a set of standard solutions prepared using American Chemical Society (ACS) grade chemicals. Sulfate and chloride standards were prepared with concentrations of 1, 5, 10, 50, and 100 mg/L. Additional standards concentrations of 20, 40, 60, and 80 mg/L were prepared to measure samples with higher expected concentrations as well as standards of 0.1, 0.5, and 0.75 mg/L when lower level analysis was necessary. Blanks, standards, and the eluents were prepared using deionized Type 1 Reagent grade water with a specific resistance of 18.2 megohm-cm. Samples were prepared by filtering each sample through a 0.20 micrometer (μm) pore size nylon syringe filter with a diameter of 33mm.

Inorganic analyses for metals including calcium and magnesium were measured using atomic optical emission spectrophotometry (OES) using a Perkin Elmer (Waltham, MA) Optima 2100 DV argon-supported inductively coupled plasma (ICP) system, equipped with an AS-93 Plus autosampler. In ICP-OES systems, samples are subjected to high temperatures to cause excitation and ionization of the sample atoms. The atoms decay to less excited states through radiative energy transitions. The intensity of light emitted at specific wavelengths is measured by a polychromator and used to determine the concentrations of the elements of interest. This method allows for the

concurrent measurements of multiple ions in each sample. This research utilized two methods for characterizing water samples. One method was used when analyzing calcium, magnesium, potassium, silica, and sodium. Iron, barium, and manganese were analyzed using a second method to minimize interference from emission lines that had similar wavelengths as other ions. Standards were prepared using ACS grade chemicals and acidified using 2% nitric acid. Concentrations for standards as well as the selected wavelength and window for each method have been provided in Table 4-8 and Table 4-9. Samples were prepared by acidifying with 2% nitric acid and stored in a refrigerator for 24 hours before analysis. Samples were analyzed in triplicate with the instrument reporting the mean, standard deviation, and relative percent difference as statistical analysis. Blanks, spikes, and standard checks were included during each analysis.

Table 4-8: ICP-OES Method 1 Specifications

Analyte	Wavelength (nm)	Standards (ppm)	Window
Calcium	317.933	1, 2, 5, 7.5, 20, 50, 60	Axial
Magnesium	285.213	1, 2, 5, 7.5, 15, 20, 30	Axial
Potassium	766.490	0.1, 0.2, 0.4, 0.5, 1, 2, 5	Axial
Silica	251.611	0.1, 0.2, 0.4, 0.5, 1, 2, 5	Axial
Sodium	589.592	0.2, 0.5, 1, 2, 5, 7.5, 10	Axial

Table 4-9: ICP-OES Method 2 Specifications

Analyte	Wavelength (nm)	Standards (ppb)	Window
Barium	455.403	5, 10, 50, 100, 200, 500, 1000	Axial
Iron	238.204	5, 10, 50, 100, 200, 500, 1000	Axial
Manganese	257.610	5, 10, 50, 100, 200, 500, 1000	Axial

Field Analysis Description

Standard filtration tests were conducted and used to develop fouling indices for the Verna water to determine the effectiveness of SF pretreatment. The fouling indices conducted in this research indicate the potential occurrence of particulate or colloidal fouling rather than biological or chemical fouling. The field tests included the silt density index (SDI), mini plugging factor index (MPFI), and modified fouling index (MFI) which have been increasingly used to qualitatively estimate pretreatment requirements for membrane systems (Alhadidi, Kemperman et al., 2012).

Silt Density Index

Periodic experiments were conducted on each of the sand filters to determine the SDI of the filtrate streams. The SDI is a test developed for measuring the rate of plugging for a particular feed water. Typically it is applicable to waters containing relatively low turbidities (<1.0 NTU) including well or filtered water. It has been empirically correlated with the fouling tendency of membrane filtration systems, specifically nanofiltration and reverse osmosis. While some manufacturers of spiral-wound membranes recommend that SDIs should not exceed a maximum of 5, most manufacturers suggest feed water quality SDIs less than 3 for reverse osmosis systems and less than 4 for nanofiltration systems (Alhadidi, 2011; Duranceau, 1990). The SDI can also be used to indicate the quantity of particulate matter in water and in this research was one method for determining the effectiveness of the two sand filters. The SDI is performed by measuring the initial time it takes to filter 500 mL of water through a filter pad with a mean pore size of 0.45 microns at a constant pressure of 30 psi. The process is repeated at time intervals of 5, 10, and 15 minutes after the start of the test. The value of the SDI is then calculated using the Equation 4-1 (ASTM, 2007).

58

$$SDI_T = \frac{100}{T}\left(1 - \frac{t_i}{t_f}\right) = \frac{\%P_{30}}{T}$$ (4-1)

Where:

$\%\ P_{30}$ = percent at 30 psi (207 kPa) feed pressure

t_i = time to collect initial 500 mL sample

t_f = time to collect final 500 mL sample

T = total time of the test, typically 5, 10, or 15 minutes

While the SDI can provide a rough estimate of the fouling potential of water, it is not based on a filtration model and does not account for temperature differences. Therefore, additional tests were conducted to verify SDI findings and assess the effectiveness of each sand filter in removing particulate matter.

Mini Plugging Factor Index

The MPFI is calculated by performing a test similar to the SDI by filtering the sample water through a filter pad with a mean pore size of 0.45 microns at a constant pressure of 30 psi using a filtration apparatus. The flow is recorded in 30 second intervals and used to create a plot similar to Figure 4-9 with flow (liters per second) on the y-axis and time (seconds) on the x-axis. The MPFI is a measurement of the decline in productivity calculated by the slope of the cake filtration region. It represents the mass transfer of water with respect to time.
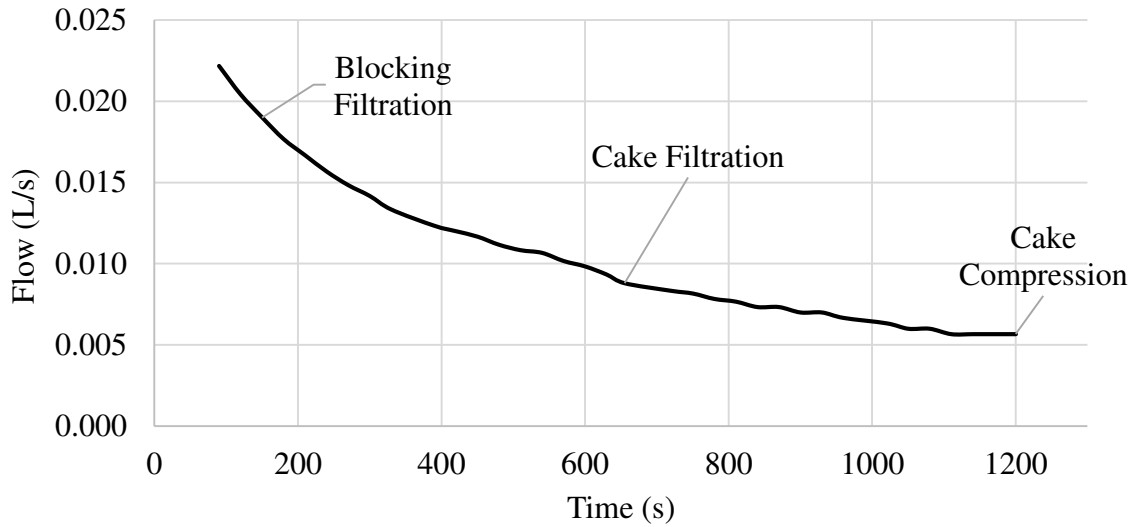
Figure 4-9: MPFI Determination Curve

Modified Fouling Index

The modified fouling index (MFI-0.45 or MFI) is another method used for estimating the fouling tendency of the feed water. The MFI was derived from the SDI by Schippers and Verdouw (1980) assuming the occurrence of a cake filtration fouling mechanism. This method is conducted using similar equipment as the SDI but incorporated pressure and temperature fluctuations as flow is measured through the membrane as a function of time. The values for flow and cumulative volume are recorded and plotted to produce a graph similar to Figure 4-10. The MFI is defined as the minimum slope (m) of the line at standard conditions that is, a temperature of 20 ℃, pressure of 30 psi (207 kPA), and active membrane filtration area for a 47 mm diameter filter pad. The minimum slope of the line is determined from Figure 4-10 and normalized to standard conditions using equations 4-2 through 4-4. Example calculations have been provided in Appendix B.
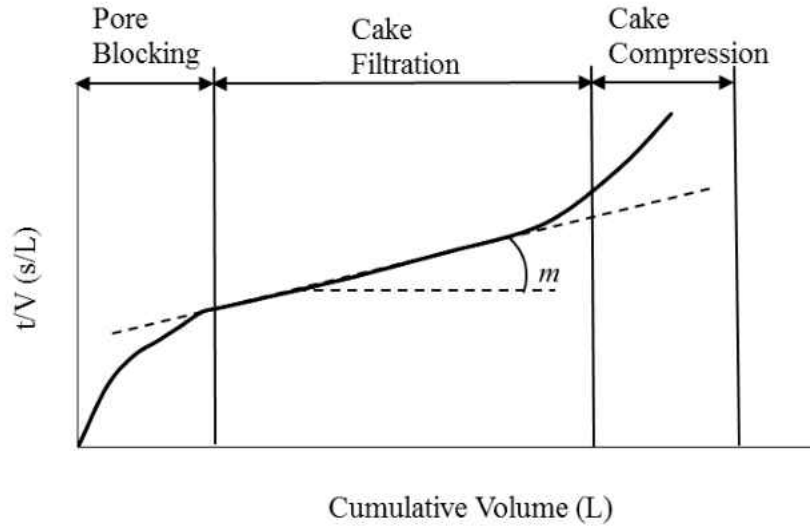
Figure 4-10: MFI Determination Curve

$$\frac{t}{V} = \frac{\mu\,R_M}{\Delta P\,A} + \frac{\mu\,I\,V}{2\,\Delta P\,A^2} \tag{4-2}$$

$$m = \frac{\mu\,I}{2\,\Delta P\,A^2} \tag{4-3}$$

$$MFI_{0.45} = \frac{\mu_{20}I}{2\Delta P_0 A_0^2} \tag{4-4}$$

Where:

t = filtration time (s)
V = cumulative filtrate volume (L)
μ = water viscosity (Ns/m^2)
I = fouling index (m^{-2})
R_m = membrane resistance (m^{-1})
ΔP = applied pressure (N/m^2)
A = active membrane filtration area (m^2)

MFI and SDI values will vary with different membrane manufacturers and membrane type. This research was conducted using white hydrophilic, mixed cellulose ester (MCE) (nitrate and acetate) membranes with a mean pore size of 0.45 µm and a diameter of 47 mm in accordance with ASTM International standards (ASTM, 2007).

61

Laboratory and Field Quality Control and Statistics

During laboratory testing, standards, reference check samples, blanks, replicates and spikes were prepared at a minimum rate of ten percent for each sample set for TOC, metal, and anion analyses. To assess the consistency of the precision of the analytical instrumentation, duplicate measurements were taken and assessed for the relative percent difference (RPD). Spike results for each parameter were used to determine the average percent recovery, warning limits, and control limits. Statistical data for accuracy and precision were displayed in Shewhart control charts.

Extensive field control measures were also implemented throughout this study. Duplicate measurements were taken to assess the consistency of the sample water quality and to assess the consistency of the sampling transport and preservation process. Duplicates for field measurements were taken every six samples, a minimum of every other sampling day. Conductivity, temperature, turbidity and pH were monitored throughout the study and calibrated using the procedure listed in Table 4-6. Quality control requirements for field data were followed according to the analytical methods listed in the Laboratory Quality Assurance Procedures for the UCF Environmental Systems Engineering Institute (ESEI) housed within the Civil, Environmental, and Construction Engineering (CECE) department (Real-Robert, 2011). Quality control measures for laboratory data collection were performed according to the *Standard Methods for the Examination of Water and Wastewater* (Eaton, Clesceri et al., 2005) and the USEPA's *Handbook of Analytical Quality Control in Water and Wastewater Laboratories*.

Accuracy

Percent recovery for each spiked sample was calculated using Equation 4-5. The percent recovery of each spike was plotted on a chart to assess the accuracy and consistency of the ICP, IC, and TOC analyzers. Recoveries were considered acceptable if the values are in the range between 80-120%.

$$\% \ Recovery = \frac{C_{sample+spike} - C_{sample}}{C_{spike}} \times 100\% \qquad (4\text{-}5)$$

Where:

$C_{sample+spike}$ = the concentration of the spiked sample (mg/L)
C_{sample} = the concentration of the sample (mg/L)
C_{spike} = the concentration of the spike (mg/L)

Upper and lower control limits (UCL & LCL) for accuracy charts are defined to be plus or minus three standard deviations from the mean and were calculated using Equation 4-6 (AWWA et al., 2005). Upper and lower warning limits (UWL & LWL) are defined to be plus or minus two standard deviations from the mean and were calculated using Equation 4-7.

$$UCL = \mu + 3s \ and \ LCL = \mu - 3s \qquad (4\text{-}6)$$
$$UWL = \mu + 2s \ and \ LWL = \mu - 2s \qquad (4\text{-}7)$$

Where:

μ = the mean of the percent recovery values
s = the standard deviation of the percent recovery values

The relative percent difference (RPD) was calculated using Equation 4-8. RPD was used in replicate and duplicate analyses and was considered acceptable if the RPD was less than 20%. Outliers are identified as values falling outside three times the standard deviations from the mean. Data found as outliers were reviewed and either repeated or removed when appropriate.

$$RPD = \frac{S-D}{(S+D)/2} \times 100\% \qquad\qquad (4\text{-}8)$$

Where:

S = sample result (mg/L)
D = duplicate sample result (mg/L)

Precision

The industrial statistic was calculated using Equation 4-9 to create Shewhart control charts for the precision of anions, DOC, and metals analyses. Control charts are a statistical, graphical method to monitor process variation due to either assignable causes or random variation (Mendenhall & Sincich, 2007). Control charts were constructed by plotting the I-statistic values over time in a sequence plot to determine if variations in the data existed due to identifiable causes or random variation.

$$I = \frac{|S-D|}{(S+D)} \qquad\qquad (4\text{-}9)$$

UCL for precision charts are defined to be the average I-value plus three standard deviations and were calculated using Equation 4-10. UWL for precision charts are defined as the average I-value plus two standard deviations of the industrial statistic values and were calculated using Equation 4-11 (Booth, 1979).

$$UCL = I_{avg} + 3s \qquad\qquad (4\text{-}10)$$
$$UWL = I_{avg} + 2s \qquad\qquad (4\text{-}11)$$

Where:

I_{avg} = the average of the industrial statistic values
s = the standard deviation of the industrial values

If a point fell above the UCL or below the LCL the data corresponding to the run of the duplicate sample were considered a control violation. Data measurements violating the LCL or UCL were repeated if possible or the data was removed from the results. If any two points were successively exceeding the warning limits the data was considered to be a control violation. Control violations were checked by analyzing another sample and corrected for bias or disregarded.

Analysis of Variance for Linear Regressions

Models were developed using statistical software and least square linear regression. The assumptions of the least squares technique include: the probability distribution of random error is normally distributed with a constant variance; the residual error associated with any two different observations are independent and not correlated; the mean of the probability distribution of random error is zero. Statistical analysis considered the coefficient of determination (R^2), root mean square error (RMSE), the sum of squares due to the regression (RegSS), the residual sum of squares (RSS), and the total sum of squares (SST). The terms can be using the Equations 4-12 through 4-16 (Brown & Mac Berthouex, 2002).

$$R^2 = \frac{RegSS}{TSS} \tag{4-12}$$

$$RMSE = \sqrt{(y_i - y)^2} \tag{4-13}$$

$$RegSS = SST - RSS \tag{4-14}$$

$$RSS = (y_i - \bar{y})^2 \tag{4-15}$$

$$SST = \sum (y_i - \bar{y})^2 \tag{4-16}$$

5. RESULTS AND DISCUSSION

This chapter presents the results and provides a discussion of the experiments conducted to determine removal capabilities, describe rejection mechanisms, and assess hydraulic performance of next generation HFNF membranes. This chapter is organized into five sections, including the results of the two bench-scale HFNF membrane treatment systems, the pilot-scale HFNF system, the pilot-scale SWNF system, and quality control.

1. The first section presents the findings of the bench-scale experiments conducted on three next generation HFNF membranes using synthetic solutions containing magnesium sulfate and sodium chloride. The operating time and testing conditions including permeate production and water recovery, and are presented for each membrane. Water flux and water MTC calculations are also provided, as well as membrane rejection capabilities. Membrane rejection mechanisms were investigated using size exclusion and diffusion-based models. An additional semi-empirical model was developed that considered HSD theory and ionic strength.

2. This second section provides water quality results and includes constituents of concern in the aerated Verna groundwater supply. An assessment of the bench-scale SF pretreatment system is discussed, which describes the performance of two filtration medias considering turbidity removal, operation pressures, and filtration indices. The section concludes with the results of HFNF membrane treated aerated Verna groundwater pretreated with the bench-scale SF system. HFNF performance data includes operating conditions, water production, water recovery, water flux, water MTC and water quality parameter removals.

3. The third section presents the results of the application of a next generation HFNF membrane on aerated groundwater using a pilot scale membrane system. Pilot testing results include operating time, permeate production, recovery, water flux, specific water flux, and permeate water quality.

4. An additional section presents the data regarding the pilot testing of traditional SWNF membranes considering water quality, hydraulic conditions, and pretreatment requirements to provide a comparison of traditional SWNF membranes to next generation HFNF membranes.

5. The fifth and last section includes the laboratory and field water quality control results including control charts reporting experimental accuracy and precision.

<u>Bench-Scale HFNF Membrane Testing Using Synthetic Solutions</u>

Time Utilization & Operating Conditions

A minimum of eighteen retention tests were completed for each membrane with each test representing a distinct combination of membrane recovery, water flux, and testing solution. Each retention test required a minimum of 15 min for system flushing, 15 min for stabilization, and 30 min to conduct an experiment. Average retention testing time was approximately 1 hour, for each retention and permeability test. Five sets of samples were collected for each retention test and analyzed for appropriate water quality parameters. A total of sixty retention tests were conducted, producing approximately 350 water samples used for model development. A complete list of experiments specifying target flows, recoveries, and solution types has been provided in Appendix A.

System Water Production & Water Recovery

The HFNF membranes were tested under three flows configurations and three recoveries during each of the bench-scale experiments. Permeate flows were targeted at 19, 25, and 31 mL/min, while concentrate flows varied from 3.4 to 10.5 mL/min to produce membrane recoveries of 50%, 75%, and 85%. A recycle stream was implemented in the design of the bench-scale system to meet the desired cross flow velocities. Feed pressures varied between 24 and 40 psi depending on membrane and permeate flows. Table 5-1 provides a summary of the operating conditions tested throughout this study for each membrane type.

Table 5-1: Operating Pressure and Flow Ranges for Experimental Testing

Type	Run / Test	Feed Pressure (psi)	Concentrate Pressure (psi)	Permeate Pressure (psi)	Feed Flow (gpm)	Concentrate Flow (mL/min)	Permeate Flow (mL/min)
A	1 – 22	24 – 40	21 – 39	0	0.3 – 1.2	3.4 – 10.5	19 – 31
B	23 – 40	24 – 40	20 – 38	0	0.6 – 1.2	3.4 – 10.5	19 – 31
C	41 – 58	30 – 42	26 – 42	0	0.2 – 1.0	3.4 – 10.5	19 – 31

Water Flux & Water Mass Transfer Coefficient

Three distinct flux values were targeted when conducting bench-scale experiments based on manufacturer recommendations. Fluxes of 9, 12, and 15 gfd were specified as target experimental set points. The water MTCs for each membrane were determined from data collected when using the synthetic 5mM magnesium sulfate testing solution recommended by the manufacturer. Mass transfer coefficients of water were determined by utilizing the HSD theory and applying Equation 3-26 to produce a scatter plot of water flux versus the pressure differential. Using linear regression statistical software, the water mass transfer coefficients for each membrane were determined from the slope of the relationship between water flux and pressure differential with forced zero intercept. The equation of the least squares line for membrane A was determined to be y = 0.388x indicating a water MTCs of 0.39 gal/sfd-psi or 0.022 days^{-1}. The linear regression for membrane A was based on 104 experimental observations and yielded a coefficient of determination of 0.996 indicating that 99.6% of the variation within the data could be explained by the linear regression. An analysis of variance was conducted using statistical software generating a RMSE of 0.75, a RegSS of 14321, a RSS of 59, and a SST of 14380 for the linear regression describing membrane A. MTCs for membrane B and C were conducted using the same procedure and displayed in Figure 5-1. Comparison of the MTCs for each membrane indicate membrane C was the least permeable with respect to water yielding a MTCs of 0.30 gal/sfd-psi or 0.018 day^{-1}. Membrane B was the most permeable with a MTC for water of 0.75 gal/sfd-psi or 0.044 days^{-1} within the conditions tested. The water MTCs for each membrane were within the expected permeability range (0.20-0.81 gal/sfd-psi) specified by the manufacturer.
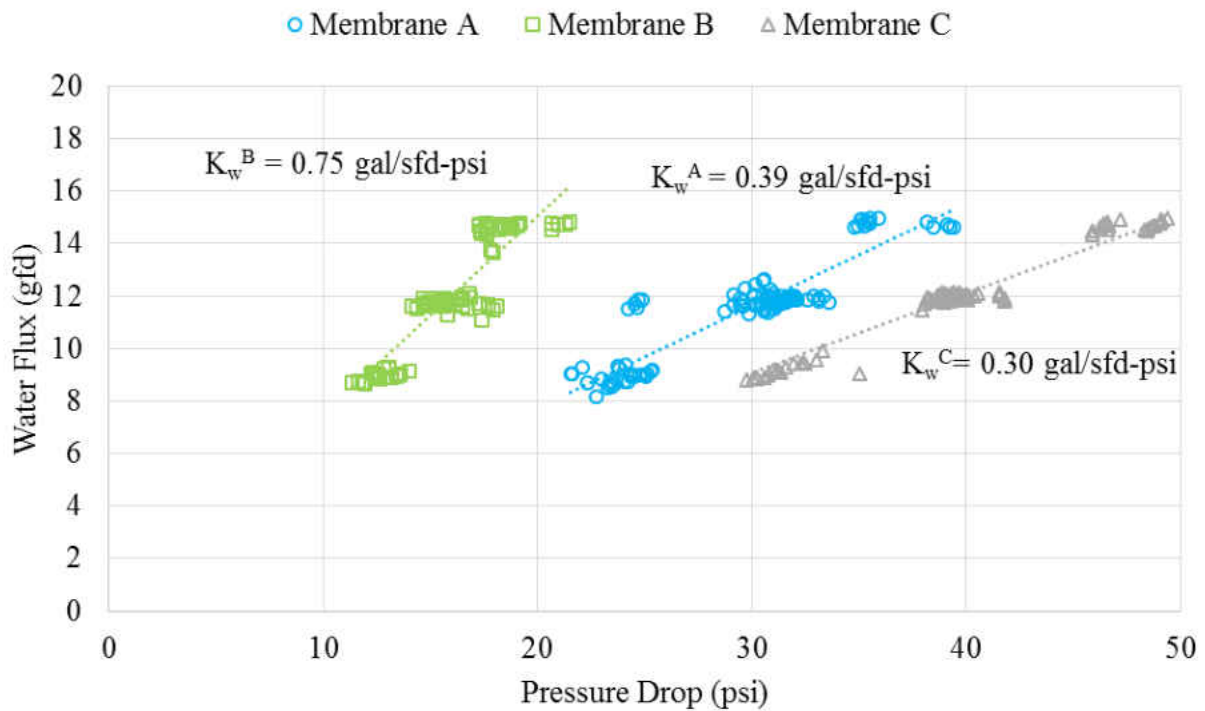
Figure 5-1: Water Flux versus Transmembrane Pressure Differential

The analysis of variance outputs for the linear regressions describing each of the MTCs of each membrane has been provided in Table 5-2. Outliner analysis revealed the presence of one outlier occurring within the data set for membrane C. The outlier was identified to have been caused by a spike in the feed pressure data. The point was not removed but it was attributed to the sensitivity of the data logger and the pressure transducer. Plots of residuals revealed the data to be normally distributed for each of the membranes.

Table 5-2: Statistics Summary for Membrane K_w Values

Membrane	No. Obs.	Coefficient of Determination	RMSE	RSS	RegSS	SST
A	104	0.996	0.754	59	14321	14380
B	89	0.995	0.904	73	13394	13467
C	89	0.999	0.359	11	13115	13127

Membrane Rejection Capabilities

UF membranes are typically used for removing large organic molecules and providing a physical barrier against viruses, whereas NF membranes are more often classified based on their rejection of divalent ions. However some overlaps exist when considering the removal capability of each technology. Alpatova, Verbych et al. (2004) has shown partial removal of divalent ions, using UF membranes and many NF membranes achieve some removal of monovalent ions (AWWA, 2007). Therefore, assessing the removal capabilities with respect to divalent and monovalent ions for each of the membranes can assist in their characterization.

The removal capabilities of divalent ions for each membrane were assessed using a standard testing solution of magnesium sulfate ($MgSO_4$) specified by the manufacture. In addition, removals were also assessed by determining the impact of varying feed concentrations and the presence of monovalent ions into the solutions using additional synthetic blends. The average removal capabilities of each membrane when using the standard solution of 5 mmol $MgSO_4$ are displayed in Figure 5-2. Membrane A rejected approximately 90% of divalent ions. Membrane B achieved 84% magnesium removal and 83% sulfate rejection. Membrane C retained significantly less divalent ions than membranes A and B removing on average less than 44% of sulfate and less than 43% of magnesium.
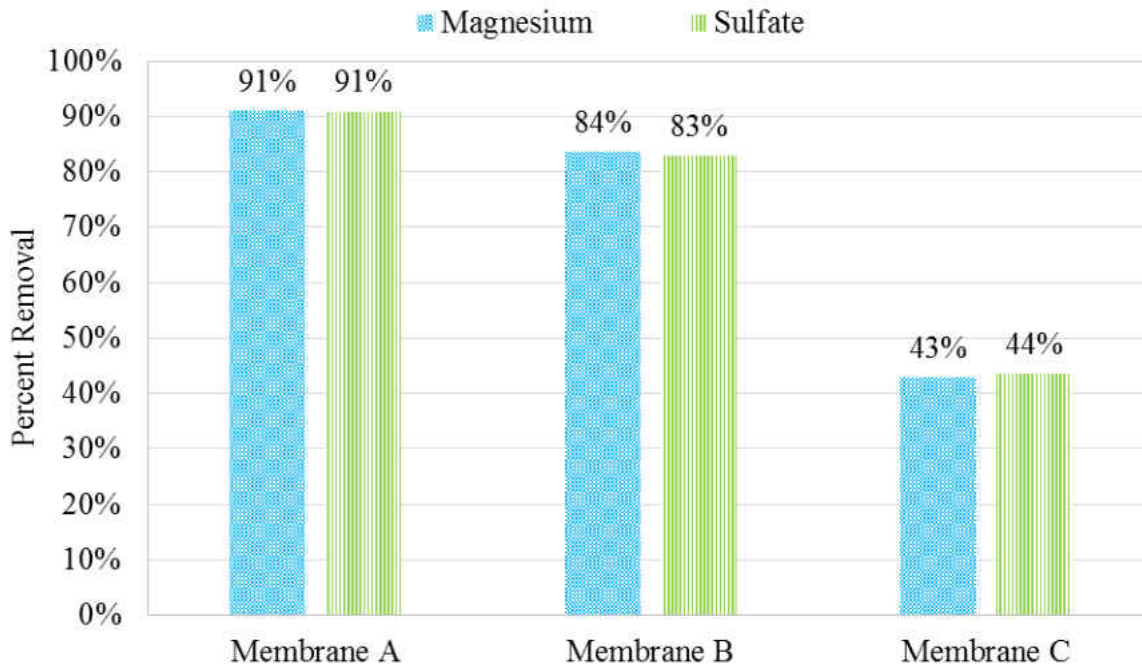
Figure 5-2: Average Magnesium and Sulfate Removals for each Membrane

The concentrations of Solutions 2 through 3 were designed to represent waters with varying levels of hardness by changing the concentration of $MgSO_4$. Recall the concentration of Solution 1 was 600 mg/L $MgSO_4$. Solutions 2 and 3 were prepared to contain concentrations of 960 and 240 mg/L $MgSO_4$, respectively. The effect of feed concentration on membrane rejection of magnesium and sulfate for each membrane are displayed in Figure 5-3 and Figure 5-4, respectively. Removals for membranes A and B are relatively constant when varying the feed concentrations of magnesium and sulfate. Membrane C was impacted by the feed concentration yielding greater removals at lesser feed concentrations.
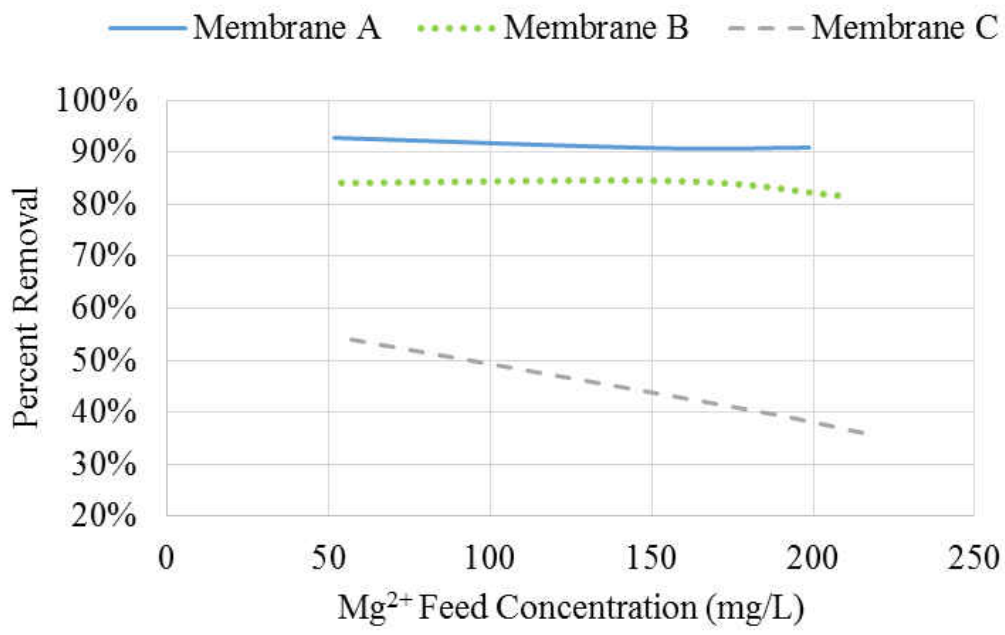
Figure 5-3: Magnesium Feed Concentration versus Percent Removal
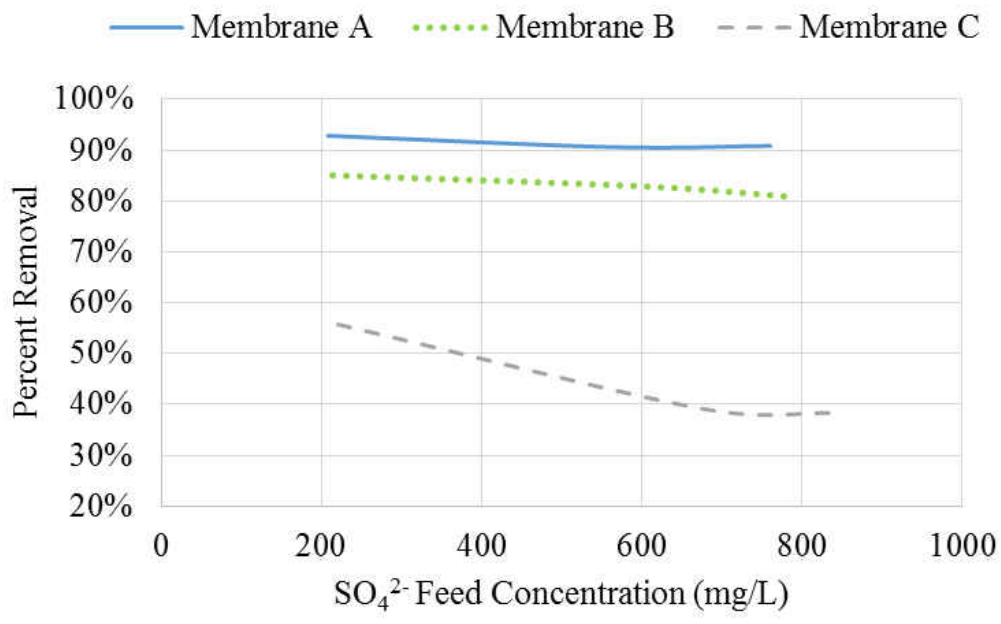
Figure 5-4: Sulfate Feed Concentration versus Percent Removal

73

Solutions 4 and 5 were tested to determine monovalent ion rejection specifically with regards to sodium chloride. Membrane A achieved removals of 13% and 11% for sodium and chloride, respectively. Membrane B achieved approximately 10% removal of sodium and less than 5% rejection of chloride. Membrane C rejected less than 6% of sodium ions and less than 1% chloride. The addition of sodium chloride into the synthetic $MgSO_4$ blend caused decreased removal with respect to magnesium and sulfate. The removals of magnesium and sulfate for membrane A decreased to 75% and 81% respectively. Membrane B and C were half as effective at removing magnesium with the introduction of NaCl while sulfate removal remained relatively constant. The significant change in the removal capabilities of each membrane presented in Figure 5-5 indicate that the presence of additional ions within the solution has a significant impact on overall cation rejection.
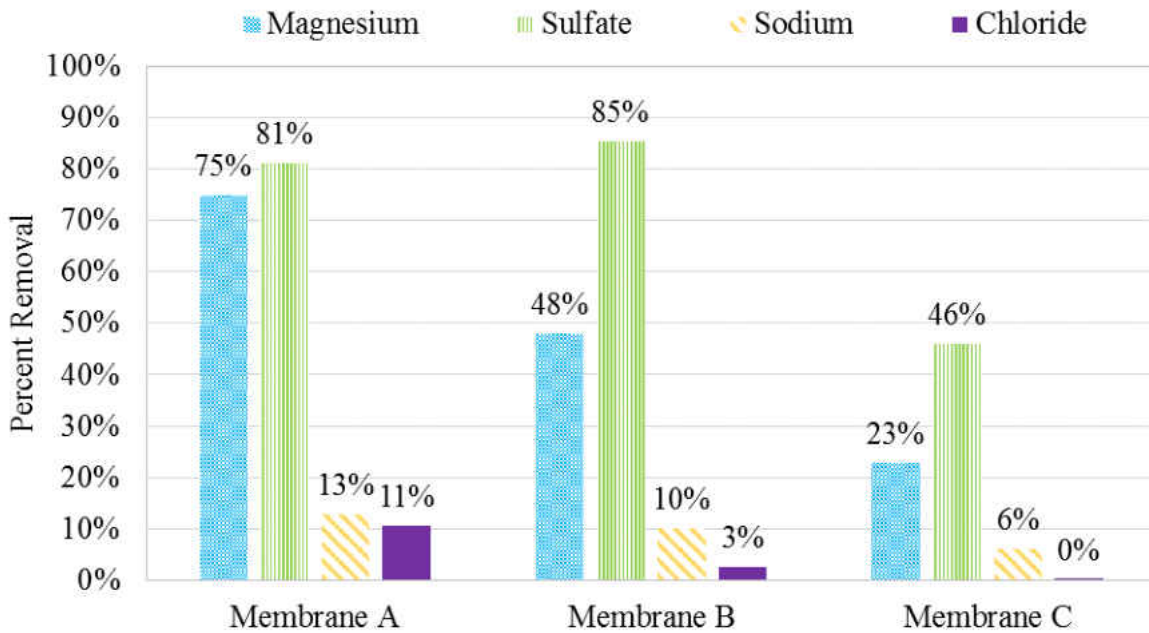
Figure 5-5: Magnesium, Sulfate, Sodium, and Chloride Removals for each Membrane

Each of the membranes investigated in this research attained varying levels of removal for the constituents of interest. The substantial divalent removals achieved using membranes A and B indicate nanofiltration-like properties. On the other hand membrane C appears to yield removals expected for that of a tighter UF membrane. While the rejection data provides some indication of the membrane type, the mechanisms that drive solute mass transport are necessary to characterize the membranes. Consequently, considering size exclusion and diffusion controlled modeling techniques may be useful in describing rejection mechanisms for the HFNF technology.

Membrane Rejection Mechanisms & Transport Models

The water quality data collected in the bench-scale experiments of this research were used to determine the rejection mechanisms of the new HF membranes by applying and assessing size and diffusion controlled transport models for the prediction of magnesium and sulfate mass transfer. The mass transfer coefficients for size and diffusion-solution models were estimated for these membranes with the aid of statistical software using the data collected in the bench-scale experiments. Modeling efforts included an investigation of previously developed models, including size exclusion (SE), homogenous solution diffusion (HSD), and HSDM-FT as well as dimensional analysis to determine MTCs and predict permeate concentrations. A modified version of the HSD model is also proposed herein, and is referred to as HSD-IS, which describes the impact of ionic strength on solutes in multi-solute solutions.

Size Exclusion Model

Pressure driven membrane process are often classified based on the driving force that causes transport through the membranes. While the suitability of diffusion based models are well known to apply to SWNF and RO, UF processes can typically be described by SE. The SE model states that the feed and permeate concentrations are linearly correlated independent of flux and recovery (Zhao, 2004). Using least squares linear regression, the size exclusion constant was determined from the slope of the relationship between solute permeate concentration and solute feed concentration with forced zero intercept for each membrane. Testing solutions 1-3 were used to provide varying feed concentrations of magnesium sulfate representing varying levels of hardness.

The SE constant for magnesium for membrane A, B, and C were determined from Figure 5-6. Solute rejection for membrane A was described by the equation y=0.903x based on 84 observations yielding a coefficient of determination of 0.92. The equation describing the solute rejection of membrane B was determined to be y=0.171x. The coefficient of determination for membrane B was approximately 0.92 indicating 92% of the variation in the data could be described by the SE model. The relationship between feed and permeate concentration for membrane C behaves according to the relationship y=0.615x. The equations for membranes B and C were based on 69 observations. The coefficient of determination for membrane C was determined to be 0.98 accounting for the most variation in the data compared to the other membranes described by the SE model.
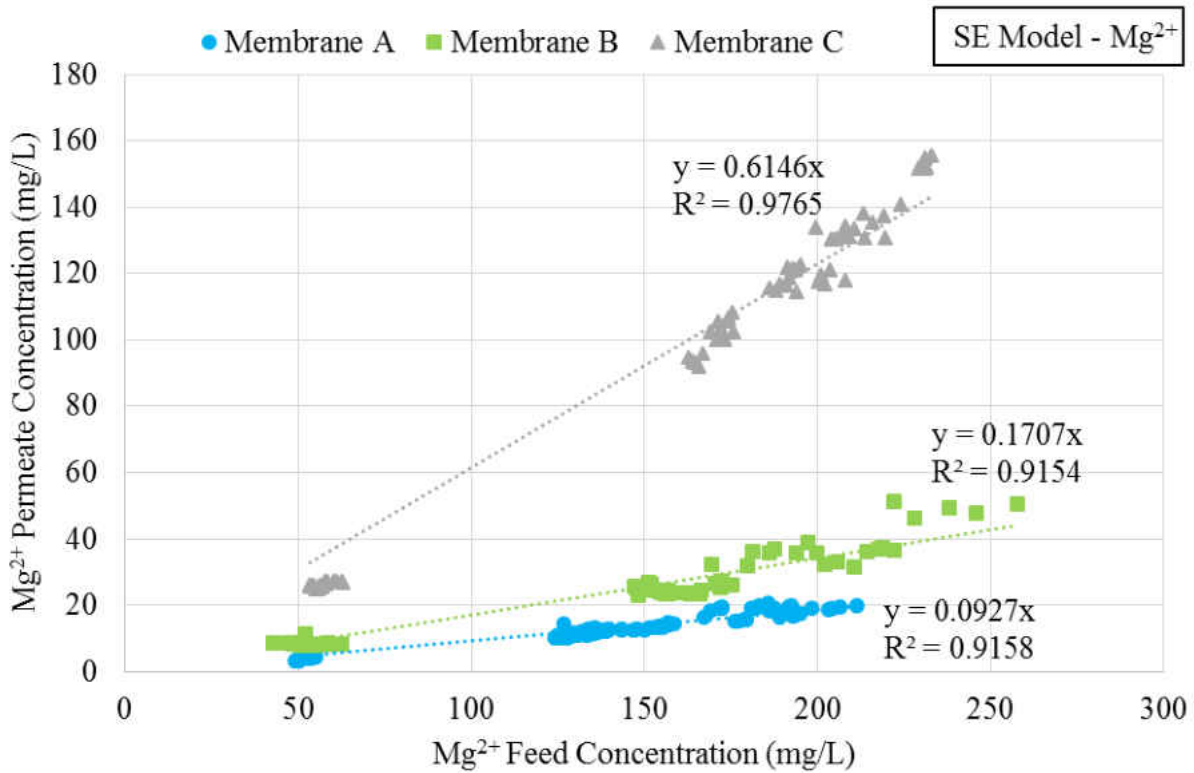
Figure 5-6: Magnesium Permeate versus Feed Concentration

The SE constants for membranes A, B, and C were also determined using sulfate data in Figure 5-7. The results are consistent with the findings from Figure 5-6 which were expected as the SE model considers mechanical sieving or steric rejection to be the dominate removal mechanism. A summary of the statistical analysis conducted with regards to the SE models has been provided in Table 5-3 including the RMSE and the RSS for both magnesium and sulfate prediction.
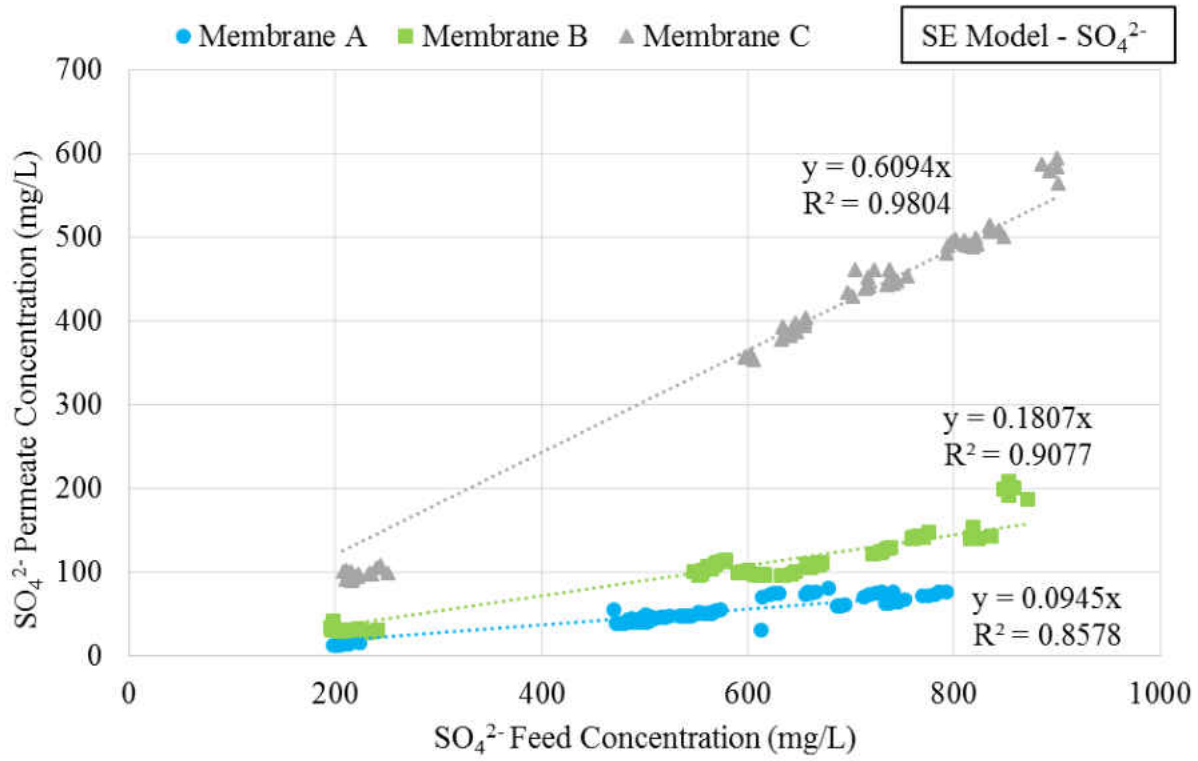
Figure 5-7: Sulfate Permeate versus Feed Concentration

Table 5-3: Summary of Regression Statistics for SEM

Membrane	No. Obs.	Magnesium Prediction		Sulfate Prediction	
		RMSE	RSS	RMSE	RSS
A	84	1	151	7	3988
B	69	3	841	15	15186
C	69	7	3369	24	39730

Homogenous Solution Diffusion Model (HSDM)

Solute mass transport can also be modeled considering the homogenous solution diffusion (HSD) theory. Parameter estimation for magnesium and sulfate was conducted by considering the relationship between solute flux and concentration gradient using Equation 3-27. The magnesium MTCs for each membrane can be determined from the slopes of the linear regressions provided in the x-y scatterplot of Figure 5-8. The magnesium MTC for membrane A was estimated to be 0.158 ft/day bases on 84 experimental observations. The experimental observations considered the solutions with varying magnesium sulfate concentrations, listed previously as solutions 1-3. The coefficient of determination for the line of best fit for membrane A was determined to be 0.97 with an RMSE of 0.2. The magnesium MTC for membrane B was calculated to be 0.318 ft/day based on 69 experimental observation indicating slightly more magnesium passage than membrane A. The coefficient of determination was determined to be 0.97 with an RMSE of 0.5. The magnesium mass transfer coefficient of membrane C was estimated to be 2.49 ft/day with a coefficient of determination of approximately 0.94. Membrane C was shown to allow the most solute passage with respect to membranes A and B. The analysis of variance output from statistical software used to perform the least squares linear regression provided the RSS, RegSS, and SST values listed in Table 5-4. Outlier analysis showed no outliers were present in the data and residual plots were normally distributed.
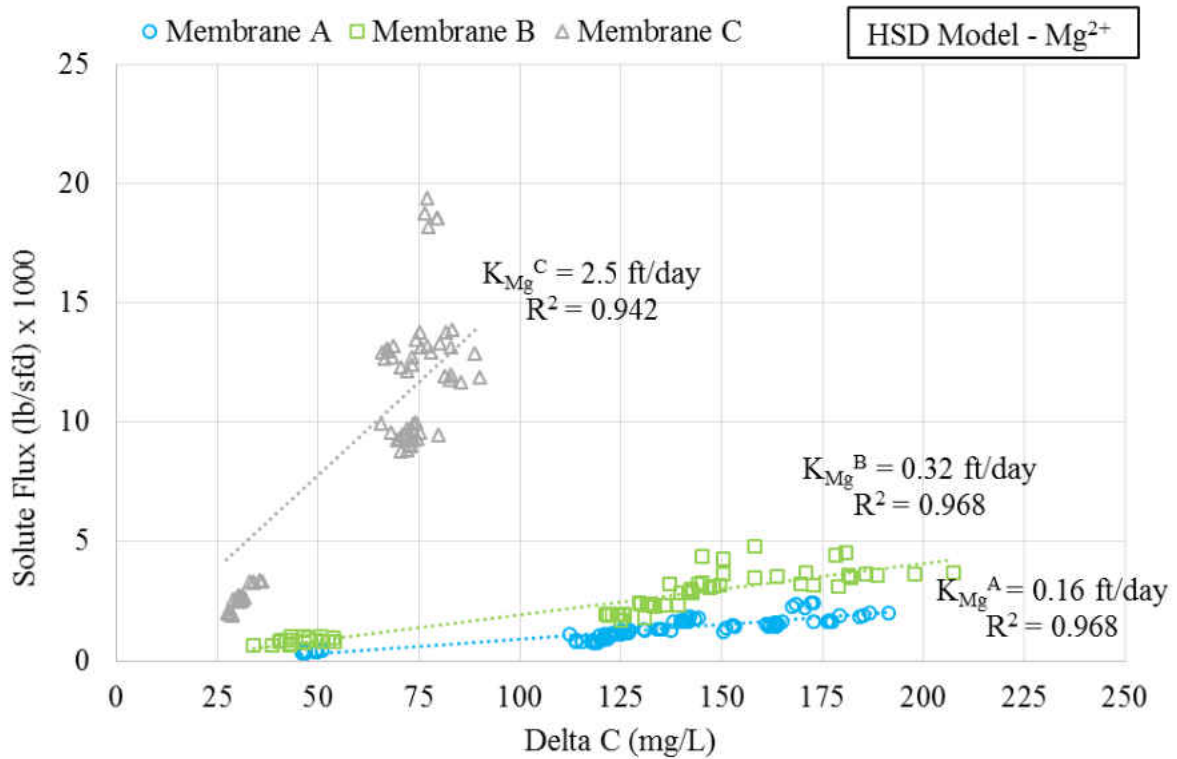
Figure 5-8: Magnesium Solute Flux versus Concentration Differential

Table 5-4: Summary of Regression Statistics for the Evaluation of Magnesium Mass Transfer Coefficients

Membrane	No. Obs.	R^2	RMSE	RSS	RegSS	SST
A	84	0.968	0.2	5	157	162
B	69	0.968	0.5	15	461	476
C	69	0.942	2.6	454	7309	7762

Similarly the MTCs for sulfate for each membrane were estimated using the HSD approach. The sulfate MTC for membrane A was determined to be 0.162 ft/day from 84 experimental observations with 97% of the variance explained by the equation y=0.162x. The MTC for membrane B was determined from 69 observations to be 0.34 ft/day. Membrane C showed the least rejection as indicated by Figure 5-9 corresponding with the magnesium removal as discussed previously. The sulfate MTC for membrane C was determined from 69 observations to be 2.45 ft/day with a coefficient of determination of 0.94. The summary of regression statistics for the determination of sulfate MTCs has been provided in Table 5-5. Comparisons of the SST indicate the estimated parameters for membranes A and B are better described by the linear regression relative to membrane C.
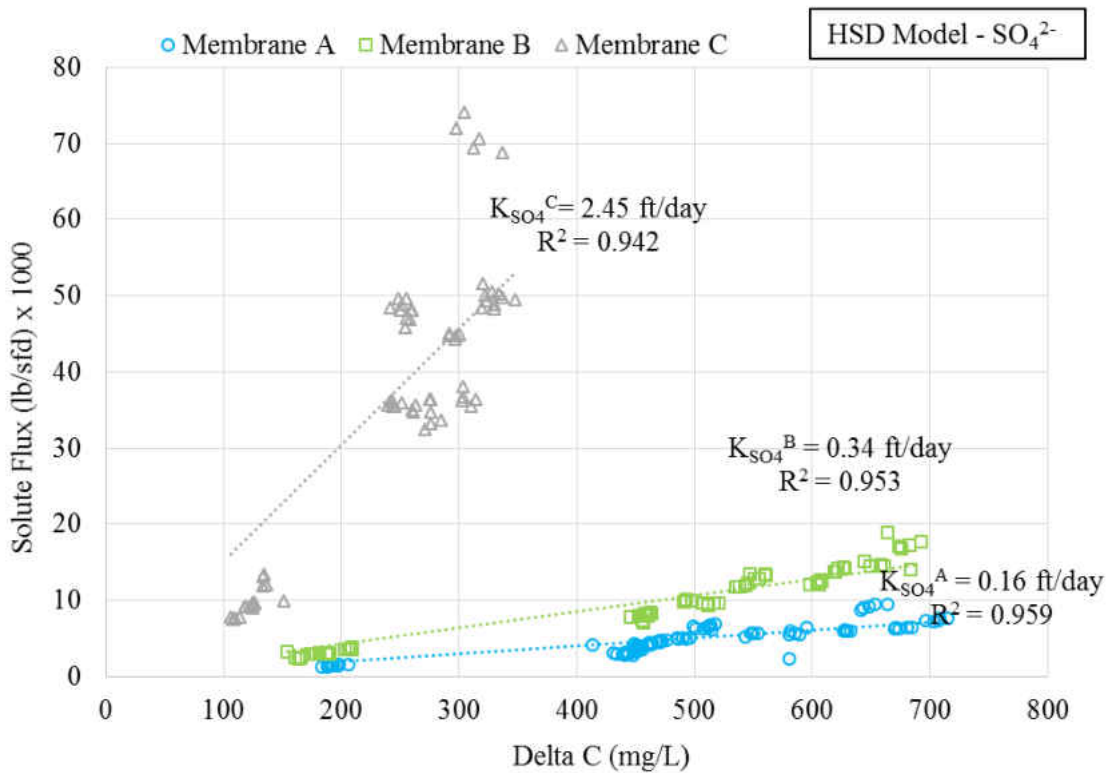
Figure 5-9: Sulfate Solute Flux versus Concentration Differential

Table 5-5: Summary of Regression Statistics for the Evaluation of Sulfate Mass Transfer Coefficients

Membrane	No. Obs.	R^2	RMSE	RSS	RegSS	SST
A	84	0.959	1.1	99	2298	2397
B	69	0.983	1.4	130	7575	7705
C	69	0.942	10	6377	103907	110283

The estimated MTCs for magnesium and sulfate were used to predict the permeate concentration using Equation 3-28 which utilizes recovery, feed concentrations, osmotic pressure, and the water MTCs for each membrane. The regression statistics for the predicted magnesium and sulfate permeate concentrations using the HSD model are provided in Table 5-6. The regression statistics indicate the descriptive models derived using the HSD approach for magnesium are better predicted than the models for sulfate. Furthermore, membranes A and B are better described by the HSD model approach than the model developed for membrane C.

Table 5-6: Summary of Regression Statistics for the HSD Model

Membrane	No. Obs.	Magnesium Prediction		Sulfate Prediction	
		RMSE	RSS	RMSE	RSS
A	84	2	362	13	190565
B	69	3	745	9	862561
C	69	9	5344	34	10663924

Dimensional Analysis

Solute mass transfer coefficients were also estimated using empirical correlations expressed in terms of Schmidt, Reynolds, and Sherwood numbers. The Schmidt numbers were calculated using Equation 3-15 which considers the solvent density and kinematic viscosity, and solute diffusion coefficient. The diffusion coefficients of single ions in infinite dilute solution were estimated using the Nernst equation provided previously as Equation 3-17. Ionic conductance for magnesium and sulfate were determined from literature as 53 cm/mol-ohm and 80 cm/mol-ohm, respectively (Perry et al., 1963). The Reynolds numbers were calculated using the solvent density, kinematic viscosity, hydraulic diameter, and the water velocity. The solute MTCs were calculated by algebraic manipulation of Equation 3-19 and Equation 3-20. The MTCs were determined for each flux set point at various water velocities for each membrane. The MTCs determined using the dimensional analysis (DA) and the Nernst diffusion coefficients for magnesium and sulfate are provided in Table 5-7 and Table 5-8, respectively. The permeate concentrations were estimated using the ionic MTC derived from the empirical relationships, the recovery, pressure and the water MTC determined for each membrane using Equation 3-28. Table 5-7 and Table 5-8 also provides a comparison of the MTCs and predicted permeate concentrations using the HSD model approach. Example calculations for the procedure discussed herein can be found in Appendix B. The data presented in Table 5-7 and Table 5-8 were used to develop predicted versus actual plots for each membrane with regards to magnesium and sulfate.

Table 5-7: Summary of Dimensional Analysis Approach for Magnesium Mass Transfer Coefficient Prediction

Type	Water Flux (gfd)	Cross Flow Velocity (ft/s)	Re	Sc	Sh	MTC (ft/day)		Cp Predicted (mg/L)		Cp Actual (mg/L)
						DA	HSD	DA	HSD	
A	9	2.03	530	1317	8	2.13	0.158	109	20	18
A	9	1.57	408	1334	8	1.94	0.158	113	21	20
A	12	1.99	518	1331	8	2.10	0.158	98	15	16
A	12	2.65	693	1332	9	2.31	0.158	88	14	13
A	12	2.43	635	1330	9	2.24	0.158	112	17	17
A	12	2.70	706	1326	9	2.33	0.158	122	19	19
A	12	3.46	903	1331	10	2.52	0.158	31	5	3
A	12	3.46	903	1328	10	2.52	0.158	34	5	4
A	15	2.27	592	1320	9	2.20	0.158	86	12	14
A	15	1.06	277	1325	7	1.71	0.158	87	14	19
B	9	3.64	950	1330	10	2.56	0.318	100	30	24
B	9	4.00	1044	1327	11	2.65	0.318	102	31	26
B	12	3.61	941	1325	10	2.56	0.318	97	26	24
B	12	2.91	759	1330	10	2.38	0.318	95	26	24
B	12	3.05	795	1322	10	2.43	0.318	119	34	32
B	12	3.30	862	1318	10	2.50	0.318	129	36	36
B	12	3.18	829	1315	10	2.47	0.318	33	9	8
B	11	3.95	1031	1313	11	2.65	0.318	33	8	9
B	15	2.45	639	1326	9	2.25	0.318	91	24	24
B	15	2.57	671	1325	9	2.29	0.318	98	26	26
C	9	2.46	642	1335	9	2.24	2.49	119	124	116
C	9	2.82	736	1318	9	2.37	2.49	125	127	121
C	12	2.96	774	1309	10	2.42	2.49	122	123	119
C	12	2.48	648	1308	9	2.28	2.49	95	98	94
C	12	3.33	868	1320	10	2.50	2.49	34	34	25
C	12	3.46	903	1309	10	2.55	2.49	36	35	27
C	12	1.81	472	1320	8	2.04	2.49	118	128	132
C	12	1.94	507	1314	8	2.10	2.49	124	134	137
C	15	0.90	234	1306	6	1.63	2.49	78	96	101
C	15	0.79	206	1304	6	1.57	2.49	78	98	106

Table 5-8: Summary of Dimensional Analysis Approach for Sulfate Mass Transfer Coefficient Prediction

Type	Water Flux (gfd)	Water Velocity (ft/s)	Re	Sc	Sh	MTC (ft/day)		Cp Predicted (mg/L)		Cp Actual (mg/L)
						DA	HSD	DA	HSD	
A	9	2.03	530	873	7	2.80	0.143	436	67	65
A	9	1.57	408	883	7	2.55	0.143	450	70	77
A	12	1.99	518	882	7	2.76	0.143	426	53	61
A	12	2.65	693	883	8	3.04	0.143	357	45	48
A	12	2.43	635	881	8	2.95	0.143	479	60	32
A	12	2.70	706	879	8	3.07	0.143	514	64	37
A	12	3.46	903	882	9	3.32	0.143	138	17	14
A	12	3.46	903	880	9	3.32	0.143	147	18	16
A	15	2.27	592	874	8	2.90	0.143	349	41	54
A	15	1.06	277	878	6	2.25	0.143	385	49	75
B	9	3.64	950	881	9	3.38	0.343	402	117	101
B	9	4.00	1044	879	9	3.49	0.343	421	124	111
B	12	3.61	941	878	9	3.37	0.343	407	108	100
B	12	2.91	759	881	8	3.13	0.343	406	108	98
B	12	3.05	795	876	8	3.20	0.343	497	136	126
B	12	3.30	862	873	9	3.29	0.343	531	146	144
B	12	3.18	829	871	9	3.25	0.343	137	35	30
B	11	3.95	1031	870	9	3.50	0.343	145	35	32
B	15	2.45	639	879	8	2.97	0.343	393	100	98
B	15	2.57	671	878	8	3.02	0.343	419	108	109
C	9	2.46	642	884	8	2.96	2.45	490	460	437
C	9	2.82	736	873	8	3.12	2.45	513	475	458
C	12	2.96	774	867	8	3.19	2.45	493	447	448
C	12	2.48	648	866	8	3.01	2.45	386	357	357
C	12	3.33	868	875	9	3.29	2.45	144	130	92
C	12	3.46	903	867	9	3.35	2.45	155	138	97
C	12	1.81	472	875	7	2.69	2.45	514	495	492
C	12	1.94	507	871	7	2.76	2.45	535	511	508
C	15	0.90	234	865	6	2.15	2.45	336	356	385
C	15	0.79	206	864	5	2.06	2.45	336	363	398

Figure 5-10A depicts the predicted magnesium concentration using the DA and the HSD approaches vs the actual permeate concentration for membrane A. The 1:1 ratio, representing an exact correlation, has been depicted as a dashed line in each figure. As seen from the Figure 5-10A, the DA approach tends to overestimate the permeate magnesium concentration for membrane A. Similar results are observed in Figure 5-10B when considering the predicted versus actual permeate concentration of sulfate. The results of membrane B are also consistent with the findings in membrane A as seen in Figure 5-11. Similar results were found by Duranceau (1990) showing the DA approach over predicted the MTCs of inorganic ions when using nanofiltration membranes. On the other hand the ionic MTCs for sulfate and magnesium calculated for membrane C show significant improvement. Both the HSD and DA approaches show fairly accurate permeate concentrations as seen in Figure 5-12A-B. The discrepancies between membranes indicate that membranes A and B exhibit nanofiltration-like removals and are better described by the HSD model, on the other hand Membrane C behaves similar to an ultrafiltration membrane with regards to removal of divalent ions.
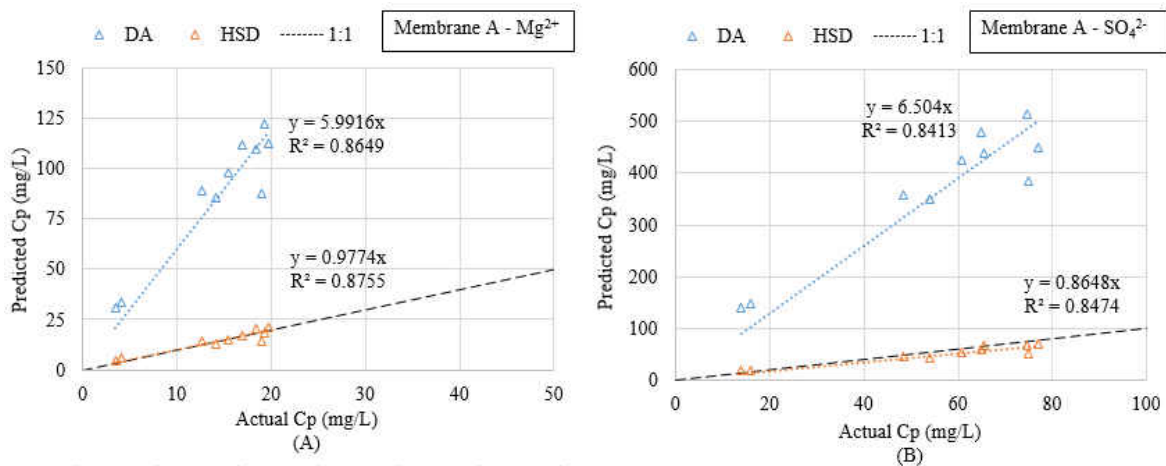
Figure 5-10: Model Comparison Magnesium (A) and Sulfate (B) for Membrane A
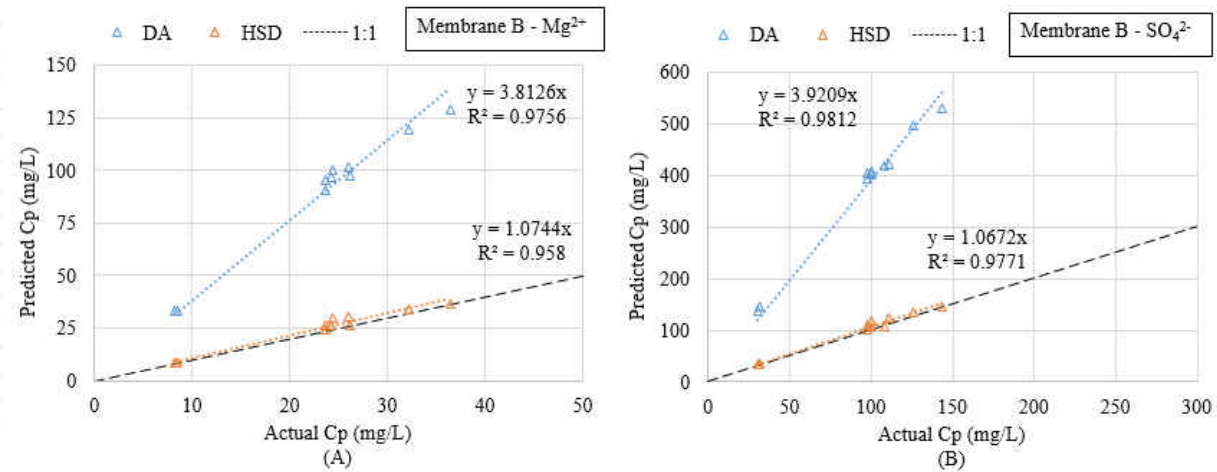
Figure 5-11: Model Comparison Magnesium (A) and Sulfate (B) for Membrane B
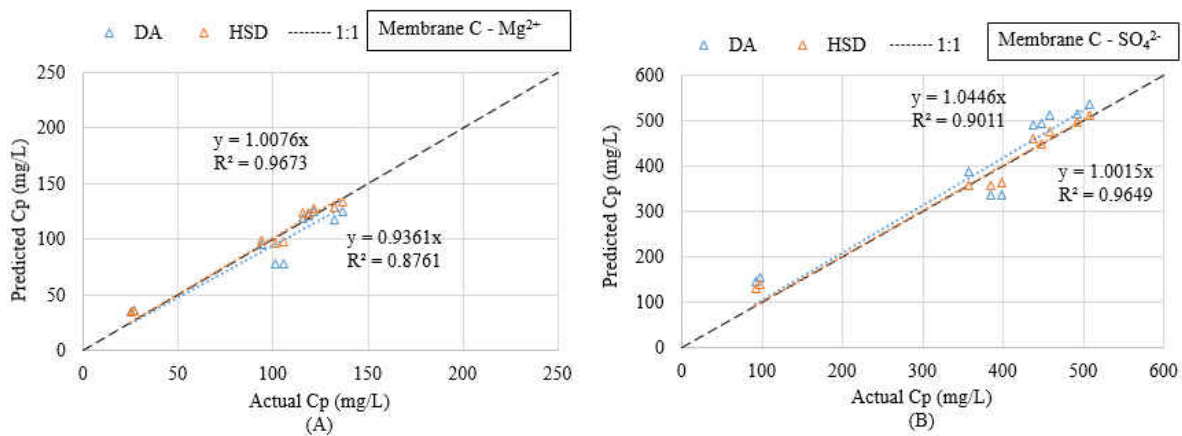
Figure 5-12: Model Comparison Magnesium (A) and Sulfate (B) for Membrane C

Comparisons between the experimentally determined MTC with those calculated theoretically show a significant discrepancy for membrane A and B. This was likely from a number of causes including the theoretical models do not consider membrane properties or the interaction effects between multiple solutes in solution. The calculation used for diffusion coefficients assumes an infinitely dilute solution but actual conditions at the membrane surface may differ for NF and RO membranes.

Concentration polarization, Donnan effects, and significant changes in the feed concentration would also affect the viscosity, density, and diffusivity of the feed solution which would influence mass transfer (Cheryan, 1986).

HSD-FT Model

Additional modeling efforts considered the effect of concentration polarization by incorporating the film theory (FT) with the HSD model (Sung, 1993). The solute back-transport MTC, k_b, for magnesium and sulfate for each membrane were estimated using laboratory bench-scale data and fitted to the HSD model using Equation 3-34. Similar studies correlated k_b values using dimensional analysis and NaCl solutions were reported by Murthy and Gupta (1997). Parameter estimation for the k_b magnesium values for Membrane A, B, and C were 69 ft/day, 128 ft/day, and 41 ft/day, respectively. The k_b values for sulfate for membrane A, B, and C were estimated to be 497 ft/day, 392 ft/day 43 ft/day, respectively. The predicted vs actual permeate concentrations for magnesium and sulfate for membrane A, B, and C have been provided in Figure 5-13 and Figure 5-14, respectively. Similar to the HSD model, the HSD-FT model accurately described the data as seen from the correlation between the model points and the 1:1 line. Membranes A and B are well fitted to the line with slightly more variation occurring from the model describing membrane C. Comparisons between the RMSE and RSS show slightly improved models when compared to the HSD descriptive models.

Table 5-9: Summary of Regression Statistics for the HSD-FT Model

Membrane	No. Obs.	Magnesium Prediction		Sulfate Prediction	
		RMSE	RSS	RMSE	RSS
A	84	2.1	376	9	7003
B	69	3.4	780	9	5489
C	69	8.6	5183	33	77066
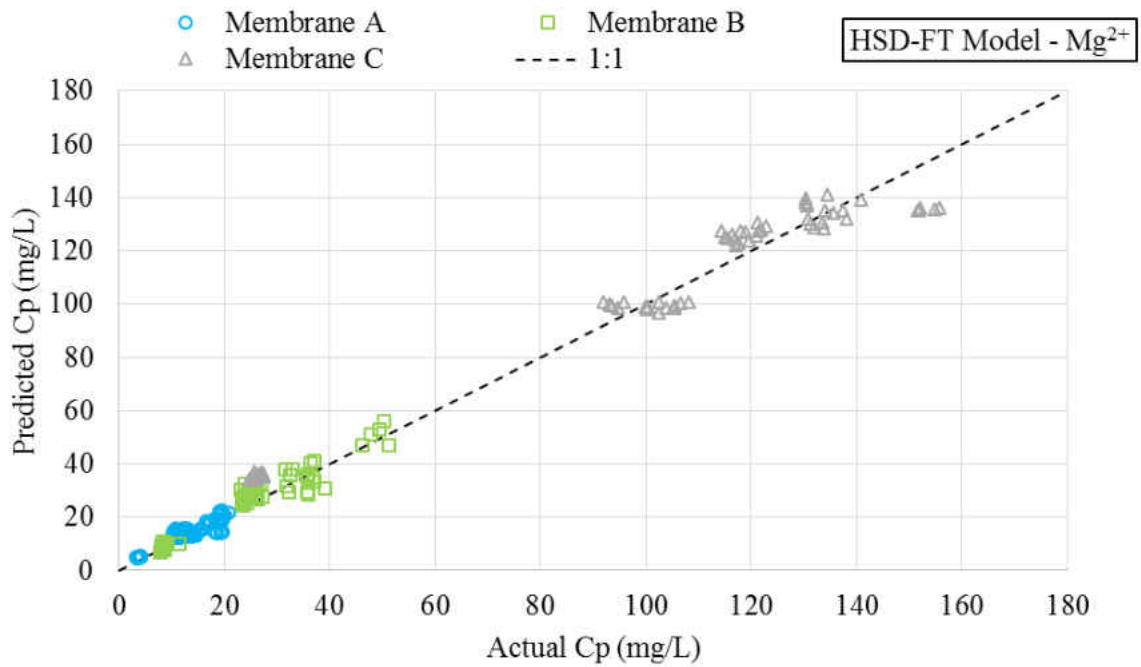
Figure 5-13: Predicted versus Actual Mg^{2+} Permeate Concentration using HSD-FT Model
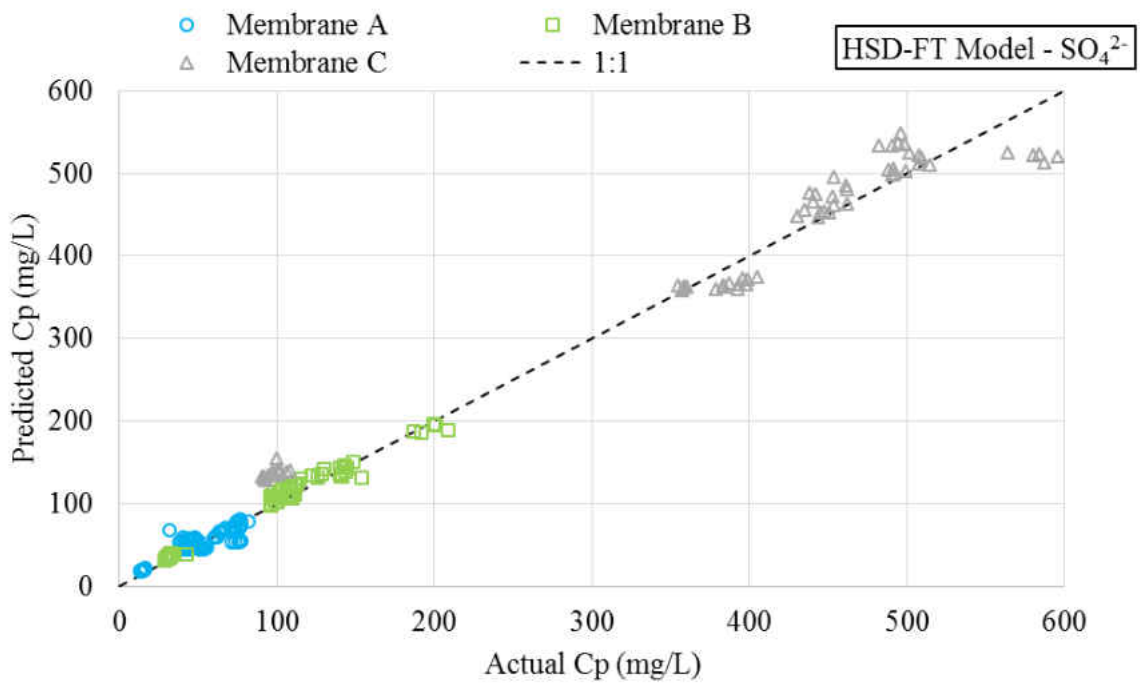
Figure 5-14: Predicted versus Actual SO$_4^{2-}$ Permeate Concentration using HSD-FT Model

While overall models were improved by incorporating concentration polarization through the use of the HSD-FT model, significant error still exists when describing the solute mass transfer. Zhao (2004) also notes the complexity of predicting solute mass transfer suggesting coefficients are also affected by the physical and chemical properties of the membrane, interface properties, module geometry and operating conditions. Significant changes in the feed concentration and composition are not accounted for in the existing models. Therefore additional experiments were performed to describe the effect multiple solutes have by incorporated additional ions to the solution in an attempt to describe fluctuations in feed water concentrations and composition.

HSD-IS Model

The previously discussed models have been developed using solutions containing magnesium sulfate (Solutions 1-3). However additional testing was conducted for each membrane using synthetic blends 4 and 5 which included the addition of sodium chloride. As discussed previously, the addition of sodium chloride showed decreased removal efficiency for each of the membranes indicating that multiple ions in solution significantly impacted solute transport. Each of the traditional size and diffusion based models investigated in this research including the SE, HSD, and HSD-FT models were used to describe the data including Solutions 1-5. Figure 5-15A displays RMSE for each model describing the permeate magnesium concentration using experimental data from solution 1-3 for each membrane. Figure 5-15B depicts the RMSE for each model when considering data collected from solutions 1-5 for each membrane. The RMSE and SS for each of the descriptive models were shown to increase indicating that the addition of solutions 4 and 5 caused the existing models to become less accurate.

A plot of predicted versus actual magnesium concentrations using the HSD model for each solution has been provided Figure 5-16. The plot confirms the data collected using solutions 4 and 5 were not described well using the HSD model. Similar results were found with the SE and HSD-FT models for magnesium as well as each of the descriptive models for sulfate.
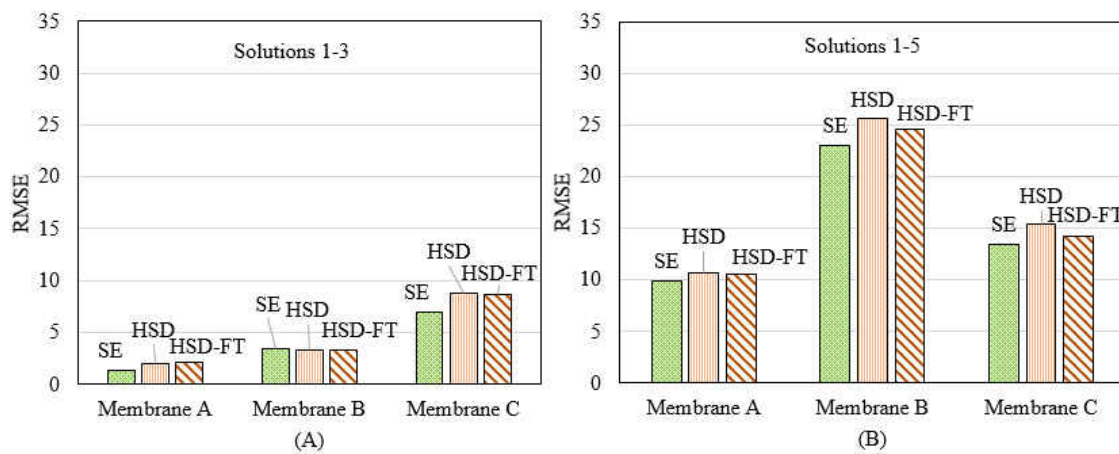
Figure 5-15: Comparison of Models for Describing Permeate Magnesium Concentration
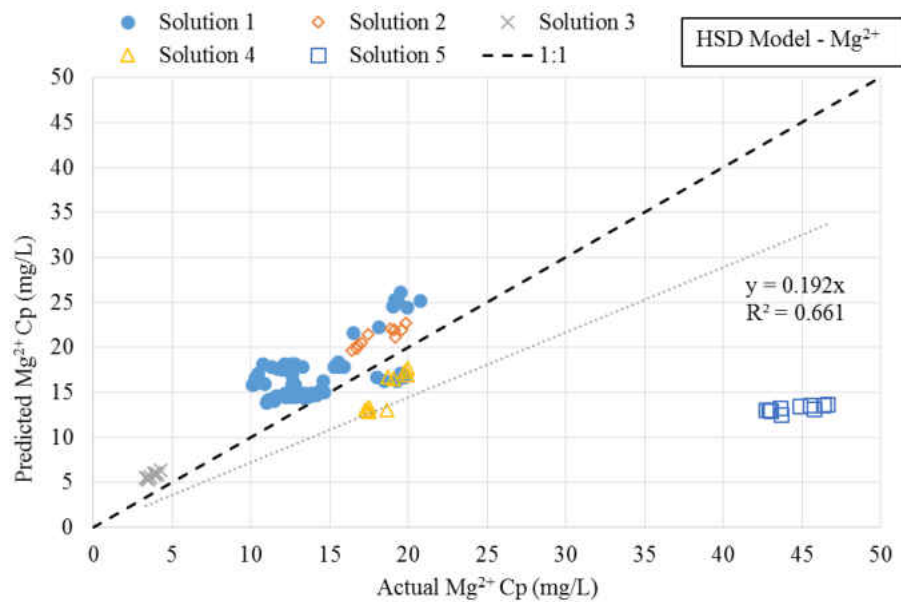
Figure 5-16: Predicted versus Actual Magnesium Permeate Concentration using HSD

In order to explain this phenomenon the effect of feed ionic strength on solute transport was considered. Few researchers have investigated the direct influence ionic strength has on solute transport in membrane processes. Yuan and Kilduff (2009) found the transport of charged fractions of NOM while primarily influenced by diffusion was largely affected by ionic strength. Sieving coefficients for charged NOM particles were shown to increase with increasing ionic strength in UF membranes. The relationship between magnesium flux and ionic strength for membrane A has been displayed in Figure 5-17. The transport of magnesium across the membrane was shown to increase as ionic strength was increased. Similar findings for divalent ion rejection were observed by Braghetta and researchers (1997).
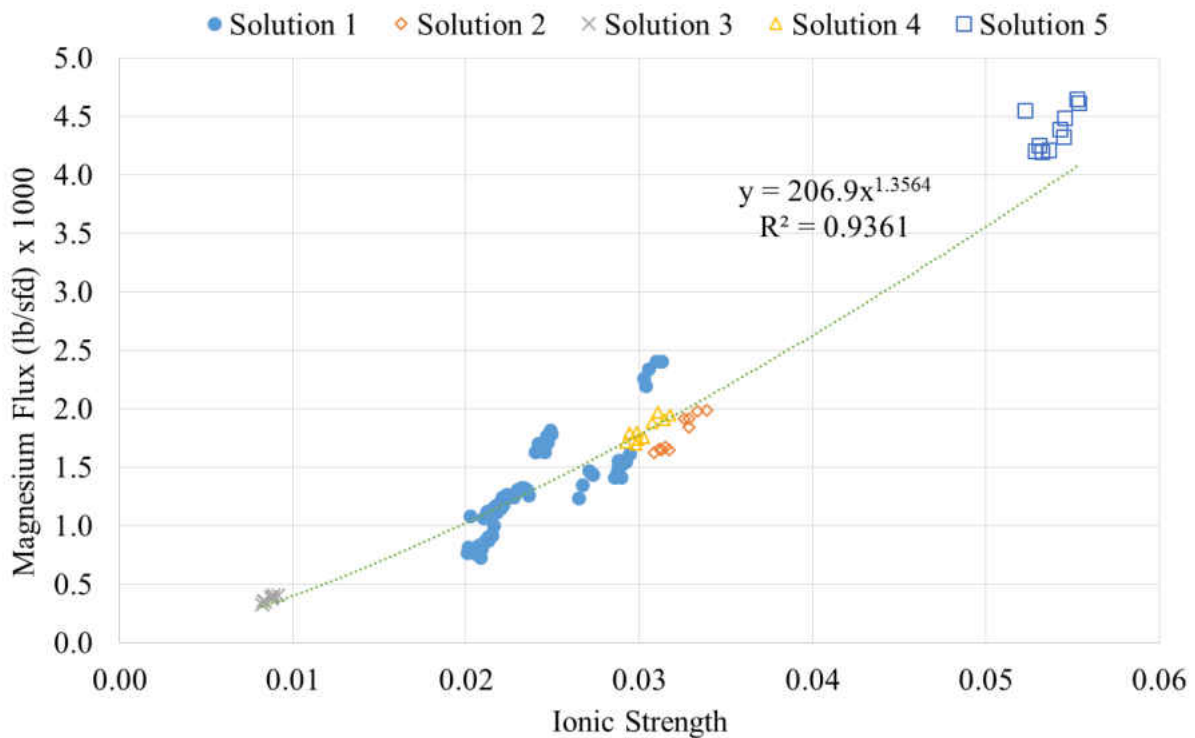
Figure 5-17: Effect of Ionic Strength on Solute Flux

Calcium rejection was shown to decrease when elevating ionic strength from 0.01 to 0.05M using NF membranes. The addition of monovalent salts (NaCl) in feed solutions has been shown to facilitate the transport of divalent ions through semipermeable nanofiltration membranes which may be explained by the reduced strength of the electrostatic double layer at the membrane surface or by the establishment of a Donnan equilibrium across the membrane. However, this effect on solute mass transport in HFNF membranes has not yet been mathematically described. Figure 5-17 depicts a parabolic relationship between solute flux and ionic strength. Therefore a parabolic term incorporating feed ionic strength was introduced to describe solute flux in addition to the solute concentration gradient term. The following derivation was developed to describe the solute transport with variations in ionic strength (IS) through the presence of sodium chloride. The model was developed using HSD theory and the Equations 5-1 through 5-6. The equations include terms for calculating water flux, solute flux, and recovery based on flow diagram provided in Figure 5-18.
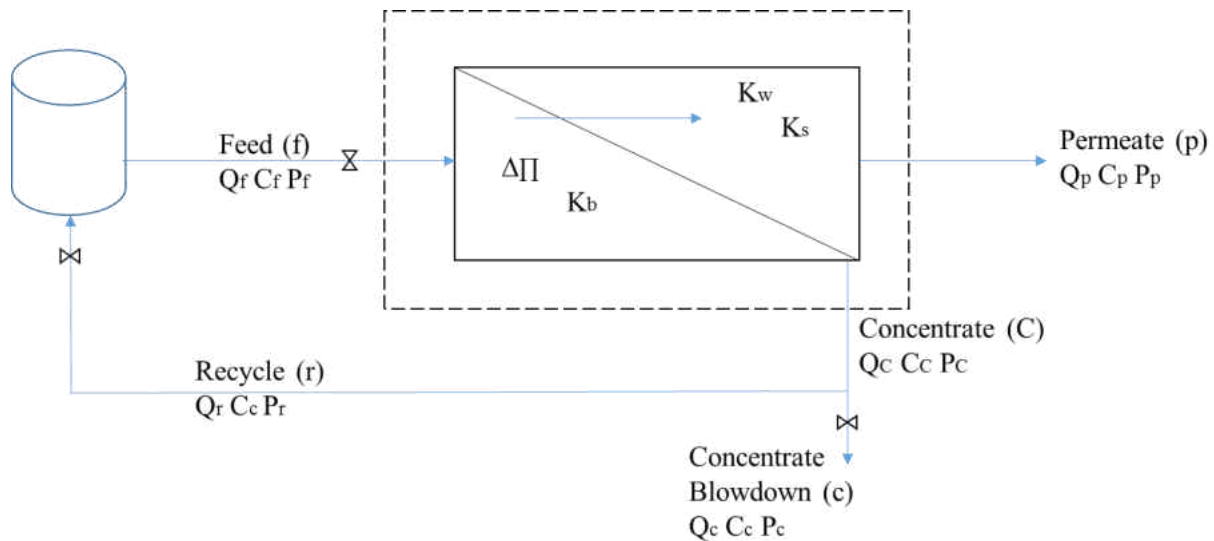
Figure 5-18: Hollow-fiber Nanofiltration Flow Diagram

$$J_W = K_w(\Delta p - \Delta \pi) = \frac{Q_p}{A}$$

(5-1)

$$J_s = K_s \Delta C + \beta_1 \mu^{\beta_2} = \frac{Q_p C_p}{A}$$

(5-2)

$$\Delta C = \left(\frac{C_f + C_c}{2}\right) - C_p$$

(5-3)

$$R = \frac{Q_p}{Q_f}$$

(5-4)

$$Q_f = Q_c + Q_p$$

(5-5)

$$Q_f C_f = Q_p C_p + Q_c C_c$$

(5-6)

The derivation of the semi-empirical HSD-IS model has been presented in steps 1 through 12.

1. Rearranging Equations 5-1 and 5-2 and equating yields:

$$J_w C_p = K_s \Delta C + \beta_1 \mu^{\beta_2}$$

2. Rearranging for ΔC and substituting Equation 5-3 produces:

$$\Delta C = \frac{J_w C_p - \beta_1 \mu^{\beta_2}}{K_s} = \left(\frac{C_f + C_c}{2}\right) - C_p$$

$$\left(\frac{C_f + C_c}{2}\right) - C_p = \frac{J_w C_p - \beta_1 \mu^{\beta_2}}{K_s}$$

3. Solving for Cc:

$$C_f + C_c = \frac{2(J_w C_p - \beta_1 \mu^{\beta_2})}{K_s} + 2C_p$$

$$C_c = \frac{2 J_w C_p}{K_s} - \frac{2 \beta_1 \mu^{\beta_2}}{K_s} + 2C_p - C_f$$

(5-7)

4. Rearranging Equation 5-5 and substituting into Equation 5-6 yields:

$$Q_f C_f = Q_p C_p + (Q_f - Q_p) C_c$$

Solving for C_f:

$$C_f = \frac{Q_p C_p}{Q_f} + \frac{(Q_f - Q_p) C_c}{Q_f}$$

$$C_f = \frac{Q_p C_p}{Q_f} + \frac{Q_f C_c}{Q_f} - \frac{Q_p C_c}{Q_f} \tag{5-8}$$

5. Substituting Equation 5-4 into Equation 5-8:

$$C_f = R C_p + + C_c - R C_c \tag{5-9}$$

6. Substituting C_c in Equation 5-9 with Equation 5-7 and simplifying:

$$C_f = R C_p + \left(\frac{2 J_w C_p}{K_s} - \frac{2 \beta_1 \mu^{\beta_2}}{K_s} + 2 C_p - C_f \right) - R \left(\frac{2 J_w C_p}{K_s} - \frac{2 \beta_1 \mu^{\beta_2}}{K_s} + 2 C_p - C_f \right)$$

$$C_f = R C_p + \frac{2 J_w C_p}{K_s} - \frac{2 \beta_1 \mu^{\beta_2}}{K_s} + 2 C_p - C_f - \frac{2 R J_w C_p}{K_s} + \frac{2 R \beta_1 \mu^{\beta_2}}{K_s} - 2 R C_p + R C_f$$

7. Rearranging to group common factors C_p and C_f yields:

$$C_f = C_p \left(R + \frac{2 J_w}{K_s} + 2 - \frac{2 R J_w}{K_s} - 2 R \right) + C_f (R - 1) + \frac{2 \beta_1 \mu^{\beta_2}}{K_s} (R - 1)$$

$$C_f + C_f (1 - R) = C_p \left(R + \frac{2 J_w}{K_s} + 2 - \frac{2 R J_w}{K_s} - 2 R \right) + \frac{2 \beta_1 \mu^{\beta_2}}{K_s} (R - 1)$$

$$C_f (1 + 1 - R) = C_p \left(R + \frac{2 J_w}{K_s} + 2 - \frac{2 R J_w}{K_s} - 2 R \right) + \frac{2 \beta_1 \mu^{\beta_2}}{K_s} (R - 1)$$

$$C_f(2 - R) = C_p \left(R + \frac{2J_w}{K_s} + 2 - \frac{2RJ_w}{K_s} - 2R \right) + \frac{2\beta_1 \mu^{\beta_2}}{K_s}(R - 1)$$

8. Solving for C_p:

$$C_p = \frac{C_f(2 - R) - \frac{2\beta_1 \mu^{\beta_2}}{K_s}(R - 1)}{\left(R + \frac{2J_w}{K_s} + 2 - \frac{2RJ_w}{K_s} - 2R \right)}$$

$$C_p = \frac{C_f(2 - R) - \frac{2\beta_1 \mu^{\beta_2}}{K_s}(R - 1)}{2 - R + \frac{2J_w}{K_s} - \frac{2RJ_w}{K_s}}$$

9. Factoring out $\frac{J_w}{K_s}$ and rearranging:

$$C_p = \frac{C_f(2 - R) - \frac{2\beta_1 \mu^{\beta_2}}{K_s}(R - 1)}{\frac{J_w}{K_s}(2 - 2R) + 2 - R}$$

10. Multiplying both sides by $\frac{K_s}{K_s}$ yields:

$$C_p = \frac{K_s C_f(2 - R) - 2\beta_1 \mu^{\beta_2}(R - 1)}{J_w(2 - 2R) + (2 - R)K_s}$$

11. Multiply both sides by $\frac{2-R}{2-R}$ yields:

$$C_p = \frac{K_s C_f - \frac{2\beta_1 \mu^{\beta_2}(R-1)}{2-R}}{J_w\left(\frac{2-2R}{2-R}\right) + K_s} \tag{5-10}$$

12. Substituting Equation 5-1 into Equation 5-10 produced the HSD-IS model provided in Equation 5-11:

$$C_p = \frac{K_s C_f - \frac{2\beta_1 \mu^{\beta_2}(R-1)}{2-R}}{K_w(\Delta P - \Delta\pi)\left(\frac{2-2R}{2-R}\right) + K_s}$$
(5-11)

The semi-empirical HSD-IS model was used to describe the experimental data including solution 4 and 5 with varying concentrations of sodium chloride. Model parameter were determined by fitting experimental data to Equation 5-11 using least squares non-linear regression. The beta1 and beta2 values for membrane A for magnesium were determined to be 257,536 and 1.63, respectively. Table 5-10 provides the model parameters for magnesium and sulfate for each membrane. Figure 5-19 depicts the predicted versus actual magnesium concentrations in the permeate stream for membrane A. By comparison of Figure 5-16, significant improvement was realized when incorporating the effect of ionic strength using the HSD-IS model.
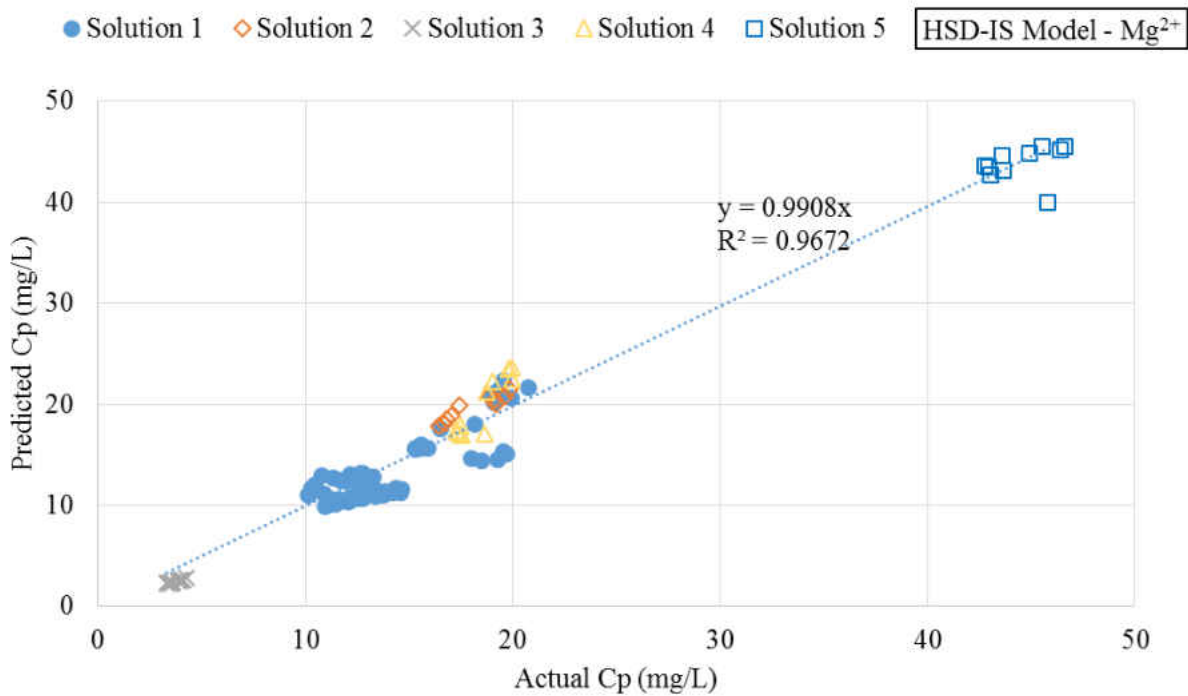
Figure 5-19: Predicted versus Actual Mg^{2+} Permeate Concentration using HSD-IS Model

Table 5-10: HSD-IS Model Parameters β1 and β2 for each Membrane

Membrane	Magnesium		Sulfate	
	β1	β2	β1	β2
A	257536	1.63	46500	0.48
B	1044640	1.83	45542	0.52
C	124462	0.68	43402	0.79

The statistical results for the regressions predicting magnesium and sulfate using the newly proposed model are presented in Table 5-11. While the mechanisms effecting facilitated solute transport are not fully understood, the incorporation of feed ionic strength to the HSD model improved overall model prediction in HFNF membranes A, B, and C when compared to previous models.

Table 5-11: Summary of Regression Statistics for the HSD-IS Model

Membrane	No. Obs.	Magnesium Prediction		Sulfate Prediction	
		RMSE	RSS	RMSE	RSS
A	105	2	371	13	18609
B	90	6	3129	19	31243
C	90	19	31122	70	436793

The development and understanding of the rejection mechanisms of individual membranes are necessary before proceeding to bench-scale wet lab testing of site specific water sources. The previous discussion identified the transport mechanisms for the three next generation HFNF membranes using synthetic solutions. Membranes A and B were best described using diffusion models while membrane C rejection was more defined by size exclusion. The rejection and performance data for each membrane were also assessed using an aerated groundwater.

<u>Bench-Scale HFNF Membrane Testing Using Aerated Groundwater</u>

The City's aerated Verna groundwater served as the testing source water for investigating membrane rejection on natural water solutions. As part of this research, the average water quality and corresponding standard deviations for select parameters of the City's aerated Verna water supply has been determined by UCF and provided in Table 5-12. The data agrees with historical values provided in Table 2-1 and includes a number of water quality constituents that are being targeted for treatment specifically calcium, magnesium, sulfate, TOC, TSS and turbidity.

Table 5-12: Verna Pilot Site Water Quality

Parameter	Units	Count	Raw Verna		
Alkalinity	mg/L as CaCO3	41	154	±	2
Barium	mg/L	53	0.14	±	0.01
Bromide	mg/L	61	< 0.20		
Calcium*	mg/L	68	125	±	7
Chloride	mg/L	61	26	±	5
Conductivity	µS/cm	41	1100	±	50
Iron	µg/L	53	3	±	2
Magnesium*	mg/L	68	60	±	3
Manganese	mg/L	53	< 0.005	±	1.36
pH	s.u.	66	7.70	±	0.05
Potassium	mg/L	68	2	±	0.1
Silica	mg/L	68	25	±	1
Sodium	mg/L	68	13	±	1
Sulfate*	mg/L	74	400	±	40
TDS*	mg/L	57	825	±	54
TOC*	mg/L	66	2.05	±	0.13
TSS*	mg/L	58	1.88	±	1.2
Temperature	˚C	41	26.9	±	0.53
Turbidity*	NTU	124	0.26	±	0.11

*Target constituent of concern

The City's concern for some of these contaminants has previously been discussed. Recall that calcium and magnesium are of concern for their contribution to the hardness of the water and the concentrations of sulfate and TDS for exceeding the secondary MCLs. While the City currently uses cation exchange for softening, NF membranes are being considered for their ability to remove hardness and divalent ions such as sulfate simultaneously. However when considering membrane softening as a treatment technique the pretreatment process becomes of significant importance. Historical and initial monitoring of the Verna water revealed significant TSS concentrations and elevated turbidity values. In addition biological testing of the Verna water supply using biological activity reaction tests and standard plate counts confirmed the presence of slime bacteria. In order to protect the membranes from fouling, a pretreatment study was conducted which implemented a parallel SF pilot to assess the performance of two distinct sand medias.

Verna Media Pretreatment Assessment

The parallel SF pilot was operated for approximately 85 runtime days over a period of four months. Filtration rates varying from 2.5 – 4.0 gpm/sf were investigated throughout the SF pilot testing. Backwashes were conducted on a weekly basis except when performing pressure accumulation tests. In this research, each media was assessed by considering turbidity removal, pressure requirements, and membrane fouling indices. The average turbidity of the Verna water has been shown to be elevated from historical levels. Additional UCF research studies have concluded that the increase in turbidity originates from various sources including biological growth. Regardless pressure vessels (PV) 1 and 2 were effective at removing turbidity to less than 0.3 NTU. As reported in Table 5-13, PV1 and PV2 achieved average turbidity reductions of 46% and 37%, respectively.

Table 5-13: Average Turbidity and Std. Deviations

Sample Location	Turbidity (NTU)	Percent Removal (%)
Raw Verna	0.44 ± 0.10	-
PV2 Coarse Sand Filtrate	0.25 ± 0.06	37 ± 14
PV1 Fine Sand Filtrate	0.21 ± 0.05	46 ± 13

Three pressure accumulation tests were conducted at distinct filtration rates to observe which media would experience greater headloss over time. The first pressure accumulation test, shown in Figure 5-22, was conducted at a filtration rate of 2.5 gpm/sf. PV1 experienced an accumulation of 0.5 psi by day 5 with an increase to 7 psi by day 9. PV2 did not experience an increase in pressure during the 10-day test. Note that pressure data for 8/30 was not collected by plant operators, but a pressure of approximately 1 psi was expected to occur within PV1. The second and third pressure accumulation tests, shown in Figure 5-21 and Figure 5-22, were conducted at filtrations rates of 3.8 gpm/sf and 3.4 gpm/sf, respectively.
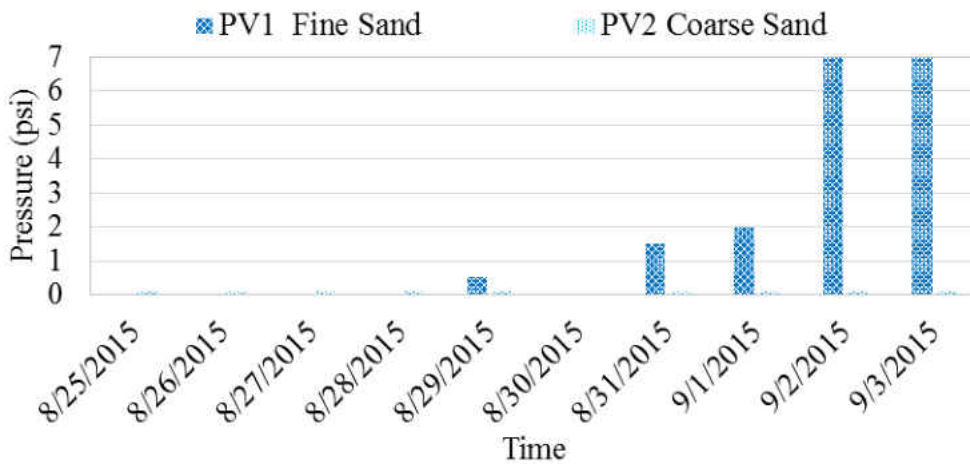
Figure 5-20: Pressure Accumulation Test (Filtration rate = 2.5 gpm/sf)

Each test consistently showed pressure accumulating in PV1 by day 7, indicating that backwashes would need to be performed to maintain productivity by day 7. On the other hand, the coarse sand in PV2 did not experienced a significant increase in pressure across the filter for each of the pressure tests. The pressure accumulation tests indicate that coarse sand was more efficient at minimizing headloss after seven days of operation. However, the water quality must also be considered before selecting a media size.
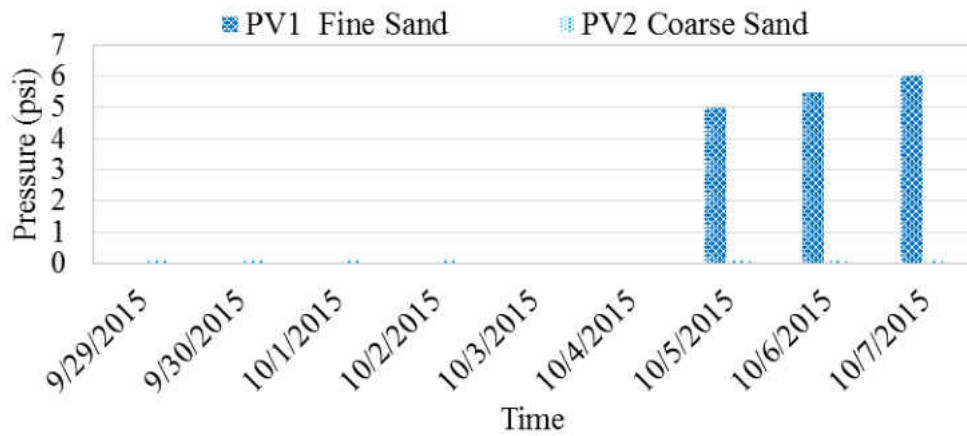
Figure 5-21: Pressure Accumulation Test (Filtration rate = 3.8 gpm/sf)
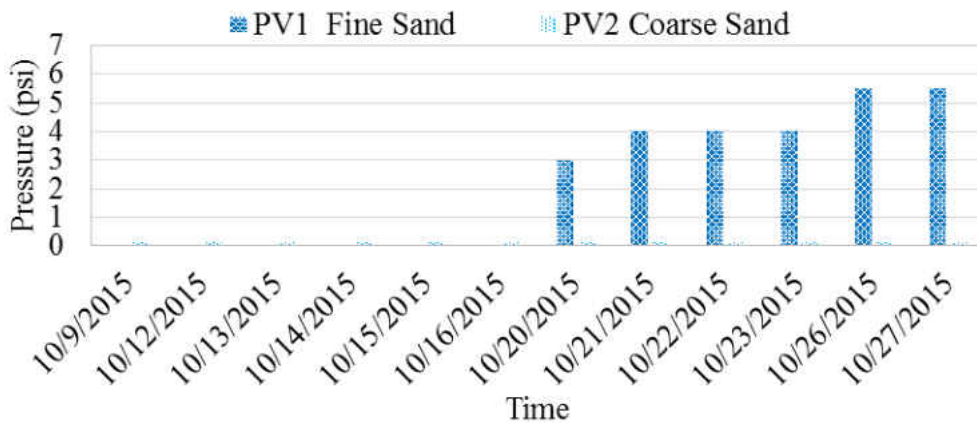
Figure 5-22: Pressure Accumulation Test (Filtration rate = 3.4 gpm/sf)

Filtration tests were conducted to develop filtration indices and determine the effectiveness of each media as a membrane pretreatment process. The results from the silt density indices are shown in Figure 5-23. The SDIs for the Verna vary from 4 to 6.1, with an average value of 5.35. SDI values for the filtrates of PV1 and PV2 are consistently lower than the raw Verna line indicating an improvement in the fouling potential of the filtered water. The average SDI value for the filtrate of PV1 and PV2 was 4.29 and 4.34, respectively. Membrane manufacturers typically recommend SDIs should be below 4 for nanofiltration membranes.
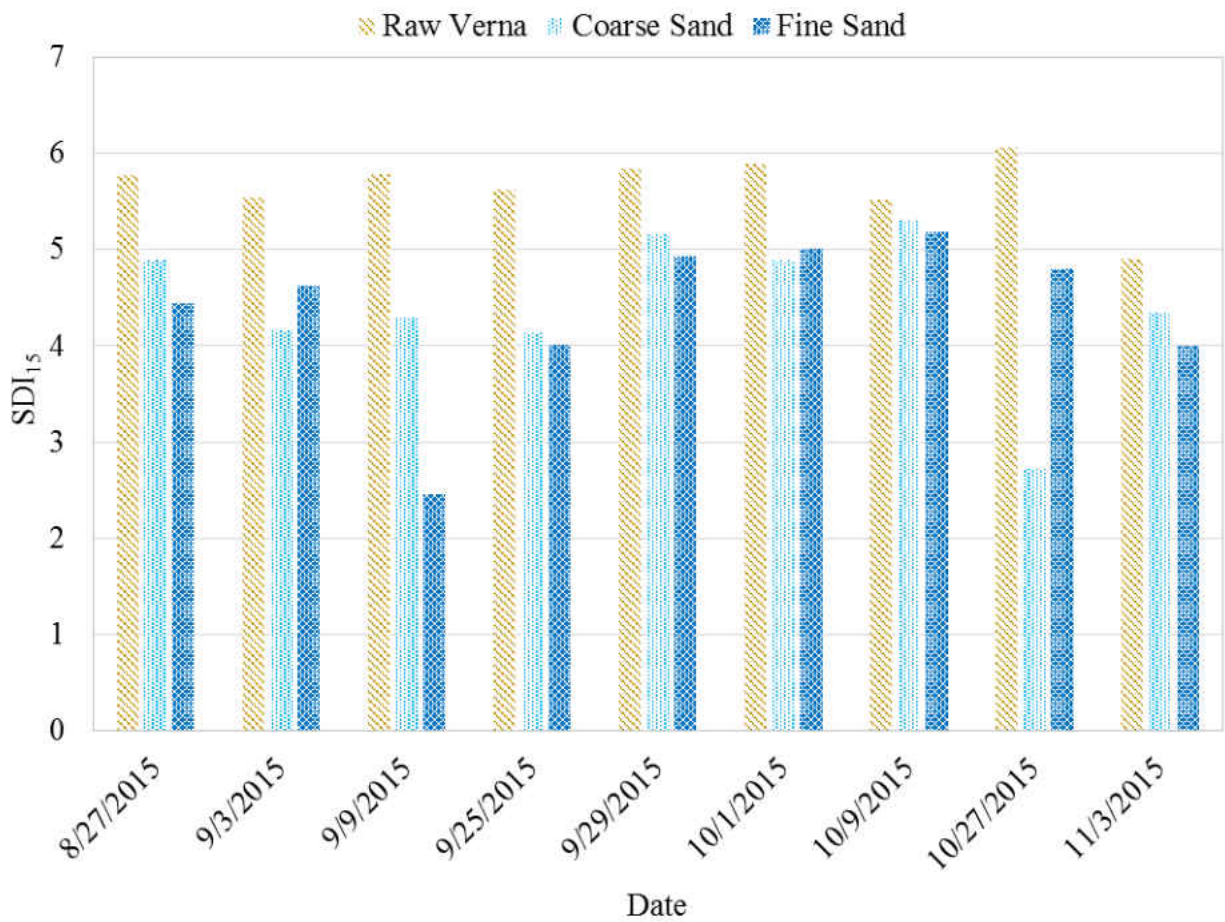
Figure 5-23: Silt Density Index Values

Alhadidi et al. (2012) found the SDI to be an unreliable fouling test and suggested the use of alternative filtration indices. However, the SDI remains a popular filtration index for estimating membrane fouling potential due to its simple design and procedure. Regardless, this research also included the use of the MPFI and MFI to estimate membrane fouling potential. Figure 5-24 plots the results of the filtration tests of the unfiltered (Raw Verna) and filtered streams (PV1 and PV2) conducted during one sampling event. The curves yielded MPFI of 1.
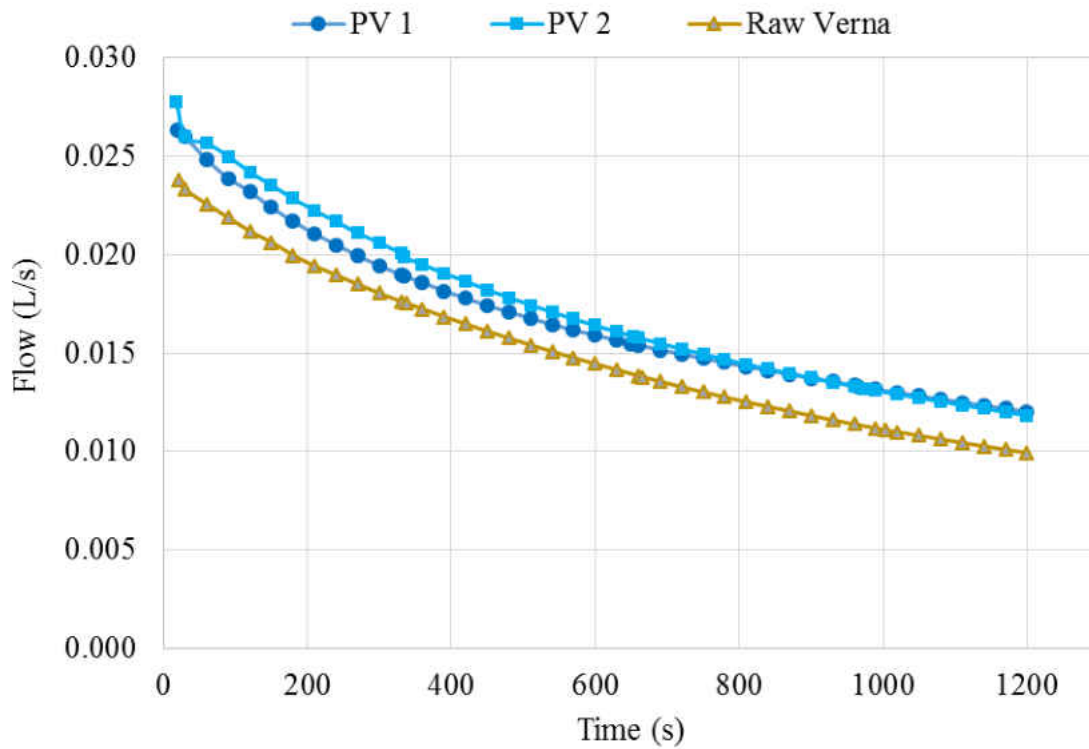
Figure 5-24: Modified Plugging Factor Index Curves

Similar to the MPFI the MFI can be determined from the slope of the linear region of the x-y scatter plot of cumulative time over volume versus cumulative volume normalized to standard viscosity and temperature. The MFIs for the Verna stream and the filtrate of PV1 and PV2 were determined for each sampling date and have been provided in Figure 5-25. The MFIs for the aerated Verna water vary significantly depending on influent water quality. On the other hand the MFIs for the filter water are consistently below 5 s/L^2. MFI values from membranes filtering water treated with the coarse sand varied from 1.9 s/L^2 to 4.3 s/L^2. MFI values from the filtrate of PV1 varied from 1.6 s/L^2 to 5.4 s/L^2. Membrane manufacturers recommend the feed water for nanofiltration and reverse osmosis membranes typically achieve less than 10 s/L^2 and 2 s/L^2, respectively.
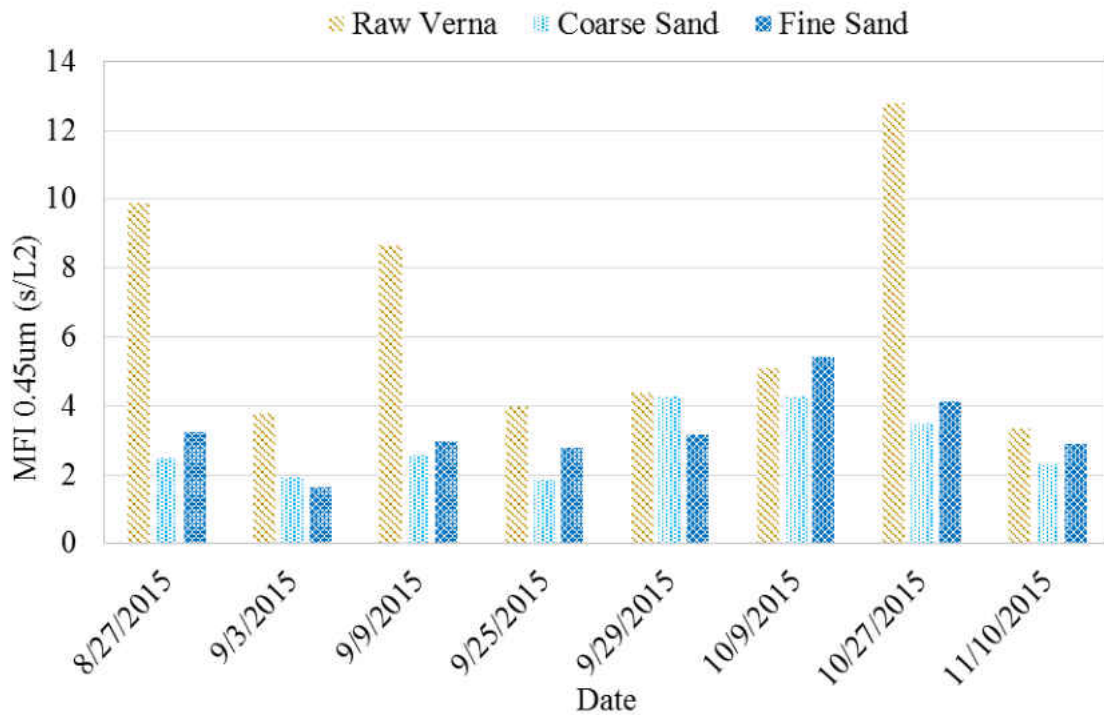
Figure 5-25: Modified Fouling Index Values

Table 5-14 provides a summary of the performance of each sand media. The difference in performance between the two medias was not statistically significant with regards to the fouling indices. However, the fine sand PV was consistently observed to accumulate larger maximum pressures during pressure testing, which indicates fine sand would require more frequent backwashes and effect overall downtime. The tradeoff in energy costs needs to be considered in conjunction with the downstream membrane processes when optimizing the performance of the overall system. The results from the pretreatment assessment of the aerated Verna water indicated that either sand media could be used for pretreating aerated Verna water for membrane treatment as long as backwashes are periodically performed. Therefore the water used for bench scale hollow fiber membrane testing was a composite sample from both sand filters effluents.

Table 5-14: Average SDI and MFI Summary

Sample Location	SDI_{15}	MPFI	$MFI_{0.45\mu m}$	Max Pressure (psi)
Raw Verna	5.5	1.70×10^{-4} L/s^2	5.4 s/L^2	-
Course Sand	4.3	1.07×10^{-5} L/s^2	3.3 s/L^2	< 0.5
Fine Sand	4.3	1.10×10^{-5} L/s^2	3.9 s/L^2	5.5-7.0

Time Utilization & Operating Conditions

The sand filtered aerated Verna water was collected in batch samples and transported to the UCF laboratories for membrane testing. A total of 15 bench-scale experiments were conducted on the pretreated aerated Verna groundwater. The bench-scale membrane testing of the aerated Verna served as a screening analysis for additional testing to be conducted on the pilot-scale.

System Water Production & Water Recovery

The bench-scale membrane testing unit was operated with conditions similar discussed in the previous section. Permeate flows were targeted at 25 and 31 mL/min, while concentrate flows varied from 5.5 to 31 mL/min to produce membrane recoveries of 50%, 75%, and 85%. Feed pressures varied between 20 and 40 psi depending on membrane and permeate flows. Table 5-15 provides a summary of the operating conditions tested throughout this study.

Table 5-15: Operating Pressure and Flow Ranges for Experimental Testing

Type	Run / Test	Feed Pressure (psi)	Concentrate Pressure (psi)	Permeate Pressure (psi)	Feed Flow (gpm)	Concentrate Flow (mL/min)	Permeate Flow (mL/min)
A	70 – 73	24 – 40	21 – 39	0	0.4 – 0.7	5.5 – 10.5	25 – 31
B	66 – 69	30 – 38	23 – 37	0	0.4 – 0.8	5.5 – 10.5	25 – 31
C	59 – 65	31 – 38	30 – 37	0	0.3 – 0.8	5.5 – 31	25 – 31

Water Flux & Water Mass Transfer Coefficient

Each membrane was tested under two flux settings. Fluxes of 12 and 15 gfd were targeted during bench-scale testing of aerated Verna water. The water mass transfer coefficients for membranes A, B, and C were determined to be 0.40 gal/sfd-psi, 0.43 gal/sfd-psi and 0.34 gal/sfd-psi, respectively. The MTCs for membranes A and C when treating Verna groundwater decreased slightly compared to the permeability values obtained when testing synthetic water. Furthermore this decrease in permeability was most significant for membrane B, decreasing from 0.75 gal/sfd-psi to 0.43 gal/sfd-psi indicating plugging or fouling may have occurred.

System Water Quality

The water quality goals of the City for treating their aerated water supply specifically include organics, calcium, magnesium, and sulfate reduction. However the water quality parameters investigated during the bench-scale membrane screening analysis also included turbidity and additional cation and anion analysis to characterize the membranes. The Verna water was pretreated for TSS and turbidity removal using sand filtration however some turbidity was still present in the sample water. Each membrane showed additional turbidity removal, producing permeates with turbidities less than 0.1 NTU. Suspended solids analysis showed removals of 92% for membrane C and 99.9% removals for membranes A and B.

TOC was used as a surrogate to measure the amount of natural organic matter (NOM) within the water samples (Wallace, Purcell et al., 2002). Although the TOC concentrations in the Verna groundwater are relatively low (< 3 mg/L), organics have been shown to react with oxidants to form carcinogenic byproducts (Chang, Chiang et al., 2001; Fang, Yang et al., 2010; Rook, 1974) and therefore are of concern for producing drinking water. The average TOC of the filtered Verna water was approximately 2 mg/L. The average TOC removals for each membrane are provided in Figure 5-26. Membranes A and B achieved the highest retention of organics yielding permeate concentrations of 0.24 and 0.26 mg/L. Membrane C rejected 66% of the influent TOC producing a permeate TOC concentration of less than 0.9 mg/L.
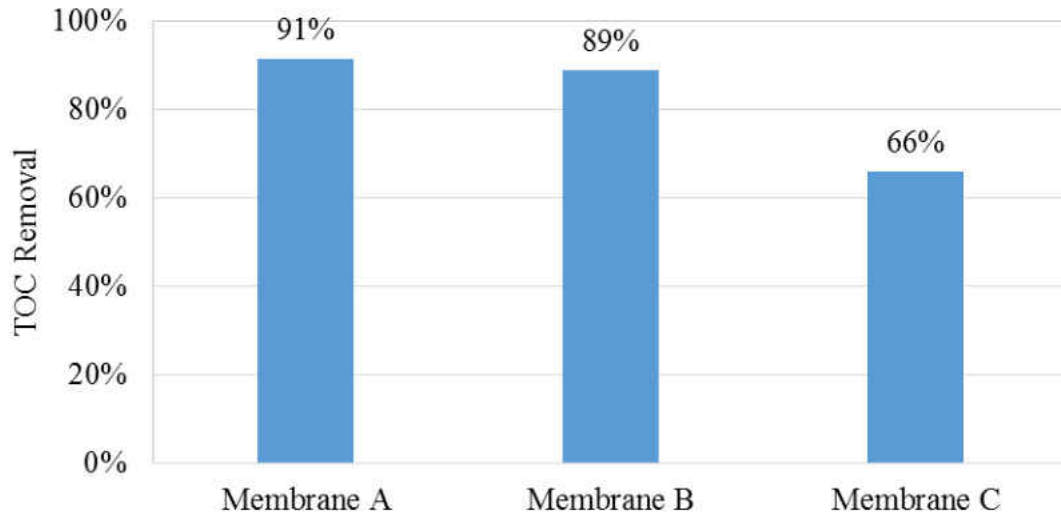
Figure 5-26: Average TOC Removals

Additional organics analysis included the use of a spectrofluorometer for characterizing the TOC using fluorescence. EEM analysis was conducted on the pretreated (aerated and media filtered) Verna water as well as the permeate samples from membranes A, B, and C. The results of the EEM analysis are provided in Figure 5-27. Significant removal of fluorescent matter was achieved for each membrane. However, membrane A appeared to have the most rejection followed by membrane B and membrane C. These results were analogous to the TOC removal data. Neither membrane A, B, nor C appeared to have a preferential removal of a particular region of the EEM plot.
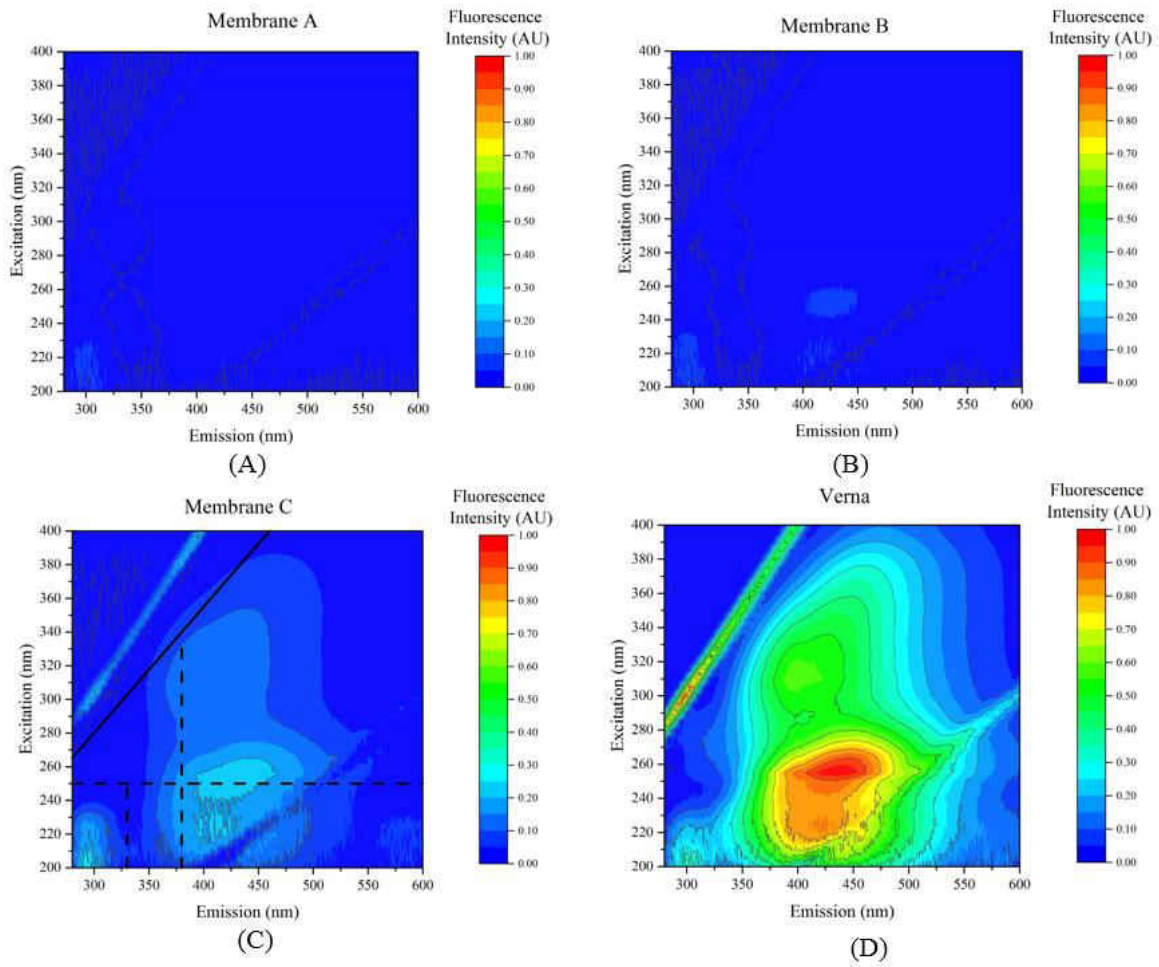
Figure 5-27: EEM Analysis for (A) Membrane A Permeate (B) Membrane B Permeate (C) Membrane C Permeate (D) and Raw Verna

The feed and permeate conductivities for each experimental run have been plotted on Figure 5-28. Recall that initial runs were performed using membrane C which decreased the conductivity of the water by 27%. Note the feed water conductivity and subsequently the permeate conductivity were shown to increase slightly over the course of each run due to the implementation of the recycle stream in the experimental design. Membranes B and A also decreased the conductivity of the samples by approximately 60% and 70%, respectively. The decrease in conductivity implies rejection of dissolved inorganic constituents such as metals and anions.
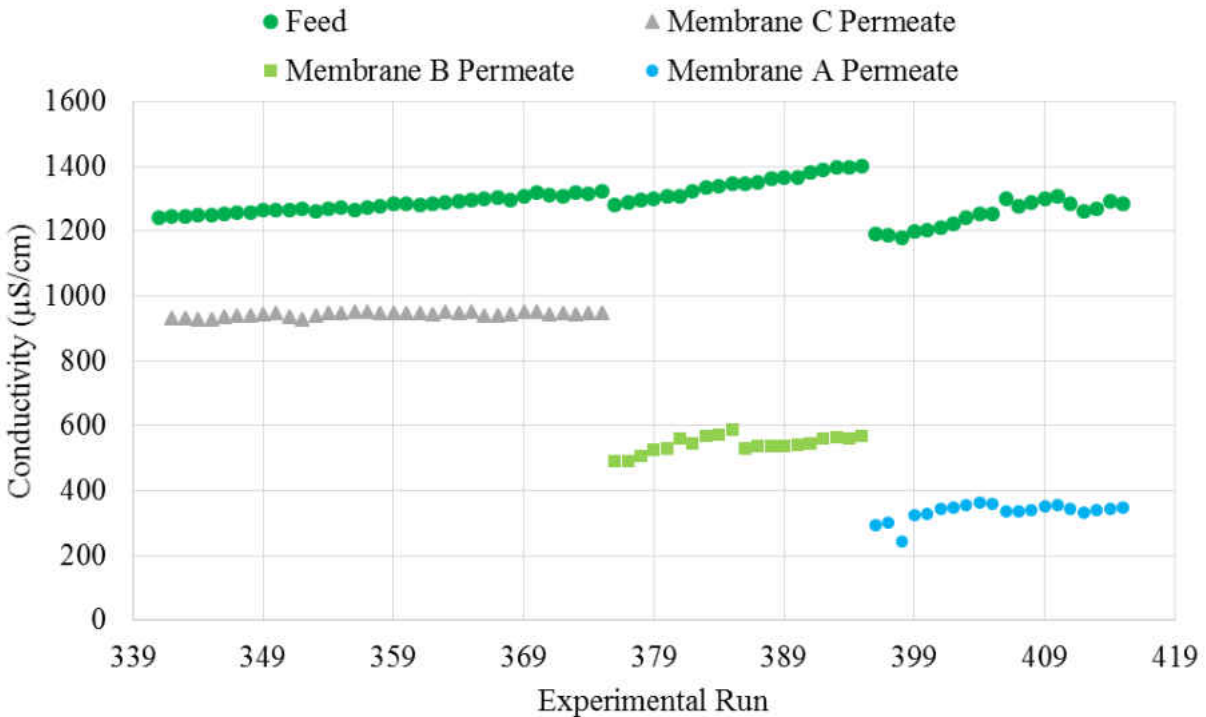
Figure 5-28: Conductivity Removal during HFNF Bench-scale Membrane Testing

Additional analysis was conducted to confirm and quantify the removal of dissolved ionic species. Figure 5-29 shows substantial removals of divalent ions specifically magnesium, sulfate and calcium. Membrane A removed over 90% magnesium and sulfate with 85% calcium reduction. Partial monovalent retention with regards to silica and chloride was also achieved. Membrane B achieved over 60% reduction in divalent ions with 25% chloride removal. Similar to bench-scale tests conducted with synthetic water, membrane C was the least effective at divalent ion removal, retaining 30% of the hardness and 40% sulfate. Overall average TDS rejection for membrane A, B, and C were 82%, 66%, and 27%, respectively. Bench-scale membrane testing was useful in evaluating the usefulness of next generation HFNF membranes for treatment of aerated sulfide-containing groundwater for the removal of sulfate, hardness, TDS, and TOC. Additional pilot testing was conducted to confirm removal capabilities of such constituents and assess hydraulic performance of a HFNF membrane at the City's WTF.
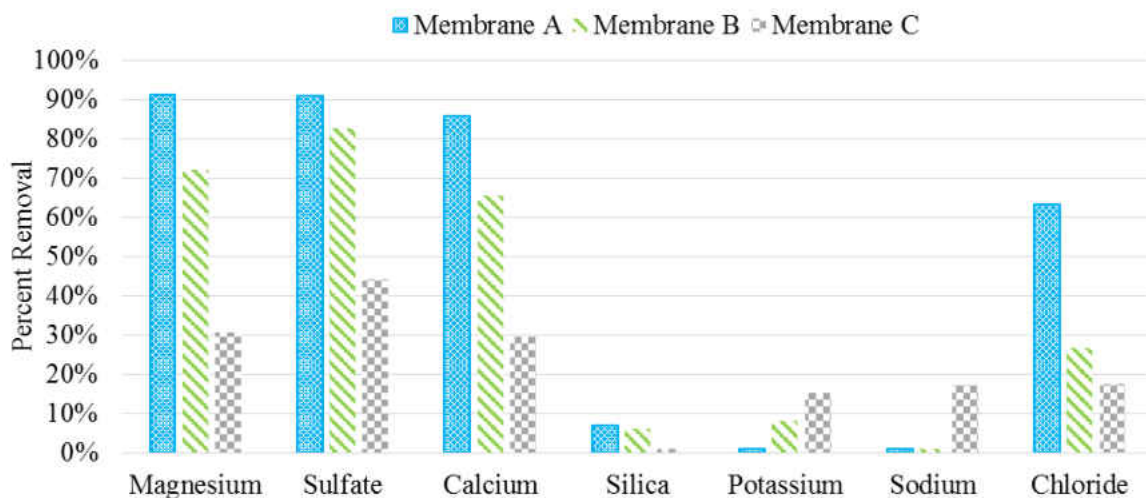
Figure 5-29: Average Inorganic Removals for each Membrane

112

Pilot-Scale HFNF Membrane Testing Using Aerated Groundwater

This section discusses the characterization of the HFW1000 membrane (Pentair X-Flow, The Netherlands) by assessing the HFNF membrane pilot performance with respect to hydraulic operations and water quality. The HFNF pilot was installed at the City's drinking water facility for treatment of the biologically active aerated Verna groundwater supply. Hydraulic assessments were conducted by determining pressure requirements, membrane permeability, and monitoring trends in TMP. Membrane performance was also analyzed with regards to water quality parameters, specifically the mass transfer and removal of sulfate, turbidity, and TOC. Table 5-16 provides a summary of the feed pressure, recoveries, and pretreatment requirements assessed during the pilot testing phase of this research.

Table 5-16: HFNF Pilot Settings

Setting	Recovery	Pressure (psi)	Pretreatment
1	50%	High (120)	Sand filter - Strainer
2	50%	Moderate (60)	Sand filter - Strainer
3	50%	Low (15)	Sand filter - Strainer
4	75%	Low (15)	Sand filter - Strainer
5	85%	Low (15)	Sand filter - Strainer
6	50%	Low (15)	Strainer
7	85%	Low (15)	Strainer

The single module pilot was operated with a cross-flow configuration under seven different settings. This approach was undertaken to obtain preliminary process optimization data by assessing the impacts on HFNF membrane performance under multiple operating conditions. The feed pressure requirements of the HFNF membrane were assessed in the first three settings. By the end of setting 3 the systematic reduction in the operating pressures was completed, providing three distinct operating pressures at a fixed recovery of 50%. Settings 4 and 5 provide a comparison of how the pilot performed under two recoveries with relatively constant flux. The last two settings (6 and 7) were conducted to identify how pilot performance was affected by removing the SF pretreatment.

Time Utilization & Operating Conditions

The operation of the HFNF pilot commenced on June 25th, 2013 and was operated with minimal interruptions until final shutdown occurred on October 1st, 2013. The total runtime included 2,074 hours over the course of nearly 100 days. Runtime refers to the time the pilot is either in forward filtration mode, backwash mode, or CEB mode. It does not include the time it took to perform pressure decay tests, clean in place events, or additional pilot maintenance. Pilot downtime was experienced due to one scheduled event and two unavoidable events. The distribution of runtime and downtime has been illustrated in Figure 5-30. The first downtime event was strategically planned and occurred between July 5th and July 11th, 2013. The pilot design supplied by the manufacturer was constrained hydraulically and modifications were conducted to incorporate a more versatile design, which allowed for recoveries, water production, and pressures to be varied.
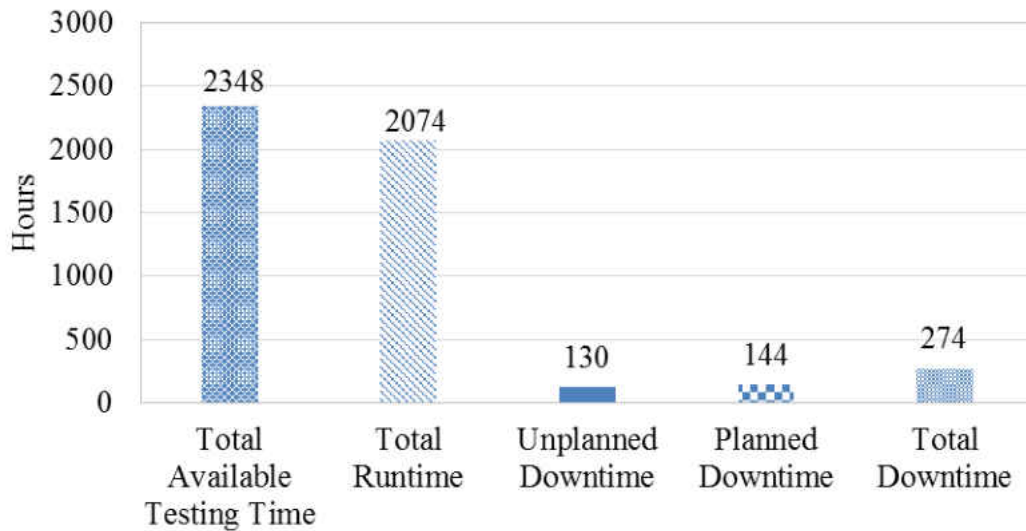
Figure 5-30: Distribution of Total Available Runtime and Downtime Events for HFNF Pilot

On July 19th, 2013 and a runtime hour of 428, the HFNF pilot data logger and acquisition system ceased to operate resulting in four days of hydraulic data loss. The HFNF pilot was taken offline to troubleshoot the data logger and repair piping which had experienced localized leaks during operation. The HFNF pilot resumed stable operation on July 23rd, 2013 after piping repairs were complete. Unfortunately, repairs to the data logger were unsuccessful therefore manual readings were conducted 3 to 4 times daily for the remainder of the pilot testing experiments. The maintenance hours on the data logger and piping along with the accumulation of sand filter backwash hours accounted for a total of 130 hours of unplanned downtime. Additional pilot information has been provided in Appendix A, including sand filter backwash log, HFNF membrane pilot parameter log list, and a field log summarizing the HFNF pilot system events.

System Water Production & Water Recovery

The SF pilot operated in declining rate rapid filtration mode and was backwashed when necessary to produce sufficient feed water to the HFNF pilot. Backwashes were typically conducted on a weekly basis for a duration of 30 minutes. The sand filter was operated in down-flow filtration during normal operations and up-flow filtration during backwashes. The sand filter filtrate was used as the feed to the HFNF pilot and the backwash water was directed to the City's wastewater system. The HFNF pilot was operated in an inside-out cross-flow configuration with up-flow filtration and an internal recycle stream. It had the ability to perform backwashes using down-flow filtration if cleanings where necessary. A flow schematic of the HFNF pilot has been provided in Figure 5-31.
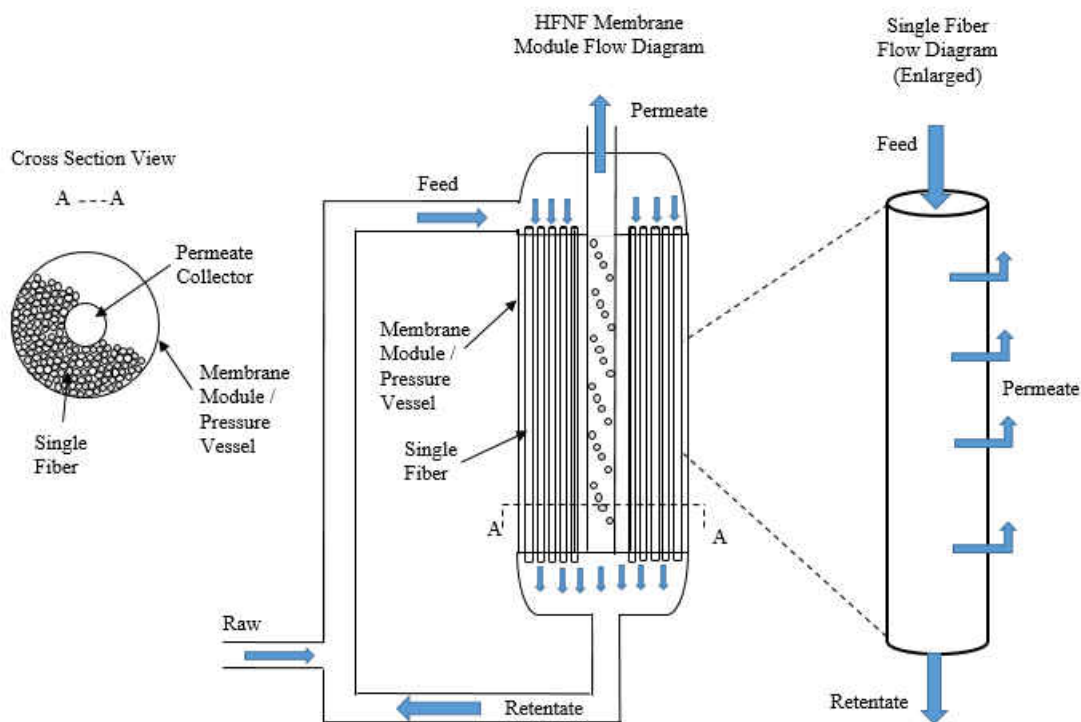
Figure 5-31: Flow Distribution Diagram for HFNF Pilot

116

Traditional SWNF membranes operate at feed pressures of approximately 100 psi. In contrast, typical feed pressures for HFUF systems operate in the 4 to 22 psi range (Nakatsuka et al., 1996; Sethi et al., 2000). The HFNF pilot under investigation in this research was tested under various pressures to determine the impact operating pressure had on pilot performance. The pressures for the feed, concentrate, and permeate streams were recorded and plotted to produce Figure 5-32. The first setting on the HFNF pilot operated at an average feed pressure of 120 psi, a conservative permeate flowrate of 3 gpm, a recovery of 50%, and incorporated a backpressure of approximately 110 psi on the permeate stream. The use of backpressure on the permeate stream was implemented to meet the manufacturer's design specifications for operating the next generation membrane.

Although typical membrane systems do not operate with significant pressures on the permeate stream, limitations in the pilot design required the use of backpressure for initial testing. Modifications to the pilot unit were performed which increased the functionality of the HFNF pilot by eliminating backpressure and consequently reducing operating pressures. Pressures were reduced in two intervals referred to as settings 2 and 3. Throughout the duration of settings 1 and 2 the flow measurements were validated by manually performing timed bucket tests. By the end of setting 2, modifications were performed on the pilot to allow the system parameters to be monitored visually by inspecting the analog flow meters and pressure gauges. Testing under setting 2 conditions began at runtime hour 243 as depicted by the vertical dashed line in Figure 5-32.
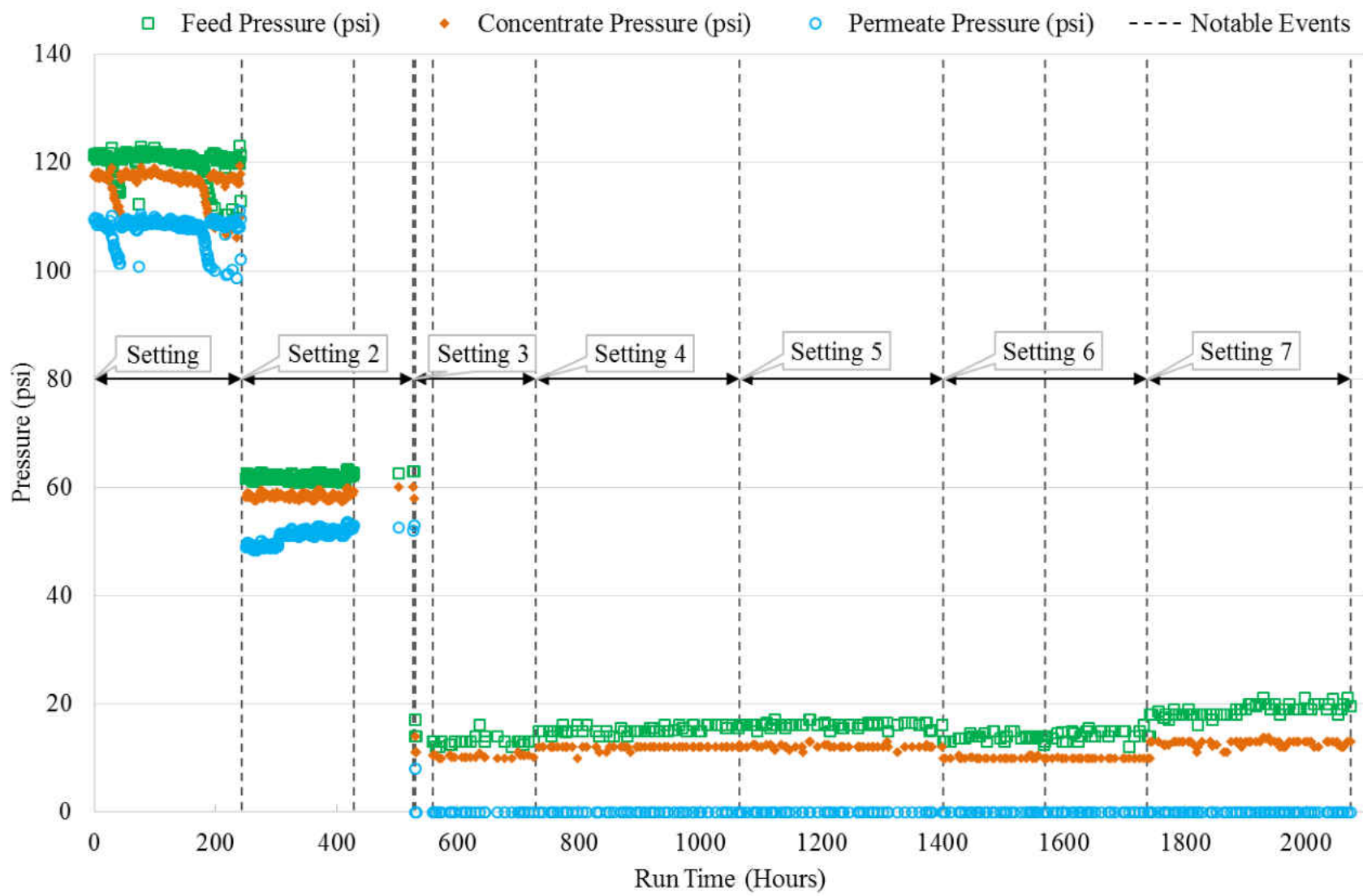
Figure 5-32: HFNF Pilot Operating Pressure Requirements

Decreasing the backpressure resulted in a 50% reduction (60 psi) in feed pressure of the system. The pilot was tested under these conditions until a runtime of 527 hours. The data logger was damaged during this setting as seen from the absence of pressure data in between the runtimes of 428 and 527 hours of Figure 5-32. After attempts to replace the data logger failed, operation resumed and manual recordings were initiated. At a runtime of 530 hours, the third pressure adjustment (setting 3) was completed reducing the backpressure to atmospheric conditions and the feed pressure to 15 psi.

The remaining experiments were conducted without implementing permeate backpressure, which decreased operating pressures and energy requirements. Settings 4 and 5 operated at a permeate flow rates of 4 and 5 gpm and recoveries of 77 and 85%, respectively. Feed pressure requirements for settings 4 and 5 were approximately 16 psi. During setting 6 the recovery was decreased to 50% and the sand filter removed as a pretreatment step. Feed pressure requirements decreased and returned to 14 psi which was similar to pressure requirements required under setting 3 conditions. The final setting targeted a recovery of 85% with a permeate flow rate of approximately 5 gpm. Operating without sand filter pretreatment caused operating feed pressures to increase to approximately 19 psi. The average operating pressures and flows for each setting have been provided in Table 5-17. Recoveries of 50%, 75%, and 85% were targeted in this research but differed slightly due to the mechanical operation and variability of the pilot controls.

Table 5-17: Averaged HFNF Pilot Parameters for Each Testing Setting

Setting	Runtime (hours)	Feed Pressure (psi)	Concentrate Pressure (psi)	Permeate Pressure (psi)	Feed Flow (gpm)	Concentrate Flow (gpm)	Permeate Flow (gpm)
1	0-243	120	117	108	49.5[b]	2.4[a]	2.9
2	243-527	62	58	51	49.5[b]	2.4[a]	3.0
3	527-729	13	10	0	49.5	3.9	3.9
4	729-1,065	15	12	0	50.5	1.5	4.9
5	1,065-1,401	16	12	0	50.7	0.9	5.0
6	1,401-1,738	14	10	0	48.7	4.0	3.8
7	1,738-2,074	19	13	0	47.9	0.8	4.9

[a] Concentrate flows were determined using bucket tests
[b] Feed flow assumed to be constant due to pilot limitations

Water Flux & Mass Transfer Coefficient

Despite hydraulic and technological limitations of the pilot skid, flux values of 10, 13, and 17 gfd were achieved during operation of the pilot. The permeate flow, feed temperature, and pressures across the membrane were recorded and used to calculate the flux, TMP, and permeability of the membrane. The flux, feed temperature, TMP, and normalized specific flux has been plotted to produce Figure 5-33. The TMP and mass transfer coefficient of water, also referred to as the specific flux, are monitored over time to assess membrane fouling and permeability.

Note the specific flux was normalized to 20 °C using Equation 3-10 but was not adjusted for the change in osmotic pressure when producing Figure 5-33. In constant production systems, increasing trends in TMP could indicate the occurrence of membrane fouling due to plugging or

the accumulation of materials on the membrane surface. In addition, decreasing trends in the specific flux indicates a decrease in the permeability of the membrane with regards to water which could also indicate membrane fouling. The TMP and specific flux is often monitored to determine backwash frequency, cleaning regiments, and fiber breakage. During the first 383 hours of runtime, the pilot was operated to produce a water flux of 10 gfd. The TMP during the operation of setting 1 was approximately 10 psi. Setting 2 operated with an average TMP value of approximately 11 psi until a correction to the permeate back pressure was performed at a runtime of 306 hours as seen in Figure 5-32. Therefore, the abrupt decline in TMP to 8 psi was not indicative of fiber breakage but rather a change in the operation. During setting 3, permeate production was increased to 4 gpm yielding a flux of 13 gfd and a TMP increase of 2 psi. Settings 4 and 5 operated at a flux of 17 gfd but the pilot experienced a slight increase in the TMP and decrease in specific flux corresponding with the system's recovery adjustment which occurred at runtime hour 1065.

Operating conditions for setting 6 were similar to setting 2, that is, a recovery of 50% and a flux of 13 gfd but without SF pretreatment. During setting 6 at runtime hour 1,570, a decrease was observed in the flux that corresponded to a slightly lower value than anticipated for the originally planned set point. The pilot was adjusted to correct the difference in flux from 12 gfd to 13 gfd as denoted in Figure 5-33 by the vertical dashed line. Setting 7 was also operated without the use of SF pretreatment. TMP increased to an average of 16 psi during while operating at a flux of 17 gfd without pretreatment. TMP varied over the course of the study from approximately 8 psi during setting 2 to a maximum of 17 psi during setting 7.
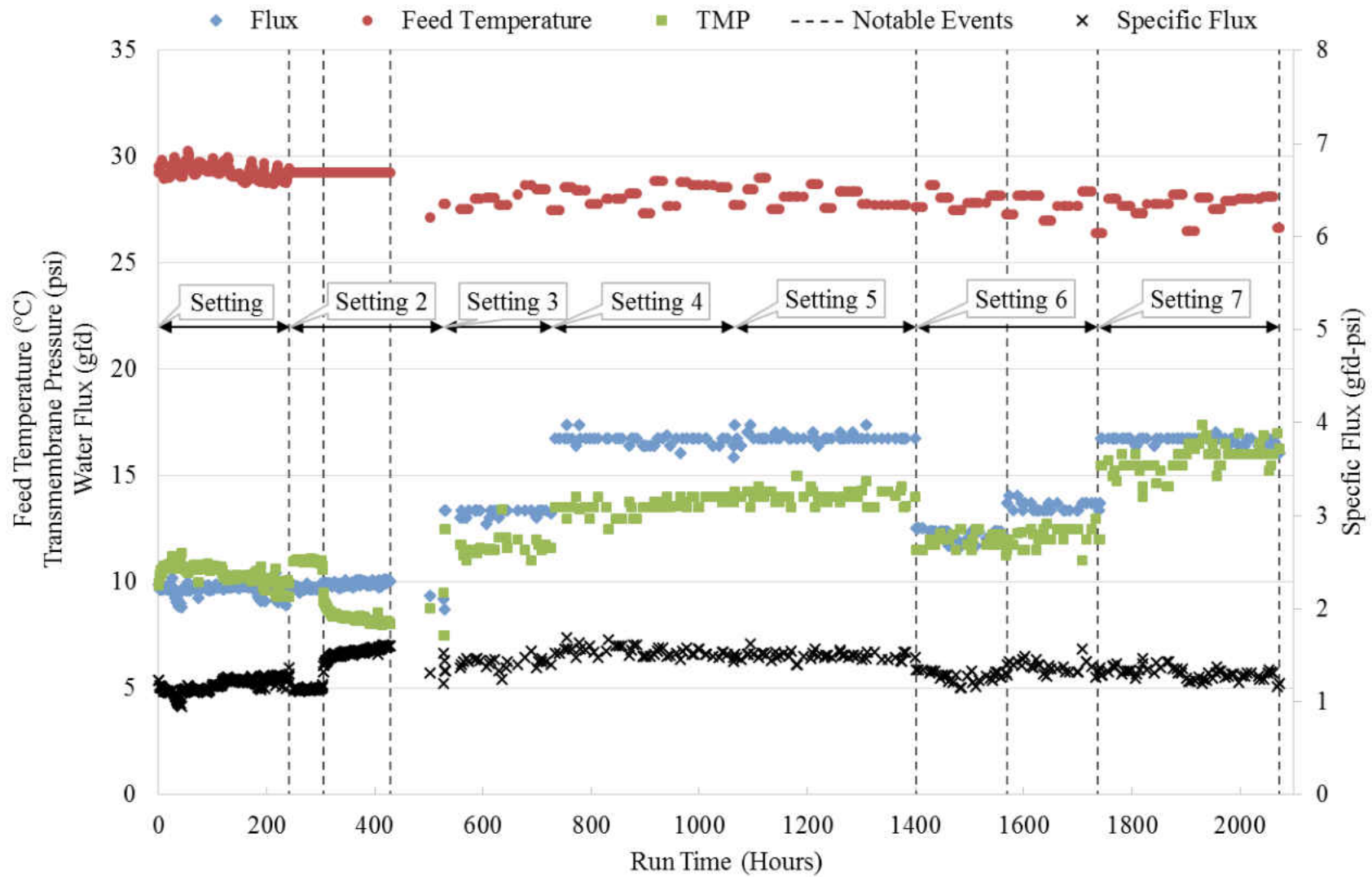
Figure 5-33: HFNF Pilot Operating Conditions

However, since the pilot hydraulics were manually adjusted throughout the study, significant differences in the measured TMP from setting to setting does not necessarily indicate fouling. Rather significant trends in TMP and specific flux within the setting intervals would illustrate fouling but were not observed. The average hydraulic parameters for each setting including recovery, water flux, TMP and temperature corrected water MTCs have been listed in Table 5-18. Example calculations for each of the hydraulic parameters have been provided in Appendix B.

The operating conditions for settings 6 and 7 were compared to settings 2 and 5, to assess the effect the SF pretreatment had on the hydraulic parameters of the membrane. Average TMP and specific flux values between settings 2 and 6 were similar indicating that fouling did not occur while operating at a flux of 13 gfd. On the other hand, hydraulic comparisons between settings 5 and 7 showed a 14% increase in TMP when operating at a flux of 17 gfd, but significant trends in specific flux or TMP were not apparent in the data therefore implementation of backwashes and cleanings were not necessary to maintain stable operation.

Table 5-18: Calculated Hydraulic Parameters Averaged for Each Testing Setting

Setting	Runtime (hours)	Recovery	TMP (psi)	Flux (gfd)	Normalized Specific Flux (gfd/psi)
1	0-243	50%	10	10	1.2
2	243-527	54%	9	10	1.4
3	527-729	50%	12	13	1.4
4	729-1,065	77%	14	17	1.5
5	1,065-1,401	84%	14	17	1.5
6	1,401-1,738	49%	12	13	1.3
7	1,738-2,074	86%	16	17	1.3

The mass transfer coefficient of water for a single stage membrane system can also be estimated using HSD theory by plotting the water flux versus the transmembrane pressure differential as shown in Figure 5-34. In this method the mass transfer coefficient of water was corrected for temperature and osmotic pressure using Equation 3-9 and Equation 3-11. The MTC was determined from the slope of the x-y scatter plot using linear regression as 0.94 gal/sfd-psi or 0.054 days^{-1}. The coefficient of determination, R^2, was determined to be 0.989 indicating that nearly 99% of the variation could be described by the regression line. The number of observations in the linear model was 60 data points. The root mean square error (RMSE), sum of squares for error (SSE), and total sum of squares (SST) and were calculated to be 1.5, 127, and 11949, respectively. The hydraulic performance of the HFW1000 membrane indicated the membrane was more permeable than membrane B tested on the bench-scale. Water quality analysis was conducted to determine if similar removals would confirm the findings and determine if the membrane could be used to meet the water quality goals of the City with regards to sulfate and hardness removal.
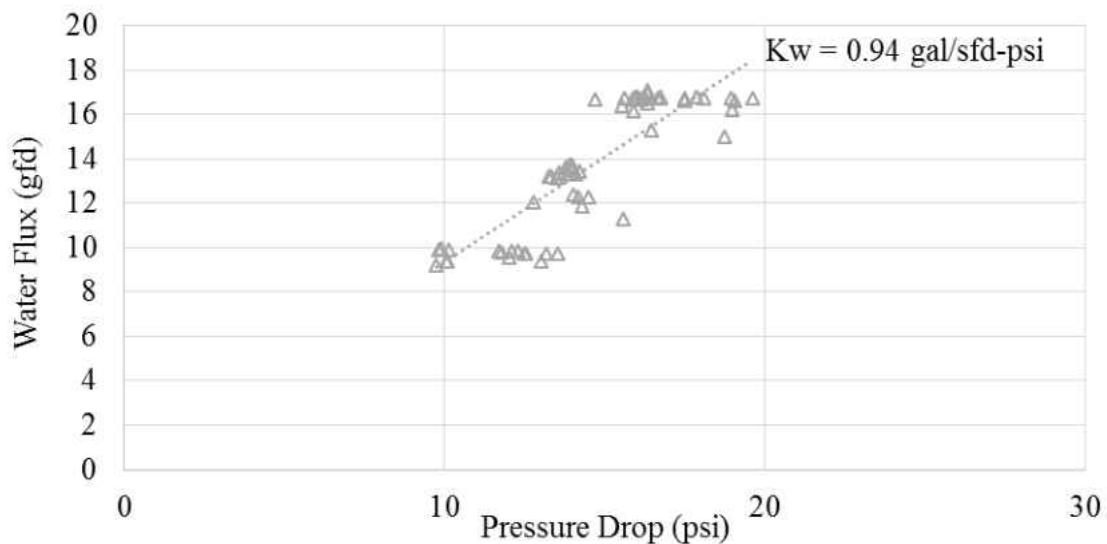
Figure 5-34: Water Flux versus Transmembrane Pressure Differential

System Water Quality

The HFNF pilot system was sampled a minimum of 5 times per week for water quality analysis. Sample locations were identified in Figure 4-6 and included the aerated Verna water, sand filter filtrate, membrane feed, concentrate, and permeate. The field water quality analysis included turbidity, conductivity, pH, temperature, and alkalinity. Figure 5-35A through Figure 5-35D describe the water quality parameters measured in the field for the feed and permeate streams of the HFNF pilot. Recall that the HFNF pilot was initially operated with SF pretreatment. The vertical dashed line in Figure 5-35A-D represent the date the SF pretreatment was bypassed.

The HFNF membrane consistently produced permeate with turbidity values less than 0.2 NTU regardless of the SF pretreatment. On average, the membrane achieved 44% turbidity removal indicating rejection of suspended solids and particles in the feed stream. Conductivity is a measure of the waters ability to conduct electrical current and is affected by the concentration, type, size, and valence of ions in the water as well as the temperature. A number of researchers have correlated the conductivity of the water with the TDS concentration (Atekwana, Atekwana et al., 2004; Thirumalini & Joseph, 2009).

The linear relationship approximating TDS and electrical conductance (EC) was proposed by Lloyd and Heathcote (1985) and is given in Equation 5-12. EC is measured in either microsiemens per centimeter (μS/cm) or microohms per centimeter ($\mu\Omega$/cm) with correlation factors (k_e) varying between 0.55 and 0.8 (Atekwana et al., 2004).

$$TDS = k_e EC \tag{5-12}$$
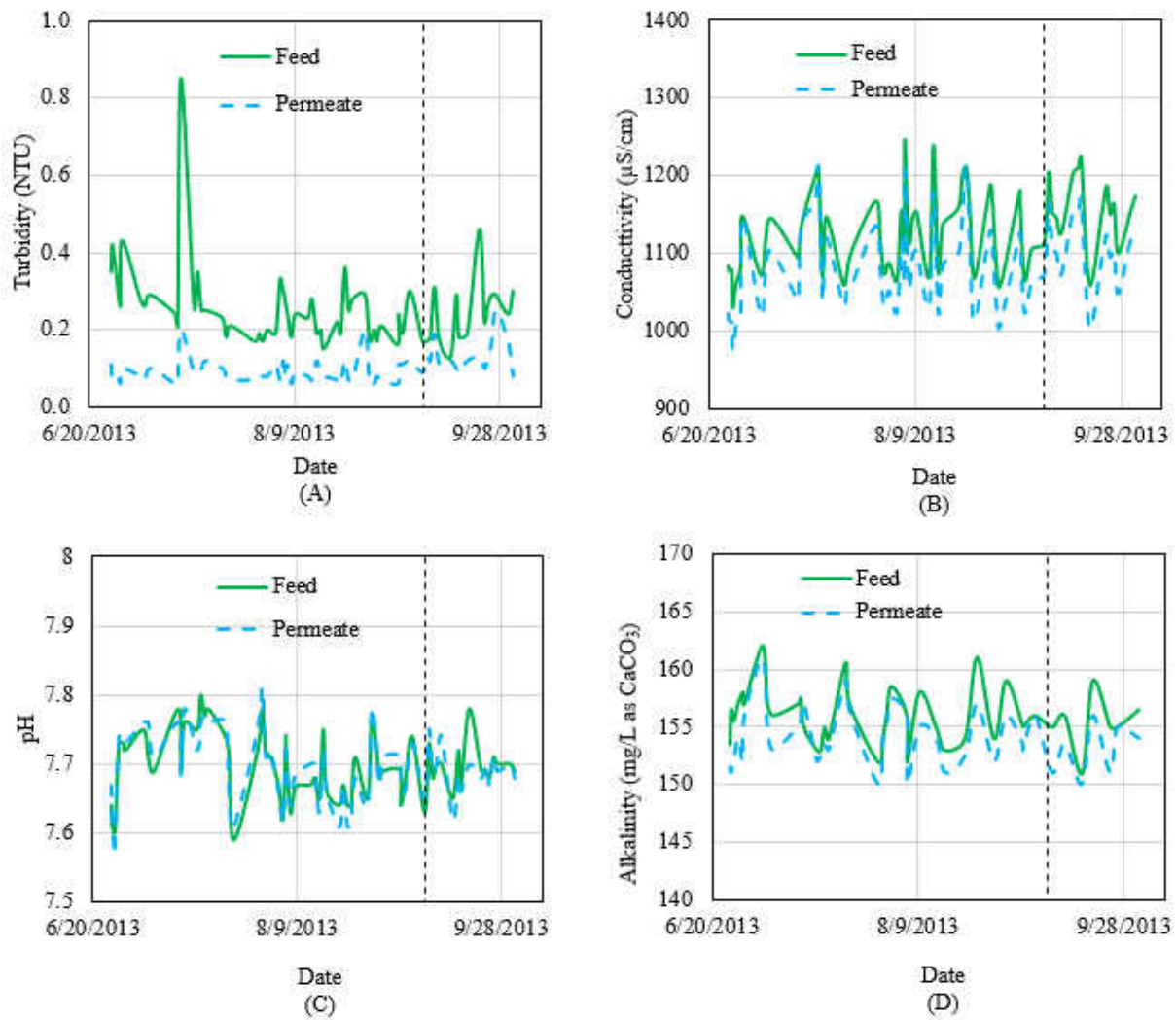
Figure 5-35: Feed and Permeate Concentration versus Time for (A) Turbidity

(B) Conductivity (C) pH and (D) Alkalinity

126

The ability to use conductivity as a surrogate measurement for TDS is advantageous in saving costs and time. However, correlation factors are water specific and it is necessary to perform TDS and EC correlations for different water sources. The conductivity plot in Figure 5-35B provides initial insight to the removal capabilities of the membrane regardless of the correlation factor. Since similar conductivity values existed in the feed and permeate streams, little TDS removal was expected when conducting solids analysis. The pH of the water did not change significantly across the membrane nor was alkalinity significantly affected. The water samples were transported to UCF facilities for additional solids and organics quantification as well as select cation and anion analysis. The suspended solids concentrations in the Verna water varies throughout the pilot testing duration reaching a concentration as high as 6 mg/L. Suspended solids were consistently reduced to less than 3 mg/L in the permeate stream. The average TDS of the Verna water was determined to be approximately 800 mg/L, and varied from 720 – 950 mg/L as show in Figure 5-36.
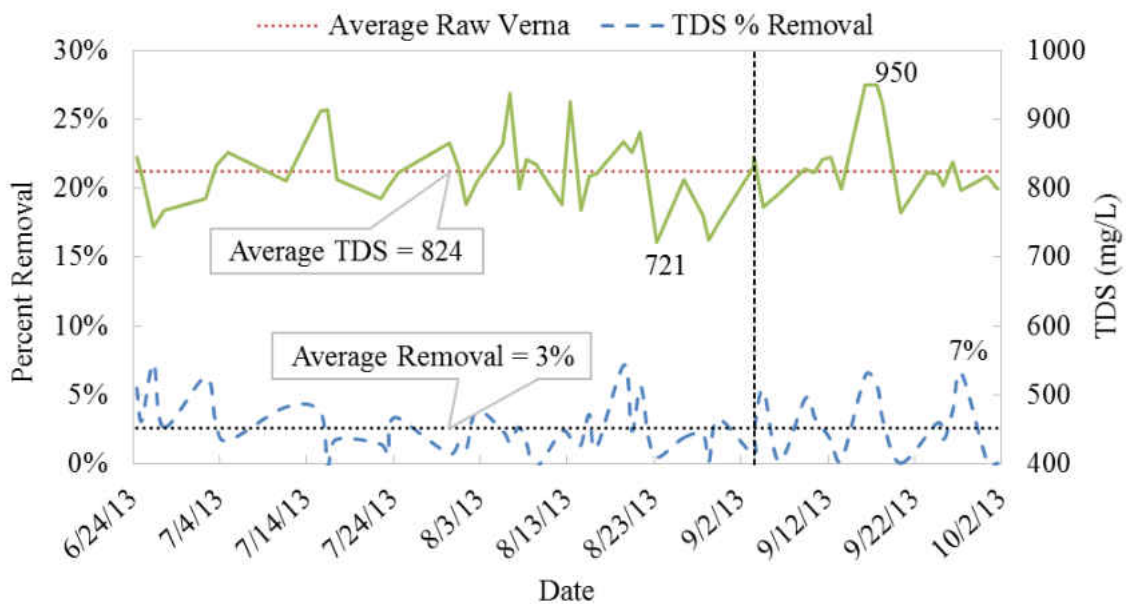
Figure 5-36: Feed TDS Concentration and Percent Removal versus Time

The variation of TDS in the feed water was likely due to the operation of multiple wells with varying water quality from the Verna wellfield. The largest observed TDS removal was 7% with an average removal of 3%. The low TDS removals correspond with the trends seen in the conductivity data presented previously. Figure 5-37 depicts the TOC variations for the feed and permeate streams over the course of pilot testing. The average maximum and minimum feed TOC concentrations ranged from approximately 2.2 to 2.5 mg/L. The top line depicts the feed TOC concentrations, while the bottom line shows the permeate TOC values. TOC removal was not affected by the removal of the pretreatment process, nor was it significantly affected by variations in flux or recovery. On average 24% of the TOC was removed using the membrane.
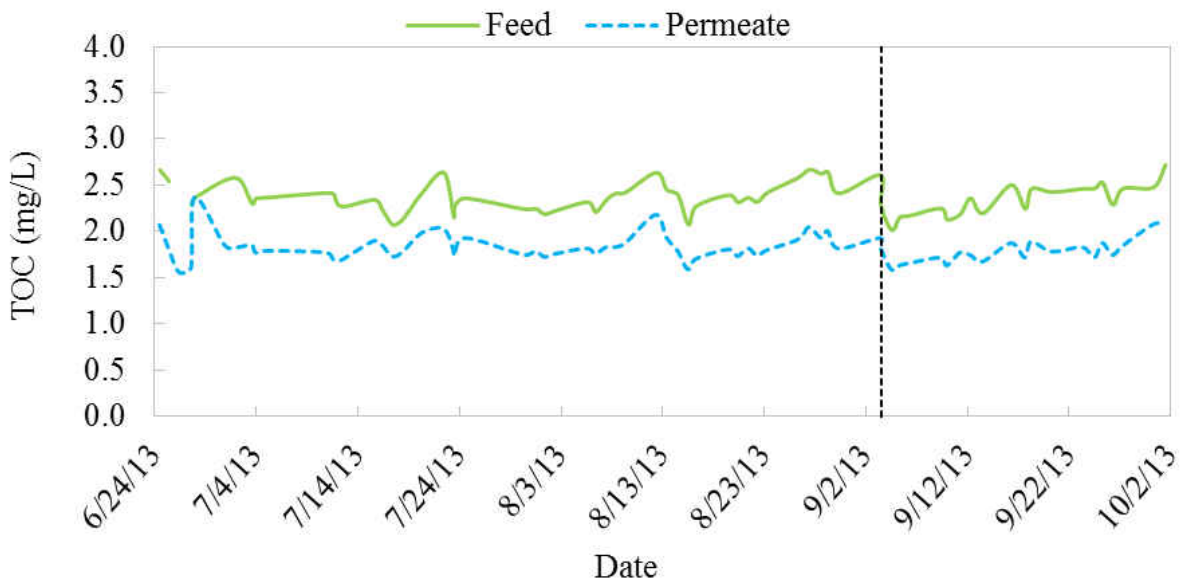
Figure 5-37: TOC Variation versus Time

Anions analysis included measurements for sulfate and chloride. Figure 5-38 shows the average sulfate concentrations for each of the three flux settings tested over the course of the study. The figure depicts the sulfate concentrations for the raw, feed and permeate streams. The membrane percent removals are calculated from the feed concentrations, which include the recycle stream, and the permeate concentrations. Although the average feed sulfate concentration was 430 mg/L the maximum and minimum feed sulfate concentrations varied from 322 mg/L to 500 mg/L, respectively. The HFW1000 membrane achieved an average removal of 7% with regards to sulfate, over the course of the study. Sulfate removals of 6% were attained operating at a flux of 10 gfd. The highest sulfate removals were met operating at a flux of approximately 17 gfd.
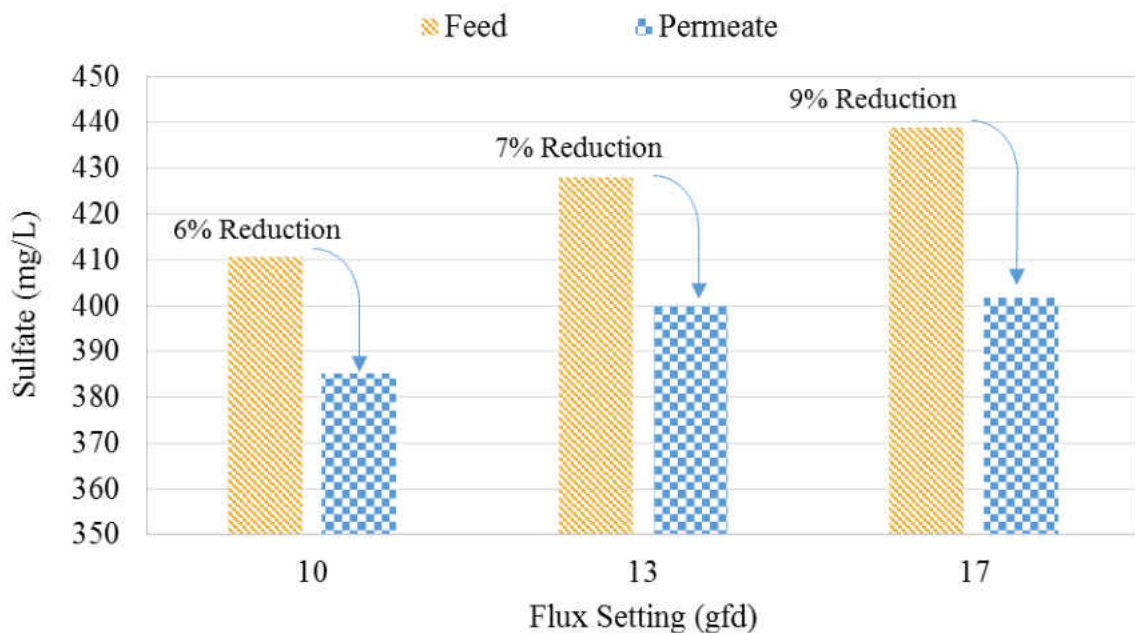
Figure 5-38: Sulfate Concentrations & Membrane Percent Removals

The removals for barium, calcium, chloride, iron, magnesium, manganese, potassium, silica, and sodium were not statistically significant and can be found in Appendix A of this document. The water quality results indicate the removal mechanism of the HFNF membrane was predominately due to size exclusion, with the ability to remove TOC and turbidity but was not sufficient at removing sulfate, hardness, and TDS.

<u>Pilot-Scale SWNF Membrane Testing Using Aerated Groundwater</u>

The results of pilot testing traditional SWNF membranes on the City's aerated groundwater supply are discussed in this section. The pilot testing included establishing baseline pressure requirements and subsequent water quality data considering two pretreatment options. The first pretreatment system evaluated was comprised of SF and HFUF while the second system evaluated considered the process without SF as a pretreatment. The successful operation of the SWNF pilot was dependent on the operation of the pretreatment process employed. Therefore the operational data of the HFUF pilot and SF events are included in this discussion.

Time Utilization & Operating Conditions

A new phase of SWNF pilot testing commenced on November 22nd, 2012 which built upon previous research conducted by Tharamapalan (2012a). Due to the extensive testing (over 300 runtime days) conducted by prior researchers (Tharamapalan, 2012b), two additional months of stable pilot data was considered acceptable to serve as a baseline for SWNF treatment. Pretreatment for the SWNF pilot employed SF in addition to HFUF for the first 516 hours. The SF utilized virgin media upon startup of the SWNF system, and operated semi-continuously with downtime occurring due to weekly backwash events.
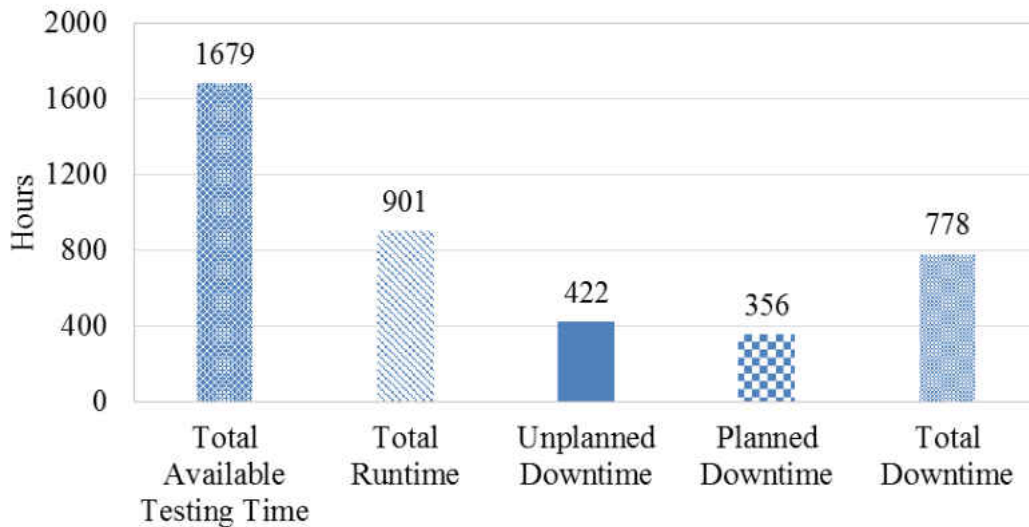
Figure 5-39: Distribution of Total Available Runtime for HFUF Pilot

After 516 hours the sand filter was bypassed, and the water fed directly to the HFUF pilot. Figure 5-39 displays the distribution of runtime for the HFUF pilot. The HFUF pilot experienced a total downtime of 778 hours, with 422 hours due to unplanned events. Unplanned downtime included sand filter backwash events, repairs to the feed pump and automatic shutdowns due to hydraulic limitations of the system. The total runtime of the HFUF pilot was 901 hours which included the time the pilot operated in dead-end forward filtration mode, backwash mode and during CEBs. Backwashes were conducted every 30 minutes for a duration of two minutes while CEBs where performed as necessary with a duration of 10 minutes.

The distribution of available testing time for the SWNF pilot has been provided in Figure 5-40. Unplanned downtime events occurred due to a number of factors including a leak in the piping of the SWNF pilot which caused air accumulation in the cartridge filter housing tank and subsequently a pilot shutdown. Further downtime accrued due to pilot power failures. The City periodically tests the standby power system of the WTF to maintain functionality of the generators

however this caused shutdowns to the SWNF pilot since the pilot was connected to the main power grid. Additional unforeseen shutdowns occurred due to failures in the SF and HFUF pretreatment pilots such as the repair of the air compressor for the HFUF pilot. Approximately 14 days of expected downtime occurred over the course of the study which included scheduled maintenance to repair the leak in the SWNF pilot and the air compressor in the HFUF pilot. Additional downtime was accumulated by the SWNF pilot due to hydraulic limitations. Shutdown of the SWNF pilot was required during sand filter backwashes and chemical cleanings on the HFUF pilot as well. Planned downtime events would not be expected in a full-scale system, as redundancy and properly sized feed tank would be implemented in the design. Overall the SWNF pilot system was operated for more than 500 hours with SF and HFUF pretreatment and nearly 400 hours without SF pretreatment. A total of 875 hours of runtime was accomplished before final shutdown occurred on January 1st, 2013. Additional pilot data has been provided in Appendix A including pilot parameter log lists, CEBs frequencies, alarm records, and field logs.
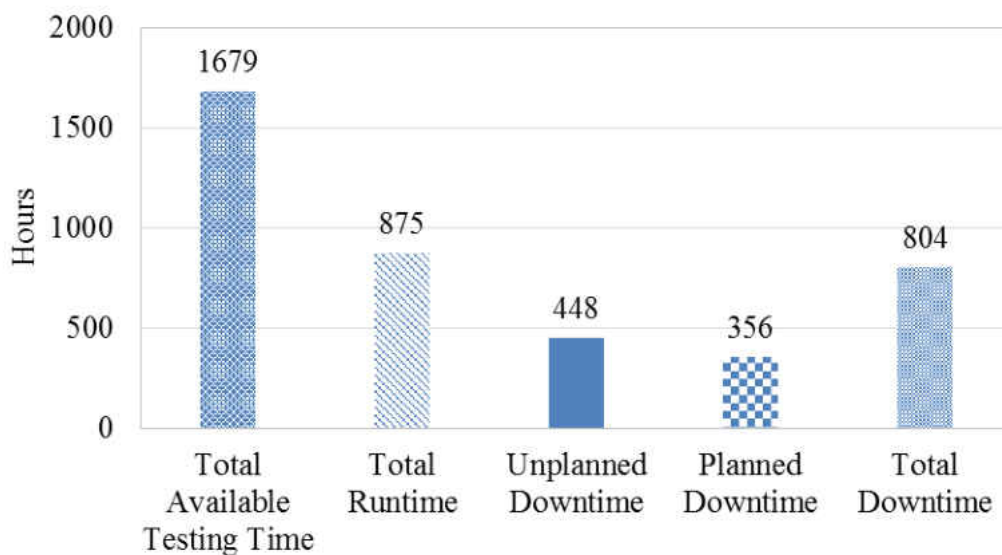
Figure 5-40: Distribution of Total Available Runtime for SWNF Pilot

132

System Water Production & Water Recovery

The SF pilot was operated in down-flow rapid filtration during normal operations and up-flow filtration during backwash events. Backwashes were conducted periodically with sand filter filtrate to maintain sufficient filtration flux. The filtrate of the sand filter was routed to the HFUF feed tank and the backwash water was directed to the City's wastewater system. The HFUF pilot was operated in inside-out dead-end up-flow filtration during normal operations. The HFUF pilot was originally set to produce a constant filtrate flow of 25 gpm and then adjusted to 37 gpm after 490 runtime hours. Water recoveries of approximately 84% and 93% were tested during the operation of the HFUF pilot. Backwashes and CEBs were conducted at a down-flow direction and rate of 120 gpm using HFUF filtrate. Flow directions during forward filtration and backwash modes have been illustrated in Figure 5-41.
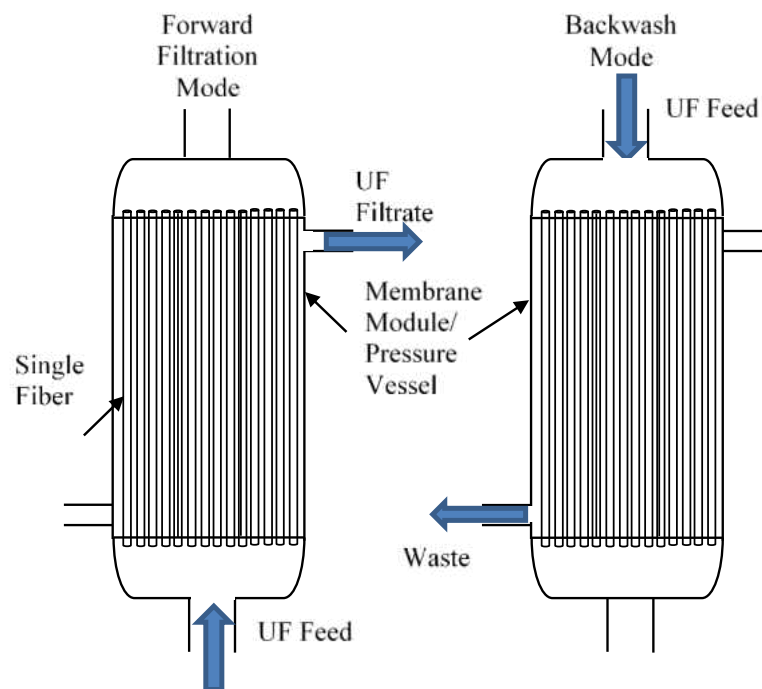
Figure 5-41: Flow Distribution Diagram for HFUF Pilot

The operating pressure requirements for the HFUF pilot are shown in Figure 5-42. The vertical dashed lines represent significant events that occurred during operation. The average feed pressure of the HFUF pilot with the use of SF was 4.5 psi with a TMP of 2.2 psi. The TMP was fairly constant until runtime hour 489 (identified by the vertical dashed line) at which point the filtrate production of the system was increased to 37 gpm yielding a recovery of 84%. The feed pressure and TMP of the HFUF pilot increased as a result of increasing the water production.
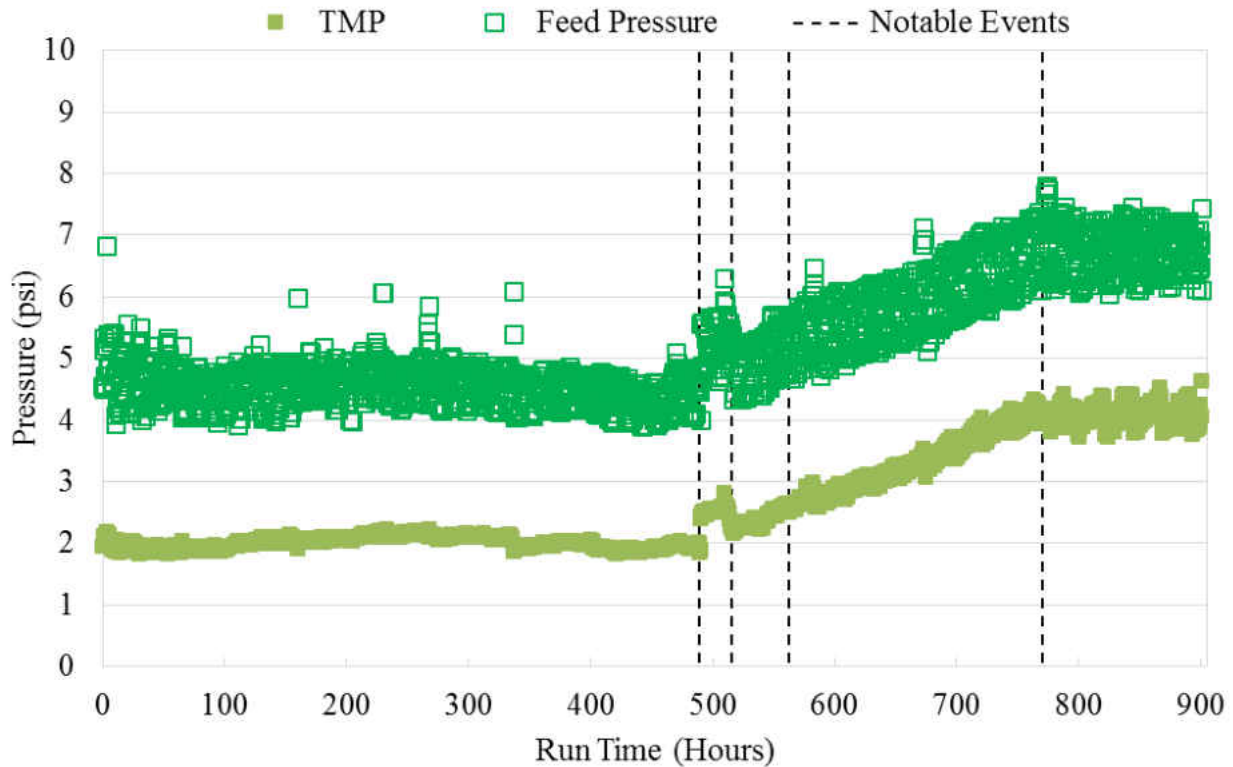
Figure 5-42: HFUF Pilot Operating Pressure Requirements

The second dashed line occurring at runtime hour 516 represents when chlorine pretreatment was removed and a CEB was performed. Chlorine pretreatment was originally added to control biofouling which was thriving in the feed and filtrate tanks due to their exposure to sunlight. The chlorine pretreatment was removed after the tanks were modified to decrease light exposure. The CEB was effective at recovering TMP and decreasing operating pressures.

The third line occurring at runtime hour 563 denotes the time at which the SF pilot was bypassed resulting in an increase in the feed and TMP pressures. After the SF was bypassed the operating pressures increased until stabilizing at an average feed pressure of 6.5 psi at a runtime hour of 770 (4th line). The TMP increased from an average of 2 psi to an average 4 psi after the SF was bypassed. The TMP continued to increase from runtime hour 770 until the end of the HFUF pilot testing (runtime hour 900) indicating SF pretreatment would likely be necessary to maintain TMPs below 4 psi.

The average flows of the feed, concentrate, and permeate streams for the two stage SWNF pilot has been displayed in Figure 5-43. The first stage membranes achieved an average recovery of 60% while the second stage achieved 62.5% yielding a total system recovery of 85%. In comparison, recoveries for RO and SWNF processes range from 75 to 95% depending on the water source, quality, and addition of scale inhibitor (Fritzmann, Löwenberg et al., 2007; Van der Bruggen & Vandecasteele, 2003; Zhao & Taylor, 2005).

Hydraulic flows were recorded automatically from flow gauges on the skid. Concentrate and permeate streams were collected and combined with the City's full-scale concentrate disposal stream. The SWNF pilot was set to produce 17 gpm of permeate by automatically adjusting the feed pressure of the membrane pilot.
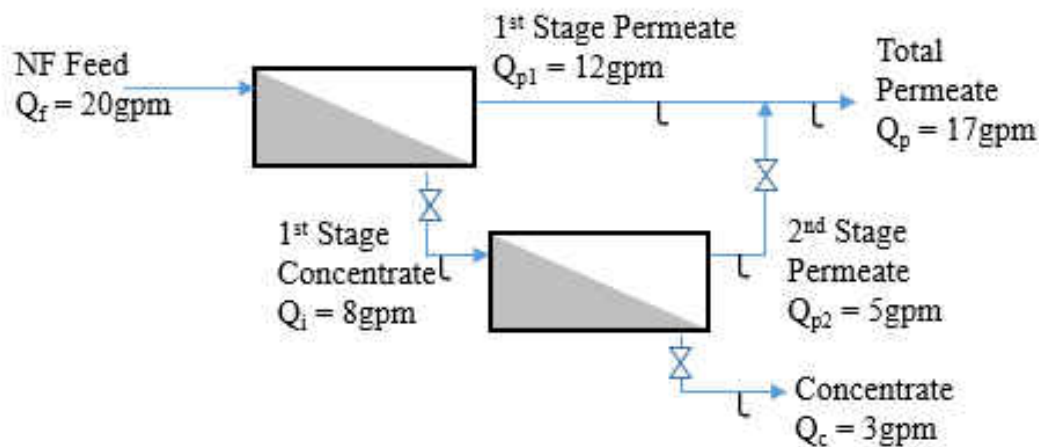
Figure 5-43: Flow Distribution Diagram for SWNF Pilot

The operational pressure requirements for the SWNF pilot are displayed in Figure 5-44. Notable events have been identified by vertical lines as formatted in Figure 5-42. Note the same event may be identified at different runtimes for Figure 5-42 and Figure 5-44 as the runtime for each pilot are distinct. The average feed pressure required by the SWNF pilot with SF and HFUF pretreatment was 96 psi. The first and second vertical dashed lines occurring at runtime hours 323 and 509, respectively, identify the period at which the pilot was operated with a leak in the cartridge filter housing unit of the SWNF pilot. The third vertical dashed line occurring at runtime hour 650, identifies the time at which chlorine dosing and SF pretreatment was removed.

The SWNF pilot was operated without SF to test the robustness of the system and assess whether SF was necessary for continuous stable operation of the SWNF system. Feed pressure requirements without the SF pretreatment increased to 105 psi. Subsequently, the 1st and 2nd stage average differential pressures increased to 53 and 69 psi, respectively. The fourth vertical line shown at runtime hour 750 identifies the time at which the SWNF pilot pressures stabilized after bypassing the SF pretreatment. This occurrence was also observed in the pressure data of the HFUF pilot displayed in Figure 5-42 at runtime hour 770.
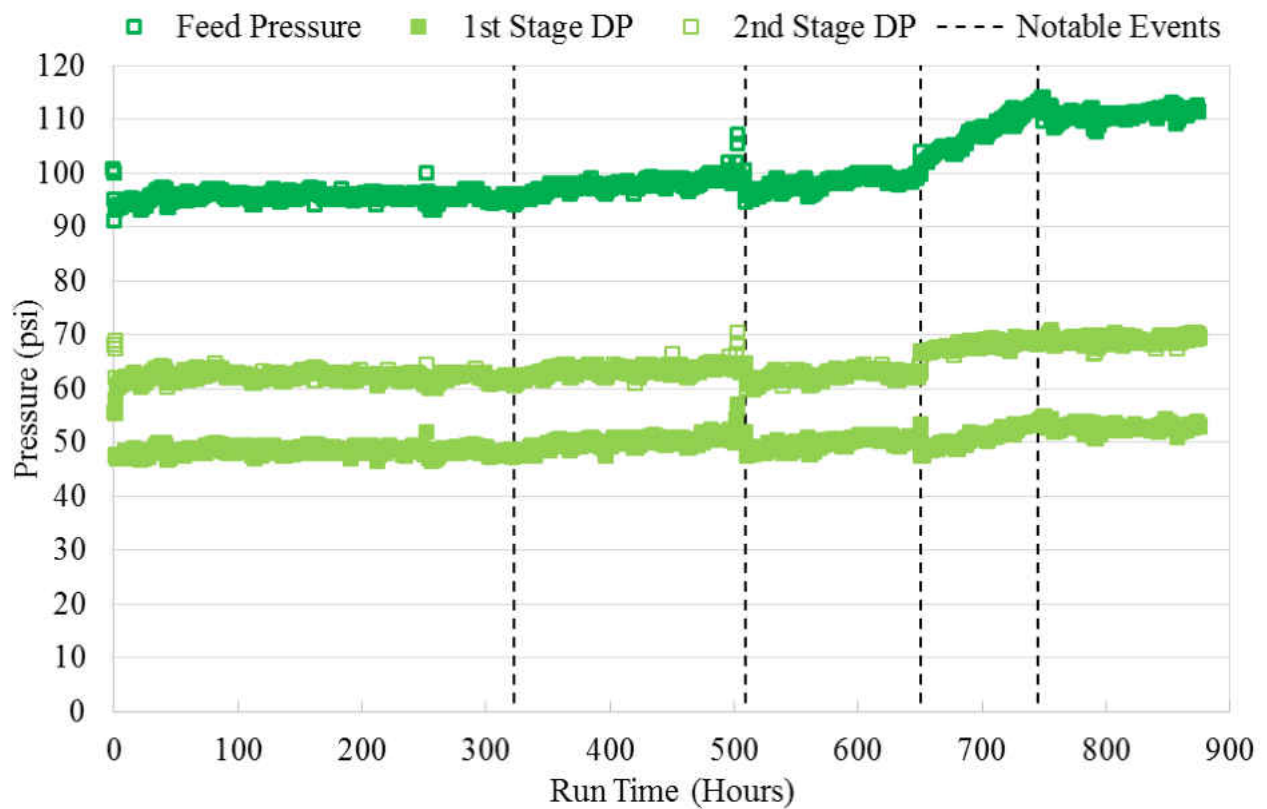
Figure 5-44: SWNF Pilot Operating Pressure Requirements

Water Flux & Mass Transfer Coefficient

The HFUF pilot recorded data at 2 min intervals and was averaged to hourly data for fouling assessment. The HFUF membrane was initially operated at a flux of approximately 30 gfd and increased to 45 gfd. The specific flux or water mass transfer coefficient and TMP were monitored over the course of testing for assessing membrane productivity and fouling. Figure 5-45 displays the flux, feed temperature, specific flux and TMP of the HFUF membrane. The feed temperature of the aerated Verna groundwater remained nearly constant over the duration of pilot testing. Regardless, the specific flux was adjusted for slight differences in temperature using Equation 3-9. During the HFUF pilot testing, the specific flux varied significantly indicating fluctuations in the membrane permeability. From runtime hours 0 to 100 variations in the specific flux occurred from normal operations of the pilot including forward filtration and backwash cycles.

CEBs were instituted after 100 hours of operation to recover specific flux and lower TMP. CEBs of sodium hypochlorite and citric acid were performed after 188 and 230 runtime hours, respectively, to stabilize the specific flux values. There was a significant recovery in specific flux on runtime hour 341 when citric acid and sodium hypochlorite CEBs were performed consecutively. At runtime hour 490 the flow rate of the pilot was adjusted to produce a flux of 45 gfd resulting in a 4 gal/sfd-psi increase in specific flux. A CEB was performed at a runtime hour of 515 to recover the membrane permeability. Following the CEB, the SF pilot was bypassed and aerated raw Verna water was fed directly to the HFUF membrane. The productivity of the HFUF pilot began to decline after the removal of the SF pretreatment. CEBs were instituted on daily basis to maintain productivity and slow the fouling of the membrane. The HFUF system stabilized after runtime hour 750 with an operating TMP of 5 psi and a specific flux of 10 gal/sfd-psi.
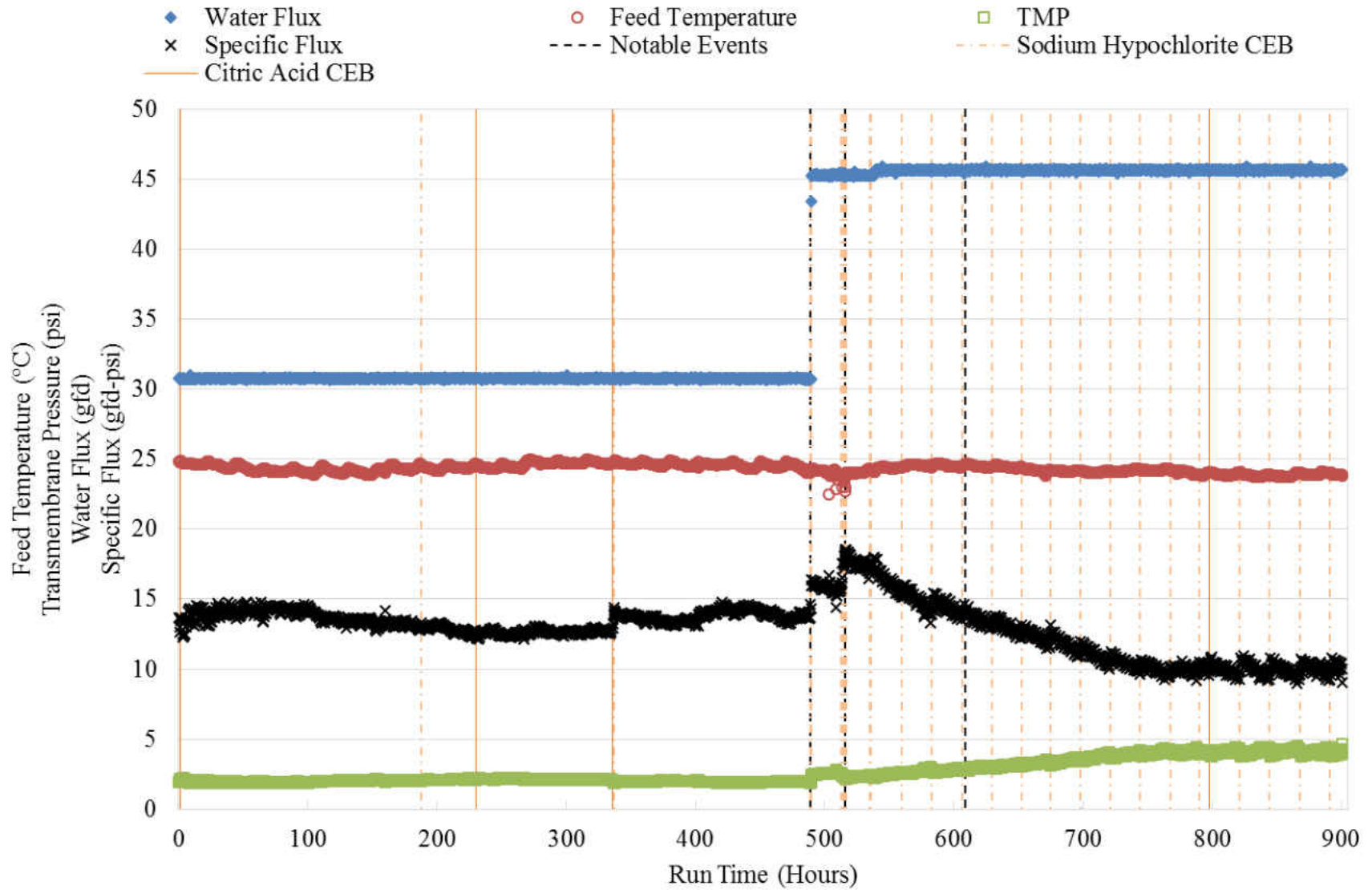
Figure 5-45: HFUF Pilot Operating Conditions

The water flux, feed temperature, TMP, and specific flux for the SWNF pilot have been plotted as a function of runtime in Figure 5-46. The SWNF water flux was designed to operate at a constant overall flux of 16 gfd. The feed temperature of the water varied from 22 ºC to 25 ºC with an average temperature of 24 ºC over the course of the study. The TMP and specific flux have been plotted for each stage of the SWNF pilot.The average TMP for the first and second stage of the SWNF pilot during pilot testing was 50 psi and 64 psi, respectively. The specific flux of the SWNF pilot was normalized to a constant temperature using Equation 3-7.

The variations in specific flux correspond with fluctuations in TMP. The specific flux of stages 1 and 2 were relatively stable for the first 500 hours of the study indicating significant fouling was not occurring while the SF and HFUF pilots were in operation. A leak occurred on the SWNF pilot resulting in slightly lower permeability values at a runtime hour 315. Permeability was restored after the leak was repaired indicated by the second dashed vertival line at runtime hour 509 hours. The average permeability for the first and second stage membranes using SF pretreatment was 0.43 gal/sfd-psi and 0.30 gal/sfd-psi, respectively. At a runtime of 650 hours, the SF pilot was bypassed which resulted in a decrease in permeability of the system. The 1st stage membranes stabilized at a specific flux of approximately 0.40 gal/sfd-psi. However the 2nd stage specific flux continued to decrease to 0.28 gal/sfd-psi, before the pilot was shutdown indicating that SF pretreatment would be necessary for stable operation.
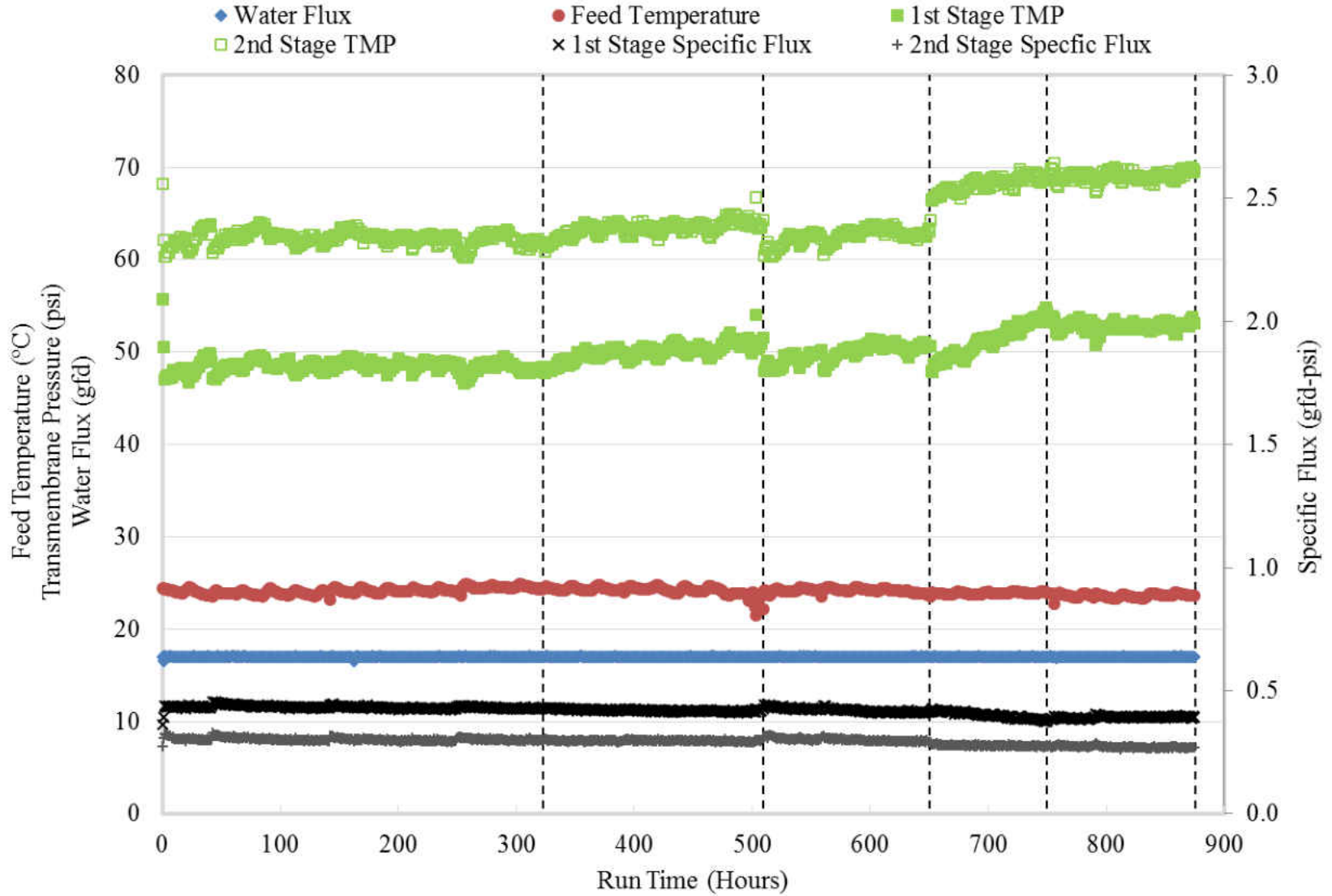
Figure 5-46: SWNF Normalized Specific Flux Variations

141

System Water Quality

The SWNF pilot system was sampled weekly for water quality parameters. Sample locations were identified in Figure 4-6 and included the aerated Verna water, sand filtrate, HFUF feed, HFUF filtrate, SWNF feed, SWNF concentrate, and SWNF permeate. The SWNF system implemented SF and HFUF pretreatment operations to protect the SWNF membranes from larger particles contributing to turbidity and suspended solids. The HFUF pilot was equipped to measure turbidity at two minute intervals using online turbidimeters. The feed turbidity and significant events experienced by the HFUF pilot over the course of the study has been displayed in Figure 5-47. The dashed line at 410 hours representing the change in flux caused a slight increase in the feed turbidity. The dashed line at 520 hours represents the addition of light resistant storage tanks and the removal of chlorine from the HFUF pilot.
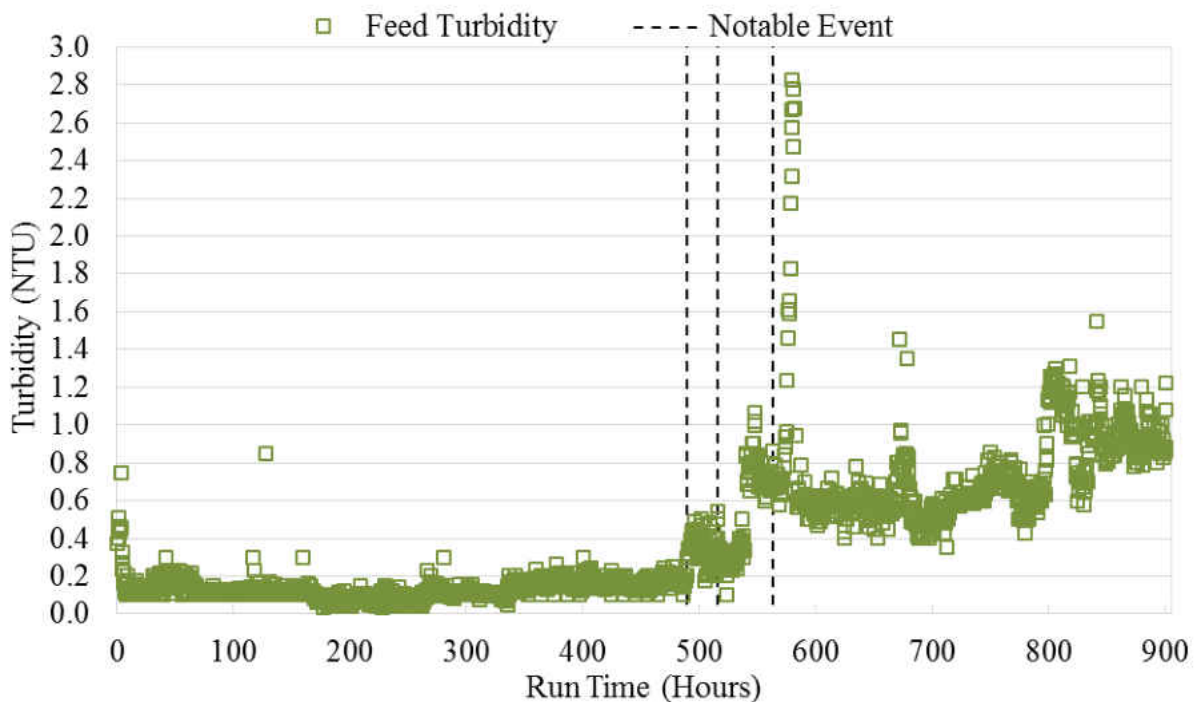
Figure 5-47: HFUF Feed Turbidity

Originally chlorine was being fed into the HFUF pilot to control biofouling. However, oxidants can irreversibly damage polyamide SWNF membranes therefore the addition of sodium bisulfite was also necessary before the water entered the SWNF pilot skid. The addition of chemicals for biogrowth prevention was a costly and temporary solution until the tanks could be modified. After the modifications, an additional increase was observed in the turbidity of the system. The vertical line at 560 hours indicated the removal of the SF pilot when the aerated Verna water was routed directly to the HFUF feed tank. A spike in feed turbidity was observed at a runtime hour of 570 indicating that the SF pilot had a significant impact on dampening high turbidity events. The SF was shown to remove 50% of the turbidity in the aerated Verna water while in operation.

The HFUF pilot produced filtrate water quality with turbidity values consistently below 0.1 NTU as illustrated in Figure 5-48. The graph not only shows the effect of increasing flux, removing chlorination, and removing the sand filter but also provides data on the impact of backwashes and CEBs. Backwashes were conducted after 45 minutes of runtime to maintain productivity and decrease TMP. The pilot operated without CEBs for the first 188 hours of runtime, allowing for cake filtration to occur. The formation of a cake layer can improve turbidity removal but also requires higher operating pressures (Choi & Dempsey, 2004; Galjaard, Buijs et al., 2001). CEBs are performed to remove foulant and restore TMP but consequently a decrease in removal effectiveness occurs. At a runtime of 188 hours a CEB was performed with sodium hypochlorite, which had little effect on TMP or filtrate turbidity. An additional CEB was performed with citric acid at a runtime of 230 hours, which improved TMP and increased filtrate turbidity. After the citric acid CEB, backwashes became more effective as seen from the periodic increases and decreases in the turbidity values. This indicated that the citric acid CEB removed a foulant layer that was resistant to the sodium hypochlorite CEB. The significant events identified in Figure 5-48

by vertical dashed black lines also affected filtrate turbidity. Increasing the filtrate production of the HFUF pilot at runtime hour 490 resulted in higher filtrate turbidity values and shifted the minimum filtrate turbidity from 0.02 to 0.025 NTU. The removal of chlorine to the HFUF pretreatment at runtime hour 520 increased filtrate turbidity to 0.04 NTU. Filtrate turbidity increased to 0.07 NTU at runtime hour 545 due to increased backwash frequency. Once the SF was bypassed at runtime hour 560, the HFUF pilot experienced greater turbidity fluctuations in the feed turbidity which consequently affected the filtrate turbidity. Regardless, an average of 60% turbidity removal was achieved using HFUF. The HFUF pilot was also monitored for sulfate, hardness, and TOC rejection; however, removals for divalent ions and TOC removals were less than 3% and 4%, respectively.
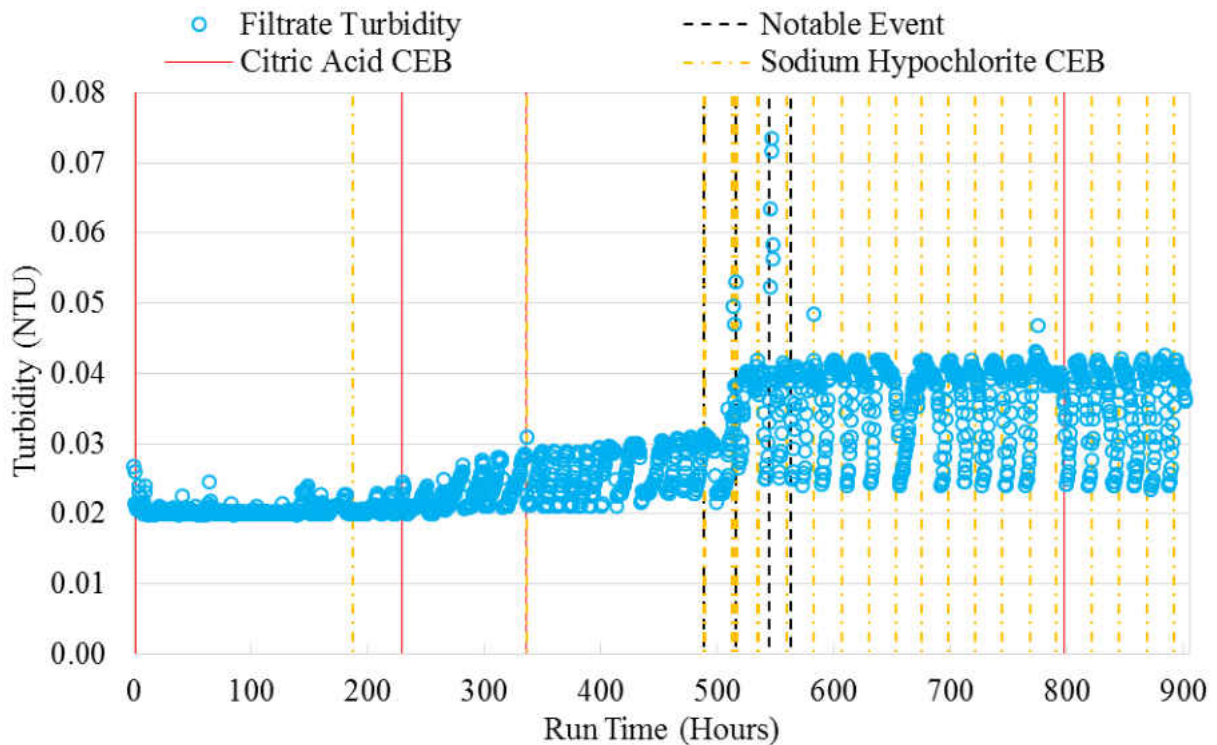
Figure 5-48: HFUF Filtrate Turbidity

144

The SWNF pilot was equipped with online conductivity meters recording data at two minute intervals. Tharamapalan (2012a) determined the EC to TDS ratio of the water source used in this research was dependent on the stage of the process, noting that feed water ratios differ significantly than permeate ratios. This research determined correlation coefficients of the feed, concentrate, and permeate streams separately and used the corresponding ratio for estimating TDS concentrations. Figure 5-49 illustrates the feed and filtrate conductivity of the SWNF pilot.

The feed conductivity of the SWNF pilot varied from 1,134 µS/cm to 1,354 µS/cm with an average of 1,236 µS/cm. Feed conductivity does not correlate with the events previously discussed as the conductivity is not significantly affected by the SF and HFUF processes. Conductivity in the permeate experienced less variation with an average conductivity of 287 µS/cm.
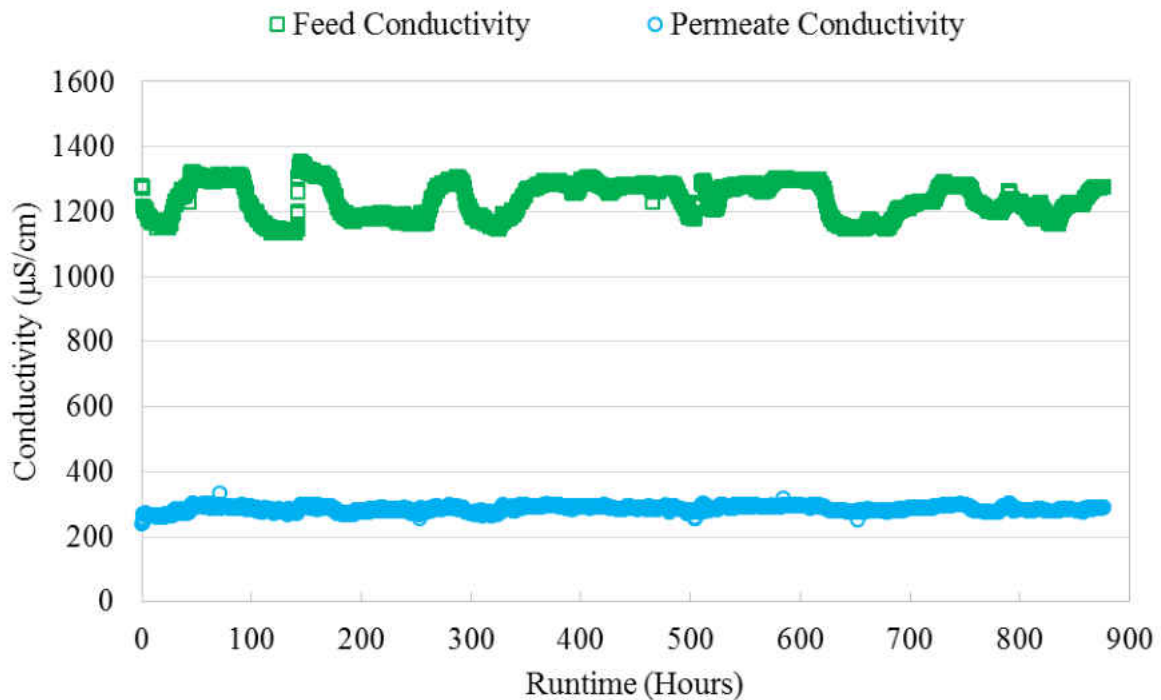
Figure 5-49: SWNF Conductivity Monitoring

Additional water quality results were similar to previously collected pilot testing data conducted by Tharamapalan (2012a). Treatment of aerated Verna water using a combination of SF, HFUF, and SWNF removed 50% of the alkalinity, 90% of the divalent ions calcium and magnesium, and 99% of the sulfate. In addition, the SWNF pilot treatment system achieved 90% TDS rejection and 96% TOC removal.

<div align="center">

Laboratory and Field Quality Control

</div>

Laboratory Quality Control

This section provides the quality control for the laboratory analysis conducted throughout this research. Laboratory analysis included TOC, metals, anion, TSS and TDS experiments. Duplicates were prepared for one out of every six samples to assess the consistency of the precision of the analytical machines. To assess the consistency of the accuracy of the TOC analyzer, one out of every six samples was spiked with 1 mL of 200 ppm TOC solution created monthly for TOC analysis. Spikes for metals and anions analyses were prepared with various concentrations dependent on varying sample concentrations and the bounds specified by the ion chromatograph (IC) and inductively coupled plasma spectrometer (ICP) manufacturers.

Control charts were constructed by plotting the I-statistic values over time in a sequence plot to determine if variations in the data existed due to identifiable causes or random variation. The control charts for precision and accuracy are provided in Figure 5-50 and Figure 5-51. There was one I-statistic value violating the UCL on the TOC control chart. The violation corresponded from a sample set taken on July 4th, 2013. The values for the original sample and replicate sample are 2.21 and 2.10 mg/L, respectively. These values show a 0.1 mg/L difference between the samples which is significant due to the small concentration of TOC present in the samples and the expected precision of the TOC equipment used by UCF.
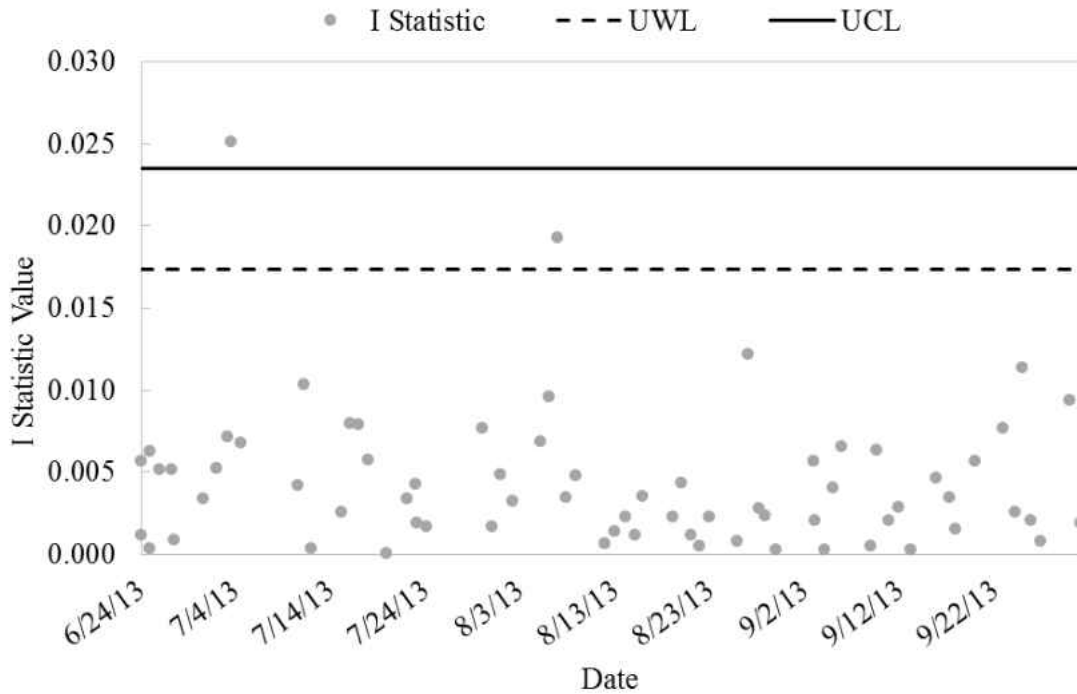
Figure 5-50: Control Chart for TOC Precision

This UCL violation corresponded to a replicate value with a relative percent difference greater than five. This error was most likely due to human error in labeling or use of contaminated glassware. Therefore, the values obtained from this particular set was not used for averaging TOC values. No other control or warning limit violations were detected in the TOC control charts.

The control chart for accuracy of TOC analysis is provided in Figure 5-51. The control limits were developed from historical TOC data analysis conducted on the equipment used in this study. The testing of this parameter was well within this range having minimum and maximum recoveries of 88% and 107%. Furthermore, the percent recoveries for accuracy is also within the limits of 80-120%. Additional control charts for metals, anions, and solids analysis have been provided in Appendix D.

147

Figure 5-51: Control Chart for TOC Accuracy

Field Quality Control

Field duplicates were taken daily for each set of samples and analyzed for alkalinity, turbidity, pH, conductivity, and temperature. The field data collected in this research was in part conducted by the City's personnel due to the frequency of sampling. Precision assessments were performed for each field parameter and used to develop precision control charts. The field data assessment for alkalinity has been provided in Table 5-19 and was used to produce Figure 5-52.

Table 5-19: Precision Assessment for Alkalinity Quality Control

Sample #	Duplicate A	Duplicate B	I Statistic	Sample #	Duplicate A	Duplicate B	I Statistic
1	153	154	0.002	24	157	155	0.007
2	155	154	0.004	25	154	153	0.003
3	154	155	0.002	26	151	153	0.005
4	154	156	0.005	27	155	153	0.005
5	157	157	0.001	28	158	159	0.003
6	157	156	0.004	29	154	152	0.006
7	160	161	0.002	30	156	158	0.006
8	156	156	0.001	31	157	154	0.008
9	153	155	0.006	32	154	154	0.001
10	156	157	0.004	33	156	156	0.001
11	157	156	0.005	34	153	154	0.002
12	152	153	0.004	35	157	155	0.006
13	152	153	0.002	36	156	158	0.005
14	155	154	0.003	37	154	154	0.000
15	153	153	0.001	38	157	156	0.003
16	159	160	0.002				
17	159	157	0.006	Average			0.0032
18	152	151	0.003	Std. deviation			0.0022
19	154	154	0.000	Minimum			0.0000
20	155	155	0.001	Maximum			0.0083
21	159	158	0.001				
22	156	156	0.001	Upper Warning Limit			0.0076
23	150	150	0.001	Upper Control Limit			0.0099
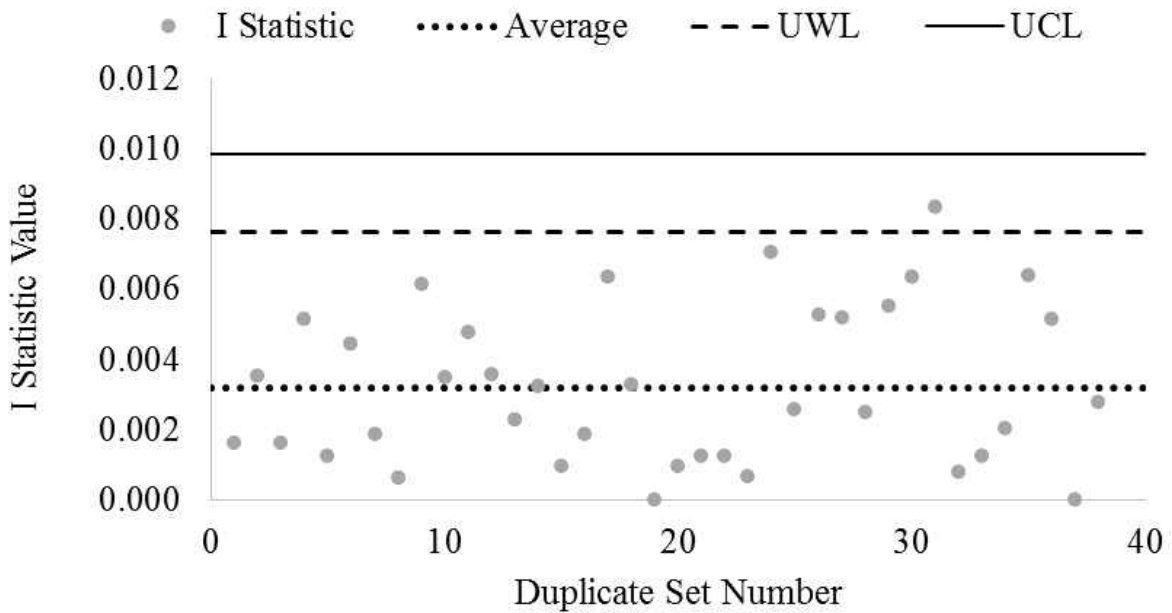
Figure 5-52: Control Chart for Alkalinity Precision

The UWL and UCL were determined to be approximately 0.008 and 0.01, respectively. The control chart for alkalinity precision indicates one sample violation of the warning limit however no violations of the control limit occurred. The precision control charts for turbidity, pH, conductivity, and temperature have been provided in Figure 5-53A-D. The figures indicate no control violations occurred for the 70 duplicate measurements conducted for each of the field parameters. The precision assessment data for additional field parameters have been provided in Appendix D.
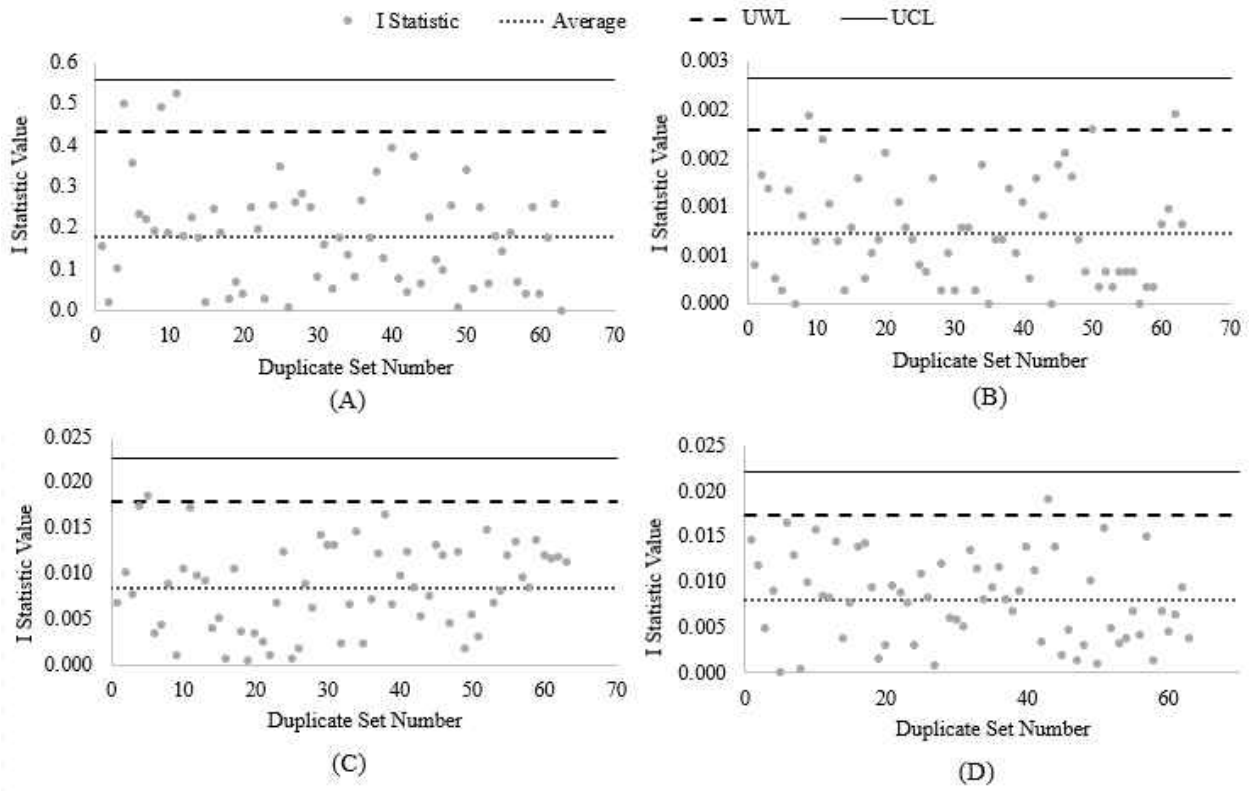
Figure 5-53: Control Charts for (A) Turbidity (B) pH (C) Conductivity and

(D)Temperature Precision

6. CONCEPTUAL PROCESS COST COMPARISON

Two process alternatives were considered for treatment of the City's Verna water supply considering the results of the pilot testing performed in this research. Two alternatives were evaluated in this analysis: (i) a traditional SWNF membrane process and (ii) a SF and HFNF process. The first treatment alternative, provided in Figure 6-1, considered the use of traditional SWNF membrane process with SF and HFUF processes required for pretreatment.
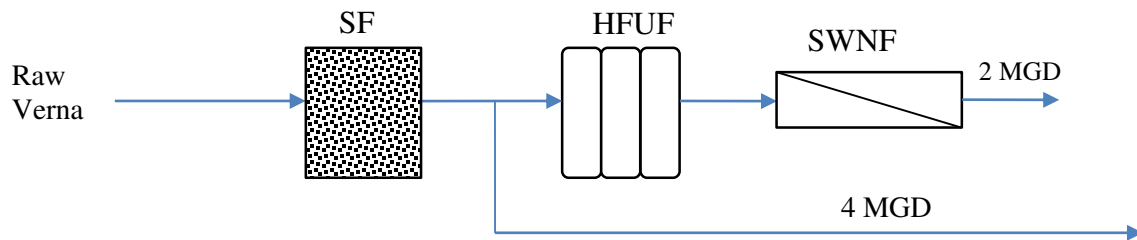
Figure 6-1: Verna Water Supply Treatment Alternative 1 – SF-HFUF-SWNF

The second treatment alternative investigated in this research considered HFNF membrane technology with SF pretreatment, shown in Figure 6-2. The permeate production flows have been included in the figures. The conceptual costs presented herein were estimating assuming recoveries of 97%, 95%, and 85% for media filtration, membrane filtration, and membrane softening processes, respectively.
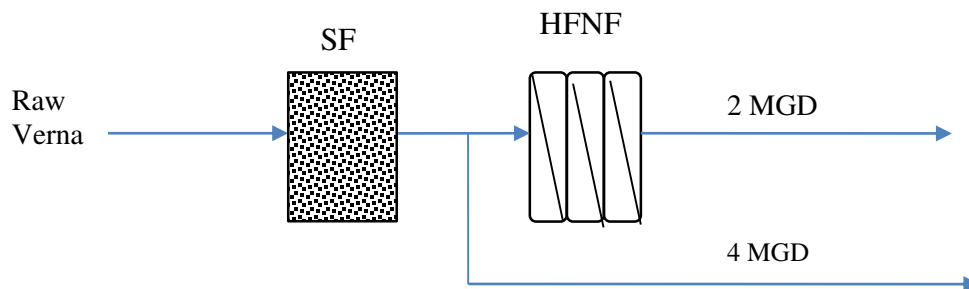
Figure 6-2: Verna Water Supply Treatment Alternative 2 – SF-HFNF

<u>Capital Costs</u>

The capital costs for the Verna water treatment alternatives is provided in Table 6-1. The costs for additional buildings, degasifiers, clearwells, transfer pumps, ground storage tanks, bulk chemical storage, emergency power, yard piping, and site development have been excluded from the conceptual cost estimations. The direct capital costs for a typical rapid SF process would include horizontal pressure filters, filter underdrains and distributors, air wash configurations, tank nozzles and manways, face piping, instrumental and controls, and filtration media. Direct capital costs for SF equipment were developed using data from an existing facility (Jupiter, 2007). The capital costs of the SF process for the WTF in Jupiter FL were adjusted for plant size by a factor of 0.09. The conceptual capital costs for a 6 MGD SF process was estimated to be approximately $602,000.

The direct capital cost for HFUF equipment includes HFUF membrane modules, cleaning equipment, high pressure pumps, backwash pumps, transfer pumps, backwash tanks, blowers, instruments and controls (I&C). The capital costs were calculated using membrane filtration cost curves found in the literature (Nemeth-Harn, 2004). Capital costs for the HFUF equipment were based upon a permeate flow of 2 MGD and were determined to be a total of $1.04 million.

The direct capital costs for SWNF equipment includes SWNF membrane modules, cleaning equipment, high pressure pumps, pretreatment chemical feed and storage, cartridge filters and I&C. Capital costs for estimating membrane softening processes were developed using cost curves similar to the HFUF cost curves which consider the process capacity (MGD) as a function of cost ($/gpd) (Nemeth-Harn, 2004). The direct capital costs for a SWNF process were estimated to be approximately 2.4 million dollars.

Table 6-1: Conceptual Capital Costs for City's Verna Treatment Alternatives

Category	Alternative 1 Cost ($1000)	Alternative 2 Cost ($1000)
Direct Capital Costs		
Media Filtration Equipment Cost	602	602
Horizontal Pressure filters (2)		
Filter Underdrains and Distributors		
Air wash Configuration		
Tank Nozzles and Manways		
Face piping		
Instrumentation and Controls		
Media 16" Gravel		
Media 24" Sand		
Membrane Filtration Equipment Cost	1,040	n/a
HFUF Membrane Modules		
Cleaning Equipment		
Feed/Permeate Pumps		
Backwash Pumps		
Blowers		
Backwash Tanks		
Chemical Feed and Storage		
Instrumentation and Controls		
Membrane Softening Cost	2,400	2,600
Membrane Modules		
Vessels and Supports		
Cleaning Equipment		
Feed Pumps		
Pretreatment Chemical Feed and Storage		
Cartridge Filters		
Backwash Pumps (n/a for SWNF)		
Blowers (n/a for SWNF)		
Instrumentation and Controls		
Total Direct Capital Costs	4,042	3,202
Indirect Capital Costs		
Construction Overhead & Profit (22%)	889	704
Insurance and Bonding (3%)	121	96
Contingencies (15%)	606	480
Total Indirect Capital Costs	1,617	1,281
Total Estimated Capital Costs	5,658	4,482
$/gallon/day Capital Installed	2.49	1.96

Indirect capital costs considered construction overhead and profit, insurance and bonding, and contingencies for each treatment alternative and were estimated to be 22%, 3% and 15% of the total direct capital costs, respectively. The total capital cost for the treatment alternative utilizing SF, HFUF, and SWNF was estimated to be approximately $5.7 million.

The capital costs estimates for the second treatment alternative utilizing SF and HFNF were estimated using SWNF and HFUF equipment conceptual estimates. The equipment required for HFNF treatment would likely include components from both treatment alternatives. For instance the addition of blowers and backwash pumps would include additional costs to the HFNF process. Previous cost estimates conducted by Sethi and researchers (2000) found HFNF to be comparable to a UF-SWNF system depending on plant size, economies of scale, and operating conditions. The conceptual capital cost for the HFNF equipment was estimated to be $2.6 million corresponding to a total capital cost of approximately $4.5 million.

The total capital costs for each treatment alternative are provided in Table 6-2. The estimated installed conceptual capital cost for the treatment alternative using SF and HFNF was determined to be $1.96/gpd. The treatment alternative using SWNF required an additional pretreatment process resulting in an increase of approximately $1.2 million, or $0.53/gpd, for a total estimated conceptual cost of $2.49/gpd.

Table 6-2: Conceptual Capital Process Costs for each Treatment Alternative

Process (Size)	Alternative 1 Cost ($/gpd)	Alternative 2 Cost ($/gpd)
Media Filtration (6 MGD)	0.14	0.14
Membrane Filtration (2 MGD)	0.67	-
Membrane Softening (2 MGD)	1.68	1.82
Total Cost ($/gal/day capital installed)	2.49	1.96

Operating & Maintenance Costs

The operating and maintenance (O&M) costs for each membrane treatment alternative would include: energy and power, chemicals, cartridge filter replacement, membrane replacement, water and sewer charges, cleaning chemicals, maintenance and labor (Byrne, 1995). A significant portion of the energy costs for NF processes are from the operation of high pressure feed pumps (AWWA, 2007). Operating feed pressures for each alternative were monitored and averaged for each of the pilots to estimate power requirements of the feed pumps. The amount of energy to drive the feed pumps for each pilot were estimated using Equation 6-1 which considers the pump pressure (P), pump efficiency (η_p), motor efficiency (η_m), and recovery (R).

$$\frac{kwh}{kgal\ permeate} = \frac{P(psi) \times 0.00728}{\eta_p \times \eta_m \times R} \tag{6-1}$$

Each of the pilots feed pumps were assumed to have a pumping efficiency of 60% and a motor efficiency of 94%. The average industrial electricity rate in the City was determined to be approximately \$0.07/kWh (Electricity Local, 2016). Additional costs from operating labor wages and fringes were not included assuming current plant personal could be utilized to operate the new treatment system. Furthermore chemical costs, administration and overhead costs were considered to be comparable for each treatment alternative. Costs for membrane replacement were calculated using the method proposed by Byrne (1995) assuming an average membrane life of five years (Sethi et al., 2000). Operating costs for the SWNF process included cartridge filter replacement which was not included in the HFNF estimate. Both treatment alternatives neglect the cost of concentrate disposal, but it is noted that the City has two options for disposal including deep well injection or sewer. The conceptual O&M conceptual cost estimates for the full-scale alternatives are provided in Table 6-3.

Table 6-3: Conceptual O&M Costs for City's Verna Treatment Alternatives

Category	Alternative 1 Cost ($1000)	Alternative 2 Cost ($1000)
O & M Costs		
Energy & Power	135	91
Chemicals	18	13
Membrane Replacement	85	41
Cartridge Filter Replacement	5	-
Administration & Supplies	6	4
Overhead (15%)	20	12
Miscellaneous	10	10
Total Estimated Annual Operating Cost	278	170
$/gallon/day O&M	0.11	0.06

The conceptual annual operating costs for the SWNF treatment alternative were estimated to be $278,000 or approximately $0.11/gpd. The conceptual annual operating costs the HFNF alternative was estimated to be $0.06/gpd resulting in a yearly savings of approximately $107,000. Capital costs components listed previously were amortized over the design life of the membrane plant assumed to be 20 years with a 4.5% interest rate to determine the total (capital and O&M) annual costs provided in Table 6-4. The total cost for the SWNF treatment alterntaive was estimated to be $278,000/year or $0.84/kgal. Alternatively the total amount for a new HFNF treatment alternative was estimated to cost approximately $170,000/year, or 0.57/kgal.

Table 6-4: Total Process Cost Summary for each Treatment Alternative

Process (Size)	Alternative 1 Cost ($/kgal)	Alternative 2 Cost ($/kgal)
Media Filtration (6 MGD)	0.07	0.07
Membrane Filtration (2 MGD)	0.27	-
Membrane Softening (2 MGD)	0.51	0.51
Total Cost	**0.84**	**0.57**

7. CONCLUSIONS AND SUMMARY

This section provides the conclusions and findings of the research. The information has been organized in terms of bench-scale and pilot-scale membrane testing as discussed in the results chapter of this document. The bench-scale membrane tests were conducted using synthetic solution to provide water quality removal data and limited hydraulic data for modeling purposes. Additional bench-scale membrane experiments were conducted using the City's aerated groundwater source to assess membrane performance with respect to permeability and site specific water quality removals. HFNF and traditional SWNF membrane pilots were assessed for hydraulic performance and water quality considerations. The results for the two membrane pilot systems considered pretreatment requirements for treating the City's aerated Verna water supply and provided cost estimations for full-scale implementation.

Bench-Scale HFNF Membrane Testing Using Synthetic Water

- Membranes A, B, and C MTCs were found to be 0.39 gal/sfd-psi, 0.75 gal/sfd-psi, and 0.30 gal/sfd-psi, respectively. Values indicated membrane C was the least permeable and membrane B was the most permeable with respect to water flux.

- Considering the retention values, permeability and molecular weight cutoffs of each membrane, membrane C should have been the most permeable relative to membranes A and B. Membrane C may have experienced plugging during the manufacturing process due to potting resin or damage to the active layer of the membrane.

- The membrane manufacturer replicated the testing conditions and confirmed the permeability values and removals for each membrane noting membrane C experienced minor plugging.

- Membrane A achieved the highest removals of magnesium and sulfate with over 90% rejection for both elements. Membrane B obtained an average rejection of 84% for magnesium and sulfate. Membrane C removed the lowest amount of magnesium and sulfate with an average removal of approximately 40%. Membranes A and B indicate nanofiltration-like removals achieving removals greater than 80%. Membrane C exhibits removals which are more indicative of a tighter HFUF membrane.

- Removals efficiency for both sulfate and magnesium decreased with the presence of sodium chloride for membranes A, B and C. Magnesium removals decreased to 75% for membrane A, 48% for membrane B, and 23% for membrane C.

- The rejection mechanisms of sulfate and magnesium for membranes A and B were determined to be driven by diffusion considering the SE, HSD, and HSD-FT models indicating nanofiltration-like removal characteristics. The dominate rejection mechanism for membrane C with regards to sulfate and magnesium mass transfer was best described using the SE model.

- Estimation of model parameters specifically inorganic solute mass transfer coefficients for magnesium and sulfate were more accurately determined using the HSD theory rather than empirical correlation using Sherwood, Schmitt and Reynolds numbers. Incorporating the concentration gradient by use of the HSD-FT model improved the predicted model.

- Previously developed models were insufficient for describing solute flux with fluctuating feed ionic strength. A new model was developed which described facilitated solute transport with the addition of NaCl by incorporating the feed ionic strength into the HSD model. The resulting model has been provided in Equation 5-11.

$$C_p = \frac{K_s C_f - \frac{2\beta_1 \mu^{\beta_2}(R-1)}{2-R}}{K_w(\Delta P - \Delta \pi)\left(\frac{2-2R}{2-R}\right) + K_s} \tag{5-11}$$

- The RMSE for each model including the newly-developed HSD-IS model are shown in Figure 7-1. The HSD-IS model was shown to produce less error for the diffusion controlled membranes A and B. However the size exclusion model remains the best fit model to describe membrane C producing the least error as indicated by an RMSE of less than 15.

- Empirical β1 and β2 values are constituent and membrane specific. The β1 and β2 values for membrane A for magnesium were determine to be 257,536 and 1.63, respectively. The β1 and β2 values for membrane B were determined to be 1,044,640 and 1.83.
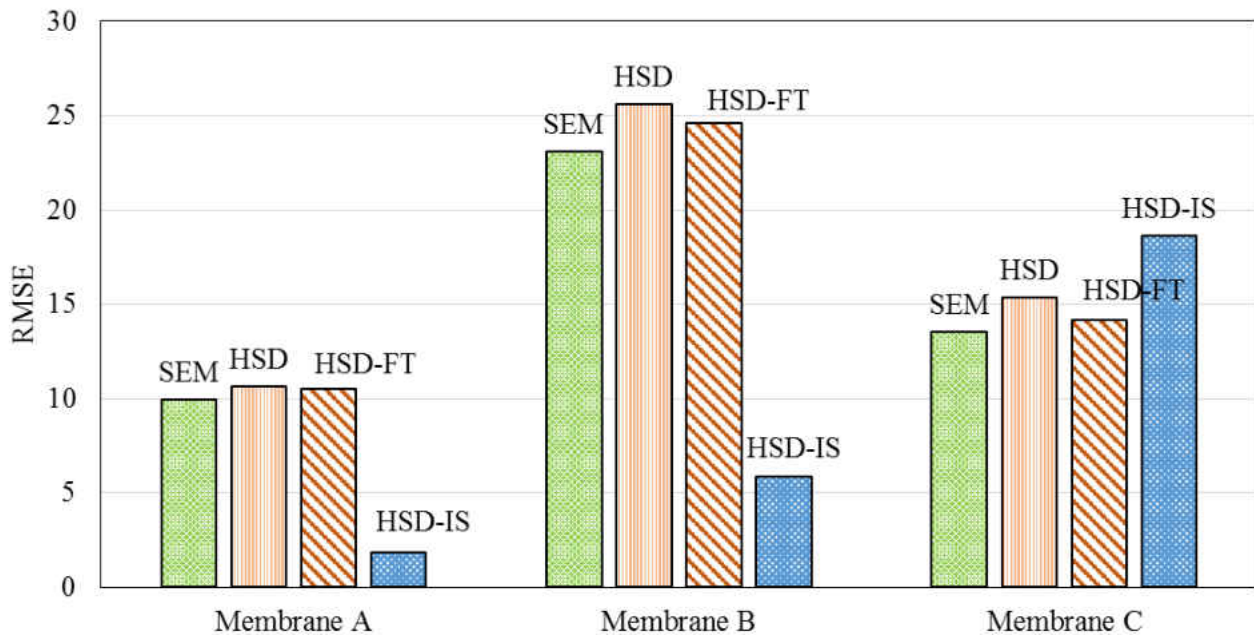
Figure 7-1: Model Comparison for Magnesium

Bench-Scale HFNF Membrane Testing Using Aerated Groundwater

The conclusions drawn from the bench-scale testing experiments of the City's biologically active aerated Verna groundwater supply are provided herein.

- Biological activity reaction tests and standard plate counts confirmed the presence of slime bacteria in the aerated water supply.

- Sand filtration using either coarse or fine sand provided sufficient removal of turbidity and suspended solids to achieve SDI and MFI values within the acceptable range for NF membranes as shown in the Verna pretreatment assessment.

- Membrane A and B were effective at removing over 65% divalent ions while also attaining some monovalent removal indicating the membranes exhibit NF removal characteristics.

- Membrane C was less effective at removing divalent ions however some rejection (approximately 30%) was attained, which could prove to be sufficient for treated aerated Verna water.

- Membranes A, B, and C were capable of removing 91%, 89%, and 66% of TOC, respectively. EEM analysis confirmed significant removals (>85%) of fluorescence organics were removed using membranes A and B.

- Newer HFNF membranes could offer significant cost savings by combining the hydraulic performance of HFUF with the removal effectiveness of SWNF. This combined technology could serve as an alternative option for the City in improving the quality of its water supply when this technique becomes commercially available in the near future.

Pilot-Scale HFNF Membrane Testing Using Aerated Groundwater

One objective of this research was to evaluate a HF membrane offering nanofiltration properties that aimed to integrate the hydraulic operation of a conventional HFUF process. The hydraulic operations of a HFUF process of this kind could provide significant operational costs savings if the water quality goals could be met. Generally, the data collected on the hydraulic parameters monitored throughout this study indicate that the membrane did not experience significant fouling. As such, cleaning chemicals were not used during the duration of this study. A pressure decay test (PDT) was conducted on the membrane at the conclusion of the study indicating no fiber breakage and no loss of performance. Additional findings regarding the HFNF pilot have been listed herein.

- As permeate backpressure was decreased from 100 to 0 psi the normalized specific flux increased from 1.2 gfd/psi to 1.5 gfd/psi, improving the productivity of the system.

- A decrease of nearly 87% in operating pressures did not significantly (<3% difference) affect the membrane removal efficiency for the targeted constituents.

- The HFNF membrane did not experience rapid fouling when treating Verna groundwater with sand filtration pretreatment. The membrane's durability and performance remained unchanged while producing a consistent water quality.

- The hydraulic performance of the HFNF pilot was not significantly affected with the removal of the SF pretreatment nor did it affect the permeate water quality, indicating the membrane could possibly be used to treat Verna water without additional pretreatment. However protecting the membrane from fouling remains a priority and it was therefore recommended to include the pretreatment process of SF in conceptual cost estimations.

- The results from the pilot testing show an average sulfate removal of 7% corresponding to a flux of 13 gfd. Sulfate removals as high as 9% were obtained at the highest flux setting tested during this study.

- The membrane achieved an average TOC removal of approximately twenty-five percent. Ninety-five percent of the TOC in the Verna water was comprised of dissolved constituents indicating partial removal of DOC.

- The membrane was successful at removing turbidity consistently producing water with less than 1.0 NTU.

- The HFNF membrane under investigation did not attain the water quality goals of the City, specifically sulfate and hardness removal and was therefore not recommended as a treatment alternative for the aerated Verna source.

Pilot-Scale SWNF Membrane Testing Using Aerated Groundwater

One of the primary objectives of the research conducted with respect to the Verna water supply was whether or not traditional SWNF membrane processes could be employed to treat the water supply, and to what degree of pretreatment would be required. It was determined that a combination of SF and HFUF processes would overcome the technical water quality challenges associated with SWNF treatment of the aerated Verna water supply. Additional findings regarding the traditional SWNF pilot include the items presented herein.

- A difference of 26 hours was observed between the unplanned downtime distributions of the two pilot systems, indicating that the majority of the unplanned downtime was not due to the SWNF pilot but rather the pretreatment processes. One item that should be considered but is difficult to measure is the operation of multiple unit processes in the water

treatment plant. As seen from the pilot data, multiple processes in series add to the complexity and operation of the plant which would likely require more maintenance and skilled operators.

- The HFUF feed and filtrate storage tanks were modified to be light resistant to control biogrowth equating in chemical cost savings but a decrease in the HFUF feed water quality.

- Increasing the flux of the HFUF system required changing the sand filter flow rates which caused a slight increase in the turbidity of the SF filtrate. Regardless, SF pretreatment, when in operation, decreased the average turbidity of the Verna water by approximately 0.4 NTU. The HFUF consistently produced turbidities below 0.08 NTU over the course of testing proving to be an adequate pretreatment in junction with SF for the removal of colloidal sulfur turbidity.

- Backwashes were sufficient for maintaining an operating TMP of approximately 2 psi when operating at a flux 31 gfd.

- HFUF filtrate turbidities of 0.02 NTU were consistently achieved under this operating condition and were in part due to a cake filtration layer present on the membrane surface. Once CEBs were initiated with citric acid, filtrate turbidity values increased and TMP decreased indicating the cake layer had been removed from the membrane. Daily CEBs were required in addition to backwashes to maintain an approximate TMP of 7 psi when producing a flux of 45 gfd.

- The increase in flux and removal of SF pretreatment caused a rise in TMP and decline in the specific flux of the membrane indicating that SF would be necessary as a pretreatment process to prevent fouling.

- Treating aerated groundwater required a combination of SF, HFUF, and CF pretreatment processes achieved 90% divalent ion removal, 99% sulfate removal, and 96% organics retention.

Conceptual Cost Comparison

- Conceptual cost comparisons were based on a 6 MGD SF process, a 2.1 MGD HFUF process, and softening processes sized for producing 2 MGD assuming an 85% recovery.

- Conceptual capital costs for the HFNF treatment alternative and the SWNF treatment alternative were estimated to be $4.4 million and $5.6 million, respectively.

- Excluding the cost of labor and fringes, conceptual operating cost for the HFNF process including SF pretreatment was estimated to be $0.57/kgal. The conceptual operating cost for the traditional SWNF process including SF, HFUF, and CF pretreatment was estimated to be $0.84/kgal.

8. RECOMMENDATIONS

From the experimental results obtained in these investigations the following recommendations were provided to the City regarding the treatment of the aerate Verna water supply:

- The SF pretreatment assessment of the Verna water supply showed 50% turbidity reduction, average effluent SDIs of 4.3, and average MFIs less than 4 s/L^2 using either sand filter media. Therefore, UCF recommended that the City (at a minimum) filter the Verna water supply in its entirety to reduce turbidity loadings to the existing water distribution system.

- If the City wished to treat the Verna wellfield for TOC, sulfate, and hardness removal within the current 5-year capital improvement plan timeframe, then integrated SF-HFUF-SWNF membrane treatment would be required.

- The results from the bench-scale testing showed increased rejections for divalent ions using two next generation membranes (membranes A and B) compared to commercially available HFNF membranes. If the City does not implement membrane treatment of Verna within the current capital improvement plan timeline, alternative next generation HFNF membranes should be assessed using full-scale modules and pilot testing.

APPENDIX A – LABORATORY AND FIELD DATA

Table A-1: Experimental Bench-Scale Testing Conditions

Phase	Type	Testing Solution	Run	Concentrate Flow (mL/min)	Permeate Flow (mL/min)	Target Flux (gfd)	Target Flux (lmh)	Membrane Recovery	Sample Set #
0	A	Deionized Water	PT					50%	N/A
0	A	Solution 1	1	29	31	14	25	51%	1-15
0	A	Solution 1	2	25	26	12	20	51%	16-30
0	A	Solution 1	3	13	13	6	10	50%	31-45
1	A	Solution 1	4	19	19	9	15	50%	45-60
1	A	Solution 1	5	24	25	12	20	51%	61-75
1	A	Solution 1	6	8.5	25	12	20	75%	76-80
1	A	Solution 1	7	4.5	25	12	20	85%	81-85
1	A	Solution 1	8	31	31	14	25	50%	86-90
1	A	Solution 1	9	10.5	31	14	25	75%	91-95
1	A	Solution 1	10	5.5	31	14	25	85%	96-100
1	A	Solution 1	11	6.5	19	9	15	75%	101-105
1	A	Solution 1	12	3.4	19	9	15	85%	106-110
1	A	Solution 1	13	8.5	25	12	20	75%	111-115
1	A	Solution 1	14	5.5	31	14	25	85%	116-120
1	A	Solution 1.1	15	8.5	25	12	20	75%	121-125
1	A	Solution 1.1	16	4.5	25	12	20	85%	126-130
1	A	Solution 1.2	17	8.5	25	12	20	75%	131-135
1	A	Solution 1.2	18	4.5	25	12	20	85%	136-140
1	A	Solution 1.3	19	8.5	25	12	20	75%	141-145
1	A	Solution 1.3	20	4.5	25	12	20	85%	146-150
1	A	Solution 1.4	21	8.5	25	12	20	75%	151-155
1	A	Solution 1.4	22	4.5	25	12	20	85%	156-160
1	A	Deionized Water	PT	25	25	12	20	50%	N/A

Table A-2: Experimental Bench-Scale Testing Conditions

Phase	Type	Testing Solution	Run	Concentrate Flow (mL/min)	Permeate Flow (mL/min)	Target Flux (gfd)	Target Flux (lmh)	Membrane Recovery	Sample Set #
2	B	Deionized Water	PT	25	25	12	20	50%	N/A
2	B	Solution 1	23	6.5	19	9	15	75%	161-165
2	B	Solution 1	24	3.4	19	9	15	85%	166-170
2	B	Solution 1	25	8.5	25	12	20	75%	170-175
2	B	Solution 1	26	4.5	25	12	20	85%	176-180
2	B	Solution 1	27	10.5	31	14	25	75%	181-185
2	B	Solution 1	28	5.5	31	14	25	85%	186-190
2	B	Solution 1.1	29	8.5	25	12	20	75%	191-195
2	B	Solution 1.1	30	4.5	25	12	20	85%	196-200
2	B	Solution 1.2	31	8.5	25	12	20	75%	201-205
2	B	Solution 1.2	32	4.5	25	12	20	85%	206-210
2	B	Solution 1.3	33	8.5	25	12	20	75%	211-215
2	B	Solution 1.3	34	4.5	25	12	20	85%	216-220
2	B	Solution 1.4	35	8.5	25	12	20	75%	221-225
2	B	Solution 1.4	36	4.5	25	12	20	85%	226-230
2	B	Solution 1.1	37	10.5	31	14	25	75%	231-235
2	B	Solution 1.1	38	6.5	19	9	15	75%	236-240
2	B	Solution 1.2	39	6.5	19	9	15	75%	241-245
2	B	Solution 1.2	40	10.5	31	14	25	75%	246-250
2	B	Deionized Water	PT	25	25	12	20	50%	N/A

Table A-3: Experimental Bench-Scale Testing Conditions

Phase	Type	Testing Solution	Run	Concentrate Flow (mL/min)	Permeate Flow (mL/min)	Target Flux (gfd)	Target Flux (lmh)	Membrane Recovery	Sample Set #
3	C	Deionized Water	PT	25	25	12	20	50%	N/A
3	C	Solution 1	41	6.5	19	9	15	75%	251-255
3	C	Solution 1	42	3.4	19	9	15	85%	256-260
3	C	Solution 1	43	8.5	25	12	20	75%	261-265
3	C	Solution 1	44	4.5	25	12	20	85%	266-270
3	C	Solution 1	45	10.5	31	14	25	75%	271-275
3	C	Solution 1	46	5.5	31	14	25	85%	276-280
3	C	Solution 1.2	47	8.5	25	12	20	75%	281-285
3	C	Solution 1.2	48	4.5	25	12	20	85%	286-290
3	C	Solution 1.1	49	8.5	25	12	20	75%	291-295
3	C	Solution 1.1	50	4.5	25	12	20	85%	296-300
3	C	Solution 1.3	51	8.5	25	12	20	75%	301-305
3	C	Solution 1.3	52	4.5	25	12	20	85%	306-310
3	C	Solution 1.4	53	8.5	25	12	20	75%	311-315
3	C	Solution 1.4	54	4.5	25	12	20	85%	316-320
3	C	Solution 1.2	55	10.5	31	14	25	75%	321-325
3	C	Solution 1.2	56	6.5	19	9	15	75%	326-330
3	C	Solution 1.1	57	6.5	19	9	15	75%	331-335
3	C	Solution 1.1	58	10.5	31	14	25	75%	336-340
3	C	Deionized Water	PT	25	25	12	20	50%	N/A

Table A-4: Experimental Bench-Scale Testing Conditions

Phase	Type	Testing Solution	Run	Concentrate Flow (mL/min)	Permeate Flow (mL/min)	Target Flux (gfd)	Target Flux (lmh)	Membrane Recovery	Sample Set #
4	C	Deionized Water	PT	25	25	12	20	50%	N/A
4	C	Filtered Verna	59	8.5	25	12	20	75%	341-345
4	C	Filtered Verna	60	25	25	12	20	50%	346-350
4	C	Filtered Verna	61	31	31	14	25	50%	351-355
4	C	Filtered Verna	62	31	31	14	25	50%	356-360
4	C	Filtered Verna	63	4.5	25	12	20	85%	361-365
4	C	Filtered Verna	64	10.5	31	14	25	75%	366-370
4	C	Filtered Verna	65	5.5	31	14	25	85%	371-375
4	C	Deionized Water	PT	25	25	12	20	50%	N/A
4	B	Deionized Water	PT	25	25	12	20	50%	N/A
4	B	Filtered Verna	66	8.5	25	12	20	75%	376-380
4	B	Filtered Verna	67	4.5	25	12	20	85%	381-385
4	B	Filtered Verna	68	10.5	31	14	25	75%	386-390
4	B	Filtered Verna	69	5.5	31	14	25	85%	391-395
4	B	Deionized Water	PT	25	25	12	20	50%	N/A
4	A	Deionized Water	PT	25	25	12	20	50%	N/A
4	A	Filtered Verna	70	8.5	25	12	20	75%	396-400
4	A	Filtered Verna	71	4.5	25	12	20	85%	401-405
4	A	Filtered Verna	72	10.5	31	14	25	75%	406-410
4	A	Filtered Verna	73	5.5	31	14	25	85%	411-415
4	A	Deionized Water	PT	25	25	12	20	50%	N/A

Table A-5: Hydraulic Data for Bench-Scale Experiments using Synthetic Water

Type	Run	Set	Flow			Pressure			Temp.
			HFC (mL/min)	HFP (mL/min)	HFR (gpm)	HFF (psi)	HFR (psi)	HFS (psi)	HFF (ºC)
A	4	46	18	19	1.2	30	25	30	20.6
A	4	47	18	19	1.2	30	25	30	20.9
A	4	48	21	19	1.2	30	25	30	21.3
A	4	49	19	20	1.2	31	25	30	21.5
A	4	50	19	19	1.2	30	24	30	21.7
A	4	51	18	19	1.2	29	23	30	21.9
A	4	52	17	17	1.2	28	22	30	22.1
A	4	53	17	18	1.2	28	23	30	22.3
A	4	54	18	18	1.2	28	23	30	22.5
A	4	55	19	19	1.2	28	23	30	22.7
A	4	56	20	19	1.2	29	23	30	22.9
A	4	57	20	18	1.2	28	22	30	23.1
A	4	58	18	18	1.2	28	22	30	23.3
A	4	59	19	19	1.2	28	22	30	23.4
A	4	60	20	19	1.2	29	23	30	23.3
A	5	61	24	25	0.9	34	29	38	23.2
A	5	62	26	25	0.9	35	30	38	23.2
A	5	63	24	25	0.9	35	30	38	23.5
A	5	64	22	25	0.9	34	30	38	23.7
A	5	65	25	26	0.9	35	30	38	23.9
A	5	66	23	25	0.9	34	29	38	24.1
A	5	67	25	25	0.9	33	29	38	24.3
A	5	68	25	25	0.9	34	29	38	24.5
A	5	69	26	24	0.9	33	29	38	24.6
A	5	70	23	25	0.9	34	29	38	24.6
A	5	71	24	24	0.9	33	29	38	24.7
A	5	72	25	25	0.9	33	29	38	24.7
A	5	73	25	26	0.9	34	30	38	24.8
A	5	74	23	25	0.9	34	29	38	25.3
A	5	75	25	25	0.9	33	29	38	25.8
A	7	81	5	26	0.8	33	30	35	22.7
A	7	82	5	27	0.8	34	30	35	23.0
A	7	83	5	27	0.8	34	30	35	23.4
A	7	84	6	27	0.8	33	29	35	23.6
A	7	85	5	26	0.8	33	28	35	23.9
A	8	86	29	32	0.7	37	35	80	24.0
A	8	87	30	31	0.7	36	34	80	24.4
A	8	88	31	31	0.7	36	33	80	24.7

Table A-5: Hydraulic Data for Bench-Scale Experiments using Synthetic Water

Type	Run	Set	Flow			Pressure			Temp.
			HFC (mL/min)	HFP (mL/min)	HFR (gpm)	HFF (psi)	HFR (psi)	HFS (psi)	HFF (ºC)
A	8	89	32	31	0.7	36	33	80	24.9
A	8	90	30	32	0.7	36	33	80	25.7
A	9	91	11	32	0.7	36	33	80	25.9
A	9	92	10	32	0.7	36	33	80	26.0
A	9	93	11	32	0.7	36	33	80	26.1
A	9	94	11	32	0.7	36	32	80	26.2
A	9	95	11	32	0.7	36	32	80	26.2
A	11	101	7	19	0.6	27	24	21	26.3
A	11	102	6	19	0.6	26	24	21	26.4
A	11	103	7	20	0.6	24	21	21	27.0
A	11	104	7	19	0.6	23	21	21	26.9
A	11	105	6	19	0.6	23	21	21	27.0
A	12	106	4	20	0.5	28	26	22	22.6
A	12	107	4	19	0.5	27	25	22	22.8
A	12	108	4	20	0.5	28	26	22	23.0
A	12	109	3	19	0.5	26	24	22	23.2
A	12	110	3	20	0.5	27	25	22	23.3
A	13	111	8	25	0.6	36	33	35	22.9
A	13	112	8	26	0.6	36	33	35	23.2
A	13	113	9	25	0.6	36	33	35	23.5
A	13	114	8	26	0.6	36	33	35	23.8
A	13	115	9	25	0.6	36	33	35	24.1
A	14	116	5	31	0.3	40	38	70	24.4
A	14	117	6	31	0.3	40	39	70	24.6
A	14	118	5	31	0.3	40	39	70	24.8
A	14	119	6	32	0.3	39	38	70	25.0
A	14	120	6	31	0.3	40	39	70	25.2
A	15	121	9	25	0.7	36	33	40	23.6
A	15	122	8	25	0.7	36	32	40	23.7
A	15	123	8	25	0.7	35	32	40	23.8
A	15	124	7	25	0.7	35	31	40	23.9
A	15	125	9	24	0.7	34	30	40	24.0
A	16	126	5	25	0.8	34	30	33	24.1
A	16	127	5	26	0.8	35	31	33	24.3
A	16	128	4	26	0.8	35	31	33	24.7
A	16	129	4	26	0.8	35	30	33	25.0
A	16	130	5	26	0.8	35	29	33	25.3
A	17	131	8	25	1.0	32	26	29	23.4
A	17	132	8	25	1.0	31	26	29	23.5

Table A-5: Hydraulic Data for Bench-Scale Experiments using Synthetic Water

Type	Run	Set	Flow HFC (mL/min)	Flow HFP (mL/min)	Flow HFR (gpm)	HFF (psi)	Pressure HFR (psi)	HFS (psi)	Temp. HFF (ºC)
A	17	133	9	26	1.0	32	27	29	23.6
A	17	134	8	26	1.0	32	26	29	23.7
A	17	135	8	25	1.0	31	25	29	23.7
A	18	136	4	26	1.0	32	26	28	23.8
A	18	137	4	25	1.0	31	25	28	24.1
A	18	138	5	25	1.0	31	25	28	24.3
A	18	139	5	25	1.0	31	25	28	24.6
A	18	140	4	24	1.0	30	24	28	24.9
A	19	141	8	25	0.8	34	30	35	23.1
A	19	142	8	25	0.8	34	30	35	23.2
A	19	143	9	26	0.8	35	31	35	23.3
A	19	144	8	25	0.8	34	30	35	23.4
A	19	145	8	26	0.8	34	30	35	23.5
A	20	146	5	25	0.9	24	29	30	23.9
A	20	147	5	25	0.9	24	28	30	24.0
A	20	148	5	25	0.9	24	28	30	24.1
A	20	149	4	25	0.9	24	28	30	24.2
A	20	150	5	25	0.9	24	28	30	24.3
A	21	151	8	25	0.8	35	31	30	22.8
A	21	152	8	25	0.8	35	31	30	23.0
A	21	153	9	25	0.8	35	31	30	23.5
A	21	154	8	25	0.8	35	31	30	24.0
A	21	155	9	25	0.8	35	31	30	24.3
A	22	156	5	25	0.8	34	30	30	25.1
A	22	157	4	25	0.8	34	30	30	25.2
A	22	158	5	25	0.8	34	30	30	25.3
A	22	159	5	25	0.8	34	30	30	25.5
A	22	160	4	26	0.8	34	30	30	25.6
B	23	161	6	19	1.6	29	24	24	23.6
B	23	162	6	19	1.	28	24	24	23.7
B	23	163	7	20	1.1	29	25	24	23.8
B	23	164	7	20	1.1	29	25	24	23.9
B	23	165	7	20	1.1	29	25	24	24.1
B	24	166	3	19	1.2	28	23	22	24.3
B	24	167	3	19	1.2	28	23	22	24.3
B	24	168	4	19	1.2	28	23	22	24.5
B	24	169	3	19	1.2	28	23	22	24.6
B	24	170	4	19	1.1	27	22	22	24.6
B	25	171	8	25	1.0	34	30	36	24.8

Table A-5: Hydraulic Data for Bench-Scale Experiments using Synthetic Water

| Type | Run | Set | Flow | | | | Pressure | | | Temp. |
			HFC (mL/min)	HFP (mL/min)	HFR (gpm)	HFF (psi)	HFR (psi)	HFS (psi)	HFF (ºC)
B	25	172	8	25	1.1	34	29	36	24.8
B	25	173	9	25	1.1	33	29	36	24.9
B	25	174	8	25	1.1	33	29	36	25.0
B	25	175	8	25	1.0	33	29	36	25.0
B	26	176	5	25	0.8	36	33	37	23.5
B	26	177	5	25	0.8	35	32	37	23.7
B	26	178	6	25	0.9	36	32	37	23.8
B	26	179	5	25	0.9	35	32	37	24.0
B	26	180	5	25	0.9	35	32	37	24.1
B	27	181	11	31	0.7	40	38	85	24.5
B	27	182	10	31	0.7	40	38	85	24.5
B	27	183	10	31	0.7	40	37	85	24.6
B	27	184	11	31	0.7	39	37	85	24.6
B	27	185	10	31	0.7	39	37	85	24.7
B	28	186	5	31	0.7	39	36	85	24.9
B	28	187	5	31	0.7	38	36	85	24.9
B	28	188	5	31	0.7	38	36	85	25.0
B	28	189	6	31	0.7	38	36	85	25.0
B	28	190	6	31	0.8	38	35	85	25.1
B	29	191	8	25	0.9	34	31	32	25.3
B	29	192	9	25	0.8	34	31	32	25.5
B	29	193	9	25	0.9	34	31	32	25.7
B	29	194	8	25	0.9	34	31	32	25.8
B	29	195	8	25	0.9	33	30	32	25.9
B	30	196	4	25	0.9	33	29	29	26.3
B	30	197	5	25	0.9	32	28	29	26.4
B	30	198	4	25	0.9	33	29	29	26.5
B	30	199	4	25	1.0	32	29	29	26.6
B	30	200	5	25	1.0	32	28	29	26.8
B	31	201	9	25	0.9	30	27	25	27.0
B	31	202	9	26	0.9	30	27	25	27.1
B	31	203	8	25	0.9	29	26	25	27.2
B	31	204	8	26	0.8	30	27	25	27.3
B	31	205	9	24	1.0	28	25	25	27.4
B	32	206	4	25	1.1	31	26	29	27.6
B	32	207	5	25	1.2	31	26	29	27.7
B	32	208	5	24	1.1	30	26	29	27.7
B	32	209	5	25	1.2	32	27	29	27.7
B	32	210	4	25	1.1	32	27	29	27.7

Table A-5: Hydraulic Data for Bench-Scale Experiments using Synthetic Water

Type	Run	Set	Flow			Pressure			Temp.
			HFC (mL/min)	HFP (mL/min)	HFR (gpm)	HFF (psi)	HFR (psi)	HFS (psi)	HFF (ºC)
B	33	211	8	25	0.8	35	32	39	23.4
B	33	212	9	25	0.8	35	32	39	23.5
B	33	213	8	25	0.8	34	31	39	23.6
B	33	214	9	25	0.8	34	32	39	23.8
B	33	215	8	25	0.8	34	31	39	23.9
B	34	216	10	29	0.6	40	37	85	24.2
B	34	217	11	31	0.6	39	37	85	24.3
B	34	218	10	29	0.7	39	37	85	24.4
B	34	219	11	32	0.6	39	36	85	24.5
B	34	220	10	31	0.6	38	36	85	24.6
B	35	221	9	26	0.9	34	31	33	24.4
B	35	222	8	25	0.9	34	30	33	24.5
B	35	223	9	25	0.9	34	30	33	24.6
B	35	224	9	25	0.9	34	30	33	24.7
B	35	225	8	25	1.0	33	30	33	24.7
B	36	226	10	31	0.8	38	35	80	25.0
B	36	227	10	31	0.8	38	35	80	25.2
B	36	228	11	31	0.8	38	35	80	25.3
B	36	229	11	31	0.8	38	35	80	25.3
B	36	230	11	32	0.8	38	35	80	25.4
B	37	231	10	31	0.8	38	36	80	26.2
B	37	232	10	31	0.8	38	35	80	26.4
B	37	233	10	31	0.8	38	35	80	26.5
B	37	234	10	31	0.8	38	35	80	26.7
B	37	235	11	31	0.8	38	35	80	26.8
B	38	236	7	19	1.1	27	22	25	27.1
B	38	237	6	18	1.2	28	23	25	27.2
B	38	238	6	19	1.1	28	23	25	27.2
B	38	239	7	19	1.1	29	25	25	27.1
B	38	240	7	19	1.1	29	24	25	27.1
B	39	241	11	31	0.9	37	34	74	27.7
B	39	242	11	32	0.9	38	34	74	27.7
B	39	243	12	31	1.0	36	33	74	27.8
B	39	244	11	31	1.0	37	33	74	27.8
B	39	245	10	32	1.0	36	32	74	27.9
B	40	246	7	20	1.0	26	22	20	25.8
B	40	247	7	19	0.9	25	21	20	26.0
B	40	248	7	19	0.9	24	21	20	26.2
B	40	249	7	19	0.9	24	21	20	26.5

Table A-5: Hydraulic Data for Bench-Scale Experiments using Synthetic Water

Type	Run	Set	Flow			Pressure			Temp. HFF (ºC)
			HFC (mL/min)	HFP (mL/min)	HFR (gpm)	HFF (psi)	HFR (psi)	HFS (psi)	
B	40	250	6	19	0.9	24	21	20	26.6
C	41	251	6	20	0.7	34	32	30	21.6
C	41	252	7	19	0.7	33	30	30	22.1
C	41	253	6	20	0.7	34	32	30	22.4
C	41	254	6	19	0.7	35	33	30	23.6
C	41	255	6	21	0.7	34	31	30	23.9
C	42	256	3	20	0.7	31	29	28	25.7
C	42	257	4	20	0.8	31	29	28	26.1
C	42	258	4	19	0.8	30	27	28	26.5
C	42	259	3	20	0.9	31	28	28	26.9
C	42	260	3	19	0.9	30	27	28	27.2
C	43	261	9	26	0.8	37	34	60	28.2
C	43	262	8	26	0.9	37	34	60	28.4
C	43	263	8	26	0.9	37	34	60	28.5
C	43	264	8	25	0.9	36	33	60	28.7
C	43	265	9	25	0.9	36	33	60	28.9
C	44	266	4	25	0.7	37	35	72	28.9
C	44	267	5	25	0.7	37	35	72	28.8
C	44	268	5	26	0.7	37	35	72	28.7
C	44	269	5	26	0.7	37	35	72	28.8
C	44	270	4	26	0.7	37	34	72	28.9
C	45	271	9	31	0.3	42	41	82	29.2
C	45	272	10	31	0.3	41	41	82	29.3
C	45	273	10	31	0.3	42	41	82	29.3
C	45	274	11	32	0.3	42	41	82	29.4
C	45	275	10	32	0.3	42	41	82	29.4
C	46	276	5	32	0.2	42	41	80	29.6
C	46	277	6	32	0.2	42	41	80	29.7
C	46	278	6	31	0.2	41	40	80	29.9
C	46	279	6	31	0.2	41	40	80	30.0
C	46	280	6	31	0.2	41	40	80	29.9
C	47	281	8	26	1.0	37	33	80	25.4
C	47	282	9	26	1.0	37	33	80	25.7
C	47	283	9	26	1.0	37	33	80	26.0
C	47	284	8	26	1.0	36	32	80	26.3
C	47	285	8	26	1.0	36	32	80	26.6
C	48	286	5	26	1.0	35	31	74	28.4
C	48	287	5	26	1.0	35	31	74	28.4
C	48	288	5	26	1.0	35	31	74	28.8

Table A-5: Hydraulic Data for Bench-Scale Experiments using Synthetic Water

Type	Run	Set	Flow			Pressure			Temp.
			HFC (mL/min)	HFP (mL/min)	HFR (gpm)	HFF (psi)	HFR (psi)	HFS (psi)	HFF (ºC)
C	48	289	5	26	1.0	35	31	74	28.0
C	48	290	5	26	1.0	35	31	74	28.7
C	49	291	8	26	0.5	38	36	53	25.4
C	49	292	9	25	0.5	37	35	53	25.7
C	49	293	9	25	0.5	37	35	53	26.0
C	49	294	8	25	0.5	37	35	53	26.2
C	49	295	9	26	0.6	37	35	53	26.5
C	50	296	4	25	0.6	36	34	48	26.8
C	50	297	4	25	0.5	36	34	48	27.1
C	50	298	5	25	0.5	36	35	48	27.3
C	50	299	4	26	0.6	37	35	48	27.6
C	50	300	5	25	0.6	36	34	48	27.8
C	51	301	9	25	0.6	37	35	51	25.2
C	51	302	10	25	0.5	37	35	51	25.5
C	51	303	11	26	0.5	37	35	51	25.8
C	51	304	11	26	0.6	37	35	51	26.0
C	51	305	11	25	0.6	36	34	51	26.2
C	52	306	4	25	0.6	36	34	40	26.6
C	52	307	5	25	0.6	35	33	40	26.7
C	52	308	5	25	0.6	36	34	40	26.8
C	52	309	5	25	0.6	35	33	40	26.9
C	52	310	4	25	0.6	36	34	40	27.1
C	53	311	11	24	0.5	36	35	43	26.2
C	53	312	12	25	0.5	37	35	43	26.6
C	53	313	12	26	0.5	37	35	43	26.8
C	53	314	10	25	0.5	36	34	43	27.0
C	53	315	10	26	0.5	36	35	43	27.2
C	54	316	4	26	0.5	36	34	36	27.6
C	54	317	4	26	0.6	36	34	36	27.8
C	54	318	5	26	0.6	36	34	36	28.0
C	54	319	4	26	0.6	36	34	36	28.1
C	54	320	5	26	0.6	36	34	36	28.3
C	55	321	11	31	0.8	40	37	85	29.0
C	55	322	9	31	0.8	40	37	85	29.2
C	55	323	10	31	0.8	40	37	85	29.3
C	55	324	11	31	0.8	40	37	85	29.3
C	55	325	11	32	0.8	40	37	85	29.5
C	56	326	8	19	1.0	31	27	30	23.5
C	56	327	6	20	1.0	31	27	30	23.8

Table A-5: Hydraulic Data for Bench-Scale Experiments using Synthetic Water

Type	Run	Set	Flow			Pressure			Temp.
			HFC (mL/min)	HFP (mL/min)	HFR (gpm)	HFF (psi)	HFR (psi)	HFS (psi)	HFF (ºC)
C	56	328	6	20	1.0	31	28	30	24.1
C	56	329	8	20	1.0	31	27	30	24.4
C	56	330	7	19	1.0	30	26	30	24.6
C	57	331	6	19	0.9	32	28	33	23.0
C	57	332	7	19	0.9	32	28	33	23.3
C	57	333	6	19	0.9	31	28	33	23.7
C	57	334	7	20	1.0	32	28	33	24.0
C	57	335	6	19	0.9	31	27	33	24.3
C	58	336	9	31	0.2	42	42	84	26.6
C	58	337	9	31	0.2	42	42	84	26.8
C	58	338	10	31	0.2	42	41	84	27.0
C	58	339	10	31	0.2	42	41	84	27.2
C	58	340	10	32	0.2	42	41	84	27.4

Table A-6: Water Quality Results for Bench-Scale Experiments using Synthetic Water

Type	Run	Set	Conductivity μS/cm		Magnesium (mg/L)		Sulfate (mg/L)		Sodium (mg/L)		Chloride (mg/L)	
			HFC	HFP	HFC	HFP	HFC	HFP	HFC	HFP	HFC	HFP
A	4	46	935	145	127	15	469	56	-	-	-	-
A	4	47	938	111	125	11	473	41	-	-	-	-
A	4	48	942	105	124	10	472	38	-	-	-	-
A	4	49	947	104	126	10	478	38	-	-	-	-
A	4	50	949	105	128	10	479	38	-	-	-	-
A	4	51	955	106	129	10	479	39	-	-	-	-
A	4	52	960	109	130	11	488	40	-	-	-	-
A	4	53	972	115	130	11	486	42	-	-	-	-
A	4	54	975	118	130	12	483	44	-	-	-	-
A	4	55	982	120	132	12	488	45	-	-	-	-
A	4	56	986	122	133	12	495	46	-	-	-	-
A	4	57	993	121	133	12	495	45	-	-	-	-
A	4	58	989	124	134	13	500	47	-	-	-	-
A	4	59	1007	127	134	13	503	48	-	-	-	-
A	4	60	1005	132	135	13	501	49	-	-	-	-
A	5	61	986	116	133	11	494	43	-	-	-	-
A	5	62	985	110	131	11	492	41	-	-	-	-
A	5	63	991	110	133	11	496	41	-	-	-	-
A	5	64	988	112	134	11	497	41	-	-	-	-
A	5	65	1001	113	135	11	502	41	-	-	-	-
A	5	66	1008	115	135	11	504	42	-	-	-	-
A	5	67	1011	116	137	12	506	43	-	-	-	-
A	5	68	1010	119	139	12	494	44	-	-	-	-
A	5	69	1013	120	139	12	509	45	-	-	-	-
A	5	70	1008	121	138	12	507	46	-	-	-	-
A	5	71	1026	123	138	12	517	46	-	-	-	-

Table A-6: Water Quality Results for Bench-Scale Experiments using Synthetic Water

Type	Run	Set	Conductivity µS/cm		Magnesium (mg/L)		Sulfate (mg/L)		Sodium (mg/L)		Chloride (mg/L)	
			HFC	HFP	HFC	HFP	HFC	HFP	HFC	HFP	HFC	HFP
A	5	72	1032	124	138	13	516	47	-	-	-	-
A	5	73	1038	125	140	13	519	47	-	-	-	-
A	5	74	1040	125	140	13	519	47	-	-	-	-
A	5	75	1034	125	143	13	524	48	-	-	-	-
A	7	81	1070	127	143	13	535	48	-	-	-	-
A	7	82	1075	128	147	13	533	48	-	-	-	-
A	7	83	1074	128	147	13	538	48				
A	7	84	1081	128	148	13	545	49	-	-	-	-
A	7	85	1081	128	150	13	542	48	-	-	-	-
A	8	86	1111	139	154	14	552	53	-	-	-	-
A	8	87	1112	134	152	13	552	51	-	-	-	-
A	8	88	1114	134	154	13	559	51	-	-	-	-
A	8	89	1123	133	155	13	565	51	-	-	-	-
A	8	90	1122	130	153	13	559	51	-	-	-	-
A	9	91	1117	133	154	14	564	52	-	-	-	-
A	9	92	1122	138	157	14	564	53	-	-	-	-
A	9	93	1127	140	155	14	568	54	-	-	-	-
A	9	94	1131	140	159	14	569	55	-	-	-	-
A	9	95	1138	143	157	15	574	56	-	-	-	-
A	11	101	1198	156	167	17	613	32	-	-	-	-
A	11	102	1205	172	169	18	614	70	-	-	-	-
A	11	103	1209	179	172	19	622	74	-	-	-	-
A	11	104	1217	183	172	19	625	75	-	-	-	-
A	11	105	1228	183	172	19	630	76	-	-	-	-
A	12	106	1275	184	182	19	660	75	-	-	-	-
A	12	107	1272	185	181	19	655	75	-	-	-	-

Table A-6: Water Quality Results for Bench-Scale Experiments using Synthetic Water

Type	Run	Set	Conductivity µS/cm		Magnesium (mg/L)		Sulfate (mg/L)		Sodium (mg/L)		Chloride (mg/L)	
			HFC	HFP	HFC	HFP	HFC	HFP	HFC	HFP	HFC	HFP
A	12	108	1279	188	183	20	659	77	-	-	-	-
A	12	109	1297	188	183	19	666	77	-	-	-	-
A	12	110	1301	198	186	21	678	82	-	-	-	-
A	13	111	1309	159	180	16	690	61	-	-	-	-
A	13	112	1288	157	176	15	687	60	-	-	-	-
A	13	113	1293	158	177	15	689	60	-	-	-	-
A	13	114	1302	160	179	16	688	61	-	-	-	-
A	13	115	1305	161	179	16	694	62	-	-	-	-
A	14	116	1333	179	189	18	712	71	-	-	-	-
A	14	117	1353	186	186	18	717	73	-	-	-	-
A	14	118	1361	190	188	19	724	76	-	-	-	-
A	14	119	1366	192	192	19	730	77	-	-	-	-
A	14	120	1369	194	192	20	741	78	-	-	-	-
A	15	121	1371	169	193	17	735	32	-	-	-	-
A	15	122	1364	168	189	16	733	32	-	-	-	-
A	15	123	1374	169	193	17	737	32	-	-	-	-
A	15	124	1383	172	194	17	746	33	-	-	-	-
A	15	125	1405	178	195	17	752	34	-	-	-	-
A	16	126	1433	189	203	19	776	36	-	-	-	-
A	16	127	1435	191	204	19	770	36	-	-	-	-
A	16	128	1436	191	198	19	781	37	-	-	-	-
A	16	129	1456	198	206	20	785	38	-	-	-	-
A	16	130	1479	198	211	20	792	38	-	-	-	-
A	17	131	443	40	50	3	197	13	-	-	-	-
A	17	132	433	40	49	3	202	14	-	-	-	-
A	17	133	436	41	49	3	202	14	-	-	-	-

Table A-6: Water Quality Results for Bench-Scale Experiments using Synthetic Water

Type	Run	Set	Conductivity μS/cm		Magnesium (mg/L)		Sulfate (mg/L)		Sodium (mg/L)		Chloride (mg/L)	
			HFC	HFP	HFC	HFP	HFC	HFP	HFC	HFP	HFC	HFP
A	17	134	441	41	50	4	204	14	-	-	-	-
A	17	135	447	42	50	4	207	14	-	-	-	-
A	18	136	455	45	53	4	209	15	-	-	-	-
A	18	137	457	45	53	4	212	15	-	-	-	-
A	18	138	459	46	54	4	212	16	-	-	-	-
A	18	139	467	48	54	4	214	16	-	-	-	-
A	18	140	475	49	55	4	223	17	-	-	-	-
A	19	141	2370	1445	121	19	438	94	223	189	391	336
A	19	142	2390	1424	118	18	442	89	219	186	390	330
A	19	143	2390	1422	123	17	451	85	222	186	396	328
A	19	144	2400	1424	121	17	454	90	221	182	395	332
A	19	145	2420	1435	124	17	459	91	224	187	397	332
A	20	146	2450	1456	126	19	474	94	223	189	400	331
A	20	147	2470	1455	128	19	444	95	222	190	373	331
A	20	148	2480	1473	131	20	476	101	221	194	396	340
A	20	149	2490	1476	131	20	489	101	223	189	402	337
A	20	150	2520	1485	134	20	493	101	223	190	398	341
A	21	151	5570	4490	118	44	441	73	697	627	1339	1256
A	21	152	5560	4480	122	43	446	72	684	623	1351	1233
A	21	153	5570	4470	123	43	451	73	665	620	1355	1242
A	21	154	5580	4500	124	43	456	73	686	609	1353	1259
A	21	155	5590	4470	127	44	465	76	691	613	1373	1260
A	22	156	5600	4520	127	45	460	81	701	615	1350	1250
A	22	157	5630	4530	130	46	426	84	701	617	1239	1283
A	22	158	5600	4550	127	46	466	83	702	620	1359	1257
A	22	159	5670	4570	131	47	474	88	710	640	1366	1284

Table A-6: Water Quality Results for Bench-Scale Experiments using Synthetic Water

Type	Run	Set	Conductivity µS/cm		Magnesium (mg/L)		Sulfate (mg/L)		Sodium (mg/L)		Chloride (mg/L)	
			HFC	HFP	HFC	HFP	HFC	HFP	HFC	HFP	HFC	HFP
A	22	160	5660	4560	131	46	481	86	700	623	1369	1290
B	23	161	1120	229	148	23	553	96	-	-	-	-
B	23	162	1122	233	155	24	554	98	-	-	-	-
B	23	163	1127	242	148	25	556	103	-	-	-	-
B	23	164	1131	239	150	25	547	101	-	-	-	-
B	23	165	1132	242	149	25	565	104	-	-	-	-
B	24	166	1137	251	150	26	562	108	-	-	-	-
B	24	167	1142	254	147	26	567	109	-	-	-	-
B	24	168	1143	257	148	26	570	111	-	-	-	-
B	24	169	1146	260	152	26	575	113	-	-	-	-
B	24	170	1153	263	151	27	578	115	-	-	-	-
B	25	171	1177	236	155	24	593	100	-	-	-	-
B	25	172	1173	235	154	24	590	99	-	-	-	-
B	25	173	1183	235	156	24	591	100	-	-	-	-
B	25	174	1186	239	154	25	594	101	-	-	-	-
B	25	175	1194	241	157	25	601	102	-	-	-	-
B	26	176	1211	235	159	24	606	99	-	-	-	-
B	26	177	1211	232	157	23	609	97	-	-	-	-
B	26	178	1211	231	156	24	609	98	-	-	-	-
B	26	179	1219	231	159	24	617	97	-	-	-	-
B	26	180	1216	232	163	24	615	98	-	-	-	-
B	27	181	1253	375	163	24	635	96	-	-	-	-
B	27	182	1250	229	166	23	635	96	-	-	-	-
B	27	183	1250	231	165	23	632	97	-	-	-	-
B	27	184	1263	234	166	24	642	99	-	-	-	-
B	27	185	1267	238	167	24	646	101	-	-	-	-

Table A-6: Water Quality Results for Bench-Scale Experiments using Synthetic Water

Type	Run	Set	Conductivity µS/cm		Magnesium (mg/L)		Sulfate (mg/L)		Sodium (mg/L)		Chloride (mg/L)	
			HFC	HFP	HFC	HFP	HFC	HFP	HFC	HFP	HFC	HFP
B	28	186	1281	248	172	25	661	106	-	-	-	-
B	28	187	1287	251	173	26	658	107	-	-	-	-
B	28	188	1290	252	175	26	670	108	-	-	-	-
B	28	189	1293	256	170	26	657	110	-	-	-	-
B	28	190	1302	258	173	27	672	112	-	-	-	-
B	29	191	1394	301	210	32	721	123	-	-	-	-
B	29	192	1393	304	180	32	729	123	-	-	-	-
B	29	193	1400	300	169	32	730	126	-	-	-	-
B	29	194	1408	310	202	32	735	128	-	-	-	-
B	29	195	1421	313	206	33	738	130	-	-	-	-
B	30	196	1445	334	200	36	760	140	-	-	-	-
B	30	197	1451	339	194	36	761	142	-	-	-	-
B	30	198	1450	340	222	36	770	143	-	-	-	-
B	30	199	1460	342	187	37	766	144	-	-	-	-
B	30	200	1480	352	219	37	775	148	-	-	-	-
B	31	201	483	91	49	8	204	31	-	-	-	-
B	31	202	478	88	51	8	204	30	-	-	-	-
B	31	203	479	89	55	8	205	30	-	-	-	-
B	31	204	482	90	59	8	208	30	-	-	-	-
B	31	205	493	91	62	8	209	31	-	-	-	-
B	32	206	497	93	51	9	213	32	-	-	-	-
B	32	207	503	93	58	9	219	32	-	-	-	-
B	32	208	500	92	55	8	218	31	-	-	-	-
B	32	209	499	95	52	9	222	32	-	-	-	-
B	32	210	507	93	61	8	222	32	-	-	-	-
B	33	211	2450	1611	132	47	463	72	254	209	400	381

Table A-6: Water Quality Results for Bench-Scale Experiments using Synthetic Water

Type	Run	Set	Conductivity µS/cm		Magnesium (mg/L)		Sulfate (mg/L)		Sodium (mg/L)		Chloride (mg/L)	
			HFC	HFP	HFC	HFP	HFC	HFP	HFC	HFP	HFC	HFP
B	33	212	2460	1618	131	48	469	75	254	199	399	388
B	33	213	2470	1623	132	47	474	75	254	200	400	390
B	33	214	2480	1628	134	48	485	75	262	203	403	386
B	33	215	2490	1641	135	48	485	76	266	205	401	389
B	34	216	2540	1636	143	48	506	78	268	202	404	387
B	34	217	2570	1633	138	48	513	84	264	206	400	390
B	34	218	2530	1638	141	48	512	78	267	206	402	387
B	34	219	2540	1646	141	48	521	78	268	201	405	387
B	34	220	2560	1651	141	48	522	79	264	201	403	388
B	35	221	5630	4740	129	92	483	68	709	689	1345	1302
B	35	222	5600	4720	130	96	486	68	714	748	1358	1323
B	35	223	5590	4740	130	91	485	68	719	684	1347	1323
B	35	224	5620	4740	132	91	493	69	701	691	1352	1318
B	35	225	5620	4740	131	93	497	71	711	686	1341	1317
B	36	226	5660	4740	135	92	522	68	704	691	1363	1310
B	36	227	5700	4740	135	92	504	72	711	683	1327	1312
B	36	228	5660	4740	136	91	515	72	717	677	1342	1323
B	36	229	5660	4740	137	92	526	72	720	669	1351	1328
B	36	230	5680	4750	138	91	525	74	713	684	1342	1366
B	37	231	1540	365	197	39	818	154	-	-	-	-
B	37	232	1543	336	186	36	817	140	-	-	-	-
B	37	233	1552	337	181	36	816	142	-	-	-	-
B	37	234	1556	340	214	36	823	140	-	-	-	-
B	37	235	1574	346	218	37	836	144	-	-	-	-
B	38	236	1606	445	238	49	848	199	-	-	-	-
B	38	237	1608	462	222	51	853	208	-	-	-	-

Table A-6: Water Quality Results for Bench-Scale Experiments using Synthetic Water

Type	Run	Set	Conductivity µS/cm		Magnesium (mg/L)		Sulfate (mg/L)		Sodium (mg/L)		Chloride (mg/L)	
			HFC	HFP	HFC	HFP	HFC	HFP	HFC	HFP	HFC	HFP
B	38	238	1611	448	258	50	858	201	-	-	-	-
B	38	239	1617	430	246	48	853	192	-	-	-	-
B	38	240	1632	423	228	46	871	187	-	-	-	-
B	39	241	530	86	55	8	232	29	-	-	-	-
B	39	242	539	87	51	8	235	29	-	-	-	-
B	39	243	535	87	62	8	238	29	-	-	-	-
B	39	244	536	89	55	8	238	31	-	-	-	-
B	39	245	545	90	59	8	240	31	-	-	-	-
B	40	246	456	121	52	11	197	43	-	-	-	-
B	40	247	456	98	52	9	195	34	-	-	-	-
B	40	248	458	94	47	8	196	32	-	-	-	-
B	40	249	461	94	43	9	196	32	-	-	-	-
B	40	250	463	96	52	9	198	33	-	-	-	-
C	41	251	1324	1054	188	115	717	442	-	-	-	-
C	41	252	1324	1045	186	116	714	438	-	-	-	-
C	41	253	1322	1044	191	117	696	435	-	-	-	-
C	41	254	1326	1041	189	117	701	430	-	-	-	-
C	41	255	1337	1051	194	114	716	441	-	-	-	-
C	42	256	1326	1076	192	119	716	453	-	-	-	-
C	42	257	1328	1084	195	123	737	461	-	-	-	-
C	42	258	1341	1078	194	121	738	454	-	-	-	-
C	42	259	1320	1084	193	121	704	462	-	-	-	-
C	42	260	1326	1093	191	122	723	462	-	-	-	-
C	43	261	1382	1053	200	118	745	447	-	-	-	-
C	43	262	1368	1051	208	118	734	443	-	-	-	-
C	43	263	1379	1047	202	117	742	450	-	-	-	-

Table A-6: Water Quality Results for Bench-Scale Experiments using Synthetic Water

Type	Run	Set	Conductivity µS/cm		Magnesium (mg/L)		Sulfate (mg/L)		Sodium (mg/L)		Chloride (mg/L)	
			HFC	HFP	HFC	HFP	HFC	HFP	HFC	HFP	HFC	HFP
C	43	264	1381	1057	201	120	741	445	-	-	-	-
C	43	265	1389	1071	204	121	754	454	-	-	-	-
C	44	266	1146	875	167	96	603	360	-	-	-	-
C	44	267	1137	862	164	94	602	357	-	-	-	-
C	44	268	1148	861	165	93	596	357	-	-	-	-
C	44	269	1151	862	166	92	601	358	-	-	-	-
C	44	270	1153	867	163	95	606	355	-	-	-	-
C	45	271	1191	931	172	104	639	384	-	-	-	-
C	45	272	1186	916	172	100	632	378	-	-	-	-
C	45	273	1179	916	171	100	641	384	-	-	-	-
C	45	274	1183	922	169	103	634	393	-	-	-	-
C	45	275	1192	928	173	100	648	387	-	-	-	-
C	46	276	1196	945	176	102	654	399	-	-	-	-
C	46	277	1195	944	174	105	646	398	-	-	-	-
C	46	278	1186	947	171	105	644	393	-	-	-	-
C	46	279	1205	939	174	107	655	396	-	-	-	-
C	46	280	1215	958	175	108	656	405	-	-	-	-
C	47	281	570	283	55	26	210	93	-	-	-	-
C	47	282	571	277	55	25	211	92	-	-	-	-
C	47	283	573	278	55	25	213	92	-	-	-	-
C	47	284	577	281	56	25	215	90	-	-	-	-
C	47	285	579	285	57	26	216	92	-	-	-	-
C	48	286	588	293	56	26	220	94	-	-	-	-
C	48	287	588	295	58	27	222	96	-	-	-	-
C	48	288	589	296	58	26	220	96	-	-	-	-
C	48	289	593	299	58	27	223	98	-	-	-	-

Table A-6: Water Quality Results for Bench-Scale Experiments using Synthetic Water

Type	Run	Set	Conductivity µS/cm		Magnesium (mg/L)		Sulfate (mg/L)		Sodium (mg/L)		Chloride (mg/L)	
			HFC	HFP	HFC	HFP	HFC	HFP	HFC	HFP	HFC	HFP
C	48	290	597	304	58	27	251	99	-	-	-	-
C	49	291	1474	1135	208	134	813	491	-	-	-	-
C	49	292	1474	1139	209	131	811	492	-	-	-	-
C	49	293	1479	1137	210	134	818	488	-	-	-	-
C	49	294	1477	1138	207	132	822	492	-	-	-	-
C	49	295	1483	1144	214	131	821	499	-	-	-	-
C	50	296	1495	1150	219	131	849	501	-	-	-	-
C	50	297	1499	1160	216	136	844	507	-	-	-	-
C	50	298	1504	1168	213	138	835	507	-	-	-	-
C	50	299	1507	1172	219	137	835	514	-	-	-	-
C	50	300	1514	1174	224	141	843	509	-	-	-	-
C	51	301	2560	2110	148	105	563	306	223	187	382	400
C	51	302	2560	2110	147	107	572	312	220	188	387	403
C	51	303	2570	2120	152	107	574	316	225	188	385	407
C	51	304	2580	2130	154	107	586	316	231	187	386	405
C	51	305	2580	2140	151	107	588	321	223	185	386	407
C	52	306	2590	2150	154	108	598	332	229	188	384	405
C	52	307	2600	2150	151	108	595	329	226	190	382	406
C	52	308	2570	2160	155	111	599	341	225	191	376	406
C	52	309	2590	2170	156	110	602	337	226	189	384	405
C	52	310	2590	2180	156	111	608	342	226	191	383	407
C	53	311	5490	5090	162	140	575	290	714	636	1415	1373
C	53	312	5580	5120	162	139	557	296	710	649	1362	1389
C	53	313	5530	5130	161	136	554	297	716	645	1343	1383
C	53	314	5540	5130	167	138	565	296	727	649	1364	1377
C	53	315	5560	5130	164	137	567	298	710	642	1356	1374

Table A-6: Water Quality Results for Bench-Scale Experiments using Synthetic Water

Type	Run	Set	Conductivity µS/cm		Magnesium (mg/L)		Sulfate (mg/L)		Sodium (mg/L)		Chloride (mg/L)	
			HFC	HFP	HFC	HFP	HFC	HFP	HFC	HFP	HFC	HFP
C	54	316	5560	5150	164	138	565	307	713	660	1335	1382
C	54	317	5590	5150	166	138	579	309	727	644	1361	1388
C	54	318	5570	5130	166	137	580	306	719	663	1357	1380
C	54	319	5590	5160	169	139	587	312	727	653	1365	1370
C	54	320	5590	5150	167	136	595	309	711	654	1371	1368
C	55	321	614	304	60	27	233	99	-	-	-	-
C	55	322	614	301	61	27	232	98	-	-	-	-
C	55	323	619	301	61	27	235	99	-	-	-	-
C	55	324	623	304	63	27	239	106	-	-	-	-
C	55	325	631	308	63	27	243	108	-	-	-	-
C	56	326	558	289	54	26	211	102	-	-	-	-
C	56	327	556	291	54	26	210	101	-	-	-	-
C	56	328	555	288	53	26	214	101	-	-	-	-
C	56	329	559	290	54	26	207	101	-	-	-	-
C	56	330	561	289	54	26	210	102	-	-	-	-
C	57	331	1431	1114	204	130	792	482	-	-	-	-
C	57	332	1432	1139	208	134	794	491	-	-	-	-
C	57	333	1438	1137	199	134	798	495	-	-	-	-
C	57	334	1441	1142	205	131	801	498	-	-	-	-
C	57	335	1445	1153	205	130	810	496	-	-	-	-
C	58	336	1605	1035	231	152	901	564	-	-	-	-
C	58	337	1592	1059	231	152	885	587	-	-	-	-
C	58	338	1591	1049	229	152	892	580	-	-	-	-
C	58	339	1599	1056	231	155	901	584	-	-	-	-
C	58	340	1611	1080	233	156	899	595	-	-	-	-
C	41	251	1324	1054	188	115	717	442	-	-	-	-

Table A-6: Water Quality Results for Bench-Scale Experiments using Synthetic Water

Type	Run	Set	Conductivity µS/cm		Magnesium (mg/L)		Sulfate (mg/L)		Sodium (mg/L)		Chloride (mg/L)	
			HFC	HFP	HFC	HFP	HFC	HFP	HFC	HFP	HFC	HFP
C	41	252	1324	1045	186	116	714	438	-	-	-	-
C	41	253	1322	1044	191	117	696	435	-	-	-	-
C	41	254	1326	1041	189	117	701	430	-	-	-	-
C	41	255	1337	1051	194	114	716	441	-	-	-	-
C	42	256	1326	1076	192	119	716	453	-	-	-	-
C	42	257	1328	1084	195	123	737	461	-	-	-	-
C	42	258	1341	1078	194	121	738	454	-	-	-	-
C	42	259	1320	1084	193	121	704	462	-	-	-	-
C	42	260	1326	1093	191	122	723	462	-	-	-	-
C	43	261	1382	1053	200	118	745	447	-	-	-	-
C	43	262	1368	1051	208	118	734	443	-	-	-	-
C	43	263	1379	1047	202	117	742	450	-	-	-	-
C	43	264	1381	1057	201	120	741	445	-	-	-	-
C	43	265	1389	1071	204	121	754	454	-	-	-	-
C	44	266	1146	875	167	96	603	360	-	-	-	-
C	44	267	1137	862	164	94	602	357	-	-	-	-
C	44	268	1148	861	165	93	596	357	-	-	-	-
C	44	269	1151	862	166	92	601	358	-	-	-	-
C	44	270	1153	867	163	95	606	355	-	-	-	-
C	45	271	1191	931	172	104	639	384	-	-	-	-
C	45	272	1186	916	172	100	632	378	-	-	-	-
C	45	273	1179	916	171	100	641	384	-	-	-	-
C	45	274	1183	922	169	103	634	393	-	-	-	-
C	45	275	1192	928	173	100	648	387	-	-	-	-
C	46	276	1196	945	176	102	654	399	-	-	-	-
C	46	277	1195	944	174	105	646	398	-	-	-	-

Table A-6: Water Quality Results for Bench-Scale Experiments using Synthetic Water

Type	Run	Set	Conductivity µS/cm		Magnesium (mg/L)		Sulfate (mg/L)		Sodium (mg/L)		Chloride (mg/L)	
			HFC	HFP	HFC	HFP	HFC	HFP	HFC	HFP	HFC	HFP
C	46	278	1186	947	171	105	644	393	-	-	-	-
C	46	279	1205	939	174	107	655	396	-	-	-	-
C	46	280	1215	958	175	108	656	405	-	-	-	-
C	47	281	570	283	55	26	210	93	-	-	-	-
C	47	282	571	277	55	25	211	92	-	-	-	-
C	47	283	573	278	55	25	213	92	-	-	-	-
C	47	284	577	281	56	25	215	90	-	-	-	-
C	47	285	579	285	57	26	216	92	-	-	-	-
C	48	286	588	293	56	26	220	94	-	-	-	-
C	48	287	588	295	58	27	222	96	-	-	-	-
C	48	288	589	296	58	26	220	96	-	-	-	-
C	48	289	593	299	58	27	223	98	-	-	-	-
C	48	290	597	304	58	27	251	99	-	-	-	-
C	49	291	1474	1135	208	134	813	491	-	-	-	-
C	49	292	1474	1139	209	131	811	492	-	-	-	-
C	49	293	1479	1137	210	134	818	488	-	-	-	-
C	49	294	1477	1138	207	132	822	492	-	-	-	-
C	49	295	1483	1144	214	131	821	499	-	-	-	-
C	50	296	1495	1150	219	131	849	501	-	-	-	-
C	50	297	1499	1160	216	136	844	507	-	-	-	-
C	50	298	1504	1168	213	138	835	507	-	-	-	-
C	50	299	1507	1172	219	137	835	514	-	-	-	-
C	50	300	1514	1174	224	141	843	509	-	-	-	-
C	51	301	2560	2110	148	105	563	306	223	187	382	400
C	51	302	2560	2110	147	107	572	312	220	188	387	403
C	51	303	2570	2120	152	107	574	316	225	188	385	407

Table A-6: Water Quality Results for Bench-Scale Experiments using Synthetic Water

Type	Run	Set	Conductivity µS/cm		Magnesium (mg/L)		Sulfate (mg/L)		Sodium (mg/L)		Chloride (mg/L)	
			HFC	HFP	HFC	HFP	HFC	HFP	HFC	HFP	HFC	HFP
C	51	304	2580	2130	154	107	586	316	231	187	386	405
C	51	305	2580	2140	151	107	588	321	223	185	386	407
C	52	306	2590	2150	154	108	598	332	229	188	384	405
C	52	307	2600	2150	151	108	595	329	226	190	382	406
C	52	308	2570	2160	155	111	599	341	225	191	376	406
C	52	309	2590	2170	156	110	602	337	226	189	384	405
C	52	310	2590	2180	156	111	608	342	226	191	383	407
C	53	311	5490	5090	162	140	575	290	714	636	1415	1373
C	53	312	5580	5120	162	139	557	296	710	649	1362	1389
C	53	313	5530	5130	161	136	554	297	716	645	1343	1383
C	53	314	5540	5130	167	138	565	296	727	649	1364	1377
C	53	315	5560	5130	164	137	567	298	710	642	1356	1374
C	54	316	5560	5150	164	138	565	307	713	660	1335	1382
C	54	317	5590	5150	166	138	579	309	727	644	1361	1388
C	54	318	5570	5130	166	137	580	306	719	663	1357	1380
C	54	319	5590	5160	169	139	587	312	727	653	1365	1370
C	54	320	5590	5150	167	136	595	309	711	654	1371	1368
C	55	321	614	304	60	27	233	99	-	-	-	-
C	55	322	614	301	61	27	232	98	-	-	-	-
C	55	323	619	301	61	27	235	99	-	-	-	-
C	55	324	623	304	63	27	239	106	-	-	-	-
C	55	325	631	308	63	27	243	108	-	-	-	-
C	56	326	558	289	54	26	211	102	-	-	-	-
C	56	327	556	291	54	26	210	101	-	-	-	-
C	56	328	555	288	53	26	214	101	-	-	-	-
C	56	329	559	290	54	26	207	101	-	-	-	-

Table A-6: Water Quality Results for Bench-Scale Experiments using Synthetic Water

Type	Run	Set	Conductivity µS/cm		Magnesium (mg/L)		Sulfate (mg/L)		Sodium (mg/L)		Chloride (mg/L)	
			HFC	HFP	HFC	HFP	HFC	HFP	HFC	HFP	HFC	HFP
C	56	330	561	289	54	26	210	102	-	-	-	-
C	57	331	1431	1114	204	130	792	482	-	-	-	-
C	57	332	1432	1139	208	134	794	491	-	-	-	-
C	57	333	1438	1137	199	134	798	495	-	-	-	-
C	57	334	1441	1142	205	131	801	498	-	-	-	-
C	57	335	1445	1153	205	130	810	496	-	-	-	-
C	58	336	1605	1035	231	152	901	564	-	-	-	-
C	58	337	1592	1059	231	152	885	587	-	-	-	-
C	58	338	1591	1049	229	152	892	580	-	-	-	-
C	58	339	1599	1056	231	155	901	584	-	-	-	-
C	58	340	1611	1080	233	156	899	595	-	-	-	-

Table A-7: Hydraulic Data for Bench-Scale Experiments using Aerated Groundwater

Type	Run	Set	HFC (mL/min)	Flow HFP (mL/min)	HFR (gpm)	HFF (psi)	Pressure HFR (psi)	HFS (psi)	Temp. HFF (ºC)
C	63	361	5	25	0.55	37	34	67	23.5
C	63	362	5	26	0.61	36	34	52	24.4
C	63	363	5	25	0.69	35	32	45	24.9
C	63	364	5	26	0.73	36	33	40	25.3
C	63	365	4	25	0.70	35	32	45	25.8
C	64	366	11	31	0.49	40	38	78	26.4
C	64	367	11	32	0.47	41	39	87	26.5
C	64	368	11	32	0.47	40	38	68	26.7
C	64	369	11	32	0.46	40	38	70	26.9
C	64	370	10	31	0.50	39	37	70	27.1
C	65	371	6	32	0.48	41	39	87	26.9
C	65	372	6	30	0.46	39	38	63	26.9
C	65	373	6	32	0.48	41	39	78	26.9
C	65	374	5	32	0.52	40	38	85	27.0
C	65	375	6	32	0.53	40	38	85	27.1
C	59	341	10	25	0.39	39	37	60	23.6
C	59	342	10	26	0.39	38	37	63	24.1
C	59	343	8	26	0.49	37	35	73	24.4
C	59	344	10	26	0.60	36	34	85	24.5
C	59	345	10	26	0.60	36	34	83	24.6
C	60	346	25	26	0.73	35	32	80	24.8
C	60	347	25	25	0.74	34	31	80	24.8
C	60	348	25	25	0.74	34	31	80	24.8
C	60	349	25	26	0.75	34	31	80	24.9
C	60	350	25	26	0.76	34	31	80	25.0
C	61	351	31	31	0.38	40	38	90	25.1
C	61	352	31	30	0.28	40	39	80	25.1
C	61	353	31	31	0.28	40	39	80	25.0
C	61	354	31	31	0.28	41	39	80	25.0
C	61	355	31	31	0.29	40	39	75	25.0
C	62	356	31	32	0.35	41	40	80	25.0
C	62	357	31	31	0.29	40	39	90	25.0
C	62	358	31	31	0.30	40	39	90	25.1
C	62	359	31	32	0.31	40	39	90	25.1
C	62	360	31	32	0.33	40	39	90	25.1
B	66	376	9	26	0.44	38	23	52	21.0
B	66	377	9	26	0.49	36	23	44	21.7
B	66	378	8	25	0.53	33	24	33	22.6
B	66	379	8	25	0.70	33	24	32	23.4
B	66	380	9	25	0.60	32	24	30	24.1

Table A-7: Hydraulic Data for Bench-Scale Experiments using Aerated Groundwater

Type	Run	Set	HFC (mL/min)	Flow HFP (mL/min)	HFR (gpm)	HFF (psi)	Pressure HFR (psi)	HFS (psi)	Temp. HFF (ºC)
B	67	381	5	25	0.60	31	29	30	22.1
B	67	382	5	26	0.58	31	29	25	24.4
B	67	383	5	25	0.57	30	28	25	25.7
B	67	384	5	25	0.57	30	28	28	26.3
B	67	385	5	27	0.56	31	30	26	26.5
B	68	386	10	31	0.42	38	37	58	22.7
B	68	387	10	31	0.42	38	37	60	23.7
B	68	388	10	31	0.60	37	36	65	24.5
B	68	389	10	31	0.70	37	34	80	25.3
B	68	390	11	30	0.71	35	33	71	25.9
B	69	391	5	32	0.80	36	33	75	26.6
B	69	392	6	30	0.80	34	31	50	27.0
B	69	393	6	31	0.80	35	32	48	27.6
B	69	394	6	32	0.80	35	33	46	27.7
B	69	395	6	30	0.81	34	31	45	27.8
A	70	396	9	25	0.35	38	37	54	22.7
A	70	397	9	25	0.38	37	35	35	23.1
A	70	398	9	25	0.35	36	35	30	23.6
A	70	399	8	25	0.38	35	33	29	24.1
A	70	400	9	25	0.43	34	32	28	24.6
A	71	401	4	25	0.42	33	31	28	25.1
A	71	402	5	25	0.41	32	31	25	25.3
A	71	403	5	25	0.42	32	31	27	25.6
A	71	404	5	25	0.40	31	30	25	25.8
A	71	405	5	25	0.43	31	30	26	25.9
A	72	406	12	32	0.68	38	35	85	26.5
A	72	407	10	32	0.68	38	35	85	26.7
A	72	408	11	31	0.70	37	34	85	27.0
A	72	409	10	31	0.70	36	34	80	27.2
A	72	410	12	31	0.71	36	33	75	27.4
A	73	411	6	31	0.40	38	36	85	27.1
A	73	412	6	31	0.67	38	35	78	26.8
A	73	413	6	31	0.67	38	35	70	26.8
A	73	414	6	31	0.71	37	35	73	26.8
A	73	415	6	31	0.72	37	34	78	26.9

Table A-8: Metals Results for Bench-Scale Experiments using Aerated Groundwater

Type	Run	Set	Calcium (mg/L)		Magnesium (mg/L)		Potassium (mg/L)		Silica (mg/L)		Sodium (mg/L)	
			HFC	HFP	HFC	HFP	HFC	HFP	HFC	HFP	HFC	HFP
C	59	341	118	75	58	36	3	2	27	24	17	12
C	59	342	118	85	59	41	3	2	26	27	17	14
C	59	343	118	86	59	41	3	2	27	27	16	14
C	59	344	117	84	59	41	3	2	26	27	16	14
C	59	345	118	85	59	41	3	2	26	27	16	14
C	60	346	118	87	59	41	3	2	26	26	16	14
C	60	347	118	85	60	41	3	2	27	26	17	14
C	60	348	118	86	59	42	3	3	26	27	16	14
C	60	349	119	87	60	41	3	2	26	26	16	14
C	60	350	117	86	59	43	3	2	26	26	16	14
C	61	351	117	86	59	42	3	2	26	26	16	14
C	61	352	120	85	60	41	3	2	27	27	17	14
C	61	353	118	87	59	43	3	3	26	27	16	14
C	61	354	120	87	60	42	3	2	26	27	17	14
C	61	355	119	85	58	42	3	2	26	26	16	14
C	62	356	122	87	61	43	3	2	27	26	17	14
C	62	357	121	87	61	42	3	2	26	26	17	14
C	62	358	121	85	60	42	3	3	26	26	17	14
C	62	359	122	87	61	43	3	2	27	27	17	14
C	62	360	121	87	61	43	3	2	27	27	17	14
C	63	361	122	87	61	43	3	2	27	27	17	14
C	63	362	123	87	61	43	3	2	27	27	17	14
C	63	363	121	85	62	42	3	3	26	26	17	14
C	63	364	122	87	61	44	3	2	26	27	17	14
C	63	365	122	85	62	43	3	2	26	26	17	14
C	64	366	124	86	63	43	3	2	27	27	17	14

Table A-8: Metals Results for Bench-Scale Experiments using Aerated Groundwater

Type	Run	Set	Calcium (mg/L)		Magnesium (mg/L)		Potassium (mg/L)		Silica (mg/L)		Sodium (mg/L)	
			HFC	HFP	HFC	HFP	HFC	HFP	HFC	HFP	HFC	HFP
C	64	367	124	85	62	42	3	2	26	26	17	14
C	64	368	124	84	63	42	3	2	26	26	17	14
C	64	369	125	84	63	42	3	2	27	26	17	14
C	64	370	125	85	63	42	3	2	26	27	17	14
C	65	371	125	85	63	43	3	2	27	27	17	14
C	65	372	125	83	63	42	3	2	26	26	17	14
C	65	373	124	86	62	43	3	2	26	27	17	14
C	65	374	123	85	62	42	3	2	26	27	17	14
C	65	375	125	84	63	42	3	2	26	26	17	14
B	66	376	126	39	60	15	3	2	29	25	17	14
B	66	377	124	40	60	15	3	2	28	25	17	15
B	66	378	125	42	60	16	3	2	28	26	17	15
B	66	379	127	43	62	17	3	3	29	27	17	15
B	66	380	126	45	61	17	3	2	28	25	17	15
B	67	381	130	47	63	19	3	2	28	26	17	15
B	67	382	128	46	62	18	3	2	28	27	17	15
B	67	383	130	48	65	19	3	2	29	26	18	14
B	67	384	129	48	63	19	3	2	28	26	17	15
B	67	385	134	49	65	19	3	2	28	27	18	15
B	68	386	133	45	65	18	3	3	29	26	18	15
B	68	387	133	48	65	19	3	3	28	27	17	15
B	68	388	131	43	64	17	3	2	29	26	17	14
B	68	389	131	43	64	17	3	2	28	25	17	14
B	68	390	136	45	65	18	3	3	28	25	18	13
B	69	391	134	45	66	18	3	2	28	26	17	14
B	69	392	135	46	66	19	3	2	29	26	18	14

Table A-8: Metals Results for Bench-Scale Experiments using Aerated Groundwater

Type	Run	Set	Calcium (mg/L)		Magnesium (mg/L)		Potassium (mg/L)		Silica (mg/L)		Sodium (mg/L)	
			HFC	HFP	HFC	HFP	HFC	HFP	HFC	HFP	HFC	HFP
B	69	393	137	47	67	19	3	2	28	25	18	14
B	69	394	137	46	67	19	3	2	29	26	18	15
B	69	395	137	47	68	19	3	2	28	27	18	15
A	70	396	137	17	66	5	4	3	30	27	17	16
A	70	397	138	17	67	5	4	3	30	27	17	16
A	70	398	138	18	67	6	3	3	30	25	17	15
A	70	399	118	75	69	6	3	2	27	24	17	16
A	70	400	118	85	69	6	3	2	26	27	17	17
A	71	401	118	86	70	6	3	2	27	27	17	17
A	71	402	117	84	73	6	3	2	26	27	17	17
A	71	403	118	85	72	7	3	2	26	27	16	18
A	71	404	118	87	72	7	3	2	26	26	16	17
A	71	405	118	85	73	7	3	2	27	26	16	17
A	72	406	118	86	74	6	3	3	26	27	16	17
A	72	407	119	87	73	6	3	2	26	26	16	16
A	72	408	117	86	74	6	3	2	26	26	16	17
A	72	409	117	86	75	7	3	2	26	26	16	17
A	72	410	120	85	76	7	3	2	27	27	16	17
A	73	411	118	87	75	6	3	3	26	27	17	16
A	73	412	120	87	73	6	3	2	26	27	16	17
A	73	413	119	85	75	6	3	2	26	26	17	16
A	73	414	122	87	73	6	3	2	27	26	16	16
A	73	415	121	87	74	6	3	2	26	26	16	17

Table A-9: Water Quality Results for Bench-Scale Experiments using Aerated Groundwater

Type	Run	Set	Conductivity (μs/cm) HFC	Conductivity (μs/cm) HFP	Temperature (°C) HFC	Temperature (°C) HFP	pH (s.u.) HFC	pH (s.u.) HFP	Sulfate (mg/L) HFC	Sulfate (mg/L) HFP	Chloride (mg/L) HFC	Chloride (mg/L) HFP
C	62	358	1242	835	23.0	22.7	7.7	7.5	377	195	27	25
C	62	359	1247	931	22.9	22.7	7.8	7.7	386	231	29	27
C	62	360	1246	931	22.8	22.7	7.8	7.8	384	229	28	27
C	63	361	1250	928	22.8	22.7	7.8	7.8	386	226	28	27
C	63	362	1252	930	22.9	22.9	7.8	7.7	390	228	28	27
C	63	363	1253	935	22.8	22.7	7.8	7.7	399	230	29	26
C	63	364	1258	940	22.7	22.8	7.9	7.8	394	232	28	27
C	63	365	1259	940	22.8	22.8	8.0	7.8	398	232	28	27
C	64	366	1266	944	22.8	22.8	7.9	7.8	393	231	29	27
C	64	367	1267	947	22.8	22.8	7.9	7.8	401	236	28	27
C	64	368	1264	937	22.9	22.9	7.8	7.8	395	229	29	27
C	64	369	1270	930	22.8	22.8	7.9	7.8	400	225	29	27
C	64	370	1261	940	22.7	22.8	8.0	7.9	403	232	29	27
C	65	371	1269	948	22.8	22.8	7.9	7.8	405	234	28	26
C	65	372	1275	949	22.8	22.8	7.9	7.8	405	237	28	26
C	65	373	1266	950	23.3	22.8	7.9	7.8	404	234	28	26
C	65	374	1275	950	22.9	22.8	7.9	7.8	406	228	28	30
C	65	375	1278	948	22.8	22.8	7.7	7.9	412	229	29	30
B	66	376	1284	947	22.7	22.7	7.9	7.9	412	228	28	30
B	66	377	1287	948	22.8	22.8	7.9	7.9	417	225	28	30
B	66	378	1280	948	21.8	22.0	7.7	7.9	412	226	29	30
B	66	379	1286	946	21.7	22.1	8.0	7.9	412	229	28	30
B	66	380	1289	950	22.0	22.1	8.1	8.1	419	230	29	30
B	67	381	1294	948	21.8	22.1	8.0	8.0	417	229	29	30
B	67	382	1295	951	22.1	22.2	8.1	8.0	420	231	29	30
B	67	383	1300	942	21.9	21.9	8.0	8.0	420	227	29	30

Table A-9: Water Quality Results for Bench-Scale Experiments using Aerated Groundwater

Type	Run	Set	Conductivity (µs/cm)		Temperature (ºC)		pH (s.u.)		Sulfate (mg/L)		Chloride (mg/L)	
			HFC	HFP	HFC	HFP	HFC	HFP	HFC	HFP	HFC	HFP
B	67	384	1305	941	22.1	21.9	7.9	8.0	421	227	28	30
B	67	385	1295	943	22.1	21.8	8.1	8.1	422	225	29	30
B	68	386	1309	950	22.2	21.8	8.0	8.0	430	232	29	30
B	68	387	1320	953	22.2	21.9	8.1	8.0	427	229	28	30
B	68	388	1312	944	22.1	21.9	8.1	8.0	426	227	28	30
B	68	389	1310	947	22.1	21.8	8.0	8.0	427	229	28	30
B	68	390	1319	946	22.0	21.8	8.1	8.0	430	230	29	30
B	69	391	1315	949	22.1	21.8	8.1	8.0	437	230	30	30
B	69	392	1322	948	22.0	22.0	8.0	8.0	438	229	30	30
B	69	393	1281	489	21.7	21.4	7.8	7.6	440	64	32	21
B	69	394	1288	491	21.7	21.2	7.8	7.6	442	64	31	20
B	69	395	1296	507	21.7	21.6	7.9	7.7	445	68	33	21
A	70	396	1299	524	21.7	21.6	7.9	7.7	450	74	32	21
A	70	397	1307	528	21.8	21.7	7.9	7.7	448	74	33	22
A	70	398	1309	560	21.6	21.4	7.9	7.7	456	87	33	22
A	70	399	1322	546	21.6	21.4	7.9	7.8	466	81	32	23
A	70	400	1334	567	21.5	21.4	7.9	7.8	472	87	33	23
A	71	401	1339	573	21.6	21.4	7.9	7.8	476	89	33	24
A	71	402	1348	588	21.7	21.8	8.0	7.8	479	87	33	24
A	71	403	1346	528	22.4	22.4	7.9	7.7	478	74	33	23
A	71	404	1351	538	22.5	22.5	8.0	7.8	479	76	33	23
A	71	405	1362	539	22.8	22.5	8.0	7.8	431	77	30	24
A	72	406	1368	537	22.9	23.0	8.0	7.8	434	77	30	23
A	72	407	1368	543	23.0	22.7	8.0	7.8	439	78	30	24
A	72	408	1380	547	22.5	22.8	7.9	7.8	445	79	30	24
A	72	409	1388	562	22.5	23.6	8.0	7.9	452	83	30	24

Table A-9: Water Quality Results for Bench-Scale Experiments using Aerated Groundwater

Type	Run	Set	Conductivity (μs/cm)		Temperature (ºC)		pH (s.u.)		Sulfate (mg/L)		Chloride (mg/L)	
			HFC	HFP	HFC	HFP	HFC	HFP	HFC	HFP	HFC	HFP
A	72	410	1399	564	22.7	22.8	8.0	7.8	458	84	30	24
A	73	411	1396	560	23.0	22.9	8.0	7.9	462	85	30	24
A	73	412	1403	568	22.8	23.2	8.0	7.9	462	85	30	25
A	73	413	1192	293	22.4	22.0	7.6	7.2	449	35	29	10
A	73	414	1190	301	22.5	22.6	7.8	7.2	453	36	29	10
A	73	415	1182	242	23.3	22.5	7.8	7.4	457	39	28	11

Table A-10: Sand Filter Backwash Log for HFNF Pilot System

Date -Time	Operator	Field Notes
05/21/2013 7:00 AM	PJP	
05/22/2013 7:30 AM	PJP	
05/24/2013 6:45 AM	PJP	
05/31/2013 7:30 AM	PJP	
06/07/2013 9:00 AM	PJP	
06/14/2013 1:30 PM	JG	
06/21/2013 11:50 AM	JG	
06/24/2013 10:30 AM	PJP	
06/28/2013 2:00 PM	JG	
07/10/2013 2:00 PM	PJP	Odorous smell in backwash tank
07/11/2013 6:45 AM	PJP	Cleaned w/Cl$_2$ (1 foam cup HTH)
07/11/2013 7:10 AM	PJP	
07/16/2013 11:40 AM	DTY	
07/20/2013 8:45 AM	PJP	
07/24/2013 2:46 PM	PJP	
07/29/2013 1:25 PM	PJP	Bill from Harn on site
08/02/2013 1:00 PM	JG	
08/06/2013 8:30 AM	PJP	
08/09/2013 1:00 PM	JG	
08/12/2013 2:30 PM	PJP	
08/16/2013 10:35 AM	JG	
08/20/2013 10:45 AM	DTY	
08/23/2013 1:26 PM	JG	
08/27/2013 11:30 AM	DTY	
08/30/2013 2:08 PM	JG	
09/03/2013 10:50 AM	DTY	Sand filter taken offline

Table A-11: HFNF Pilot Sequence of Events

June 24, 2013	HF pilot start up, operating at 50% recovery, sand filter online as pretreatment, sand filter backwash frequency 2 times/week
June 24-July 5, 2013	Stable operations at 50% recovery
July 5 -11, 2013	HF pilot at HARN RO for modifications and maintenance Pressure gauges and flow meters installed
July 11, 2013	Pilot adjusted to decrease operating pressures, flows set to meet 50% recovery
July 19, 2013	Data logger damaged and offline
July 23, 2013	Pilot adjusted to decrease operating pressures, flux adjusted to 13 gfd to meet 50% recovery
July 24-29, 2013	Pilot shutdown due to maintenance
August 6, 2013	Flux adjusted to 17gfd to meet 77% recovery
August 20, 2013	Pilot adjusted to 85% recovery
September 3, 2013	Sand filter bypassed, pilot adjusted to 50% recovery
September 3-10, 2013	Pilot decreased recovery from 50% to 47%.
September 10, 2013	Readjusted manually to 50% recovery
September 17, 2013	Pilot adjusted to 85% recovery
October 1, 2013	Pilot shutdown

Table A-12: Water Quality Averages and Corresponding Standard Deviations

Parameter	Units	Raw Verna	SF Filtrate	HF Feed	HF Permeate	HF Concentrate
Alkalinity	mg/L as $CaCO_3$	154 ± 2	154 ± 3	156 ± 2	154 ± 3	156 ± 2
Barium	mg/L	0.14 ± 0.01	0.14 ± 0.01	0.14 ± 0.01	0.13 ± 0.01	0.14 ± 0.01
Calcium	mg/L	124.8 ± 7.3	124.5 ± 7.3	128.5 ± 8.9	122.5 ± 8.0	128.9 ± 8.3
Chloride	mg/L	26.4 ± 4.8	25.8 ± 8.0	27.0 ± 1.9	25.9 ± 1.9	25.8 ± 1.8
Conductivity	µS/cm	1101 ± 51	1095 ± 54	1129 ± 53	1083 ± 55	1133 ± 54
Iron	µg/L	3.09 ± 2.78	0.30 ± 0.82	1.93 ± 2.84	0.77 ± 1.65	2.21 ± 3.46
Magnesium	mg/L	59.1 ± 3.1	59.2 ± 3.2	60.6 ± 3.8	58.3 ± 3.2	60.8 ± 3.2
Manganese	µg/L	3.02 ± 1.36	1.71 ± 0.49	2.54 ± 1.35	2.44 ± 1.27	2.58 ± 1.32
pH	s.u.	7.69 ± 0.05	7.69 ± 0.06	7.69 ± 0.05	7.69 ± 0.05	7.69 ± 0.05
Potassium	mg/L	2.4 ± 0.1	2.4 ± 0.1	2.4 ± 0.1	2.4 ± 0.1	2.5 ± 0.1
Silica	mg/L	25.2 ± 1.3	25.4 ± 1.4	25.2 ± 1.4	25.3 ± 1.1	25.3 ± 1.3
Sodium	mg/L	12.8 ± 1.2	13.0 ± 1.1	13.0 ± 1.2	12.7 ± 1.0	13.0 ± 1.1
Sulfate	mg/L	406 ± 41	425 ± 43	404 ± 42	394 ± 39	425 ± 44
TDS	mg/L	825 ± 54	819 ± 52	849 ± 52	804 ± 53	854 ± 51
TOC	mg/L	2.05 ± 0.13	2.06 ± 0.13	2.37 ± 0.17	1.82 ± 0.15	2.41 ± 0.20
TSS	mg/L	1.88 ± 1.21	2.10 ± 1.42	1.82 ± 0.93	1.68 ± 1.18	1.96 ± 0.98
Temperature	˚C	26.9 ± 0.53	27.0 ± 0.54	28.0 ± 0.70	28.0 ± 0.76	28.0 ± 0.79
Turbidity	NTU	0.26 ± 0.11	0.11 ± 0.05	0.16 ± 0.09	0.10 ± 0.04	0.17 ± 0.10

Table A-13: SWNF Pilot Parameter Log List

Month	1st Stage Concentrate Pressure
Day	2nd Stage Feed Pressure
Year	Total Concentrate Pressure
Hour	1st Stage Permeate Flow
Minute	2nd Stage Permeate Flow
Feed Temp.	Total Permeate Flow
Feed pH	Concentrate Flow
Feed Conductivity	1st Stage Permeate Pressure
Feed ORP	Total Permeate Pressure
Feed Pressure	1st Stage dP
HPP Speed	2nd Stage dP
Permeate Conductivity	

Table A-14: HFUF Pilot Parameter Log List

Month	Backwash Flow
Day	Filtrate TMP
Year	Backwash TMP
Hour	Filtration Timer Setpoint
Minute	CEB Cylcle Setpoint
System Mode	Type of CEB
Feed Turbidity	Filtration Timer Value
Feed Temp.	Backwash Timer Value
Filtrate Turbidity	CEB Cycle Counter Value
Feed Pressure	Particle Counter Ch. 1
Concentrate Pressure	Particle Counter Ch. 2
Filtrate Pressure	Particle Counter Ch. 3
Filtrate Flow	Particle Counter Ch. 4

Table A-15: SWNF Pilot Testing Summary Timeline

November 19th	Sand filter media changed
November 20th	SWNF – restarted after membranes cleaned HFUF – Performed a CEB with citric acid (chemical A)
December 4th	UCF Remote Access - Performed a CEB with sodium hypochlorite solution (old solution) (chemical B)
December 6th	UCF Site Visit Replaced the HFUF sodium hypochlorite solution (chemical B) Informed HARN of split feed tube to Chemical B Performed a PDT results 0.01psi/min Performed a CEB with citric acid (chemical A)
December 13th	UCF Site Visit Observed SWNF cartridge filter tank was accumulating air Performed a CEB with citric acid (chemical A) Performed a CEB with sodium hypochlorite solution (chemical B) pH=8
December 21st	UCF Remote Access - Recovery = 84.1% (water) Performed a CEB with sodium hypochlorite solution (chemical B) pH=10 Increased the HFUF filtrate flow to 36.8 GPM for a flux of 45 GFD
December 24th	The HFUF pilot shut down during a regularly scheduled CEB during the rinse cycle because the filtrate tank level became low
December 31st	Glenn pressurized the SWNF suction piping and identified the leak causing air to build up in the SWNF cartridge filter tank
January 7th	HARN site visit The SWNF leak was repaired The SWNF start/stop float was adjusted up to stop the SWNF pilot sooner during a CEB and the low filtrate tank level flow was adjusted down to allow more filtrate volume to be useable during CEBs The SBS pump was disabled and unplugged since chlorine is no longer being fed for algae control The CEB rinse duration was also decreased by 20 seconds so that less filtrate is used during the CEB cycle The HFUF pilot was restarted and was able to complete a CEB after the first cycle without running out of filtrate water
January 11th	UCF Remote Access Bypassed the sand filter Performed a CEB with sodium hypochlorite solution (chemical B)
January 15th	Recovery = 92.8% (water)
January 15th - 29th	Normal operations sodium hypochlorite CEB once a day
January 24th	Performed Citric acid CEB
January 29th	SWNF shutdown and HFUF cleaning performed.
February 1st	HFUF shutdown and removed

APPENDIX B – EXAMPLE CALCULATIONS

Temperature Correction Factors

Temperature correction factors for the HFUF and HFNF membranes were calculated using TCF equations provided by the manufacturer whereas the TCF for SWNF was calculated using the ASTM standard provided in Equation 3-7.

The TCF for the HFUF membrane was calculated using Equations 3-9:

$$\text{TCF}_{(20°C)} = \frac{0.99712}{1.855 \text{-} 0.05596\text{T} + 0.0006533\text{T}^2} \tag{3-9}$$

$$\text{TCF}_{(20°C)} = \frac{0.99712}{1.855 \text{-} 0.05596\text{T} + 0.0006533\text{T}^2} = \frac{0.99712}{1.855 \text{-} 0.05596(26.5) + 0.0006533(26.5)^2} = 1.200$$

The TCF for the HFNF membrane was calculated using Equations 3-10:

$$\text{TCF}_{(20°C)} = 0.002024 \times (42.5 + T)^{1.5} \qquad (3\text{-}10) \quad \text{TCF}_{(20°C)} = 0.002024 \times (42.5 + 20.6)^{1.5} = 1.014$$

$$\text{TCF}_{(20°C)} = 0.002024 \times (42.5 + 20.6)^{1.5} = 1.014$$

The TCF for the SWNF was calculating using Equation 3-7:

$$\text{TCF} = \frac{J_{T°C}}{J_{25°C}} = 1.026^{(T-25)} \tag{3-7}$$

$$\text{TCF} = \frac{J_{T°C}}{J_{25°C}} = 1.026^{(T-25)} = 1.03^{(24.2-25)} = 0.9766$$

Osmotic Pressure and Ionic Strength

The osmotic pressure of the bench-scale testing using synthetic water was calculated using Equation 3-13. The change in osmotic pressure was calculated by the difference of the osmotic pressure of the feed and permeate streams. Sample calculations provided herein refer to Run 4 Set 46 shown in Row 1 of Table A-6. Similar calculations were performed for each bench-scale membrane test.

$$\Pi = cR_gT \tag{3-13}$$

$$\Pi = cR_gT = \left(\frac{127mg/L}{24.305g/mol} + \frac{469mg/L}{96.06g/mol}\right)\left(\frac{0.08206L - atm}{mol - K}\right)(273.15 + 20.6)K = 3.58psi$$

$$\Pi = cR_gT = \left(\frac{15mg/L}{24.305g/mol} + \frac{56mg/L}{96.06g/mol}\right)\left(\frac{0.08206L - atm}{mol - K}\right)(273.15 + 20.6)K = 0.42psi$$

$$\Delta\Pi = \Pi_{feed} - \Pi_{permeate} = 3.58psi - 0.42psi = 3.16psi$$

Osmotic pressure for bench-scale and pilot scale systems treating aerated groundwater was calculated using Equation 3-14 and the TDS concentrations of the feed, permeate, and concentrate streams.

$$\Delta\Pi = \frac{1psi}{100mg/L}\left(\frac{C_f + C_c}{2} - C_p\right) \tag{3-14}$$

$$\Delta\Pi = \frac{1psi}{100mg/L}(862mg/L - 798mg/L) = \frac{1psi}{100mg/L}(64mg/L) = 0.64psi$$

The ionic strength of the solutions were as determined by Lewis and Randall (1921).

$$I = \frac{1}{2}\sum_i C_iZ_i^2 = \frac{1}{2}\left(\left(\frac{127mg/L}{24.305g/mol} \times 2^2\right) + \left(\frac{469mg/L}{96.06g/mol} \times 2^2\right)\right) = 0.020$$

210

Water Flux and Water Mass Transfer Coefficient

The water flux and incremental mass transfer coefficients for each bench-scale testing experiments were calculated using Equation 3-26.

$$J_w = K_w(\Delta P - \Delta \Pi) = \frac{Q_p}{A} \tag{3-26}$$

$$J_w = K_w(\Delta P - \Delta \Pi) = \frac{Q_p}{A} = \frac{(19mL/min)(1440min/day)}{(0.812ft^2)\left(\frac{3785mL}{ft^3}\right)} = \frac{8.9gal}{ft^2\ day} = 8.9gfd$$

Where:

$$\Delta P = \left(\frac{P_F + P_C}{2} - P_P\right)$$

$$K_W = \frac{J_W}{(\Delta P - \Delta \Pi)} = \frac{8.9gfd}{(28.2psi - 3psi)} = \frac{0.356gal}{ft^2\ day\ psi}$$

Solute Flux and Solute Mass Transfer Coefficient

The magnesium flux and incremental magnesium mass transfer coefficients for each bench-scale testing experiments were calculated using Equation 3-27.

$$J_s = K_s(\Delta C) = \frac{Q_p C_p}{A} \tag{3-27}$$

$$J_{Mg} = \frac{Q_p C_p}{A} = \frac{(19mL/min)(15mg/L)}{0.812ft^2} = \frac{491mg}{ft^2 day} = 1.08lb/sfd$$

$$K_{Mg} = \frac{J_{Mg}}{(\Delta C)} = \frac{491mg/sfd}{127mg/L - 15mg/L} = 0.15ft/day$$

The following example calculations were conducted for Row 1 in Table 5-7 and repeated for each experiment.

Crossflow Velocity

$$Q_F = Q_R + Q_P + Q_c = \left(\frac{0.60gal}{min}\right) + \left(\frac{6.5mL}{min}\right) + \left(\frac{19mL}{min}\right) = \frac{0.77gal}{min} = 1.32 \times 10^{-3} \frac{ft^3}{s}$$

Fiber diameter, $d_h = 0.0008m = 0.002624ft$

Active Length = Module Length − (2) potting length = 0.03m − (2) (0.024m) = 0.25m = 0.82ft

Membrane Area: $A = \pi d_h Ln = \pi(0.0008m)(0.25m)(120 fibers) = 0.0754\ m^2 = 0.812 ft^2$

Lumen Crossflow Area $= \pi(d/2)^2 = \pi(0.0008m/2)^2 = 5.03 \times 10^{-7}m^2$

Total Crossflow Area $= 5.03 \times 10^{-7}m^2\ (120) = 6.03 \times 10^{-5}m^2 = 6.49 \times 10^{-4}ft^2$

$$V = \frac{Q_F}{A} = \frac{1.32 \times 10^{-3}ft/s}{6.49 \times 10^{-4}ft^2} = 2.03\ ft/s$$

The Nernst diffusion coefficients for synthetic membrane testing using magnesium and sulfate were calculated using Equation 3-17

$$D_i^o = \psi_i^0 \left(\frac{R_g T}{z_i F^2}\right) \tag{3-17}$$

$$D_{Mg}^o = \Psi_{Mg}^o \left[\frac{R_g T}{z_{Mg}F^2}\right] = \left[53\frac{cm^2}{ohm\ eq}\right]\left[\frac{\left(8.314\frac{J}{K\ mol}\right)(300\ K)}{2\left(96500\frac{C}{eq}\right)^2\left(\frac{amp^2s^2}{C^2}\right)}\right] = 7.09 \times 10^{-10}m^2/s$$

Estimating mass transfer coefficients using dimensional analysis were calculated using the Schmidt, Reynolds and Sherwood numbers:

$$Sc = \frac{\mu}{\rho D_0} \tag{3-15}$$

$$Sc_{Mg} = \frac{\mu}{\rho D_{Mg}{}^o} = \frac{(9.325 \times 10^{-4} \ kg/(m*s))}{\left(998\frac{kg}{m^3}\right)(7.09 \times 10^{-10} \ m^2/s)} = 1317$$

$$Re = \frac{d_h V \rho}{\mu} \tag{3-18}$$

$$Re = \frac{d_h V \rho}{\mu} = \frac{(0.0008m)(2.03ft/s)(1ft/3.281m)(998kg/m^3)}{9.326 \times 10^{-4} \ kg/m - s} = 530$$

Assuming the effective concentration layer to be fully developed:

$$Sh = 0.664(Re)^{0.33}(Sc)^{0.33}\left(\frac{d_h}{L}\right)^{0.33} \tag{3-20}$$

$$S_h = 0.664(R_e, S_c, d_h/L)^{0.33} = 0.664\left[(530)(1317)\left(\frac{0.0008m}{0.25m}\right)\right]^{0.33} = 8$$

$$Sh = \frac{kd_h}{D_0} \Rightarrow \quad k = \frac{ShD_o}{d_h} \tag{3-19}$$

$$K_s = \frac{S_h D_{mg}{}^o}{d_h} = \frac{(8)\left(7.09 \times 10^{-10}\frac{m^2}{s}\right)\left(86400\frac{s}{day}\right)}{0.0008m} = 0.65\frac{m}{day} = 2.13\frac{ft}{day}$$

The permeate concentration can be predicted using Equation 3-28:

$$C_p = \frac{C_f K_s}{K_w(\Delta P - \Delta \Pi)\left(\frac{2-2R}{2-R}\right) + K_s} \tag{3-28}$$

$$C_{p,Mg} = \frac{C_f K_s}{K_w(\Delta P - \Delta \Pi)\left(\frac{2-2R}{2-R}\right) + K_s} = \frac{(147mg/L)(0.158ft/day)}{\left(\frac{0.05ft}{day}\right)(30psi)\left(\frac{2-2(0.01)}{2-0.01}\right) + \left(\frac{0.158ft}{day}\right)} = 20mg/L$$

APPENDIX C – FIELD SAMPLING SHEET

Project Name: City of Sarasota HF Study			Comments:				
Sampled by:							
Date:							
			Parameter / Analysis				
Sort Code	Matrix Type	Sample ID	pH (s.u)	Temp (˚C)	Conductivity (µS/cm)	Turbidity (NTU)	Alkalinity (mg/L as CaCO$_3$)
1	GW	Raw Verna					
2	GW	SF Filtrate					
3	GW	HF Feed					
4	GW	HF Concentrate					
5	GW	HF Permeate					
6	GW	Dupe:					

Time	Temp(˚C)	Flow (gpm)			Pressure (PSI)		
	HF Feed	HF Concentrate	HF Permeate	HF Feed	HF Concentrate	HF Permeate	HF Feed

APPENDIX D – FIELD AND LABORATORY QUALITY CONTROL DATA

Table D-1: Precision Assessment for Turbidity Quality Control

Sample #	Duplicate A	Duplicate B	I Statistic	Sample #	Duplicate A	Duplicate B	I Statistic
1	0.19	0.26	0.1556	37	0.07	0.10	0.1765
2	0.17	0.16	0.0180	38	0.11	0.22	0.3333
3	0.23	0.19	0.1005	39	0.09	0.12	0.1262
4	0.07	0.21	0.4964	40	0.28	0.12	0.3930
5	0.08	0.17	0.3548	41	0.17	0.20	0.0761
6	0.07	0.11	0.2308	42	0.09	0.10	0.0426
7	0.10	0.16	0.2188	43	0.20	0.09	0.3699
8	0.08	0.12	0.1919	44	0.13	0.11	0.0656
9	0.09	0.26	0.4915	45	0.07	0.11	0.2222
10	0.10	0.15	0.1870	46	0.08	0.10	0.1209
11	0.05	0.16	0.5238	47	0.31	0.26	0.0973
12	0.20	0.29	0.1803	48	0.11	0.19	0.2542
13	0.09	0.14	0.2241	49	0.28	0.28	0.0090
14	0.10	0.14	0.1736	50	0.34	0.17	0.3399
15	0.15	0.14	0.0204	51	0.16	0.18	0.0519
16	0.25	0.15	0.2438	52	0.12	0.20	0.2500
17	0.10	0.15	0.1870	53	0.22	0.25	0.0638
18	0.11	0.12	0.0265	54	0.24	0.17	0.1779
19	0.11	0.13	0.0678	55	0.12	0.16	0.1429
20	0.10	0.11	0.0385	56	0.30	0.21	0.1881
21	0.19	0.11	0.2500	57	0.19	0.17	0.0704
22	0.07	0.10	0.1954	58	0.32	0.30	0.0407
23	0.10	0.11	0.0291	59	0.12	0.20	0.2500
24	0.11	0.19	0.2542	60	0.25	0.23	0.0417
25	0.28	0.14	0.3462	61	0.42	0.30	0.1748
26	0.28	0.28	0.0090	62	0.16	0.27	0.2558
27	0.08	0.14	0.2593	63	0.22	0.22	0.0000
28	0.09	0.16	0.2800				
29	0.06	0.10	0.2500	Average			0.179
30	0.15	0.13	0.0791	Std deviation			0.126
31	0.08	0.11	0.1579	Minimum			0.000
32	0.13	0.14	0.0511	Maximum			0.524
33	0.19	0.13	0.1728				
34	0.09	0.12	0.1346				
35	0.10	0.12	0.0826	Upper Warning Limit			0.431
36	0.19	0.11	0.2667	Upper Control Limit			0.557

Table D-2: Precision Assessment for pH Quality Control

Sample #	Duplicate A	Duplicate B	I Statistic	Sample #	Duplicate A	Duplicate B	I Statistic
1	7.61	7.62	0.0004	37	7.68	7.67	0.0007
2	7.61	7.59	0.0013	38	7.61	7.63	0.0012
3	7.59	7.57	0.0012	39	7.65	7.64	0.0005
4	7.62	7.62	0.0003	40	7.68	7.70	0.0010
5	7.73	7.73	0.0001	41	7.65	7.65	0.0003
6	7.71	7.73	0.0012	42	7.78	7.76	0.0013
7	7.72	7.72	0.0000	43	7.69	7.70	0.0009
8	7.76	7.75	0.0009	44	7.68	7.68	0.0000
9	7.7	7.73	0.0019	45	7.69	7.71	0.0014
10	7.69	7.70	0.0006	46	7.71	7.69	0.0016
11	7.69	7.72	0.0017	47	7.67	7.65	0.0013
12	7.76	7.78	0.0010	48	7.67	7.66	0.0007
13	7.75	7.74	0.0006	49	7.74	7.74	0.0003
14	7.77	7.77	0.0001	50	7.65	7.62	0.0018
15	7.76	7.75	0.0008	51	7.74	7.74	0.0002
16	7.75	7.77	0.0013	52	7.68	7.69	0.0003
17	7.74	7.74	0.0003	53	7.7	7.70	0.0002
18	7.7	7.69	0.0005	54	7.73	7.73	0.0003
19	7.6	7.61	0.0007	55	7.64	7.64	0.0003
20	7.75	7.73	0.0016	56	7.67	7.67	0.0003
21	7.71	7.77	0.0000	57	7.74	7.74	0.0000
22	7.69	7.71	0.0010	58	7.68	7.68	0.0002
23	7.72	7.71	0.0008	59	7.68	7.68	0.0002
24	7.67	7.66	0.0007	60	7.7	7.71	0.0008
25	7.64	7.65	0.0004	61	7.67	7.69	0.0010
26	7.74	7.74	0.0003	62	7.67	7.70	0.0020
27	7.72	7.70	0.0013	63	7.68	7.69	0.0008
28	7.64	7.64	0.0001				
29	7.66	7.67	0.0005	Average			0.001
30	7.69	7.69	0.0001	Std deviation			0.001
31	7.67	7.68	0.0008	Minimum			0.000
32	7.67	7.68	0.0008	Maximum			0.002
33	7.64	7.64	0.0001				
34	7.75	7.73	0.0014				
35	7.66	7.66	0.0000	Upper Warning Limit			0.002
36	7.63	7.62	0.0007	Upper Control Limit			0.002

Table D-3: Precision Assessment for Conductivity Quality Control

Sample #	Duplicate A	Duplicate B	I Statistic	Sample #	Duplicate A	Duplicate B	I Statistic
1	1041	1055	0.0067	37	1200	1171	0.0122
2	1069	1048	0.0101	38	1157	1196	0.0164
3	1064	1048	0.0076	39	1108	1123	0.0065
4	972	1006	0.0173	40	1027	1047	0.0096
5	1004	1042	0.0185	41	1105	1132	0.0122
6	1058	1065	0.0034	42	1178	1158	0.0085
7	1147	1137	0.0044	43	1058	1069	0.0052
8	1070	1051	0.0089	44	1015	1030	0.0075
9	1102	1104	0.0009	45	1021	1048	0.0131
10	1103	1126	0.0105	46	1181	1153	0.0120
11	1037	1073	0.0172	47	1165	1155	0.0045
12	1139	1117	0.0098	48	1024	1050	0.0124
13	1164	1185	0.0091	49	1088	1092	0.0016
14	1209	1199	0.0040	50	1111	1099	0.0054
15	1070	1059	0.0050	51	1186	1193	0.0030
16	1137	1138	0.0006	52	1104	1137	0.0147
17	1030	1052	0.0104	53	1146	1131	0.0068
18	1073	1065	0.0036	54	1127	1109	0.0081
19	1090	1091	0.0004	55	1154	1182	0.0119
20	1161	1153	0.0035	56	1233	1200	0.0135
21	1097	1102	0.0024	57	1018	1038	0.0095
22	1057	1059	0.0010	58	1151	1132	0.0083
23	1088	1073	0.0068	59	1095	1125	0.0136
24	1024	1050	0.0124	60	1162	1135	0.0119
25	1137	1138	0.0005	61	1100	1075	0.0115
26	1088	1092	0.0016	62	1116	1143	0.0117
27	1209	1230	0.0088	63	1173	1147	0.0112
28	1076	1089	0.0061				
29	1092	1123	0.0142	Average			0.008
30	1157	1127	0.0130	Std deviation			0.005
31	1026	1053	0.0130	Minimum			0.000
32	1210	1216	0.0023	Maximum			0.018
33	1038	1052	0.0065				
34	1077	1109	0.0146				
35	1104	1109	0.0022	Upper Warning Limit			0.018
36	1117	1133	0.0071	Upper Control Limit			0.023

Table D-4: Precision Assessment for Temperature Quality Control

Sample #	Duplicate A	Duplicate B	I Statistic	Sample #	Duplicate A	Duplicate B	I Statistic
1	28.2	29.0	0.0147	37	27.6	27.2	0.0080
2	29.9	29.2	0.0118	38	27.8	28.2	0.0068
3	28.8	28.5	0.0049	39	27.8	28.3	0.0089
4	28.6	29.1	0.0090	40	26.4	27.1	0.0138
5	28.3	28.3	0.0000	41	28.7	28.1	0.0113
6	27.0	27.9	0.0164	42	27.5	27.3	0.0033
7	28.4	27.7	0.0128	43	26.7	27.7	0.0191
8	27.3	27.3	0.0004	44	27.0	27.8	0.0139
9	26.7	27.2	0.0100	45	27.4	27.3	0.0018
10	27.9	27.0	0.0157	46	27.5	27.2	0.0047
11	28.5	28.0	0.0085	47	27.4	27.5	0.0014
12	27.9	27.4	0.0083	48	28.6	28.4	0.0031
13	28.3	27.5	0.0143	49	26.8	27.4	0.0102
14	27.0	26.8	0.0037	50	28.0	28.1	0.0009
15	27.6	27.2	0.0077	51	26.4	27.3	0.0158
16	26.4	27.1	0.0138	52	28.2	27.9	0.0049
17	27.7	26.9	0.0143	53	28.1	27.9	0.0031
18	27.8	27.3	0.0094	54	26.5	26.7	0.0038
19	27.4	27.5	0.0015	55	28.3	27.9	0.0067
20	27.0	27.2	0.0030	56	28.0	27.8	0.0040
21	27.0	27.5	0.0095	57	26.4	27.2	0.0149
22	27.1	27.6	0.0088	58	28.1	28.2	0.0013
23	27.8	27.4	0.0076	59	28.1	27.7	0.0067
24	28.6	28.4	0.0031	60	27.5	27.3	0.0046
25	27.4	28.0	0.0108	61	27.9	27.6	0.0063
26	26.9	27.4	0.0083	62	28.4	27.9	0.0093
27	26.6	26.6	0.0008	63	26.5	26.7	0.0038
28	27.3	28.0	0.0119				
29	28.3	28.0	0.0060	Average			0.008
30	27.6	27.3	0.0058	Std deviation			0.005
31	28.2	27.9	0.0050	Minimum			0.000
32	26.2	26.9	0.0136	Maximum			0.019
33	27.7	28.3	0.0114				
34	27.6	27.2	0.0080				
35	27.6	28.1	0.0093	Upper Warning Limit			0.017
36	27.4	28.0	0.0115	Upper Control Limit			0.022
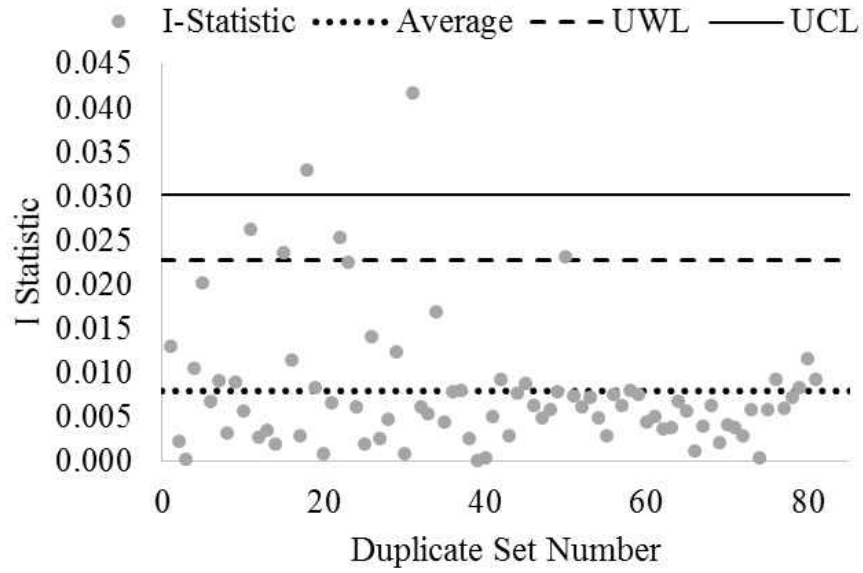
Figure D-1: Precision Control Chart for Sulfate
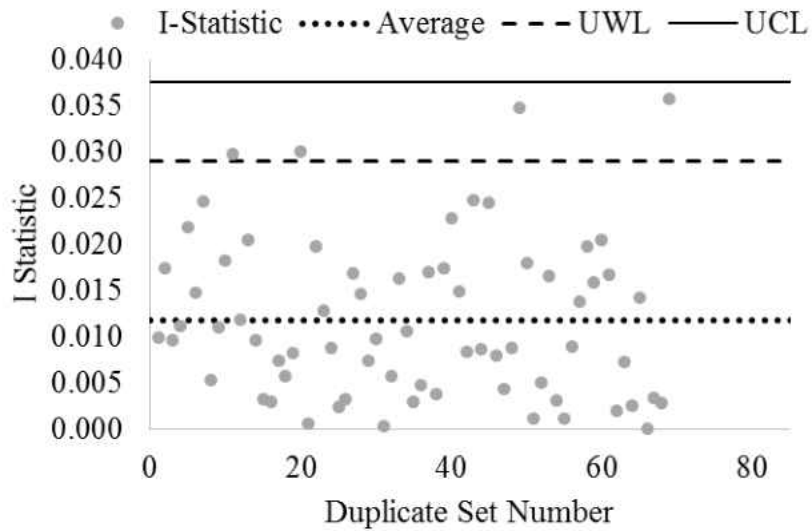
Figure D-2: Precision Control Chart for Magnesium
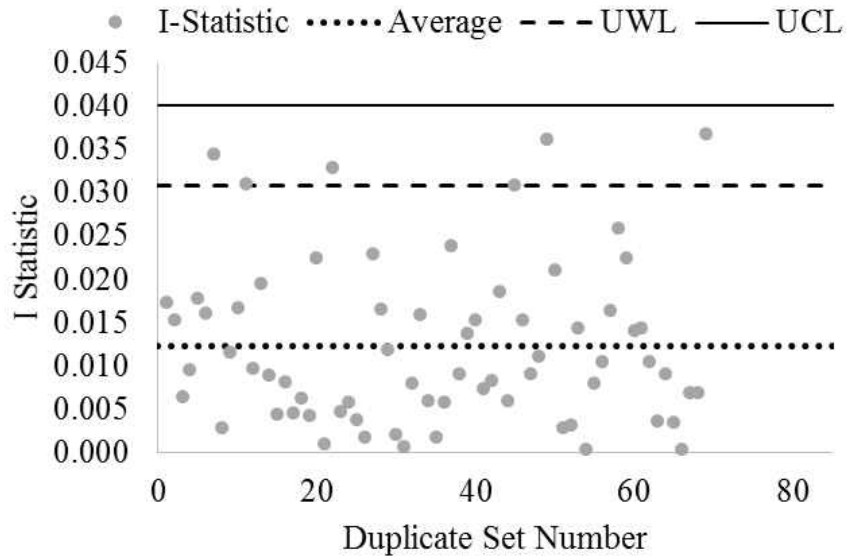
Figure D-3: Precision Control Chart for Calcium
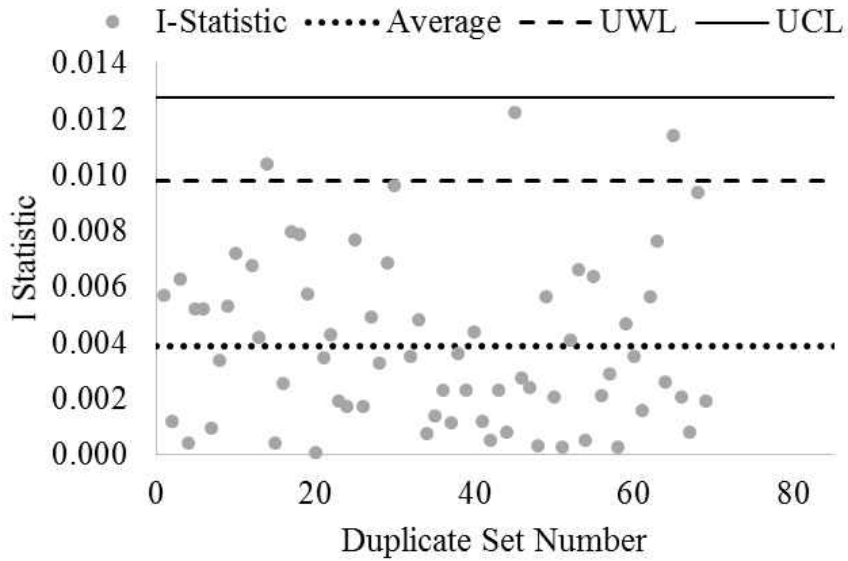
Figure D-4: Precision Control Chart for TOC

222
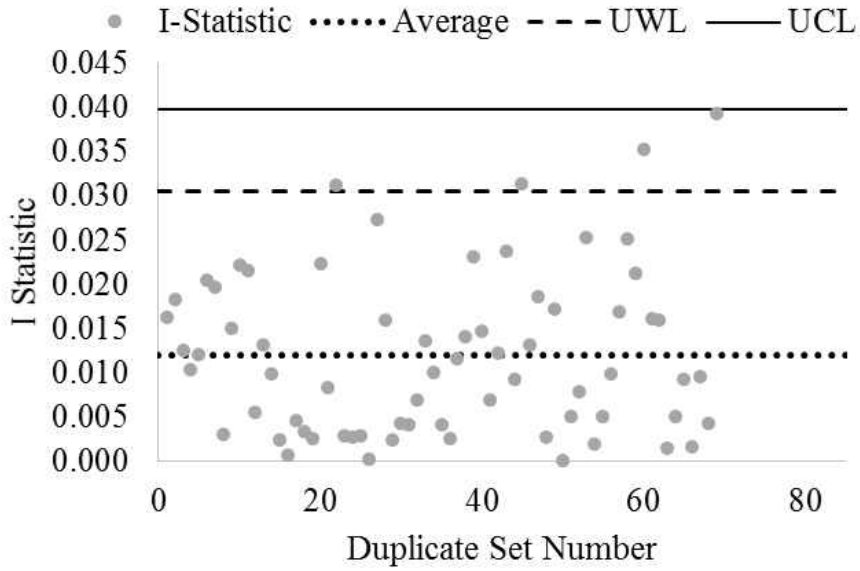
Figure D-5: Precision Control Chart for Silica
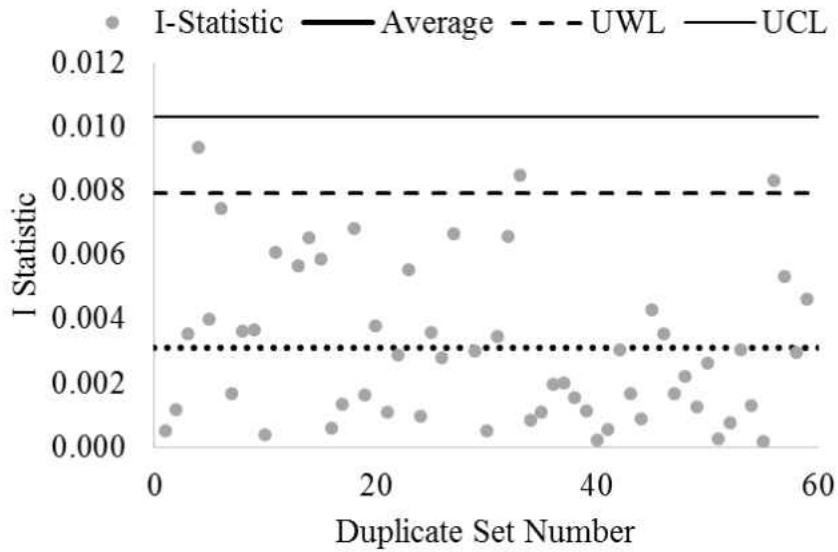
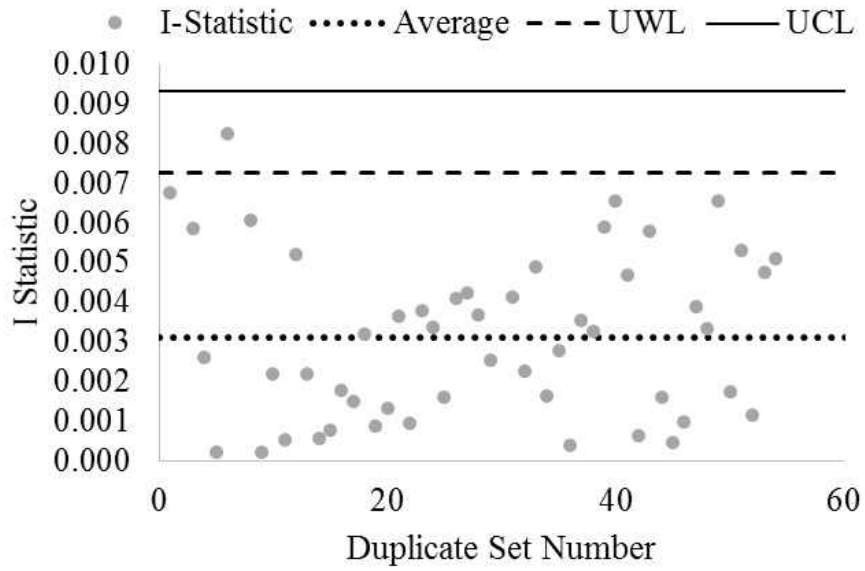**Figure D-6: Precision Control Chart for Chloride**

223

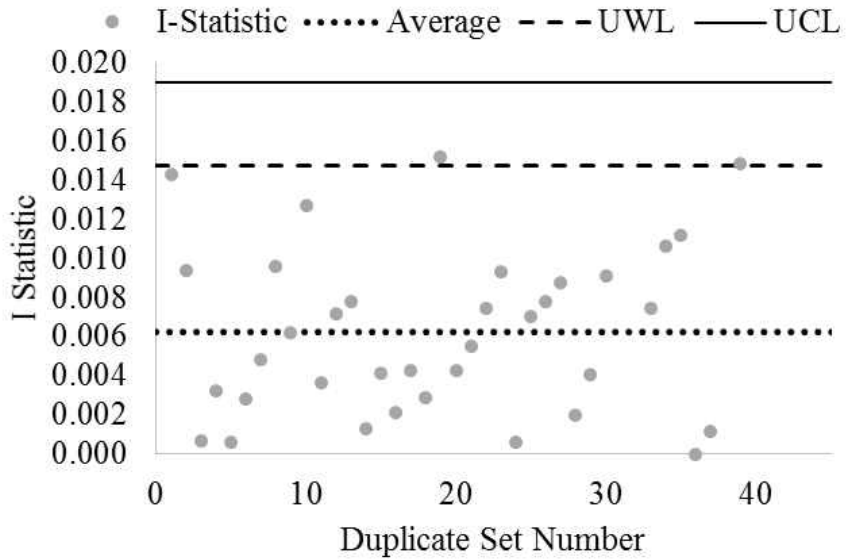**Figure D-7: Precision Control Chart for Barium**
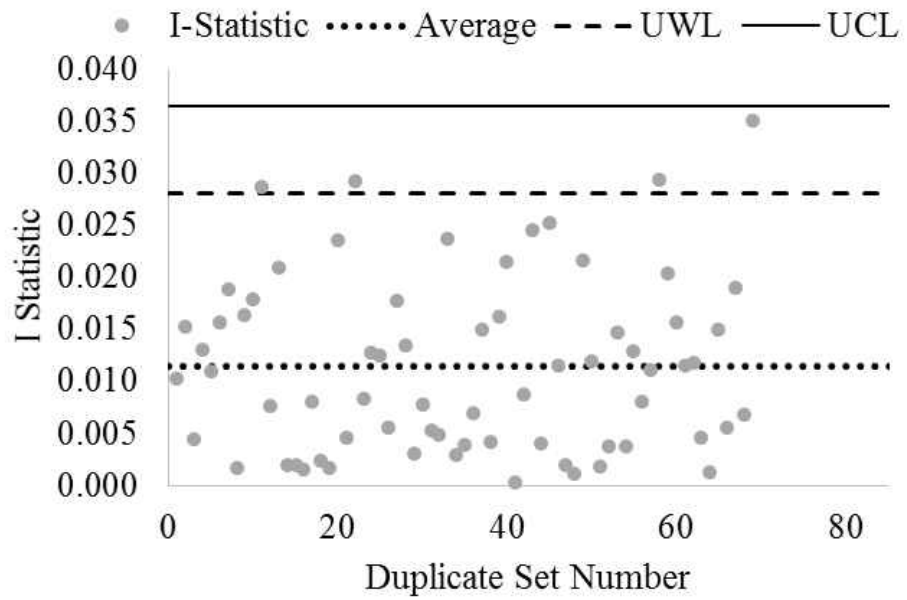

Figure D-8: Precision Control Chart for TDS

Figure D-9: Precision Control Chart for Potassium

REFERENCES

Ahmad, A. L., Ismail, S., & Bhatia, S. (2005). Membrane Treatment for Palm Oil Mill Effluent: Effect of Transmembrane Pressure and Crossflow Velocity. *Desalination, 179*(1–3), 245-255. doi: http://dx.doi.org/10.1016/j.desal.2004.11.071

Alhadidi, A., Kemperman, A. J. B., Schippers, J. C., Wessling, M., & van der Meer, W. G. J. (2012). SDI: Is It a Reliable Fouling Index? *Desalination and Water Treatment, 42*(1-3), 43-48.

Alhadidi, A. M. M. (2011). *Limitations, Improvements, Alternatives for the Silt Density Index.* University of Twente.

Alpatova, A., Verbych, S., Bryk, M., Nigmatullin, R., & Hilal, N. (2004). Ultrafiltration of Water Containing Natural Organic Matter: Heavy Metal Removing in the Hybrid Complexation–Ultrafiltration Process. *Separation and Purification Technology, 40*(2), 155-162. doi: http://dx.doi.org/10.1016/j.seppur.2004.02.003

ASTM. (2007). Standard Test Method for Silt Density Index (SDI) of Water. West Conshohocken, PA: ASTM International.

ASTM. (2010). Standard Practice for Standardizing Reverse Osmosis Performance Data (Vol. D4516-00). West Conshohocken, PA: ASTM International.

Atekwana, E. A., Atekwana, E. A., Rowe, R. S., Werkema Jr, D. D., & Legall, F. D. (2004). The Relationship of Total Dissolved Solids Measurements to Bulk Electrical Conductivity in an Aquifer Contaminated with Hydrocarbon. *Journal of Applied Geophysics, 56*(4), 281-294. doi: http://dx.doi.org/10.1016/j.jappgeo.2004.08.003

AWWA. (2005). *Microfiltration and Ultrafiltration Membranes for Drinking Water (M53)*: American Water Works Association.

AWWA. (2007). *Reverse Osmosis and Nanofiltration (M46)* (2nd ed.). Denver, CO: American Water Works Association.

AWWA. (2011). *Water Quality & Treatment A Handbook on Drinking Water* (J. K. Edzwald Ed. 6th ed.). 6666 Quincy Ave., Denver, CO 80235.

AWWA, WEF, & APHA. (2005). *Standard Methods for the Examination of Water and Wastewater* (21st ed.). Washington, DC American Public Health Association.

Bellona, C., Drewes, J. E., Xu, P., & Amy, G. (2004). Factors Affecting the Rejection of Organic Solutes During NF/RO Treatment—A Literature Review. *Water research, 38*(12), 2795-2809.

Bergman, R. A. (1995). Membrane Softening Versus Lime Softening in Florida: A Cost Comparison Update. *Desalination, 102*(1–3), 11-24. doi: http://dx.doi.org/10.1016/0011-9164(95)00036-2

Bonné, P. A. C., Hiemstra, P., van der Hoek, J. P., & Hofman, J. A. M. H. (2003). Is Direct Nanofiltration with Air Flush an Alternative for Household Water Production for Amsterdam? *Desalination, 152*(1–3), 263-269. doi: http://dx.doi.org/10.1016/S0011-9164(02)01072-X

Booth, R. L. (1979). Handbook for Analytical Quality Control in Water and Wastewater Laboratories. Cincinnati, Ohio.

Boyd, C. C. (2013). *Assessment, Optimization, and Enhancement of Ultrafiltration (UF) Membrane Processes in Potable Water Treatment.* (PhD Dissertation), University of Central Florida, University of Central Florida.

Boyle Engineering Corporation. (1998). Hollow Fine-Fiber Reverse Osmosis Water Treatment Plant Investigating, Pilot Study, and Assessment of Existing Conditions (pp. 5.6-5.7). Sarasota, FL.

Braghetta, A., DiGiano, F. A., & Ball, W. P. (1997). Nanofiltration of Natural Organic Matter: pH and Ionic Strength Effects. *Journal of Environmental Engineering, 123*(7), 628-641.

Briggs, J. C., & Ficke, J. F. (1977). Quality of Rivers of the United States, 1975 Water Year - Based on the National Stream Quality Accounting Network (NASQAN) (pp. 436): U.S. Geological Survey.

Brigmon, R. L., Bitton, G., Zam, S. G., & O'Brien, B. (1995). Development and Application of a Monoclonal Antibody Against Thiothrix spp. *Applied and Environmental Microbiology, 61*(1), 13-20.

Brown, L. C., & Mac Berthouex, P. (2002). *Statistics for Environmental Engineers*: CRC press.

Byrne, W. (1995). *Reverse Osmosis: A Practical Guide for Industrial Users*. Littleton, CO: Tall Oaks Publishing.

Cadena, F., & Peters, R. W. (1988). Evaluation of Chemical Oxidizers for Hydrogen Sulfide Control. *Journal Water Pollution Control Federation, 60*(7), 1259-1263. doi: 10.2307/25043633

Cadotte, J., Forester, R., Kim, M., Petersen, R., & Stocker, T. (1988). Nanofiltration Membranes Broaden the Use of Membrane Separation Technology. *Desalination, 70*(1–3), 77-88. doi: http://dx.doi.org/10.1016/0011-9164(88)85045-8

Chang, E., Chiang, P.-C., Ko, Y.-W., & Lan, W.-H. (2001). Characteristics of organic precursors and their relationship with disinfection by-products. *Chemosphere, 44*(5), 1231-1236.

Cheryan, M. (1986). *Ultrafiltration Handbook*. Lancaster, Pennsylvania: Technomic Publishing Company, Inc.

Cheryan, M. (1998). *Ultrafiltration and Microfiltration Handbook* (Second Edition ed.). Boca Raton, FL: CRC Press LLC.

Choi, K. Y.-j., & Dempsey, B. A. (2004). In-line Coagulation with Low-Pressure Membrane Filtration. *Water research, 38*(19), 4271-4281. doi: http://dx.doi.org/10.1016/j.watres.2004.08.006

Cissé, M., Vaillant, F., Pallet, D., & Dornier, M. (2011). Selecting Ultrafiltration and Nanofiltration Membranes to Concentrate Anthocyanins from Roselle Extract (Hibiscus sabdariffa L.). *Food Research International, 44*(9), 2607-2614. doi: http://dx.doi.org/10.1016/j.foodres.2011.04.046

Comerton, A. M., Andrews, R. C., Bagley, D. M., & Hao, C. (2008). The Rejection of Endocrine Disrupting and Pharmaceutically Active Compounds by NF and RO Membranes as a Function of Compound and Water Matrix Properties. *Journal of membrane science, 313*(1–2), 323-335. doi: http://dx.doi.org/10.1016/j.memsci.2008.01.021

Conlon, W. J., Hornburg, C. D., Watson, B. M., & Kiefer, C. A. (1990). Membrane Softening: The Concept and Its Application to Municipal Water Supply. *Desalination, 78*(2), 157-175. doi: http://dx.doi.org/10.1016/0011-9164(90)80040-I

Cussler, E. L. (2009). *Diffusion Mass Transfer in Fluid Systems* (3rd ed.). New York: Cambridge University Press.

Darvishmanesh, S., Tasselli, F., Jansen, J. C., Tocci, E., Bazzarelli, F., Bernardo, P., . . . Van der Bruggen, B. (2011). Preparation of Solvent Stable Polyphenylsulfone Hollow Fiber

Nanofiltration Membranes. *Journal of membrane science, 384*(1–2), 89-96. doi: http://dx.doi.org/10.1016/j.memsci.2011.09.003

de França Doria, M. (2010). Factors Influencing Public Perception of Drinking Water Quality. *Water policy, 12*(1), 1-19.

DiGiano, F. A., Braghetta, A., Utne, B., & Nilson, J. (1995). *Hollow-fiber Nanofiltration for Treatment of a Surface Water High in Natural Organic Matter*: Water Resources Research Institute of the University of North Carolina.

Dockins, W. S., Olson, G. J., McFeters, G. A., & Turbak, S. C. (1980). Dissimilatory Bacterial Sulfate Reduction in Montana Groundwaters. *Geomicrobiology Journal, 2*(1), 83-98. doi: 10.1080/01490458009377752

Duin, O., Wessels, P., van der Roest, H., Uijterlinde, C., & Schoonewille, H. (2000). Direct Nanofiltration or Ultrafiltration of WWTP Effluent? *Desalination, 132*(1–3), 65-72. doi: http://dx.doi.org/10.1016/S0011-9164(00)00136-3

Duranceau, S. J. (1990). *Modeling of Mass Transfer and Synthetic Organic Compound Removal in a Membrane Softening Process.* (PhD. Dissertation), University of Central Florida, Orlando, Florida.

Duranceau, S. J., & Taylor, J. S. (2011). Membrane Processes *Water Quality & Treatment: A Handbook on Drinking Water* (6th ed., pp. 1-106). New York, NY, USA: McGraw-Hill.

Duranceau, S. J., Tharamapalan, J., Yonge, D. T., & Roque, J. (2014). Verna Treatment Assessment (Vol. 2). Orlando, FL: University of Central Florida.

Duranceau, S. J., Trupiano, V. M., Lowenstine, M., Whidden, S., & Hopp, J. (2010). Innovative hydrogen sulfide treatment methods: moving beyond packed tower aeration. *Florida Water Resources Journal*.

Dykes, G. M., & Conlon, W. J. (1989). Use of Membrane Technology in Florida. *American Water Works Association, 81*(11), 43-46.

Eaton, A. D., Clesceri, L. S., Rice, E. W., & Greenberg, A. E. (2005). *Standard Methods for the Examination of Water and Wastewater*. Washington: American Public Health Association, American Water Works Association, Water Environment Federation.

Electricity Local. (2016). Sarasota, FL Electricity Rates. 2016, from http://www.electricitylocal.com/states/florida/sarasota/

Fang, J., Yang, X., Ma, J., Shang, C., & Zhao, Q. (2010). Characterization of algal organic matter and formation of DBPs from chlor(am)ination. *Water research, 44*(20), 5897-5906. doi: http://dx.doi.org/10.1016/j.watres.2010.07.009

Fang, W., Shi, L., & Wang, R. (2014). Mixed polyamide-based composite nanofiltration hollow fiber membranes with improved low-pressure water softening capability. *Journal of membrane science, 468*, 52-61.

Fritzmann, C., Löwenberg, J., Wintgens, T., & Melin, T. (2007). State-of-the-Art of Reverse Osmosis Desalination. *Desalination, 216*(1–3), 1-76. doi: http://dx.doi.org/10.1016/j.desal.2006.12.009

Futselaar, H., Schonewille, H., & van der Meer, W. (2002). Direct Capillary Nanofiltration—A New High-Grade Purification Concept. *Desalination, 145*(1), 75-80.

Galjaard, G., Buijs, P., Beerendonk, E., Schoonenberg, F., & Schippers, J. Ç. (2001). Pre-coating (EPCE®) UF membranes for Direct Treatment of Surface Water. *Desalination, 139*(1–3), 305-316. doi: http://dx.doi.org/10.1016/S0011-9164(01)00324-1

Hasson, D., Drak, A., & Semiat, R. (2001). Inception of CaSO4 Scaling on RO Membranes at Various Water Recovery Levels. *Desalination, 139*(1–3), 73-81. doi: http://dx.doi.org/10.1016/S0011-9164(01)00296-X

He, T., Frank, M., Mulder, M. H. V., & Wessling, M. (2008). Preparation and Characterization of Nanofiltration Membranes by Coating Polyethersulfone Hollow Fibers with Sulfonated Poly(ether ether ketone) (SPEEK). *Journal of membrane science, 307*(1), 62-72. doi: 10.1016/j.memsci.2007.09.016

Hilal, N., Al-Zoubi, H., Darwish, N. A., Mohamma, A. W., & Abu Arabi, M. (2004). A Comprehensive Review of Nanofiltration Membranes:Treatment, Pretreatment, Modelling, and Atomic Force Microscopy. *Desalination, 170*(3), 281-308. doi: http://dx.doi.org/10.1016/j.desal.2004.01.007

Hirata, T., & Hashimoto, A. (1998). Experimental Assessment of the Efficacy of Microfiltration and Ultrafiltration for Cryptosporidium Removal. *Water Science and Technology, 38*(12), 103-107. doi: http://dx.doi.org/10.1016/S0273-1223(98)00809-9

Howe, K. J., Marwah, A., Chiu, K.-P., & Adham, S. S. (2007). Effect of Membrane Configuration on Bench-scale MF and UF Fouling Experiments. *Water research, 41*(17), 3842-3849. doi: http://dx.doi.org/10.1016/j.watres.2007.05.025

Jacangelo, J. G., Adham, S. S., & Laîné, J. M. (1995). Mechanism of Cryptosporidium, Giardia, and MS2 Virus Removal by MF and UF. *American Water Works Association, 87*(9), 107-121.

Jacangelo, J. G., & Laine, J.-M. (1994). Evaluation of Ultrafiltration Membrane Pretreatment and Nanofiltration of Surface Waters. Denver, CO: AWWA Research Foundation.

Jacangelo, J. G., Rhodes, T., & Watson, M. (1997). Role of Membrane Technology in Drinking Water Treatment in the United States. *Desalination, 113*(2), 119-127.

Kiso, Y., Mizuno, A., Othman, R. A. A. b., Jung, Y.-J., Kumano, A., & Ariji, A. (2002). Rejection Properties of Pesticides with a Hollow Fiber NF Membrane (HNF-1). *Desalination, 143*(2), 147-157. doi: http://dx.doi.org/10.1016/S0011-9164(02)00236-9

Knops, F. (2016). [Personal Communication Enschede Netherlands].

Knops, F., Dekker, R., Spenkelink, F., & Blankert, B. (2012). *New Developments in Hollow Fiber Nanofiltration*. Netherlands.

Kucera, J. (2010). *Reverse Osmosis - Industrial Applications and Processes*. Salem: John Wiley & Sons and Scrivener Publishing LLC.

Kuznetsova, E. M. (2007). A New Method for Describing the Concentration Dependence of the Diffusion Coefficients of Strong Electrolytes in Aqueous Solutions at 298.15 K. *Russian Journal of Physical Chemistry A, 81*(8), 1234-1241. doi: 10.1134/S0036024407080109

Ladner, D. A., Subramani, A., Kumar, M., Adham, S. S., & Clark, M. M. (2010). Bench-scale Evaluation of Seawater Desalination by Reverse Osmosis. *Desalination, 250*(2), 490-499. doi: http://dx.doi.org/10.1016/j.desal.2009.06.072

Lewis, G. N., & Randall, M. (1921). The Activity Coefficient Of Strong Electrolytes. *Journal of the American Chemical Society, 43*(5), 1112-1154. doi: 10.1021/ja01438a014

Liu, C., Caothien, S., Hayes, J. C., & Otoyo, T. O. (2001). *Membrane Chemical Cleaning: From Art of Science*. AWWA 2000 Water Quality Technology Conference. Denver, CO.

Lloyd, J. W., & Heathcote, J. A. A. (1985). Natural Inorganic Hydrochemistry in Relation to Ground Water.

Lonsdale, H. K. (1982). The Growth of Membrane Technology. *Journal of membrane science, 10*(2), 81-181.

Lonsdale, H. K., Merten, U., & Riley, R. L. (1965). Transport Properties of Cellulose Acetate Osmotic Membranes. *Journal of applied polymer science, 9*(4), 1341-1362. doi: 10.1002/app.1965.070090413

Lovins, W. A., & J., D. S. (2003). *Achieving Effective Hydrogen Sulfide Odor Control at Minimal Cost – Pilot Testing Conventional and Emergent Technologies at a Central Florida Water Treatment Facility.* Paper presented at the Water Environment Federation WEFTEC.

Lyn, T. L., & Taylor, J. S. (1992). Assessing Sulfur Turbidity Formation Following Chlorination of Hydrogen Sulfide in Groundwater. *Journal (American Water Works Association), 84*(9), 103-112. doi: 10.2307/41293854

Macpherson, G. L. (2009). CO2 distribution in Groundwater and the Impact of Groundwater Extraction on the Global C Cycle. *Chemical Geology, 264*(1-4), 328-336. doi: 10.1016/j.chemgeo.2009.03.018

Maung, H., & Song, L. (2009). Effect of pH and Ionic Strength on Boron Removal by RO Membranes. *Desalination, 246*(1–3), 605-612. doi: http://dx.doi.org/10.1016/j.desal.2008.06.025

Mendenhall, W., & Sincich, T. (2007). *Statistics for Engineering and the Sciences.* Upper Saddle River, New Jersey: Pearson Prentice Hall.

Murthy, Z. V. P., & Gupta, S. K. (1997). Estimation of Mass Transfer Coefficient Using a Combined Nonlinear Membrane Transport and Film Theory Model. *Desalination, 109*(1), 39-49. doi: http://dx.doi.org/10.1016/S0011-9164(97)00051-9

Nakatsuka, S., Nakate, I., & Miyano, T. (1996). Drinking Water Treatment by Using Ultrafiltration Hollow Fiber Membranes. *Desalination, 106*(1–3), 55-61. doi: http://dx.doi.org/10.1016/S0011-9164(96)00092-6

Nemeth-Harn, J. (2004). Capital and O&M Costs for Membrane Treatment Facilities. from http://www.harnrosystems.com/papers/CapitalandOMCostforRO_Presentation.pdf

Olivieri, V. P., Parker Jr, D., Willinghan, G., & Vickers, J. (1991). *Continuous Microfiltration of Surface Water.* Paper presented at the AWWA Membrane Technology Conference Proceedings, Orlando, FL.

Ozaki, H., Sharma, K., & Saktaywin, W. (2002). Performance of an Ultra-Low-Pressure Reverse Osmosis Membrane (ULPROM) for Separating Heavy Metal: Effects of Interference Parameters. *Desalination, 144*(1–3), 287-294. doi: http://dx.doi.org/10.1016/S0011-9164(02)00329-6

Pentair. (2011). HFC Quickscan Pilot Manual.

Perry, R. H., Chilton, C. H., & Kirkpatrick, S. D. (1963). *Chemical Engineers Handbook.* New York: Mcgraw Hill Inc.

Powell, S. T., & von Lossberg, L. G. (1948). Removal of Hydrogen Sulfide from Well Water. *Journal (American Water Works Association), 40*(12), 1277-1290. doi: 10.2307/41234873

Real-Robert, M. (2011). *Environmental Engineering Laboratories: Quality Assurance/Quality Control.* University of Central Florida - Department of Civil, Environmental, and Construction Engineering, Orlando, FL.

Reid, C. E., & Breton, E. J. (1959). Water and Ion Flow Across Cellulosic Membranes. *Journal of applied polymer science, 1*(2), 133-143.

Ridgway, H. F., Justice, C. A., Whittaker, C., Argo, D. G., & Olson, B. H. (1984). Biofilm Fouling of RO Membranes—Its Nature and Effect on Treatment of Water for Reuse. *American Water Works Association, 76*(6), 94-102. doi: 10.2307/41273154

Rook, J. (1974). Formation of Haloforms During Chlorination of Natural Waters. *Water Treatment and Examination, 23*(2), 234-243.

Safar, M., Jafar, M., Abdel-Jawad, M., & Bou-Hamad, S. (1998). Standardization of RO Membrane Performance. *Desalination, 118*(1–3), 13-21. doi: http://dx.doi.org/10.1016/S0011-9164(98)00070-8

Sawyer, C. N., McCarty, P. L., & Parkin, G. F. (2003). *Chemistry for Environmental Engineering and Science* (5th ed.). New York, NY: McGraw Hill.

Schippers, J. C., & Verdouw, J. (1980). The Modified Fouling Index, a Method of Determining the Fouling Characteristics of Water. *Desalination, 32*, 137-148. doi: http://dx.doi.org/10.1016/S0011-9164(00)86014-2

Semiat, R., Sutzkover, I., & Hasson, D. (2003). Characterization of the Effectiveness of Silica Anti-Scalants. *Desalination, 159*(1), 11-19. doi: http://dx.doi.org/10.1016/S0011-9164(03)90041-5

Sethi, S., & Wiesner, M. R. (2000). Simulated Cost Comparisons of Hollow-Fiber and Integrated Nanofiltration Configurations. *Water research, 34*(9), 2589-2597. doi: http://dx.doi.org/10.1016/S0043-1354(00)00017-8

Shannon, M. A., Bohn, P. W., Elimelech, M., Georgiadis, J. G., Mariñas, B. J., & Mayes, A. M. (2008). Science and Technology for Water Purification in the Coming Decades. *Nature, 452*(7185), 301-310.

Sieder, E. N., & Tate, G. E. (1936). Heat Transfer and Pressure Drop of Liquids in Tubes. *Industrial & Engineering Chemistry, 28*(12), 1429-1435.

Simmons, O. D., Sobsey, M. D., Heaney, C. D., Schaefer, F. W., & Francy, D. S. (2001). Concentration and Detection of Cryptosporidium Oocysts in Surface Water Samples by Method 1622 Using Ultrafiltration and Capsule Filtration. *Applied and Environmental Microbiology, 67*(3), 1123-1127. doi: 10.1128/aem.67.3.1123-1127.2001

Smith, P. J., Vigneswaran, S., Ngo, H. H., Ben-Aim, R., & Nguyen, H. (2006). A New Approach to Backwash Initiation in Membrane Systems. *Journal of membrane science, 278*(1), 381-389.

Solutions, D. W. (2010). Filmtec Reverse Osmosis Membranes Technical Manual. Retrieved July 9, 2014, from http://www.scribd.com/doc/24498057/FILMTEC-RO-Membranes-Technical-Manual

Sourirajan, S., & Kimura, S. (1967). Correlations of Reverse Osmosis Separation Data for the System Glycerol-Water Using Porous Cellulose Acetate Membranes. *Industrial & Engineering Chemistry Process Design and Development, 6*(4), 504-516. doi: 10.1021/i260024a019

Stevens, D., & Loeb, S. (1967). Reverse Osmosis Desalination Costs Derived from the Coalinga Pilot Plant Operation. *Desalination, 2*(1), 56-74.

Sung, L. (1993). *Film Theory and Ion Coupling Models for a Diffusion Controlled Membrane Process.* (PhD. Dissertation), University of Central Florida, Orlando, FL.

Taylor, J. S., Mulford, L. A., Duranceau, S. J., & Barrett, W. M. (1989). Cost and Performance of a Membrane Pilot Plant. *American Water Works Association, 81*(11), 52-60. doi: 10.2307/41292729

Teuler, A., Glucina, K., & Laine, J. M. (1999). Assessment of UF Pretreatment Prior RO Membranes for Seawater Desalination. *Desalination, 125*(1), 89-96.

Tharamapalan, J. (2012a). *Application and Optimization of Membrane Processes Treating Brackish and Surficial Groundwater for Potable Water Production.* (Doctor of Philosophy), University of Central Florida, Orlando, FL.

Tharamapalan, J. (2012b). *Application and Optimization of Membrane Processes Treating Brackish and Surficial Groundwater for Potable Water Production.* (Doctor of Philosophy), University of Central Florida, Orlando, FL.

Tharamapalan, J., Duranceau, S. J., & Perez, P. (2011). *Demonstration of Sulfuric Acid Elimination in a Brackish Water Reverse Osmosis Membrane Process*. American Membrane Technology Association and Southeast Desalting Association Joint Conference. Miami Beach.

Thirumalini, S., & Joseph, K. (2009). Correlation Between Electrical Conductivity and Total Dissolved Solids in Natural Waters. *Malaysian Journal of Science, 28*(1), 55-61.

USEPA. (2005). *Membrane Filtration Guidance Manual*. (815-R-06-009). USEPA Office of Water.

Van der Bruggen, B., Hawrijk, I., Cornelissen, E., & Vandecasteele, C. (2003). Direct nanofiltration of surface water using capillary membranes: comparison with flat sheet membranes. *Separation and Purification Technology, 31*(2), 193-201.

Van der Bruggen, B., & Vandecasteele, C. (2003). Removal of Pollutants from Surface Water and Groundwater by Nanofiltration: Overview of Possible Applications in the Drinking Water Industry. *Environmental Pollution, 122*(3), 435-445. doi: http://dx.doi.org/10.1016/S0269-7491(02)00308-1

Verberk, J. Q. J. C., & Van Dijk, J. C. (2006). Air Sparging in Capillary Nanofiltration. *Journal of membrane science, 284*(1), 339-351.

Vrouwenvelder, J. S., & van der Kooij, D. (2001). Diagnosis, Prediction and Prevention of Biofouling of NF and RO Membranes. *Desalination, 139*(1–3), 65-71. doi: http://dx.doi.org/10.1016/S0011-9164(01)00295-8

Wallace, B., Purcell, M., & Furlong, J. (2002). Total Organic Carbon Analysis as a Precursor to Disinfection Byproducts in Potable Water: Oxidation Technique Considerations. *Journal of Environmental Monitoring*, 35-42.

Watson, B. M., & Hornburg, C. D. (1989). Low-Energy Membrane Nanofiltration for Removal of Color, Organics and Hardness from Drinking Water Supplies. *Desalination, 72*(1), 11-22.

Weber, W. A. (1972). *Physicochemical Processes for Water Quality Control*. New York: John Wiley and Sons.

Westrick, J. J., & Allgeier, S. C. (1996). *ICR Manual for Bench-and Pilot-scale Treatment Studies*: Technical Support Division, Office of Ground Water and Drinking Water, US Environmental Protection Agency.

White, G. C. (1999). *Handbook of Chlorination* (4th ed.). New York: John Wiley & Sons, Inc.

Wilf, M., Awerbuch, L., & Bartels, C. (2007). *The Guidebook to Membrane Desalination Technology Reverse Osmosis, Nanofiltration, and Hybrid Systems Process, Design, Applications and Economics*. Hopkinton, MA: Balaban Desalination Publications.

Wilke, C. R., & Chang, P. (1955). Correlation of Diffusion Coefficients in Dilute Solutions. *American Institute of Chemical Engineers Journal, 1*(2), 264-270. doi: 10.1002/aic.690010222

Wintgens, T., Salehi, F., Hochstrat, R., & Melin, T. (2008). Emerging Contaminants and Treatment Options in Water Recycling for Indirect Potable Use. *Water Science and Technology, 57*(1), 99-108.

Xu, J., Ruan, G., Gao, X., Pan, X., Su, B., & Gao, C. (2008). Pilot Study of Inside-out and Outside-in Hollow Fiber UF Modules as Direct Pretreatment of Seawater at Low Temperature for Reverse Osmosis. *Desalination, 219*(1), 179-189.

Xu, P., Drewes, J. E., & Heil, D. (2008). Beneficial Use of Co-Produced Water through Membrane Treatment: Technical-Economic Assessment. *Desalination, 225*(1–3), 139-155. doi: http://dx.doi.org/10.1016/j.desal.2007.04.093

Younos, T., & Tulou, K. E. (2005). Overview of Desalination Techniques. *Journal of Contemporary Water Research & Education, 132*(1), 3-10. doi: 10.1111/j.1936-704X.2005.mp132001002.x

Yuan, Y., & Kilduff, J. E. (2009). Hydrodynamic Modeling of NOM Transport in UF: Effects of Charge Density and Ionic Strength on Effective Size and Sieving. *Environmental science & technology, 43*(14), 5449-5454.

Zhao, Y. (2004). *Modeling of Membrane Solute Mass Transfer in NF/RO Membrane Systems.* (Doctor of Philosophy), University of Central Florida, Orlando, Florida.

Zhao, Y., & Taylor, J. S. (2005). Incorporation of Osmotic Pressure in an Integrated Incremental Model for Predicting RO or NF Permeate Concentration. *Desalination, 174*(2), 145-159. doi: http://dx.doi.org/10.1016/j.desal.2004.09.008

Zhao, Y., Taylor, J. S., & Chellam, S. (2005). Predicting RO/NF Water Quality by Modified Solution Diffusion Model and Artificial Neural Networks. *Journal of membrane science, 263*(1–2), 38-46. doi: http://dx.doi.org/10.1016/j.memsci.2005.04.004